Institute for Energy Technology, Norway

and

National Academy of Sciences of Ukraine

Інститут енергетичних технологій, Норвегія

та

Національна Академія наук України

ВОДНЕВІ ТЕХНОЛОГІЇ ЗБЕРІГАННЯ ЕНЕРГІЇ:

СТАН ТА ПЕРСПЕКТИВИ РОЗВИТКУ

За редакцією

В. А. Яртися
Ю. М. Солоніна та
І. Ю. Завалія

Львів
Видавництво «Простір-М»
2021

HYDROGEN BASED ENERGY STORAGE:

STATUS AND RECENT DEVELOPMENTS

Edited by

Volodymyr Yartys
Yuriy Solonin and
Ihor Zavaliy

LVIV
Publishing office “Prostir-M”
2021

.

The publication was funded by the NATO Science for Peace and Security Programme, Project G5233 “Portable Energy Supply” (2017-2021).

This monograph has been reviewed and accepted for publication by the Scientific Council of the Programme of Fundamental Research of the National Academy of Sciences of Ukraine “Development of Scientific Principles for Hydrogen Production, Storage and Use in Autonomous Energy Supply Systems”.

Monograph

Hydrogen based energy storage: status and recent developments

Edited by Volodymyr A. Yartys, Yurii M.Solonin, Ihor Yu.Zavaliy,
Lviv, Prostir-M., 2021, - 268 p.

ISBN 978-617-8055-08-0

The latest advances in the use of renewable energy sources (solar and wind), chemical processes, biomaterials for the efficient production of hydrogen, its storage and use in the fuel cells powered energy supply systems are presented. New important results were obtained within two research programs, namely, the NATO Science for Peace and Security Programme Project G5233 "Portable Energy Supply" (2017-2021) and the priority program of the NAS of Ukraine "Development of scientific principles of the production, storage and use of hydrogen in autonomous energy supply systems” (2019-2021). The book is aimed for the researchers, engineers, professors and graduate students specializing in materials science, energy storage and conversion, particularly focusing on the studies of the hydrogen energy-related materials and technologies.

ISBN 978-617-8055-08-0

Introduction

The European Commission and the Department of Energy in USA consider hydrogen as an energy carrier with a great potential for supplying a clean, efficient power for the stationary, portable and transport applications. The growing use of hydrogen fuelled transportation started in the 20th century with high profile technology breakthroughs such as powering Apollo 11 to the moon. Optimistic predictions of a quick commercialization of hydrogen energy technologies have been witnessed worldwide at the beginning of the 21st century. Unfortunately, these expectations failed to be fulfilled according to the plans at that time. However, recently the topic of use of hydrogen as an energy carrier experiences a global revival as hydrogen is getting unprecedented focus worldwide and is on track to achieve its outstanding potential as a clean energy solution.

The share of hydrogen in Europe's energy mix is projected to grow from the current less than 2% to 14% by 2050. The goal of exclusively using blue hydrogen (with CO_2 sequestration) and green hydrogen with a CO_2-free footprint is an ultimate target.

Several aspects of the technology - hydrogen production, hydrogen storage and transportation and hydrogen fuel cell technologies - were all recently significantly developed allowing to observe their synergy in reaching new and much advanced opportunities for the use of hydrogen-based energy storage and supply solutions. Improved quality of the products and markedly reduced costs of the energy systems and their components, bring much down and make well competitive the prices of hydrogen energy systems as compared to the alternative technologies of

energy storage and supply. The hydrogen energy playground is maturing through a growing fleet of hydrogen fuel cell vehicles, hydrogen fuel cell trains commercially operating in Germany, France and the UK, and hydrogen driven ferries in Norway. This is in addition to the high-capacity metal hydride fast recharging battery systems for trains and trams in France and in Japan. Nevertheless, hydrogen storage remains a key challenge in rolling out infrastructure to support hydrogen fuelled transportation.

To enable the wide-spread commercialization of hydrogen fuel cell technologies, the primary focus of the development of hydrogen storage research is in the development of both small and compact H storage solutions enabling efficient use of fuel cell electric vehicles, and large, on a scale of tons of H_2, hydrogen stores where it can be accumulated over long periods of time, allowing efficient integration of the variable sources of renewable energy into the energy system for generate power and heat.

The progress on hydrogen-based energy storage is based on the international research and development in the field. As the world's leading energy authority covering exploration of all fuels and related technologies, the International Energy Agency (IEA) is ideally placed to lead global policy on hydrogen. The IEA Technology Collaboration Program (TCP) supports advancing the research, development and commercialization of energy technologies. IEA Hydrogen TCP coordinates research on hydrogen within various tasks. IEA Hydrogen Task 32 (finished) and Task 40 (active) include the efforts of the scientific community in various areas of energy storage based on hydrogen. IEA Hydrogen Tasks 32/40 are executed by the largest international collaboration group in this field with contributions from more than 50 experts coming from 17 countries. The specific activities focus on intermetallic alloys and magnesium-based hydrides as energy storage materials, complex and liquid hydrides, electrochemical storage of energy, heat storage, hydrogen storage systems for stationary and mobile applications and on porous materials. Prof. V.A. Yartys has been leading the group activities on magnesium- and aluminium-based hydrides and intermetallic alloys which resulted in several highly cited publications [1-4]. These papers revealed a great potential which have the

alloys and hydrides of the light metals – Mg and Al – as the materials for hydrogen storage [1-4] and also when integrated into the hydrogen storage systems with fuel cells [5].

The potential of materials in efficiently generating hydrogen becomes even higher when a chemical process of their interaction with water – hydrolysis – is taking place. The current monograph presents an outcome of the project G5233 "Portable Energy Supply" belonging to the NATO Science for Peace and Security Programme, under SPS Key Priority Area Energy Security. Hydrogen can be stored, transported and used in fuel cells for a direct conversion of the accumulated chemical energy, via its electrochemical oxidation, to electricity. Despite of a reasonable efficiency of this process, its broad use is rather limited because of the necessity to have available efficient hydrogen generation and storage technologies, particularly when special demands for hydrogen use in portable applications should be implemented. Metal hydrides (MH) can accumulate large amounts of hydrogen and reversibly absorb-release hydrogen gas following the changes in temperature and H_2 pressure. Hydrogen storage tanks accommodating metal hydrides are broadly utilized for this purpose; however, for the portable applications these tanks should be minimized in their weight and volume, while providing the required high reversible hydrogen capacities. An alternative scenario when generating hydrogen by a hydrolysis reaction, is based on the use of the metals, metal hydrides or complex hydrides. The latter reaction takes place at relatively low temperatures and results in reaching high hydrogen supply efficiencies. The project G5233 "Portable Energy Supply" was executed in collaboration between Institute for Energy Technology in Norway (NATO country) and three research institutes of the National Academy of Science of Ukraine from the NATO partner country – Ukraine (Physico-Mechanical Institute in Lviv, Institute for Problems of Materials Science in Kyiv and Institute of General and Inorganic Chemistry in Kyiv) and was focused on the development of the efficient alloys and metal hydride materials, namely on the Al-based alloys and magnesium dihydride (MgH_2) composites with catalytic additives (CA), for hydrogen generation via their interaction with water. The influence of

nanostructuring of the materials, detailed physico-chemical studies of the role of the CA on hydrogen evolution, together with the development of the efficient approaches in controlling the hydrogen generation rate and/or in stopping the hydrolysis process on demand within the main challenges successfully addressed in the performed research. Weight efficient H_2 generation device was constructed by using synthesized and optimised materials. The units for hydrogen storage and generation using the technologies of hydrogen supply to the portable FC were tested and allowed to develop a lightweight, reliable and silent electrical power supply (high-energy-density portable power source) combining hydrogen storage and generation and a portable ~25 W FC. This system will be used as a prototype for further upscaling and developing the technology in the future, after the present project will be completed. The website of the project (http://nato-sps-portableenergy.ipm.lviv.ua) presents further details of the work done including presentation of the partners and lists the publications highlighting the outcome of the work with more than 15 joint papers published in the international journals with high impact factors.

The NATO SPS program is presented and described in this book later in a special contribution from the NATO SPS Programme officers Dr. Deniz Beten, Senior Science for Peace Security and Partnership Cooperation Advisor, and Richard Brewin, Programme Manager Energy and Environmental Security and Science for Peace, Security Adviser, both associated with NATO Emerging Security Challenges Division.

Another important related activity in the NATO partner country – Ukraine – is the second major topic presented in the book and highlights the outcome of the work on the research programme of the National Academy of Science of Ukraine devoted to the hydrogen-based technologies. Over the past ten years, the institutes of this Academy worked on the implementation of a comprehensive program of scientific research dedicated to the production, transportation, storage, and use of hydrogen. Within the framework of this program, new highly efficient hydrogen storage and hydrogen generating materials based on magnesium hydride were developed, a technology for manufacturing light composite high-pressure cylinders for hydrogen storage was proposed, new efficient

polymer electrolyte membrane fuel cells were made and tested, modern technologies for producing hydrogen from various renewable raw materials were proposed, technological schemes for producing hydrogen based on use of geothermal energy sources, solar radiation, and wind energy were developed, biotechnologies for the utilization of the food rests with simultaneous synthesis of an environmentally friendly energy carrier – hydrogen were proposed, a number of promising magnesium-based alloys and composites obtained by mechanochemistry were created, which can be recommended for the stationary hydrogen storage systems. The results of the program execution are presented in the Chapter II. Detailed information can also be obtained at the Program website (http://www.materials.kiev.ua/Hydrogen_2019-2021/otr_H.html).

This work shows a great benefit brought by scientific research performed in international collaboration while jointly funded by the national and international sources, allowing to grow scientific competence in the field, to exchange scientific and technological expertise and to obtain novel scientific outcome with research output published in the internationally leading scientific journals with high impact factors.

References

[1] M. Hirscher, V. Yartys, M. Baricco et al. Materials for hydrogen based energy storage – past, recent progress and future outlook, *J. Alloys and Compounds,* 2020, vol. 827,153548. https://doi.org/10.1016/j.jallcom.2019.153548. (223 citations).

[2] J.-C. Crivello, B. Dam, … V.A. Yartys. Review of magnesium hydride-based materials: development and optimisation, *Applied Physics A: Materials Science and Processing,* 2016, vol. 122, issue 2, article 97. https://doi.org/10.1007/s00339-016-9602-0 (261 citations).

[3] V. A. Yartys, M.V. Lototskyy, E. Akiba, et al. Magnesium based materials for hydrogen based energy storage: past, present and future. *Int. J. of Hydrogen Energy*, 2019, vol.44, pp. 7809-7859. https://doi.org/10.1016/j.ijhydene.2018.12.212. (238 citations).

[4] J. Graetz, J.J. Reilly, V.A. Yartys, et al. Aluminium hydride as a hydrogen and energy storage material: past, present and future, *J. of Alloys and Compounds*, 2011, vol.509, Supplement 2, pp.S517-S528. http://dx.doi.org/10.1016/j.jallcom.2010.11.115. (208 citations).
[5] M.V. Lototskyy, I.Tolj, V.Yartys. The use of metal hydrides in fuel cell applications, *Progress in Natural Science: Materials International,* 2017, vol. 27, issue 1, pp. 3-20.
http://dx.doi.org/10.1016/j.pnsc.2017.01.008 . (173 citations).

The Editors

Volodymyr Yartys, Prof.	Yuriy Solonin, Prof.	Ihor Zavaliy, Prof.
Institute for Energy Technology, Norway	Frantsevich Institute for Problems of Materials Sciences, National Academy of Sciences of Ukraine	Karpenko Physico-Mechanical Institute, National Academy of Sciences of Ukraine

5 November 2021

CHAPTER 1

Research outcome of the project
G5233 "Portable Energy Supply" (2017-2021)
supported by the NATO
Science for Peace and Security Programme

Preface

The Science for Peace and Security (SPS) programme is an established brand for NATO and has been contributing to the core goals of the Alliance for more than six decades. The Programme enhances security-related civil science and technology to address emerging security challenges and their impact, and is an integral component of NATO's Emerging Security Challenges (ESC) Division. In pursuit of NATO's Strategic Objectives, SPS activities align with a set of key priorities, which include, for instance, supporting NATO efforts to counter terrorism, the development of security-related advanced technologies, and dealing with questions related to cyber defence, detection of explosives, and defence against chemical, biological, radiological and nuclear (CBRN) agents. Of note for this publication, SPS key priorities also focus on energy and environmental security challenges, for instance by facilitating practical cooperation dealing with the protection of critical energy infrastructure as well as on innovative energy technologies.

SPS activities connect researchers, experts and officials from NATO and partner nations, who address shared challenges through practical scientific cooperation and capacity building. By supporting security-relevant activities in the form of grants for Multi-Year Projects (MYP), Advanced Research Workshops (ARW), Advanced Training Courses (ATC), and Advanced Study Institutes (ASI), SPS fosters the creation and expansion of international expert networks, the sharing of best practice, and the exchange of expertise and know-how among scientific communities in NATO and partner nations.

In the last decade, SPS has launched more than 400 new activities. Working with a balanced 360^{o} approach, the Programme involves partners across all of NATO's partnership frameworks, engaging approximately 2000 experts every year. The Programme also invests in the development of the next generation of researchers, by actively supporting the participation and training of young scientists in its activities. As a testament to the scientific excellence supported by SPS, 21 Nobel Laureates have been involved in its activities.

SPS activities have also a high public diplomacy value for NATO, participating countries, and individual scientists. In particular, the Programme contributes to enriching the public's perception of NATO beyond the military dimension. By focusing on non-military, practical scientific cooperation and capacity building, SPS often proves essential in establishing new lines of communication with partners by addressing broad and unconventional security challenges. This is demonstrated by

the large number of publications and scientific articles developed in the framework of SPS activities, the Programme provides a platform for experts and scientists to contribute to the progress of the scientific disciplines they excel in.

As the world moves closer towards a clean energy transition, and with the endorsement of NATO's Climate Change and Security Action Plan by NATO Heads of State and Government at their 2021 Summit in Brussels, the role of science and technology will become increasingly important in realizing NATO's aim to become the leading international organization when it comes to understanding and adapting to the impact of climate change on security. In addition, science and technology will also be vital to facilitate NATO's aim to reduce greenhouse gas emissions from military activities and installations without impairing personnel safety, operational effectiveness and its deterrence and defence posture. The SPS programme provides a solid foundation to support this level of ambition.

Dr. Deniz Beten,
Senior Science for Peace, Security & Partnership Cooperation Advisor

Richard Brewin,
Programme Manager: Energy & Environmental Security and Science for Peace & Security

NATO Emerging Security Challenges Division,

Brussels, Belgium

Hydrogen generation by hydrolysis of metals and hydrides for portable energy supply

(An overview of the tasks and outcome of the NATO SPS Project G5233; NATO country: Norway; NATO Partner country: Ukraine)

V. Yartys, I. Zavaliy, Yu. Pirskyy, Yu. Solonin, V. Berezovets, F. Manilevich, Yu. Verbovytskyy, A. Kytsya, A. Kutsyi

NATO project G 5233 "Portable energy supply" was executed by 4 teams (Institute for Energy Technology, Norway and 3 Institutes of the National Academy of Sciences of Ukraine). G5233 Project was focused on the development of hydrogen fueled portable energy supply systems integrating hydrogen generation and storage units based on use of light metals, metal and complex hydride materials and portable fuel cells. The weight efficient energy supply device was developed by using these selected materials and performance-optimised $NaBH_4$ complex hydride. Besides, various new relevant units of equipment for the samples preparation and characterization were ordered and accommodated in the participants labs and the program of training of young scientists at IFE, Norway was accomplished.

Different types of materials for hydrogen generation were synthesized and characterized (activated aluminium alloys, Mg-Al alloys, MgH_2 and their composites, $NaBH_4$ with catalytic additives). The challenging objective of reaching a completeness of the hydrolysis of MgH_2 was achieved; the reaction conditions were optimized and the particular focus applications integrating efficient hydrogen generation systems were identified. The mechanism and the kinetics model of the hydrolysis process of MgH_2 in water solutions have been proposed which successfully describe the experimental data. In parallel with the hydrolysis reaction resulting in hydrogen generation and formation of $Mg(OH)_2$, the process involves passivation of the MgH_2 surface by the formed $Mg(OH)_2$ precipitate followed by its re-passivation with the rate constants of these processes being established. Increase of the concentration of $MgCl_2$ leads to just a minor increase in the rate constant of the interaction of MgH_2 with water but leads to a sharp increase of the rate constant of the re-passivation of MgH_2 surface.

To achieve efficient hydrolysis of $NaBH_4$, different types of catalysts (heterogeneous on the basis of Pt and "homogeneous" - salts of Ni^{+2} and Co^{+2})

were studied and optimized. Several systems were selected as candidates to provide the required hydrogen flow to operate a 30 W fuel cell over a given time exceeding 1 hour, based on a use of inexpensive and affordable hydrogen-containing materials and catalytic additives. 3 individual hydrolysis workstations (1 in Norway and 2 in Ukraine) were built, tested and optimized. The plan of the work to reach the objectives of the Project G5233 "Portable energy supply" is completely accomplished, all the milestones are successfully fulfilled and the overall goal of the Project is reached.

Keywords: *Portable energy systems; Hydrogen generation; Complex hydrides; Catalyst additives; Hydrolysis*

1. Motivation and project goals

In the development of renewable energy systems, hydrogen plays a central role because of its record-high specific energy density (120 MJ/kg), "green", i.e., pollution-free technology of its synthesis using the renewables, its easy and convenient conversion to electricity. Hydrogen can be stored, transported, and used in fuel cells driven energy systems allowing for a direct conversion of the chemical energy, through electrochemical oxidation, to electricity. Despite a reasonable efficiency of this process, its broad use is rather limited because of the necessity to have in the possession efficient hydrogen generation and storage technologies, particularly, when targeted demands for hydrogen use in portable applications should be implemented.

In contrast to the compressed H_2 gas and liquid hydrogen, an effective and safe way is to store H_2 in its chemical compounds, namely, in metal hydrides (MH). MH can store large amounts of hydrogen and reversibly release it following an increase in temperature and/or a decrease in pressure. The hydrogen storage tanks accommodating MH are extensively used for this purpose. However, for portable applications they should be optimized by reducing their weight and volume, while showing high hydrogen storage capacity. $LaNi_5$ intermetallic and many other alloys (TiFe, Ti_2Ni, Ti,Zr-based Laves phases, bcc Ti-V-based alloys) can absorb 1.5-4.0 wt.% H at ambient conditions (near room temperature and at pressures close to 1-2

bar H_2) and reversibly release it following an increase in temperature or a decrease in pressure. Unfortunately, these values are insufficient to allow their efficient practical applications as hydrogen storage sources for the portable FC applications.

A promising group of H-storage materials is based on magnesium hydride. Magnesium metal can reversibly store large amounts of hydrogen - up to 7.6 wt.% H. However, there are principal challenges in utilizing Mg-based alloys. Indeed, due to a sluggish kinetics and unfavorable thermodynamics of hydrogen absorption-desorption processes, they require application of elevated operation temperatures (> 300 °C) while also investing a significant amount of heat because of high decomposition enthalpy of MgH_2 (74 kJ/Mol H_2). A great improvement in the hydrogen sorption kinetics by Mg was achieved by using suitable catalysts and adopting proper preparation methods [1, 2]. Mechanical alloying of Mg with different additives (and particularly its reactive ball milling in hydrogen gas) results in acceleration of the hydrogenation process and in a substantial decrease of the hydrogenation-dehydrogenation temperatures. However, the working temperatures (250-300 °C) are too high [3-5], thus a direct use of MgH_2 for the storage of gaseous H_2 should be ruled out meets practical limitations. At the same time, very intensive development of the complex hydrides, which are characterized by a high H-content (>10 wt.%), have not resulted in the development of the efficient hydrogen storage systems due to their low reversible capacity, limited cycle life and poor kinetics of hydrogen exchange [6,7]. Thus, the grand challenge of finding efficient, reversible at ambient temperatures solid hydrogen storage materials providing a high H storage capacity for use in portable FC applications remains to be solved [3,8].

An alternative and efficient way to generate hydrogen is in utilizing the hydrolysis reaction by using the metals, metal hydrides or complex hydrides. Such hydrolysis process takes place at relatively low temperatures and shows promising practical hydrogen supply efficiencies. The most frequently used hydrogen generation alloys include Al and Mg based materials [9,10]. The reason is in their light weight, high natural abundance, low cost, and environmental compatibility. However, there are practical challenges as aluminum forms a dense surface oxide layer which creates a

barrier for the progression of the hydrogen evolution reaction, while, in turn, for Mg, the hydrolysis reaction is rapidly interrupted because of the formation of a blocking layer of magnesium hydroxide.

A great benefit of metal hydrides is in a fact that during the hydrolysis they generate a double amount of hydrogen as compared to the corresponding individual metals. A large number of metal hydrides have been studied as a portable source of hydrogen for fuel cell applications, including LiH, CaH_2, MgH_2, $NaBH_4$, $LiBH_4$, and $LiAlH_4$ [11]. Among them, LiH, CaH_2, and $LiAlH_4$ can react with water so violently that the uncontrollable reaction leads to a handicapped practicability. In turn, production of hydrogen using $NaBH_4$ is safe and well controllable, but the regeneration of $NaBH_4$ from the reaction product $NaBO_2$ is not simple and needs to apply an energy intensive catalytic process. In contrast, at room temperature MgH_2 can generate hydrogen in absence of a catalyst. However, the hydrolysis of MgH_2, even though it occurs immediately when MgH_2 comes in contact with water, is interrupted by the formation of a passive magnesium hydroxide layer covering the particles. Luckily, the use of aqueous acidic solutions and other “proton-containing compounds” results in a substantial increase of hydrogen yield.

Recent advances in a development of electronic equipment for soldiers at the battlefield witness an increased deployment of night-vision equipment, laptops, and communication devices to GPS and sensors. Due to the fact that these devices must operate autonomously, soldiers typically have to carry up to 17 kg of the batteries to power an individual device [12]. Therefore, necessity of the lightweight, reliable, portable and silent high-energy-density power sources for military use is in increased demand. Portable hydrogen-fueled fuel cells are considered as a prospective solution offering a number of advantages as compared to the battery systems.

The goal of the project G5233 PORTABLE ENERGY SUPPLY is in the development of the effective materials for hydrogen generation. The work is based on utilizing several innovative solutions allowing to enhance the efficiency of hydrogen generation process, to favorably affect the properties of the utilized materials thus providing an efficient solution to the task of the development of the technologies in the field of hydrogen storage and generation systems.

2. Consortium members

This project has been funded by NATO Science for Peace and Security Programme and joined forces of four institutions representing a NATO country – Norway (one participant), and a partner country – Ukraine (three participants). The project consortium included academic partners.

Coordinator: Institute for Energy Technology (IFE, Norway, *https://www.ife.no).*

IFE is an independent foundation and conducts research for a better future. Since its foundation in 1948, IFE has been a frontrunner in international energy research. IFE contributes to new solutions in renewable energy, petroleum and industry-oriented R&D. IFE develops zero-emission transport solutions based on novel batteries and hydrogen as an energy carrier, digital systems and ground-breaking cancer medicine. The Institute strives for a climate friendly energy supply. The annual turnover is approximately NOK 1 billion, with about 600 employees.

Coordinator of the project: Prof. V.A. Yartys (NATO Country Project Director).

Karpenko Physico-Mechanical Institute, NAS of Ukraine (PhMI-NASU, Lviv, Ukraine; *www.ipm.lviv.ua).*

PhMI-NASU was established in 1951 on the basis of the existing academic institutions. Scientific studies of the Institute in the field of fracture mechanics, materials strength and influence of hydrogen on materials properties provide the leading position in the world scientific community. PhMI-NASU is the biggest scientific institution of the Western Ukraine - it has about 400 employees (~180 researchers with PhD or DSci degrees).

Participants of the project: Prof. I. Zavaliy (Partner Country Project Director), Dr. A. Kytsia, young scientists: Dr. V. Berezovets, Dr. Yu. Verbovytskyy, Dr. P. Liutyy, Dr. I. Oshchapovskyy.

Frantsevich Institute for Problems of Materials Science, NAS of Ukraine (IPMS-NASU, Kyiv, Ukraine; *www.ipms.kiev.ua).*

IPMS-NASU was founded in 1952 (before 1964 it was named as the Institute of Metalloceramics and Special Alloys of Ukrainian Academy of Sciences). The institute has been involved in the investigations of high-temperature strength of metallic, nonmetallic and composite materials and development of new materials for high-temperature applications. Development of the theoretical principles and a variety of waste-free technologies to produce materials with predetermined properties is the current emphasis of the institute. IPMS-NASU is the leading institution in the field of materials science in Ukraine, it has 900 employees (~270 researchers with PhD or DSc degrees).

Participants of the project: Prof. Yu. Solonin (Partner Country Project Co-Director), young scientists: Dr. D. Korabliov, Dr. O. Bezdorozhev.

Vernadsky Institute of General and Inorganic Chemistry, NAS of Ukraine (IGIC-NASU, Kyiv), *www.ionc.kar.net***).**

The Institute was founded in 1918, when academician V. Vernadsky, the first President of the Academy of Sciences, set up a chemical laboratory within the Physical-and-Mathematical Department. It was transformed into the Institute of Chemistry in 1929-30. The institute consists of thirteen departments, and it has nearly 350 employees.

Participants of the project: D. Sc. Yu. Pirskyy (Partner Country Project Co-Director), Dr. F. Manilevich, young scientists: A. Kutsyi, T. Panchyshyn.

4. Project organization and communication

The overall management was carried out jointly by NPD, Prof. V. Yartys and PPD, Prof. I. Zavaliy. They defined the long-term project strategy, prepared and controlled the execution of the work plan, reaching the milestones and providing deliverables on time, and arranged regular joint project discussions (a kick-off meeting; an interim workshop, of- and on-line project meetings, the final workshop). Fig.1 shows project co-directors at the workshop 2019 (Lviv-Shepilske,Ukraine).

Fig. 1. Project co-directors at the workshop at Lviv-Shepilske, Ukraine on 6 September, 2019 (from left to right side: Prof’s Yu. Solonin, V. Yartys, Yu. Pirskyy and I. Zavaliy).

All research groups exchanged experimental samples and discussed the results on a monthly basis using E-mail communication, internet (Skype) or telephone calls. The minutes of the meetings and reports were disseminated between the participants of the project by NPD and PPD.

Young Ukrainian scientists from PhMI-NASU (Dr. Berezovets), from IPMS-NASU (Dr. Korablov. Dr. Bezdorozhev) and from IGAC-NASU (Mr. Kutsyj) accomplished training visits to the partner institution – IFE, Norway. They participated in the development of the hydrolysis setup, preparation and testing of the new materials, testing of the hydrogen generation setup integrated with a FC device. They have successfully fulfilled the training programs.

5. Development of the dedicated equipment

According to the project plans, several units of equipment were purchased, and existing labs at the institutes were modernized. Description and photos of the selected equipment are given below (Table 1 and Fig. 2).

Table 1. Purchased materials and equipment.

Institute	Equipment
IFE	A flowmeter "SIERRA-100", Horizon 30W PEM Fuel Cell. Laboratory modernization and equipment installation. Hydrolysis setup Turbopump vacuum station. Retsch planetary mill.
PhMI-NASU	Ball mill "Pulverisette 6 classic line", 30W PEM Fuel Cell Stack, A flow-meter "SIERRA-100", X-ray tube "BSV27-Cu", Computer's software, Vacuum pump and welding device, pH meter ADWA 1020, Magnetic stirrer MS-H280, SNOL resistance furnace, Laboratory scale PS600, Glove Box (individual order).
IPMS-NASU	High Pressure Milling Vial/Gas-Temperature-Monitoring system.
IGIC-NASU	A Potentiostat/Galvanostat model EC301, Power Booster model O200BS.A flow-meter "SIERRA-100", Two Fuel Cell Stacks FCS-B30:H30 (B).

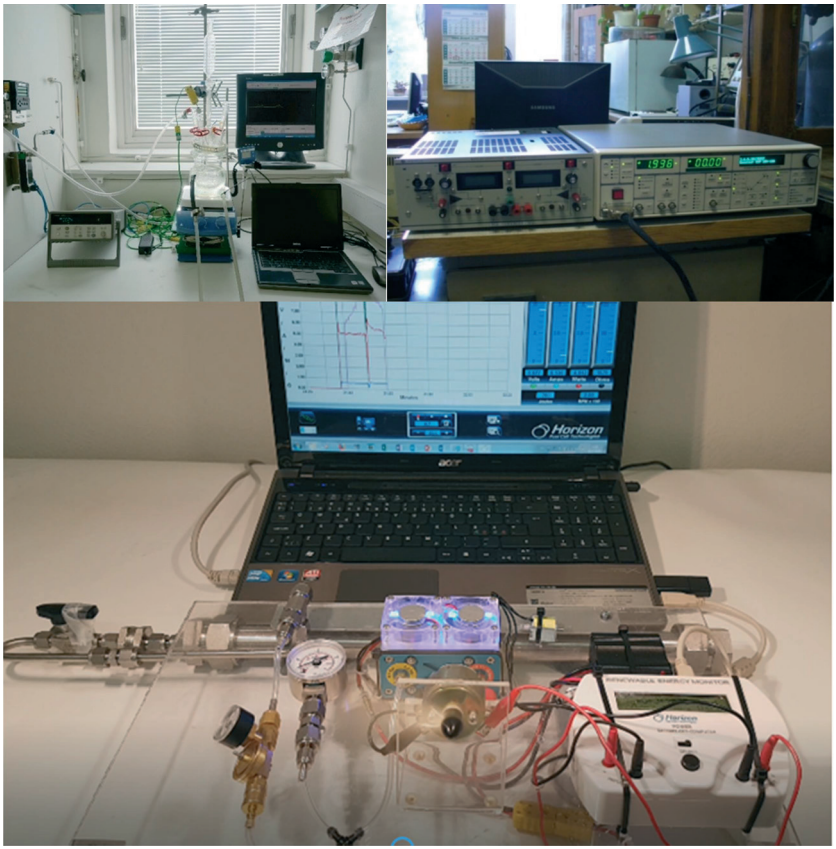

Fig. 2. Equipment for the testing of the materials for hydrolysis and hydrogen storage integrated with a FC unit

6. Results

6.1. Mg-based materials for hydrogen generation by hydrolysis

Materials preparation and characterization. Magnesium and MgAl commercial powders of a specific type: PAM-5, have been chosen as promising materials due to their low density, low cost, and as their components are locally available in Ukraine. They can be easily milled with different additivities (salts, metallic catalysts) as well as easily

hydrogenated to produce nanoscale MgH_2. Pure MgH_2, Mg, MgAl or their composites with different additives were obtained by ball milling in hydrogen atmosphere using Fritsch Pulverisette P6 mill. Hydrogenation reaction studies were conducted for the following systems: MgH_2 + Al, MgH_2 + 5 wt.% $ZrCl_4$, MgH_2 + 5 wt.% $AlCl_3$, MgH_2 + 5 wt.% citric acid, MgH_2 + 5 wt.% EDTA, MgAl + KCl, MgH_2 + *x* $MgCl_2$, MgH_2 + +5 wt.% TiC-2TiB_2. From a practical point of view, the binary MgH_2 + $MgCl_2$ system was concluded to be the most promising. The above-mentioned system was studied in detail.

Hydrolysis reaction studies. The influence of $MgCl_2$ concentration on the kinetics of MgH_2 hydrolysis has been studied in a broad range of $MgCl_2/MgH_2$ relative ratios (between mole ratios of 0/100 and 19/100). Kinetic curves of hydrogen release show that the addition of $MgCl_2$ has a significant positive effect on the extent of MgH_2 conversion, when compared with pure MgH_2 without $MgCl_2$. The hydrolysis kinetics curves show, in each case, an exponentiality and consist of two parts: (a) Initial fast release of hydrogen for approximately 10 minutes, the H_2 generation rate reaching 800 $mL \cdot min^{-1} \cdot g^{-1}$ MgH_2 at maximum; (b) Slow ascending H_2-generation for up to 150 minutes, the amount of hydrogen produced increasing continuously and rates of hydrogen release decreasing. MgH_2 conversion peaked at 89 %. Efficiency should however also account for the overall mass of the system, including the $MgCl_2$. Therefore, in Fig. 3, we present the generation efficiency in terms of the unit of mass of MgH_2 and per 1 g of the "MgH_2 + $MgCl_2$" mixture. It can be concluded from the data in Figure 4*b* that the best "MgH_2 + $MgCl_2$" system performance was achieved at a $MgCl_2/MgH_2$ weight ratio of 12.75/100. This gave hydrogen yield of 1025 $mL(H_2)/g$ per 1 g of the "MgH_2 + $MgCl_2$" system.

The addition of small amounts (17/100 wt. parts) of $MgCl_2$ leads to a factor of ~4 increase in the yield of the hydrolysis reaction, a factor of ~1 decrease in the pH of the working solution and an increase in the hydrolysis product - $Mg(OH)_2$ - precipitate crystallinity. pH of a working solution and conversion of the MgH_2 hydrolysis reaction linearly depend on the logarithm of $MgCl_2$ concentration. pH of the reaction mixture in presence of $MgCl_2$ is well described by considering a system "weak base and its salt with strong acid" type buffer solution. The mechanism of MgH_2 hydrolysis in $MgCl_2$ solutions includes the formation of the buffer

solution that controls the pH of the reaction mixture. This leads to a decreasing supersaturation coefficient for the solution by $Mg(OH)_2$ and corresponding increase in the size of the critical nuclei and crystallinity of the precipitates. This is followed by the formation of an inhomogeneous passivation film on the surface of MgH_2.

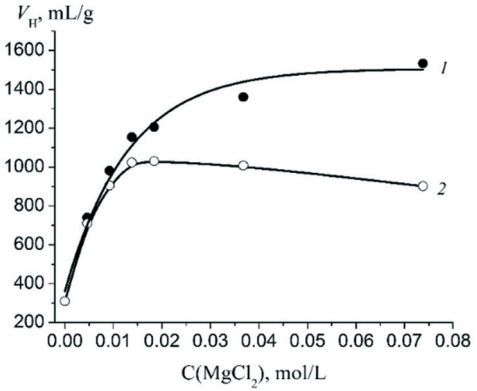

Fig. 3. Dependencies of the volume of H_2 generated per 1 g of MgH_2 and per 1 g of "MgH_2 + $MgCl_2$" system on the $MgCl_2$ weight fraction.

The MgH_2 hydrolysis process involves the hydrolysis reaction, resulting in the generation of hydrogen, and in the formation of $Mg(OH)_2$. It, however, also involves passivation of the MgH_2 surface by the $Mg(OH)_2$ precipitate, followed by its re-passivation. The rate constants for these processes were defined. An increase in $MgCl_2$ concentration leads to just a minor increase in the rate constant for MgH_2 interaction with water. This, however, also leads to a sharp increase in the rate constant of the re-passivation of the MgH_2 surface. Such behavior agrees well with XRD data for the precipitates, which show the formation of a well crystallized $Mg(OH)_2$, causing the formation of an inhomogeneous passivation film on the MgH_2 surface and improved water access to MgH_2.

6.2. Al-based materials for hydrogen generation by hydrolysis

Materials preparation and characterization. Both home lab- prepared using the in-house laboratory facilities and commercial aluminum powders were used. Modifications of Al were performed by using low melting

eutectic Ga-based alloys. The following composite materials were studied for the hydrolysis reaction: Al + Ga-In-Sn (3, 5, 7 or 10 wt.%) at 25, 40, 55, 70 °C, PA-4 + 5 wt.% Ga-In-Sn + 0, 1, 3 wt.% C, PA-4 + 5 wt.% Ga-In-Sn-Zn + 3 wt.% C, ASD-1 + 5 wt.% Ga-In-Sn + 1, 3 wt.% C, ASD-1 + 5 wt.% Ga-In-Sn-Zn + 3 wt.% C at 5 and 25 °C.

Hydrolysis reaction studies. Unoxidized aluminum is one of the most promising metals for hydrogen generation from water by the hydrolysis process because it has a very negative value of the standard electrode potential ($E^0(Al^{3+}/Al^0)$ = –1.662 V) and reacts with water at ambient temperature. Different methods can be used to activate aluminum by removing or cracking the protective oxide layer at its surface. Our studies showed that alloying of aluminum with low-melting (Ga, In, Sn, Zn) and electropositive (Bi, Sb) metals can be used to obtain active aluminum-based alloys that release hydrogen from water in a broad temperature range. Particularly, aluminum doped with 3, 5, 7 or 10 wt.% of the eutectic Ga-In-Sn alloy (68/22/10 wt.%, melting point 10.7 °C) reacts with water at the temperature of 25 °C, and the rate of the process increases for the higher content of ternary eutectic present in the aluminum alloy [13]. Alloying metals however do not participate in the hydrolysis reaction.

Bismuth and antimony, which have close and very positive values of standard electrode potentials ($E^0(Bi^{3+}/Bi^0)$ = 0.20 V, $E^0(Sb^{3+}/Sb^0)$ = 0.24 V) and form the corrosive galvanic couples with aluminum, were used as extra additives (3 wt.%) for the aluminum activated by the Ga-In-Sn eutectic (5 wt.%). We showed that the use of Bi and Sb led to a slowdown in the hydrolysis of activated aluminum, which was particularly considerable when Bi was added (Fig. 4*a*) [14]. However, the alloy of aluminum with Ga-In-Sn eutectic and Bi releases hydrogen from water with a practically constant rate for a long time, what is an important advantage when the hydrogen is used for feeding the fuel cells. On the other hand, the use of zinc as an extra additive (3 wt.%) to aluminum activated by the Ga-In-Sn eutectic led to a significant acceleration of the hydrolysis, particularly at lower temperatures (25 and 5 °C) (see Fig. 4*a*) [15]. Thus, the variation of the qualitative and quantitative compositions of aluminum-based alloys makes it possible to significantly change the rate of aluminum hydrolysis and hydrogen generation.

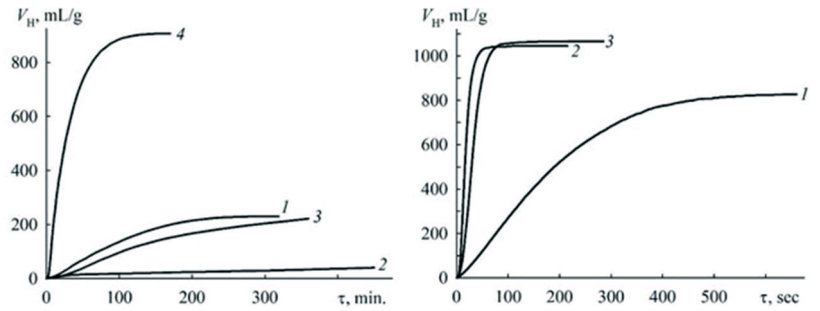

a b

Fig. 4. Time dependencies of the volume of the evolved hydrogen during the hydrolysis of aluminum from: *a* – aluminum alloys with 5 wt.% of eutectic Ga-In-Sn alloy (*1*) and 3 wt.% of Bi (*2*) or Sb (*3*) or Zn (*4*) at 25 °C; *b* – pellets from PA-4 powder activated by Ga–In–Sn eutectic (5 wt.%) (*1*) and graphite (3 wt.%) (*2, 3*) at 25 °C (*1, 2*) and 5 °C (*3*).

It is obvious that the high rate of hydrogen generation can be increased by using activated aluminum powders with a large surface area because the hydrolysis is a heterogeneous reaction. We used the aluminum powders PA-1 (grain size ≤ 100 μm) and ASD-1 (grain size <30 μm), which were mechanochemically activated by the Ga-In-Sn or Ga-In-Sn-Zn eutectic alloys (5 wt.%) and graphite (1 - 3 wt.%). Mechanochemical activation was carried out in the SPEX SamplePrep 8000D® Mixer/Mill in an argon atmosphere. Then the activated powders were compressed into the pellets with a mass of 0.2-0.3 g. It was shown that the use of graphite as an extra additive to the activated aluminum powders led to an increase in the rate of aluminum hydrolysis for more than an order of magnitude, and it easily proceeds at temperatures exceeding 5 °C (see Fig. 4*b*). The rate of hydrogen generation and its yield significantly increase with increasing graphite content in the pellets and duration of the mechanochemical treatment of the powders, as well as with decreasing the grain size of the aluminum powders and increasing the hydrolysis temperature [16].

6.3. Hydrogen generation by hydrolysis of $NaBH_4$

Materials preparation and characterization. Commercial $NaBH_4$ and NaOH were used for the hydrolysis reaction. A series of catalysts to enhance the hydrogen generation rate was prepared by chemical reduction processes. The catalysts were used in as-prepared form or when deposited on the supports (synthetic zeolite or cordierite). Single Co, Ni, Pt, and binary Co-B, Ni-B, (CoNi)-B, Ni-Cu, Ni-Ag catalysts systems were used. Effects of temperature and concentration of $NaBH_4$ and NaOH were studied to optimize the hydrolysis reaction.

Hydrolysis reaction studies. The Ni and Co powders and borides of these elements possess high catalytic activity in the reaction of $NaBH_4$ hydrolysis: $NaBH_4 + 2H_2O \rightarrow NaBO_2 + 4H_2$. We have studied the catalytic activity of the freshly prepared Ni and Co (marked as Ni-A and Co-A). To prevent a possible oxidation of Ni and Co borides, Ni-A and Co-A were synthesized in situ in the reaction mixture used for the hydrolysis experiment (concentration of $NaBH_4$ varied between 0.25…1 mol/L and pH was 12) via a reaction: $2M^{2+} + 4NaBH_4 + 9H_2O \rightarrow 4Na^{+} + M_2B + B(OH)_3 + 12.5H_2$. Concentrations of Ni^{2+} and Co^{2+} varied from 0.017 to 0.067 mol/L which corresponds to 1 and 4 mg/mL of the formed catalysts, respectively. We found that (a) the kinetic curves of H_2 evolution are characterized by a presence of a prolonged near-linear section extending to the completion of the reaction which is very attractive for the practical utilization of such systems (Fig. 5); (b) Co-A is a more active catalyst as compared to Ni-A and the values of the specific rate of hydrogen evolution (the rates of hydrogen evolution per 1 g of $NaBH_4$) are equal to 26 and 54 mL/min for Ni-A and Co-A, respectively.

Synthesized zeolite supported samples (Ni-Z and Co-Z) were tested as catalysts of the hydrolysis of $NaBH_4$. It was found that both granulated and milled samples accelerate the hydrolysis reaction.

We have also studied the catalytic activity of zeolite-supported catalysts (Ni-Z and Co-Z). It was found that both granulated and milled samples accelerate the hydrolysis reaction.

A series of hydrolysis experiments was conducted by using two types of the reactors with an aqueous solutions of sodium borohydride and platinum-based catalysts.

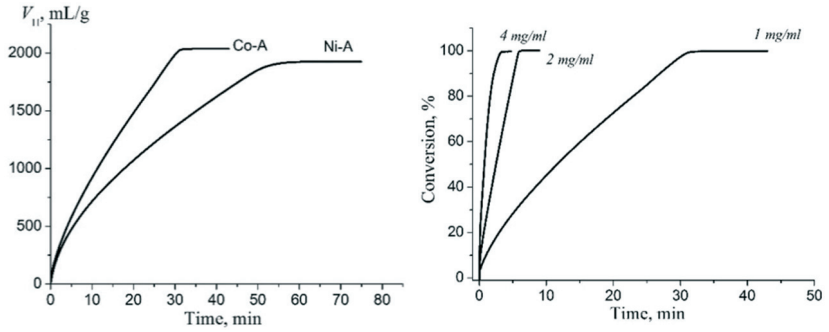

a b

Fig. 5. Dependencies of the volume of H_2 generated per 1 g of $NaBH_4$ as related to the type of the catalyst (*a*) and a conversion extent of $NaBH_4$ hydrolysis on the Co-A concentration (*b*).

The catalyst used in a flat reactor consisted of a nanodispersed platinum deposited on carbon black (XC-72), which, in turn, was immobilized on the surface of carbon cloth (1-2 mg/cm^2). The measured rate of hydrogen evolution in such a reactor at 24 °C was directly proportional to the solution pumping speed and reached 400 mL/min at a circulation rate of sodium borohydride solution of 7.8 mL/min, which is sufficient to provide a stable 30 W power of the hydrogen-oxygen FC with hydrogen used as a fuel. The progression of decomposition of sodium borohydride slows down with increasing rate of pumping the solution through the generator (see Fig. 6*a*).

For a cylindrical reactor, platinum catalysts were prepared by their deposition on various substrates. The regularities of hydrogen evolution in such a reactor are shown in Fig. 6*b*. It can be seen that platinized titanium is less active than the catalyst obtained by the polyol method. During the formation of a roll from the carbon cloth with applied platinum catalyst, the latter peeled off. That is why its activity was lower than in the flat reactor. From the reference data and from our experiments, it follows that it is promising to use a synthetic honeycomb cordierite as a substrate for platinum catalyst. Its use will allow creating a stable and highly efficient reactor for the decomposition of sodium borohydride solution.

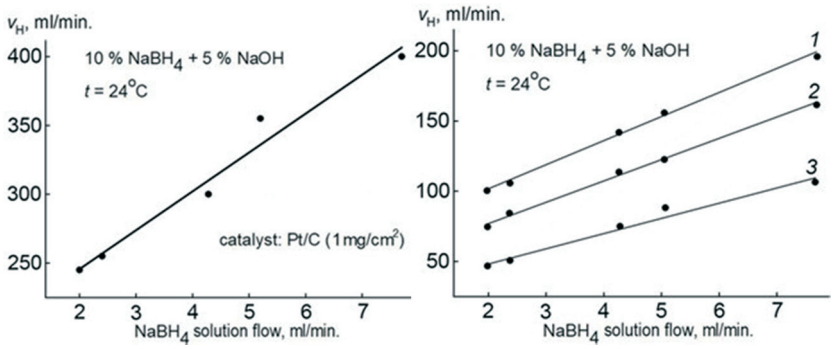

Fig. 6. Dependencies of the hydrogen evolution rate on the $NaBH_4$ solution flow rate: *a* – in the flat reactor (catalyst - 13 mg Pt/C on carbon cloth), *b* - in the cylindrical reactor (catalysts: *1* - 100 mg Pt/C on carbon cloth, *2* – 150 mg Pt on 2 g of active carbon (AG-3), *3* – 70 mg Pt on 5g of porous titanium).

6.4. Tests of a pilot hydrogen energy device

Apparatus and installation. Scheme of the fuel cell based hydrogen energy system consisting of a fuel cell stack and hydrogen generator is shown in Fig. 8. The setup for the monitoring of hydrogen generation efficiency during sodium borohydride hydrolysis when using released and supplied to the fuel cell hydrogen includes: a tank with a catalyst (hydrolysis reactor), electronic system for optimizing the performance; peristaltic pump; dc-dc converter; Li-ion battery pack; super-capacitor and a fuel cell connected to the hydrolysis reactor and control system.

Setup testing and technology verification. To ensure a stable operation of a fuel cell and reaching its required performance parameters, the following measures should be adopted: (1) Define the procedures for the system start-up; (2) Ensure start and termination of the operation; (3) Achieve stabilization of the output voltage and control over the hydrogen flow depending on the load (from idle to full power); (4) Monitor the performance parameters during the operation, perform data transfer using computerized recording and data analysis. H-30 Fuel Cell Stack was used as a FC. Output voltage and current depend on a hydrogen supply rate,

while the other parameters can considerably vary. The payload is required to keep the voltage stable (12 V), and when the current (i.e., output power) changes, to control the fuel cell, hydrogen flow, and the water pump. For this purpose, a dedicated electronic system has being developed, which consists of a converter-stabilizer of the FC voltage, a battery, a supercapacitor, switches SW1-SW3 and a microcontroller.

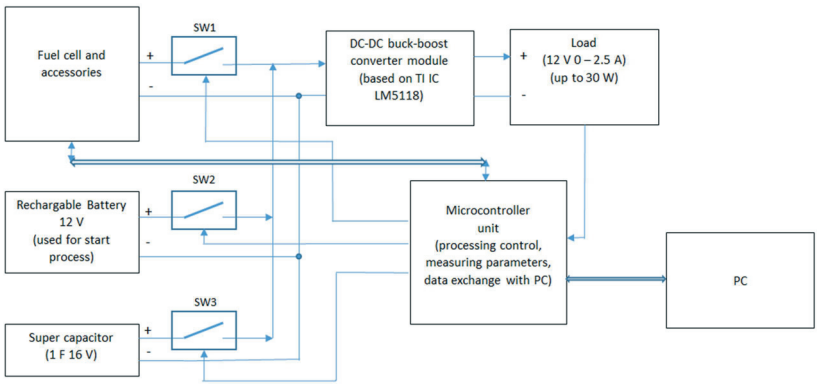

Fig. 7. Scheme of the fuel cell system consisting of a fuel cell stack and hydrogen generator.

The main function of the voltage stabilization is achieved by using a so-called buck-boost converter, which allows to keep a constant output voltage while the input can vary in a broad range (from lower than the output to higher than the output values) while providing a sufficiently high conversion efficiency. A module based on a commercial chip from a renowned supplier was used, which provides an output voltage of 12 V when changing the input from 5 to 16 V.

For initial start-up procedures it is necessary to have an external power supply – a 12 V battery is suitable. When entering the operating mode, the output voltage of the fuel cell may change, and the voltage instabilities are possible. To smoothen them, we use a super-capacitor (SC), which has certain advantages over the battery. The SC is capable of two or three orders of magnitude higher number of the charge-discharge cycles, with a smaller internal resistance as compared to a battery and,

because of that a better stabilization efficiency is expected. For switching on-off the current as related to the voltage, the switches SW1-SW3 will be utilized, and the latter will be controlled by a microcontroller (MOSFET or diode, the best options EWMOVW will be selected).

The function of the overall control over the system, measurements of the current and voltage parameters will be performed by an electronic circuit based on a microcontroller (EFM8LB12F64 from Silicon Labs with a rather wide analog peripheral). It will also transfer the measurements data via USB port to a computer to analyze the system performance. The pilot device is shown in Fig. 8.

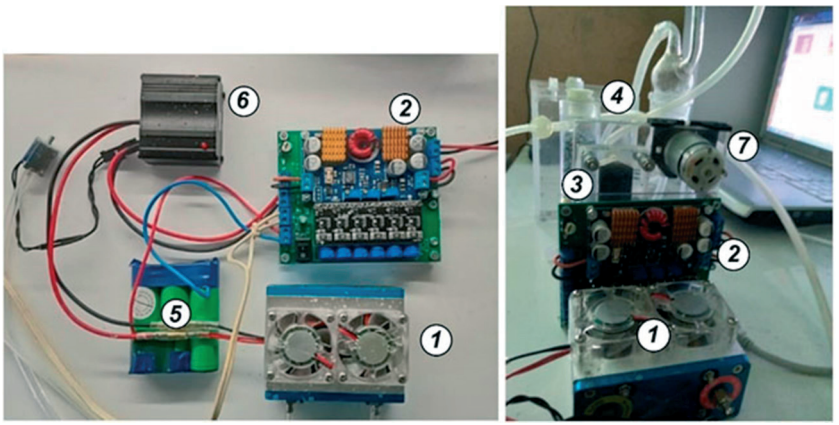

Fig. 8. The pilot device “H_2 generator – Fuel Cell”: 1 - Fuel Cell 30 W Horizon, 2 - voltage stabilizer and device control system, 3 - reactor, 4 - tank for a borohydride solution, 5 - Li-ion battery, 6 - fuel cell control unit, 7 - water pump RS385-635.

Conclusions

1. Portable power supply unit was built by using commercially available components together with parts constructed and manufactured in-house. Different types of hydrolysis reactors and catalytic systems were tested and obtained results show a feasibility of the proposed technology in achieving the goals of the project. We found that PtNPs immobilized on cordierite of honeycomb structure when applied in a cylindrical flow reactor provide

sufficient flow of hydrogen gas used as a fuel to achieve operation of a 30 W stack of fuel cells for 9-10 hours with the weight of the portable setup not exceeding 7 kg. Hydrogen is generated by the hydrolysis of 1.1 L of the $NaBH_4$ solution.

2. Hydrolysis is an expedient and convenient method for hydrogen generation, which allows to conveniently obtain the required amounts of H_2 with controlled rate. Studied in the project catalyzed aluminum powders, magnesium hydride, and sodium borohydride are all efficient materials for hydrogen generation from water for portable power supply.

3. The optimal conditions for the hydrolysis for aluminum are in use of its catalyzed by additives powders. MgH_2 is best hydrolyzed in the solutions of magnesium chloride providing hydrogen generation rate of 80 mL/min per 1 g of MgH_2. For the efficient hydrolysis of sodium borohydride the choice and efficiency of the catalyst is a decisive factor. Due to a low cost combined with the high efficiency (providing the rate of H_2 evolution up to 6000 mL/min per 1g of $NaBH_4$) and reliability, cobalt-based catalysts are considered particularly promising.

4. The work resulted in a publication of 7 papers in the peer-reviewed scientific journals and in 15 conference presentations.

Acknowledgment

This work was supported by the NATO Programme "Science for Peace and Security" (Project G5233 "Portable Energy Supply").

References

[1] Sakintuna B., Lamari-Darkrim F., Hirscher M. Metal hydride materials for solid hydrogen storage: A review. *Int. J. Hydrogen Energy*, 2007, vol.32, pp. 1121-1140.

[2] Huot J., Ravnsbæk D.B., Zhang J., *et al*. Mechanochemical synthesis of hydrogen storage materials*, Prog. Mater. Sci.*, 2013, vol.58, pp.30–75.

[3] Ross D.K. Hydrogen storage: The major technological barrier to the development of hydrogen fuel cell cars, *Vacuum*, 2006, vol.80, pp. 1084-1089.

[4] Gandía Luis M., Arzamendi Gurutze, Diéguez Pedro M. (Eds.). Renewable Hydrogen Technologies. Production, Purification, Storage, Applications and Safety, Elsevier, Amsterdam, 2013, 472 pp.

[5] Yartys V. A., Lototsky M. V. An overview of hydrogen storage methods, *Hydrogen Mat. Sci. Chem. of Carbon Nanomat. (Proceed. ICHMS'2003),* 2004, pp. 75-104.
[6] Jain I.P., Jain P., Jain A. Novel hydrogen storage materials: A review of lightweight complex hydrides, *J. Alloys Compd.,* 2010, vol. 503, pp. 303-339.
[7] Ley M.B., Jepsen L.H., Lee Y.-S. *et al*. Complex hydrides for hydrogen storage – new perspectives, *Mat. Today*, 2014, vol.17, pp. 122-128.
[8] Rango P., Marty P., Fruchart D. Hydrogen storage systems based on magnesium hydride: from laboratory tests to fuel cell integration, *Appl. Phys. A*, 2016, vol.122, 126 (1-20 pp.).
[9] Wang H.Z., Leung D.Y.C., Leung M.K.H., Ni M. A review on hydrogen production using aluminum and aluminum alloys, *Renew. Sustain. Energy Reviews,* 2009, vol.13, pp. 845-853.
[10] Grosjean M.-H., Zidoune M., Roué L., Huot J.-Y. Hydrogen production via hydrolysis reaction from ball-milled Mg-based materials, *Int. J. Hydrogen Energy*, 2006, vol.31, pp. 109-119.
[11] Ouyang L., Ma M., Huang M. *et.al*. Enhanced Hydrogen Generation Properties of MgH_2-Based Hydrides by Breaking the Magnesium Hydroxide Passivation Layer, *Energies*, 2015, vol.8, pp. 4237-4252.
[12] Lewis N.S., Abarbanel H., Bildsten L., et al. JASON report JSR-02-135, The MITRE Corp., McLean, Virginia, June, 2003.
[13] Manilevich F.D., Kozin L.Kh., Danil'tsev B.I., Kutsyi A.V., Pirskyy Yu. K. Regularities of the hydrolysis of aluminum activated with the eutectic alloy of gallium, indium, and tin. *Ukr. Khim. Zh.,* 2017, vol. 83, pp. 51-59.
[14] Manilevich F.D., Pirskyy Yu.K., Kutsyi A.V., Danil'tsev B.I. Regularities of hydrolysis of aluminum activated by Ga-In-Sn eutectic alloy and zinc. *Ukr. Khim. Zh.,* 2020, vol. 86, pp. 63-77.
[15] Manilevich F.D., Pirskyy Yu.K., Danil'tsev B.I., Kutsyi A.V., and Yartys V.A. Studies of the hydrolysis of aluminum activated by additions of Ga–In–Sn eutectic alloy, bismuth or antimony. *Mater. Sci*., 2020, vol. 55, pp. 536–547.
[16] Manilevich F.D., Pirskyy Yu.K., Kutsyi A.V., Berezovets V.V., Yartys V.A. Studies of mechanochemically activated aluminum powders for hydrogen generation from water. *Powder Metallurgy*, 2021, No. 5/6. pp. 14-24.

List of project publications

Journal articles:

1. F.D. Manilevich, Yu.K Pirskyy, B.I. Danil'tsev, A. Kutsyi, V.A.Yartys. Studies of the Hydrolysis of Aluminum Activated by Additions of Ga–In–Sn Eutectic Alloy, Bismuth, or Antimony. *Materials Science,* 2020, vol. 55 , pp. 536–547.
https://doi.org/10.1007/s11003-020-00336-x

2. Yu.V. Verbovytskyy, V.V. Berezovets, A.R. Kytsya, I.Yu. Zavaliy, V.A. Yartys. Hydrogen generation by hydrolysis of MgH_2. *Materials Science,* 2020, vol. 56, pp. 1–14. *https://doi.org/10.1007/s11003-020-00390-5*

3. D.S. Korablov, O.V. Bezdorozhev, S. Gierlotka, V.A. Yartys, Yu.M. Solonin. Effect of various additives on the hydrolysis performance of nanostructured MgH_2 synthesized by high-energy ball milling in hydrogen. *Powder Metallurgy*. 2020. № 9/10. pp. 3–12.

4. F.D. Manilevich, Yu.K. Pirskyy, A.V. Kutsyi, V.V. Berezovets, V.A. Yartys Studies of mechanochemically activated aluminum powders for hydrogen generation from water. *Powder Metallurgy*, 2021, No. 5/6. pp. 14-24.

5. A.Kytsya, V.Berezovets, Yu.Verbovytskyy, L. Bazylyak, I. Zavaliy, V. Yartys'. Zeolite Supported Ni and Co Catalysts for Hydrogen Generation via Hydrolysis of $NaBH_4$. *Proc. of the Intern Conf. "Nanomaterials: application and properties"* (NAP-2021), 5-11 Sept., Odesa - Ukraine), pp. 1–4, http://doi.org/10.1109/NAP51885.2021.9568617

6. V. Berezovets, A. Kytsya, I. Zavaliy, V. Yartys. Kinetics and mechanism of hydrolysis of MgH_2 in $MgCl_2$ solutions. *Int. J. Hydrogen Energy*, 2021, vol. 46, pp. 40278-40293.
http//doi.org/10.1016/j.ijhydene.2021.09.249.

7. A. Kytsya, V. Berezovets, Yu.Verbovytskyy, L. Bazylyak, V. Kordan, I. Zavaliy, V. Yartys. Hydrogen generation by hydrolysis of sodium borohydride catalyzed by bimetallic Ni-Co nanoparticles. *J. Alloys and Comp.*, 2021, *in preparation.*

Selected Conference presentations and public lectures:

1. V. Berezovets, Yu. Verbovytskyy, I. Zavaliy, D. Korablov, Yu. Solonin, R. Denys, F. Manilevich, A. Kutsyi, V. Yartys. Mg and Al based hydrides for the efficient hydrogen generation by hydrolysis process. Col. Abstr. of Int. Symp. on Metal-Hydrogen Systems: Fundamentals and Applications. MH-2018, October 28-November 2, 2018 – Guangzhou (China), 2018, p.286.
2. V. Berezovets, Yu. Verbovytskyy, D. Korablov, Yu. Solonin, I. Zavaliy, V. Yartys. Mg-based hydrides as a source of hydrogen for autonomous energy devices. Proceedings of the XX International Scientific Conference on Renewable Energy and Energy Efficiency in the 21st Century, May 15-16, 2019, Kyiv, Ukraine, 2019, pp.198-201.
4. V. Berezovets, Yu. Verbovytskyy, I. Zavaliy, V. Yartys. Mg-based materials for application hydrogen supply systems. 6th Intern. conf. «HighMathTech–2019», 28–30 October, 2019, Kyiv, Ukraine, p.143.
5. A.Kytsya, V. Berezovets, Yu. Verbovytskyy, I. Zavaliy, V. Yartys Modeling of kinetics of MgH_2 hydrolysis. XVII Scient. Conf. « Lviv Chemical Readings-2019», 02–05 June, 2019, Lviv, Ukraine, - M3.
6. V. Berezovets, I. Zavaliy, O. Pavlovska, L. Vasylechko, Yu. Kosarchyn. Composites of magnesium hydride with catalytic nanoadditives. Intern. research and practice conference «Nanotechnology and nanomaterials (Nano-2019)», August 27-30, – 2019, Lviv, Ukraine. p.208.
7. F. Manilevich, Yu. Pirskyy, B. Danil’tsev, A. Kutsyi. Activation of aluminum by doping with low-melting metals and regularities of its hydrolysis. Proc. of Ukrainian Conf. with International Participation "Chemistry, Physics and Technology of Surface" and Workshop “Metal-based biocompatible nanoparticles: synthesis and applications”. – Kyiv, 2019, p. 116.
8. Yu. Pirskyy, F. Manilevich, T. Panchyshyn, Ya Kolosovskiy. Bifunctional iridium electrocatalysts for modifying surface of fuel cell proton-conducting membranes. Proc. of Ukrainian Conf. with International Participation "Chemistry, Physics and Technology of Surface" and Workshop “Metal-based biocompatible nanoparticles: synthesis and applications”. – Kyiv, 2019, p. 144.

9. A. Kutsyi, F. Manilevich, B. Danil’tsev, Yu. Pirskyy. Effect of magnesium additions on hydrogen generation in the hydrolysis of aluminum activated with Ga-In-Sn alloy. Proc. of XVI Intern. Conf.“Hydrogen Materials Science and Chemistry of Carbon Nanomaterials”. – Kiev, 2019, pp. 28-29.
10. D.S. Korablov, O.V. Bezdorozhev, Yu.M. Solonin. Nanostructured materials based on refractory compounds for hydrogen energy technologies, Abstract book of 7th International conference “Nanotechnology and Nanomaterials” (NANO-2019) 27 - 30 August 2019, Lviv, Ukraine, p.173.
11. D.S. Korablov, O.V. Bezdorozhev, Yu.M. Solonin. Effect of 2D titanium carbide (MXene) on hydrogen storage properties of magnesium, Abstract book of VI conference NANSYS-2019, 4-6 December 2019, Kyiv, Ukraine, 78.
12. A. Kytsya, V. Berezovets, L. Bazylyak, Yu. Verbovytskyy, O. Kos Ni-based nanopowders as catalysts of $NaBH_4$ hydrolysis . Book of abstracts Ist International research and practice conference «Nanoobjects & Nanostructuring» (N&N–2020) September 20–23, 2020, Lviv, Ukraine.
13. F.D. Manilevich, Yu.K. Pirskyy, A.V. Kutsyi, V.V. Bereszovets. Mechanical activation of the surface of aluminium powders and regularities of their hydrolysis. Proceedings of Ukrainian Conference with International participation “Chemistry, Physics and Technology of Surface” dedicated to the 90th birthday of Aleksey Chuiko, Academician of NAS of Ukraine. 21-23 October 2020. – Kyiv, 2020, p. 117, poster
14. A. Kutsyi, F. Manilevich, Yu. Pirskyy, T. Panchyshyn. Obtaining hydrogen by hydrolysis of sodium borohydride to power fuel cells. IV Ukrainian scientific conference "Actual problems of chemistry: research and prospects". (Zhytomyr, April 29, 2020). - Proceedings of the conference,pp. 145-147.
15. F. Manilevich, Yu. Pirskyy, A. Kutsyi, B. Danil’tsev. Influence of zinc on hydrolysis of aluminum activated by Ga-In-Sn eutectic alloy. Proceedings of XXI International Scientific-Practical Conference "Renewable Energy and Energy Efficiency in the XXI Century". (Kyiv, May 14-15, 2020),pp. 239-242.

Hydrolysis of MgH_2 in $MgCl_2$ solutions as an effective way for hydrogen generation

V. Berezovets[1], A. Kytsya[1], Yu. Verbovytskyy[1], I. Zavaliy[1], V. Yartys[2]

[1]*Karpenko Physico-Mechanical Institute, NASU, Lviv, Ukraine*
[2]*Institute for Energy Technology, Kjeller, Norway*

Magnesium hydride (MgH_2) has a high hydrogen storage capacity (7.6 wt%) and the Mg element is abundant on the earth. Due to its strong reduction ability, even at room temperature it can provide the hydrogen yield reaching 15.2 wt% H (1703 mL/g) when interacting with water, which makes it very attractive for the application in supplying hydrogen for autonomous H energy systems. However, the hydrolysis reaction is rapidly inhibited by the $Mg(OH)_2$ passivation layer formed on the surface of MgH_2. In order to remove the passivation film and improve the efficiency of the MgH_2 hydrolysis process, several methods including alloying, ball milling, changing the aqueous solution, have been successfully utilized.

In this paper the process of hydrolysis of magnesium hydride in aqueous solutions of $MgCl_2$ used as a promotor of the interaction has been studied in detail. It was found that the initial hydrolysis rate, pH of the reaction mixture, and overall reaction yield are all linearly dependent of the logarithm of $MgCl_2$ concentration. It has been shown that pH of the reaction mixture in the presence of $MgCl_2$ is well described by considering a system "weak base and its salt with strong acid" type buffer solution. Reference data for this hydrolysis reaction were also carefully analyzed.

The mechanism and the kinetic model of the process of MgH_2 hydrolysis in water solutions involved passivation of the MgH_2 surface by the formed $Mg(OH)_2$ precipitate followed by its repassivation have been proposed. The obtained after the hydrolysis reactions precipitates were studied using XRD and EDS. It was found also that the final products of reaction consist of $Mg(OH)_2$ (brucsite type) and remaining MgH_2. This fact shows that the formation of solid species such as $MgCl_2 \cdot xMgO \cdot yH_2O$ at the studied conditions is unlikely and decreasing of pH the reaction mixture has a different nature.

Keywords: *Hydrolysis; Magnesium hydride; Magnesium chloride; Kinetics; Acid-base equilibrium*

Introduction

Magnesium hydride (MgH_2) has been widely investigated as a promising candidate for hydrogen generation by a hydrolysis process due to the low cost and high abundance of magnesium. MgH_2 has a high theoretical hydrogen storage capacity (7.6 wt. %) and due to its strong reducibility, even at room temperature the hydrogen yield can reach 15.2 wt. % H (1703 mL/g) when it reacts with water. The most critical issue is that hydrolysis reaction of MgH_2 can be rapidly interrupted by the formation of a $Mg(OH)_2$ passivation layer surrounding the MgH_2 particles. To address this challenge, several methods have been proposed, e.g. ball-milling, addition of catalysts, surface modification, element substitution, changing the aqueous solution, and a combined approach.

The ball-milling method can effectively increase the reaction rate and yield of hydrogen gas. This phenomenon could be ascribed to the fact that the ball milling process refines the particle and grain sizes and increases the specific surface area. In addition, the introduction of structural defects and formation of nanocrystalline structures are also beneficial for the MgH_2 hydrolysis [1]. According to [2], the highest reactivity is observed for 30 min milled MgH_2, which shows a conversion yield of 26 % as compared to 9 % for the unmilled MgH_2 powder. The specific surface area of 30 min milled powder displays a maximum of 12.2 m^2/g. Further milling reduces the specific surface area due to the particle's agglomeration. The specific surface area of 7.8 m^2/g and conversion yield of 16 % were observed for the 10 h milled MgH_2 powder. From extrapolation of the fitting curve of conversion yield of MgH_2 powders vs their specific surface area, a yield of 100 % might be reached for MgH_2 powder having a surface area of 23 m^2/g [3].

At room temperature the acids provide a remarkable increase of the MgH_2 conversion during the hydrolysis reaction. Significant amounts of hydrogen can be obtained using inorganic acids [4], organic acids, for example, acetic acid with a platinum catalyst [5], or when heating the reaction mixtures [6] in laboratory experiments. However, a commercial application of acids appears to meet the drawbacks being both expensive and not practically viable due to a significant corrosion of the reactor interior in acidic solutions. Thus, a considerable attention is

recently focused on the studies of the effect of citric acid on the reaction with magnesium hydride [7, 8].It should be noted that in a dilute citric acid solution beside the hydrolysis reaction, a direct interaction between MgH_2 and $C_6H_8O_7$ or the formation of a salt due to a reaction of the acid with magnesium hydroxide occur.

The studies of the salt additives effects on the hydrolysis kinetics of magnesium hydride were performed as related to the content of the additives. In particular, the following solutions of salts [2, 3, 9] or acidic salts and MgH_2 [9, 10] and MgH_2/salt composites [11–13] were hydrolysed using distilled/tap/sea water. The mechanism of MgH_2 hydrolysis directly depends on the pH of the formed solution. Hydrolysis of MgH_2 with acidic salt solutions gives a maximum conversion and shows a high hydrogen release rate. Increase of the salt content (but to a certain limiting value) in solution or composite leads to the increase of hydrogen yield.

The influence of the composition of the selected ammonium salts and their concentration in aqueous solutions on the hydrolysis of magnesium hydride were studied in [9, 14]. The presence of even a small amount of NH_4Cl (0.5% solution) considerably promotes the hydrolysis: the amount of hydrogen released in 5 min exceeds the amount of hydrogen released within 24 h during the hydrolysis process in a pure water (60 and 57%, respectively). As the concentration of ammonium chloride increases from 0.5 to 7.5%, the hydrolysis rate increases and the conversion in the latter case becomes significantly higher (92 % in 5 min).

The influence of the nature of the cations contained in the chloride salts and the amount of the salts were studied in [13]. The composites MgH_2/NaCl, MgH_2/$MgCl_2$, and MgH_2/NH_4Cl were prepared with 3; 5 and 10 % salt and MgH_2 synthesized by a combustion synthesis. Hydrogen yield increased with increasing the salt content in the sequence NaCl – $MgCl_2$ – NH_4Cl. The NH_4Cl has the strongest effect on the kinetics of the hydrolysis process as compared to two other chlorides. At room temperature, MgH_2−10% NH_4Cl composite exhibited the best performance with the hydrogen generation yield of 1311 mL/g and a conversion rate of 85.69 % in 60 min.

The hydrolysis reaction of MgH_2 in aqueous solution of magnesium chloride was studied in [14, 15]. It can be noticed that in the

presence of $MgCl_2$ the hydrogen yield is higher than that for pure water. According to [14, 15], the hydrogen yield was 1635 ml/g and 1137 ml/g in 0.5 M $MgCl_2$ and in 0.05 M $MgCl_2$ after 50 and 90 min, respectively. However, the effect of chlorine ions on the process of crystallization of magnesium hydroxide at the surface of MgH_2 is not completely understood even though it clearly affects the extent of the hydrolysis.

The effect of the nature of the cations on the hydrolysis of MgH_2/salt composites was studied in more detail in [12], where several chlorides including NaCl, $ZnCl_2$, $AlCl_3$, $ScCl_3$, $FeCl_3$, $TiCl_3$, $MgCl_2$, and $ZrCl_4$ were used. The effect of the anions was studied by replacing the chlorides with bromides using the salts of sodium, magnesium, and zirconium. Hydrogen yield (86% and 99% after 1 h by using $MgBr_2$ and $ZrBr_4$ as additives) was not significantly different between the two salts, but the bromides showed a faster reaction kinetics. Furthermore, it should be noted that zirconium bromide acts as the best activator of the hydrolysis reaction among all tested salts.

An increase in the rates of hydrolysis reaction is observed when using the mixtures or composites of MgH_2 with different additives. When using the milled mixture MgH_2-20.3 mol % CaH_2, the reaction yield reaches 80 % after 30 min of hydrolysis [16]. The 1 h ball-milled $Mg_{17}Al_{12}$ + 10 wt. % CaH_2 mixture produced 1389 mL H_2/g at 70 ºC after 1 h of hydrolysis in pure water (hydrogen yield was 94.8%) [17]. The MgH_2/LaH_3 composites with the atomic ratio of 3:1 and 8.5:1 can generate 706.7 mL/g of H_2 in 40 min and 473.0 mL/g of H_2 in 60 min, respectively [14]. The highest observed hydrolysis yield equals to 1195 mL/g of H_2 in 80 min and belongs to the composite with the optimal mole ratio of 5:1. The MgH_2/LaH_3/Ni composite obtained by hydrogenation of La_2Mg_{17}/Ni during the milling at a pressure of 7 MPa H_2 showed the best results [18]. It released 1208 L/g of hydrogen during 40 min at room temperature and showed reduced activation energy of the hydrolysis process of 52.9 kJ/mol. The air-stable $MgH_2/LiNH_2$ composites were another system investigated in the hydrolysis reaction in [19]. The composition $4MgH_2$-$LiNH_2$ milled for 5 h generates 887.2 mL/g of hydrogen in just one minute and 1016 mL/g of hydrogen in the next 50 min. The $LiOH{\cdot}H_2O$ and NH_4OH phases which are formed as hydrolysis products during the interaction of $LiNH_2$

with water may prevent formation of the passivation layer of $Mg(OH)_2$ at the surface and supply enough channels for MgH_2 hydrolysis.

An increase of the hydrolysis temperature, as expected, leads to an increase in both reaction rates and hydrogen yields [8, 18–22]. Evaluation of the apparent activation energy of the hydrolysis reactions calculated using the Arrhenius equation and based on the analysis of the kinetic curves of hydrogen generation at different temperatures showed that different additives were able to significantly decrease the activation energy.

Importantly, magnesium chloride may be considered as a perspective material to improve the efficiency of the hydrolysis of magnesium hydride as it is an ecofriendly material, has an affordable price and a low molecular mass (this defines overall hydrogen generation efficiency of the mixtures MgH_2+$MgCl_2$). Unfortunately, the mechanisms of chemical interactions in the systems MgH_2–MCl_n–H_2O in general and in the system MgH_2–$MgCl_2$–H_2O in particular, are studied insufficiently. One can however assume that facilitation of the hydrolysis of magnesium hydride in the presence of metal chlorides is caused by their hydrolysis resulting in the formation of hydrochloric acid. Nevertheless, many aspects relevant for describing the catalytic or promoting behaviors of the metal chlorides remain unclear, including the fact that typically used amounts of metal chlorides are significantly smaller as compared to the amount of magnesium hydride involved into the process. Thus, the amount of hydrochloric acid formed via the hydrolysis of chloride is insufficient to allow a complete conversion of MgH_2.

Thus, in presented work we studied the dependence of the kinetics of H_2 evolution via the hydrolysis of constant masses of MgH_2 on the concentration of constant volumes of solutions of $MgCl_2$ with the aim to eliminate the impact of the process of dissolution of dry magnesium chloride on the chemical equilibria.

Experimental Details

MgH_2 was prepared by a reactive ball milling of magnesium (Fluka, grit, 50-150 mesh, 99.8%) in hydrogen gas using a planetary ball mill Fritsch Pulverisette-6. Milling was carried out in a custom-made SS vial with a volume of 550 mL. The vial was equipped with two Swagelok

needle valves for hydrogen inlet and outlet. As grinding bodies, the stainless steel balls (50 with a diameter of 16 mm; m_{balls}=817 g) were used. The weight ratio of the grinding bodies to the weight of the sample was 40:1. The grinding was performed at a rotational speed of 400 rpm and an initial hydrogen pressure of 2.5 MPa.

Kinetics of MgH_2 hydrolysis was investigated at 20^o C in pseudo-isothermal conditions in a setup consisting of a two-neck glass vessel immersed into a water bath equipped with a magnetic stirrer and injectors of the solutions of $MgCl_2$ and citric acid. Typically, 0.2 g of MgH_2 was introduced into the reactor. After that, 20 mL of an aqueous solution prepared using deionized water (pH=7.00) was quickly added. The generated hydrogen was released through Allihn-type fluid-cooled condenser connected to a bottle filled with water at room temperature. Then, H_2 was collected by replacing the water in a beaker. To evaluate an extent of the MgH_2 conversion, the solution of citric acid (2 mol/L; 20 mL) was introduced after the hydrolysis reaction slowed down in order to measure the amount of the unreacted MgH_2.

The pH of the reaction mixtures was monitored after 100 min from the start of the hydrolysis experiment using a carefully calibrated prior to the measurements pH electrode. The pH electrode was calibrated using the standard buffer solutions having pH = 7.00, pH = 9.21, and pH = 11.00.

The XRD patterns were measured at a diffractometer DRON-3.0 using Cu-Kα radiation. Elemental analysis of the precipitates was performed using an EVO-40 XVP (Carl Zeiss) scanning electron microscope equipped with Inca Energy 350 (Oxford Instruments) microprobe analysis system.

Results and Discussion

The influence of $MgCl_2$ on the kinetics of MgH_2 hydrolysis has been studied in a broad range of concentrations of $MgCl_2$ (Table 1). It was found that in all the cases $MgCl_2$ solutions have increased the rate of hydrolysis (Fig. 1) as well as the conversion of reaction (Table 1). It was observed that the kinetics curves are characterized by exponential shape and contain two parts: initial fast release of hydrogen lasting for approximately 10 minutes and a slow H_2-generation part lasting for up to 150 minutes (Fig. 1). One of the assumptions explaining a high promotive

activity of $MgCl_2$ is the formation of complex solid precipitates similar to Sorel cement which are less soluble than $Mg(OH)_2$ leading to a decreasing of pH [12]. Therefore, the obtained after the hydrolysis reactions precipitates were studied using XRD and EDS. However, it was found that the final products of reaction consist of $Mg(OH)_2$ (brucsite type) and remaining unreacted MgH_2. This fact shows that the formation of solid species such as $MgCl_2 \cdot xMgO \cdot yH_2O$ [12] at the studied conditions is unlikely and decreasing of pH of the reaction mixture has a different nature.

Table 1. The dependence of conversion of MgH_2 hydrolysis and pH of reaction mixture on $MgCl_2$ concentration.

C($MgCl_2$), mol/L	Conversion after 150 min, %	pH(exp)	pH(calc)	Equation used for pH calculation
0	18	10.89	11.07	(1.4)
0.0046	43	–	10.48	(2.7)
0.0092	57	10.22	10.18	(2.7)
0.0138	67	–	10.00	(2.7)
0.0184	70	10.10	9.88	(2.7)
0.0368	79	9.89	9.58	(2.7)
0.0738	89	9.63	9.28	(2.7)

Hence with the aim of evaluation of the mechanism of MgH_2 hydrolysis in the presence of $MgCl_2$ the values of pH of reaction mixtures at high degrees of conversion of reaction when the acidity of solutions is stationary were measured. It was found that pH of reaction mixtures decreases with increasing $MgCl_2$ concentration (Table 1).

For evaluation of the mechanism of hydrolysis, the reaction system MgH_2–H_2O–$MgCl_2$ must be considered in details. The sets of all possible chemical transformations can be written as follows.

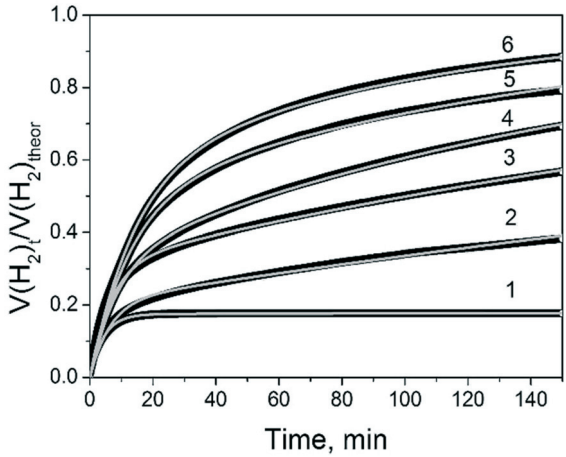

Fig. 1. Kinetic curves of H_2 evolution during MgH_2 hydrolysis at different initial concentrations of $MgCl_2$: 1 – 0; 2 – 0.0046; 3 – 0.0092; 4 – 0.0184; 5 – 0.0368; 6 – 0.0738 mol/L. Points are the experimental data and lines are the fitted by eqs. (3.4) – (3.6) curves.

Hydrolysis of MgH_2 in pure water:

$$MgH_2 + 2H_2O = Mg(OH)_2 + 2H_2\uparrow \quad (1.1)$$

$$Mg(OH)_2 \Leftrightarrow Mg(OH)_2\downarrow \quad (1.2)$$

$$Mg(OH)_2 \Leftrightarrow Mg(OH)^+ + OH^- \quad (1.3)$$

$Mg(OH)_2$ is a weak alkali with a low solubility in water. The basicity constant (pK_1) and the value of the solubility product (pSP) of a freshly precipitated $Mg(OH)_2$ are equal to 2.58 and 9.22, respectively. Please note that $Mg(OH)_2$ dissociates only partially (eq. 1.3). With the progressing conversion reaction, when the $Mg(OH)_2$ precipitate is formed, the calculated concentrations of Mg^{2+} and OH^- become equal to $5.3 \cdot 10^{-4}$ and $10.6 \cdot 10^{-4}$ mol/L, respectively. Then, pH of the solution can be calculated as follows:

$$pH = 14 - \tfrac{1}{2} pK_1 + \tfrac{1}{2} \log(C_B) \quad (1.4)$$

Here C_B is the $Mg(OH)_2$ concentration and can be considered as equal to the concentration of the dissolved hydroxide, i.e. to $5.3 \cdot 10^{-4}$ mol/L.

The calculated pH of the solution of 11.07 is in a good agreement with the experimentally measured one (see Table 1) validating the evaluation.

Hydrolysis of MgH_2 in a $MgCl_2$ solution

In $MgCl_2$ solutions, we can expect the following reactions to occur:

$$MgCl_2 + H_2O \Leftrightarrow Mg(OH)^+ + H^+ + 2Cl^- \quad (2.1)$$

$$MgH_2 + 2H^+ = Mg^{2+} + 2H_2\uparrow \quad (2.2)$$

$$MgH_2 + 2H_2O = Mg(OH)_2 + 2H_2\uparrow \quad (2.3)$$

$$Mg(OH)_2 \Leftrightarrow Mg(OH)_2\downarrow \quad (2.4)$$

$$Mg(OH)_2 \Leftrightarrow Mg(OH)^+ + OH^- \quad (2.5)$$

As can see be seen, the reaction solution is acidic before the introduction of MgH_2. pH of such a solution can be calculated by using an equation

$$pH = 7 - ½\ pK_1/2 - \log([MgCl_2]) \quad (2.6)$$

At the applied experimental conditions pH of the initial MgCl2 solutions are within 6.88 – 6.28 showing the formation of close to neutral solutions. After adding the MgH_2, the hydrolysis reaction and the formation of $Mg(OH)_2$ are taking place and after some time magnesium hydroxide precipitates are formed. As a result, the reaction system appears to contain two solid species, namely, MgH2 and Mg(OH)2 which are in equilibrium with the solution providing the stable concentrations of Mg(OH)2 and $MgCl_2$ soluble species. Such $MgCl_2$ + $Mg(OH)_2$ solution can be considered as a buffer solution "weak base and its salt with a strong acid", and pH of such a solution can be calculated by using an equation:

$$pH = 14 - pK_1 + \log([Mg(OH)_2]/[MgCl_2]) \quad (2.7)$$

As mentioned above, magnesium hydroxide has a low solubility in water. Consequently, after its precipitation, the concentration of $Mg(OH)_2$ in the solution will be constant and it can be calculated using pSP. Therefore, pH of a reaction mixture should be linearly dependent on $\log([MgCl_2])$. The latter assumption is in a good agreement with experimental observations, see Table 1. Based on the abovementioned experimental data and modeling, the mechanism of $MgCl_2$ action in the

reaction of MgH_2 hydrolysis can be described as follows. Due to a minor influence of the hydrolysis of the initial $MgCl_2$ solutions on the pH of the starting reaction mixture, the reaction of MgH_2 and water forming soluble $Mg(OH)_2$ is suggested to occur as a very fast process. Such a reaction leads to the formation of a buffer solution "$MgCl_2$ + $Mg(OH)_2$" which determines pH of the reactive solution. pH of such a solution increases with the increasing conversion up to the reaching of the solubility product of magnesium hydroxide when the precipitation of $Mg(OH)_2$ starts. After starting the precipitation of $Mg(OH)_2$, its concentration in the solution remains constant and pH will remain stable (eq. 2.7).

As it was mentioned above pH of working solution is inversely proportional to the logarithm of $MgCl_2$ concentration (see eq. 2.7). It was found that the volumes of released H_2 (or degree of conversion of reaction) are proportional to $\log(MgCl_2)$ (Fig. 2).

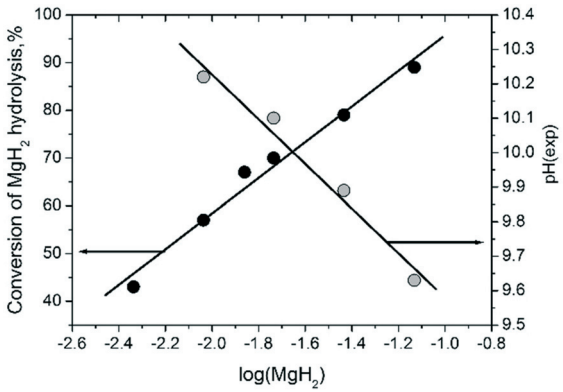

Fig. 2. The dependencies of the conversion of MgH_2 hydrolysis reaction and measured pH of the solutions on $\log(MgCl_2)$.

To describe the kinetics of hydrolysis of MgH_2 in the $MgCl_2$ solutions we propose to use a simplified kinetics scheme, which is based on the following simplifying assumptions.

It appears that only initial stages of the process show rapid changes (quick increase of the pH of the reaction mixture). Thus, the values of pH needed to initiate $Mg(OH)_2$ sedimentation are reached at early stages of the hydrolysis, when the conversion level is just 0.04 – 1 %. As after the start of $Mg(OH)_2$ sedimentation the value of pH of the solution becomes

stable and concentration of H^+ will be accounted when determining the rate constants of various contributing reactions. Thus, an overall kinetics scheme includes three pseudo-elementary reactions (3.1) – (3.3):

$$MgH_2 \rightarrow 2H_2\uparrow \quad (3.1)$$

$$MgH_2 \rightarrow P \quad (3.2)$$

$$P \rightarrow 2H_2\uparrow \quad (3.3)$$

(3.1) Fast interaction of solid MgH_2 with water releasing H_2; k_1 is the rate constant of the process.

(3.2) $Mg(OH)_2$ is formed during the hydrolysis process and blocks the surface of the remaining MgH_2 and forms low-active product P. k_2 is the rate constant of the process.

(3.3) Despite blocking the MgH_2 surface by $Mg(OH)_2$, water molecules can still slowly diffuse through its layer reaching MgH_2 and reacting with MgH_2. k_3 is the rate constant of the process.

Fitting of the kinetics curves of MgH_2 hydrolysis yielding the values of the rate constants of the reactions were performed using COPASI software [23]. By using the described kinetic model, we were able to satisfactory describe experimental curves, as can be evidenced from the Fig. 1. At the same time, the rate constants of the studied reactions exhibit a dependence on the concentration of $MgCl_2$, as show the data in Table 2.

Table 2. Dependences of the refined from the model rate constants of MgH_2 hydrolysis on the $MgCl_2$ concentration.

$[MgCl_2]$, mol/L	Rate constants, min^{-1}		
	k_1	k_2	k_3
0	0.031±0,004	0.19±0.02	0.000015±0.0000003
0.0046	0.034±0.003	0.12±0.01	0.0017±0.0004
0.0092	0.036±0.004	0.10±0.02	0.0031±0.0004
0.0138	0.038±0.002	0.07±0.02	0.0048±0.0007
0.0184	0.040±0.002	0.07±0.03	0.0054±0.0008
0.0368	0.041±0.002	0.037±0.006	0.0064±0.0009
0.0738	0.043±0.002	0.021±0.004	0.009±0.001

Such observed dependencies can be summarized as follows:

(1) A slight increase in the rate constant k_1 takes place with increasing concentration of $MgCl_2$ and can be related to the changes in the acidity of the solution;

(2) A decrease in the values of k_2 is observed with an increase of the $MgCl_2$ concentration which can be related to a decreased number of the blocking $Mg(OH)_2$ particles at an interface between the solution and the surface of MgH_2 thus resulting in reduced passivation of MgH_2;

(3) A more distinct increase of k_3 as compared to k_1 observed with increasing $MgCl_2$ concentration is associated not only with the changes of pH of the solution, but is mainly caused by the growth of the size of $Mg(OH)_2$ crystallites and, correspondingly, with a higher rate of the diffusion of water through the inhomogeneous passivation film.

Such an explanation of the promoting action of the metal chlorides of different nature during the reaction of MgH_2 hydrolysis, in spite of its simplicity, well describes the observed experimental dependencies and is expected to be further developed in the future.

Conclusions

The hydrolysis reaction of MgH_2 in the $MgCl_2$ solutions was investigated at pseudo-isothermal conditions. Based on the analysis of the process kinetics, changes of the pH of the solutions and the phase-structural composition of the reaction products it can be concluded:

– pH of a working solution linearly depends on the logarithm of $MgCl_2$ concentration;

– pH of the reaction mixture in the presence of $MgCl_2$ is well described by considering a system “weak base and its salt with strong acid” type buffer solution.

The mechanism of hydrolysis of MgH_2 in $MgCl_2$ solutions includes formation of the buffer solution controlling the pH of the reaction mixture leading to the formation of inhomogeneous passivation film on the surface of MgH_2. The kinetic model of the hydrolysis of MgH_2 in $MgCl_2$ solutions involved passivation of the MgH_2 surface by the formed $Mg(OH)_2$ precipitate followed by its repassivation has been proposed.

Acknowledgment

This work was supported by the NATO Programme "Science for Peace and Security" (Project G5233 "Portable Energy Supply").

References

[1] Lukashev R. V., Yakovleva N. A., Klyamkin S. N., Tarasov B. P. Effect of mechanical activation on the reaction of magnesium hydride with water, *Russian J. Inorg. Chem,* 2008, vol. 53, No. 3, pp. 343–349.

[2] Grosjean M.-H., Zidoune M. and Roué L. Hydrogen production from highly corroding Mg-based materials elaborated by ball milling, *J. Alloys Compd.,* 2005, vol.404, pp. 712–715.

[3] Grosjean M.-H., Zidoune M., Roué L. and Huot J.-Y. Hydrogen production via hydrolysis reaction from ball-milled Mg-based materials, *Int. J. Hydrogen Energy*, 2006, vol. 31, pp. 109–119.

[4] Tayeh T., Awad A.S., Nakhl M., Zakhour M., Silvain J.-F. and Bobet J.-L. Production of hydrogen from magnesium hydrides hydrolysis, *Int. J. Hydrogen Energy,*2014, vol. 39, pp. 3109–3117.

[5] Kojima Y., Suzuki K.-I., Kawai Y. Hydrogen generation by hydrolysis reaction of magnesium hydride, *J. Mat. Sci.,* 2004, vol. 39, pp. 2227–2229.

[6] Adeniran J. A., Akinlabi E. T., Chen H.-S., Fono-Tamo R., Jen T.-C. Organic acid-catalyzed hydrolysis of magnesium hydride for generation of hydrogen in a batch system hydrogen reactor, *Proc. of the World Congress on Eng. and Computer Sci*., 2017, vol II, WCECS 2017, October 25–27, 2017, San Francisco, USA.

[7] Hiraki T., Hiroi S., Akashi T., Okinaka N., Akiyama T. Chemical equilibrium analysis for hydrolysis of magnesium hydride to generate hydrogen, *Int. J. Hydrogen Energy*, 2012, vol. 37, pp. 12114–12119.

[8] Chao C.H., Jen T.C. Reaction of magnesium hydride with water to produce hydrogen, *Applied Mech. Mat.*, 2013, vol. 302, pp. 151–157.

[9] Makhaev V. D., Petrova L. A., Tarasov B. P. Hydrolysis of magnesium hydride in the presence of ammonium salts, *Russian J. Inorg. Chem.,* 2008, vol. 53, No. 6, pp. 858–860.

[10] Kushch S. D., Kuyunko N. S., Nazarov R. S., Tarasov B. P. Hydrogen-generating compositions based on magnesium. *Int. J. Hydrogen Energy*, 2011, vol. 36, pp. 1321–1325.
[11] Grosjean M.-H., Roué L. Hydrolysis of Mg–salt and MgH_2–salt mixtures prepared by ball milling for hydrogen production*, J. Alloys Compd.,*2006, vol. 416, pp. 296–302.
[12] Tegel M., Schöne S., Kieback B., Röntzsch L. An efficient hydrolysis of MgH_2-based materials, *Int. J. Hydrogen Energy,* 2017, vol. 42, pp. 2167–2176.
[13] Li S., Gan D., Zhu Y., Liu Y., Zhang G., Li L. Influence of chloride salts on hydrogen generation via hydrolysis of MgH_2 prepared by hydriding combustion synthesis and mechanical milling, *Trans. Nonferrous Met. Soc. China,* 2017, vol. 27, pp. 562–568.
[14] Ouyang L., M. Ma, Huang M., Duan R., Wang H., Sun L., Zhu M. Enhanced hydrogen generation properties of MgH_2-based hydrides by breaking the magnesium hydroxide passivation layer, *Energies,* 2015, vol. 8, pp. 4237–4252.
[15] Zhao Z., Zhu Y., Li L. Efficient catalysis by $MgCl_2$ in hydrogen generation via hydrolysis of Mg-based hydride prepared by hydriding combustion synthesis, *Chem. Commun.,*2012, vol.48, pp.5509–5511.
[16] Tessier J.-P., Palau P., Huot J., Schulz R., Guaya D. Hydrogen production and crystal structure of ball-milled MgH_2–Ca and MgH_2–CaH_2 mixtures, *J. Alloys Compd.,* 2004, vol. 376, pp. 180–185.
[17] Xiao Y., Wu C., Wu H., Chen Y. Hydrogen generation by CaH_2-induced hydrolysis of $Mg_{17}Al_{12}$ hydride, *Int. J. Hydrogen Energy,* 2011, vol. 36, pp. 15698–15703.
[18] Zhong H., Wang H., Liu J. W. *et.al*. Enhanced hydrolysis properties and energy efficiency of MgH_2-base hydrides, *J. Alloys Compd.*, 2016, vol. 680, pp. 419–426.
[19] Ma M., Ouyang L., Liu J., Wang H. *et.al.* Air-stable hydrogen generation materials and enhanced hydrolysis performance of MgH_2–$LiNH_2$ composites, *J. Power Sources,* 2017, vol. 359, pp. 427–434.
[20] Uesugi H., Sugiyama T., Nakatsugawa I., Ito T. Production of hydrogen storage material MgH_2 and its application, *J. Japan Inst. Light Met.*, 2010, vol. 60, pp. 615–618.

[21] Huang M., Ouyang L., Wang H., Liu J., Zhu M. Hydrogen generation by hydrolysis of MgH_2 and enhanced kinetics performance of ammonium chloride introducing, *Int. J. Hydrogen Energy,*2015, vol. 40, pp. 6145–6150.
[22] Gan D., Liu Y., Zhang J., Zhang Y., Cao C., Zhu Y., Li L. Kinetic performance of hydrogen generation enhanced by $AlCl_3$ via hydrolysis of MgH_2 prepared by hydriding combustion synthesis, *Int. J. Hydrogen Energy,* 2018, vol. 43, pp. 10232–10239.
[23] Hoops S., Sahle S., Gauges R. *et.al*, COPASI—a complex pathway simulator, *Bioinformatics*, 2006, vol. 22, pp. 3067–3074.

Mg-based composites as effective materials for storage and generation of hydrogen for FC applications

D. Korablov[1], O. Bezdorozhev[1], V. Yartys[2], Yu. Solonin[1]

[1]*Frantsevich Institute for Problems of Materials Science, NASU, Kyiv, Ukraine*
[2]*Institute for Energy Technology, Kjeller, Norway*

Today, hydrogen is considered as an ideal choice for storing and carrying energy produced by renewable power sources since it is renewable, eco-friendly and has a high energy density. However, due to the low hydrogen storage capacity, high cost and safety issues of the conventional storage methods, several challenges need to be resolved to effectively use hydrogen in mobile applications. Solid-state hydrogen storage in atomic form in hydrides is a promising method of storage for this purpose, particularly because a double amount of hydrogen can be produced via hydrolysis reaction of chemically active hydrides. Among the metal hydrides, magnesium hydride (MgH_2) is considered to be one of the most attractive candidates. However, the hydrolysis reaction is rapidly hindered by the passivation layer formed on the surface of MgH_2. In order to improve MgH_2 hydrolysis efficiency various approaches have been applied. This paper reviews recent progress on the modifications of MgH_2-based materials by adding different type of additives, including metals, oxides, hydroxides, halides and surfactants. The introduced additives possess different catalytic properties due to their intrinsic physical and chemical characteristics, and therefore can strongly influence the hydrolysis reaction of MgH_2. The most promising results were obtained for various salt additives showing that the reaction rate depends mostly on the additive type rather than on concentration. The effect of preparation technique on the hydrolysis of $MgH_2 – MgCl_2$ composites was studied in detail. The obtained results indicate that efficient hydrolysis performance can be achieved by ball milling of the freshly synthesized MgH_2 with 5 wt.% $MgCl_2$ and 1 wt.% $TiC–2TiB_2$ additives. The combination of the applied approaches exhibited a notable synergistic effect on the hydrogen generation.

Keywords: *Hydrogen generation, Hydrogen accumulation, Mg-based composites, Renewable power sources, Hydrolysis*

1. Introduction

Increase of the energy consumption and challenges appearing from the environmental pollution issues (such as global warming and associated climate changes) caused by industrialization, urbanization and extensive consumption of non-renewable fossil fuels triggered a huge interest to the exploration of green and renewable energy sources. Renewable energy technologies will play a key role in the transition from the fossil fuel economy toward a "green" energy system [1, 2]. In this context, hydrogen is considered as an ideal choice for future clean energy production because of its high energy density, environmental friendliness and renewability. However, the main challenges in the transition to the hydrogen energy are the issues associated with its production, storage and delivery.

Although hydrogen is abundant in nature element, it is primarily bound to other elements forming very stable compounds (water, hydrocarbons), and thus, hydrogen production always requires energy inputs. Hydrogen can be extracted from fossil fuels, biomass, and water by using economically efficient techniques, for example, electricity obtained from renewable energy sources. Although a significant progress has been achieved in hydrogen production, development of the effective methods of hydrogen storage remains on the agenda since the existing solutions have some limitations. Hydrogen can be stored in gaseous state, liquid state or in solid metal hydrides [3, 4]. Conventional high pressure gas storage system has maneuverability, but is costly, requires a high energy consumption and transportation costs, while liquid hydrogen-based storage systems require use of cryotemperatures, show a high energy consumption and cost, thus increasing the requirements to the features of the required equipment. Compared with these storage systems, the solid-state hydrogen storage has the potential to achieve high energy efficiency, good cycle stability, high safety and low cost for use in hydrogen storage applications [3].

On the other hand, solid-state hydrogen storage is characterized by a rather low gravimetric energy density even while considering the material itself only instead of the mass of the system [5]. Moreover, in

solid-state storage systems hydrogen is released in an endothermic reaction, which limits the rates of hydrogen supply due to the poor thermal conductivity of hydrides. Solid-state hydrogen storage is based on metal hydrides, intermetallic hydrides, and complex hydrides showing a variable performance at various P-T conditions [6].

Among the metal hydrides, MgH_2-based materials have attracted considerable attention due to the high natural abundance of magnesium, low cost of magnesium metal, good reversibility of hydrogen uptake and release, light weight, and high hydrogen storage capacity [3, 4, 7–9]. Pure magnesium can absorb hydrogen up to 7.6 wt.%, but has a slow absorption/desorption kinetics. High thermal stability of MgH_2 and its easy surface oxidation in air impede its applications. To overcome these limitations, a significant amount of research has been performed on the nanosizing, nanoconfinement, alloying, and modifying with intermetallic compounds, metal oxides, halides, carbon materials, hydrides, borohydrides, their mixtures, etc. [7–12]. Although much progress has been achieved, their performance still cannot meet requirements for mobile applications. In this context, small portable applications attract interest as they could be used to power a fuel cell coupled to a hydrogen source that provides the H_2 fuel on demand. An attractive way to implement this concept is to take advantage of the hydrolysis of various metals (e.g., Al-based alloys, Mg [13, 14]) and metal hydrides (e.g., LiH, $LiBH_4$, $NaBH_4$, MgH_2 [5, 15]). Compared with other hydrolysis materials, MgH_2-based materials have promising features [16] due to the high hydrogen yield (15.2 wt.% H_2, when hydrolyzed), relatively low cost, and a formation of the environmentally friendly by-product $Mg(OH)_2$ [5, 17]. The chemical reaction between MgH_2 and H_2O is as follows (1):

$$MgH_2 + 2H_2O \rightarrow Mg(OH)_2 + 2H_2\uparrow,\ \Delta H_r = -277\ \text{kJ/mol} \quad (1)$$

The hydrolysis reaction of MgH_2 can proceed spontaneously in contact with water at room temperature. However, the hydrolysis of MgH_2 immediately terminates due to the formation of a passive $Mg(OH)_2$ layer on the MgH_2 surface. The passivation layer prevents the diffusion of water molecules toward the surface of MgH_2, causing the hydrolysis to

rapidly stop, while the initial reaction rate is high. Magnesium hydroxide has a poor solubility in water (1.22 mg/100 mL at 20 °C) [6], and the maximum reaction yield after 1 h does not exceed 30 % [5]. Eliminating the cladding effect of magnesium hydroxide passivation layer on MgH_2 has become an urgent problem to be solved to increase the hydrogen yield by hydrolysis [18].

To address this issue, various approaches, such as nanostructuring, the addition of acids, alkali metals, salts, inert additives at ambient conditions or when under heating, ultrasonic irradiation, stirring, were tested to achieve higher hydrogen yield [5, 14, 16, 17, 19]. These approaches improve the hydrolysis performance, while their combination exhibits the notable synergistic effects. However, some aspects of hydrolysis of MgH_2-based materials require further investigations and optimization. The hydrolysis reaction is strongly influenced by the characteristics of the hydrolyzed materials, solution composition as well as by the preparation procedure. Since it is possible to improve the hydrolysis of MgH_2-based materials by optimizing their preparation procedure, we studied its effect on the hydrolysis performance of MgH_2 + 5 wt.% $MgCl_2$. Moreover, in this study, we summarized the recent advances in the hydrolysis of the MgH_2-based materials.

2. Recent trends in the hydrolysis of MgH_2-based materials

2.1. Hydrolysis of MgH_2-based materials with metal additives

Several metals and their hydrides have been tried as doping catalysts and/or as the components involved into the reaction in order to change the hydrolysis kinetics of Mg-based materials. The ball milling of Mg or MgH_2 with catalytic metal agents offers advantages of synergy between nanostructuring and alloying resulting in the synthesis of new products with improved hydrogen generation properties, as was shown, for example, in the case of Mg_3RE [20, 21], Mg–Al [22] and Mg–Ca alloying systems [23].

In this connection, the work of Awad et al. [17] should be mentioned, who studied the effect of transition metals such as Ni, Fe and Al on the hydrolysis performance of Mg-based materials in a 3.5 wt.%

NaCl solution. They found that the presence of metal elements improves the efficiency of the ball milling process by decreasing the particle size and by creating more microstructural defects which leads to a more efficient synthesis of MgH_2. As the result, the weight content of MgH_2 after 5 h of ball milling was 4% and 24% for Mg – 10 wt.% Ni and Mg – 10 wt.% Fe mixtures, respectively, while no MgH_2 was detected in the case of Mg – 10 wt.% Al mixture. The composites with Fe, Ni and Al released respectively 81%, 97% and 45% of the theoretical hydrogen yield after 30 min. The improved hydrogen yield of composites with Ni and Fe is attributed to the formation of micro-galvanic cells between Mg and transition metals that facilitate the corrosion of Mg. However, MgH_2 formed on the surface of the particles limits the galvanic connection and corrosion processes due to the low electrical conductivity of the hydride (band gap of 5 eV), which explains low H_2 yield in case of Fe addition in comparison to Ni one.

Recently, Mao et al. [24] studied the solid-solution effect of 10 wt.% In and 5 wt.% Ag on the hydrogen storage and hydrolysis properties of Mg. They found that upon hydrogenation of the Mg(In) or Mg(Ag) solid-solution, MgH_2–MgIn or MgH_2–MgAg composites are formed. The obtained materials show improved hydrogen sorption performances as well as hydrolysis behavior. Particularly, after hydrolysis at 25 ^oC for 500 s, MgH_2–MgIn releases 895.2 mL/g H_2 that is relatively higher than in the system MgH_2–MgAg (733.6 mL/g) and also for the individual MgH_2 (631.1 mL/g). This corresponds to about 91%, 92% and 64% hydrogen release for the hydrogenated MgH_2–MgIn, MgH_2–MgAg and MgH_2, respectively. The enhanced hydrolysis performance of the samples the authors attributed to the evenly dispersed nano MgIn or MgAg intermetallics that not only serve as dispersants controlling the growth of MgH_2 particles and enhancing the contact area with $MgCl_2$ aqueous solution but also act as reactants directly participating in the hydrolysis reaction.

The effect of adding 5–20 wt.% Ge on the hydrolysis of MgH_2 was investigated in [25]. In such a case, Ge does not interact with MgH_2 under the ball milling conditions, but forms Mg_2Ge at T>370 °C. By studying the hydrolysis of MgH_2–Ge composites, it was found that the unmodified

MgH_2 exhibits 1.5–2.5 slower H_2 generation rates than MgH_2–Ge materials even in concentrated (50 wt.%) acetic acid. Introduction of 5–20 wt.% Ge significantly improves the hydrolysis performance of MgH_2 when about 100 % H_2 yield is observed after less than 1 minute at the optimal hydrolysis conditions (30–50 wt.% solution of acetic or citric acid at T=30 °C). It should be noted that the hydrogen evolution kinetics was faster for the acetic acid probably due to the different pKa values of the acetic and citric acids related to their reactivity with the substrate. The highest hydrogen generation capacity (~1.56 NL/g) was achieved for the composites containing 5 wt.% Ge, while the increase of Ge content to 20 wt.% results in the lowering of the amount of the generated H_2 to 1.26 NL/g. The improvements of hydrolysis reaction by the addition of Ge, authors explained by the increase of the reaction surface area, number of nucleation centers and creation of micro-galvanic cells between Mg and Ge. The variation of ball milling time from 1 h to 10 h and hydrolysis temperature from 30 ^oC to 50 ^oC does not significantly change the kinetics of hydrolysis.

Ma et al. [26] investigated the hydrolysis properties of MgH_2–CaH_2 composites in-situ hydrogenated using the $CaMg_2$ and $CaMg_{1.9}Ni_{0.1}$ intermetallic alloys. The XRD analysis revealed that after the hydrogenation $CaMg_2$ predominantly formed MgH_2 and $Ca_4Mg_3H_{14}$, while $CaMg_2$, $MgNi_2$ and $Ca_5Mg_9H_{28}$ phases appeared after the hydrogenation of $CaMg_{1.9}Ni_{0.1}$ alloy. Ma et al. [26] found that after 12 min of hydrolysis in pure water the hydrogen yield of H-$CaMg_{1.9}Ni_{0.1}$ (1053 mL/g) was higher than that of H-$CaMg_2$ (800 mL/g). However, the hydrolysis kinetics of H-$CaMg_{1.9}Ni_{0.1}$ is sluggish during the first 5 minutes of the reaction. A possible reason for the improved hydrolysis performance of H-$CaMg_{1.9}Ni_{0.1}$ is in a catalytic effect of $MgNi_2$, which promotes the hydrolysis reaction around the interface region.

In order to improve the hydrolysis performance of Mg-based materials, Jiang et al. [27] prepared MgLi hydrides via the milling and hydrogenation of MgLi alloy. The prepared hydrides mostly consisted of $Mg(Li)H_2$ and Mg with small amounts of MgO and Li_2O. When hydrolyzed, the samples can produce 1542 mL/g and 1773 mL/g (15.8

wt.%) hydrogen after 5 min and 30 min of reaction with $MgCl_2$ water solution, respectively. The initial rapid hydrogen generation is mainly the result of the violent reaction of LiH with water, while the following reaction happens in a slow pace during the destabilization of the $Mg(OH)_2$ layer on the MgH_2 and Mg particles by chloride ions.

In the study by Naseem et al. [28], $Al_{12}Mg_{17}$ alloy was used to obtain a mixture of MgH_2 and Al, which was milled with 1.5 wt.% Mo and 3.5 wt.% B_2O_3 as grinding agents. The maximum conversion yield of 97.9% and the hydrogen generation of 1420.2 mL/g were observed for the prepared composite after hydrolysis in a 1 M $AlCl_3$ solution for 50 min. The hydrolysis process of MgH_2 and Al is catalyzed by Mo and B_2O_3 additives, where Mo forms a galvanic cell with Al accelerating its dissolution, and B_2O_3 forms boric acid, which along with $AlCl_3$ facilitates the dissolution of hydroxide layers on the MgH_2 and Al particles.

2.2. Hydrolysis of MgH_2-based materials with oxide and hydroxide additives

The role of addition of oxide on the hydrolysis performance of MgH_2 was firstly investigated by Hong et al. [29], who showed that the milling of MgH_2 with 5 wt.% MgO significantly increases the reactivity of the MgH_2 particles towards water due to the creation of numerous defects and clean surfaces along with the particle size refining. This study was followed by Awad et al. [17], who also showed that milling Mg with V_2O_5 and Nb_2O_5 leads to the higher density of defects, fracture and cracking of Mg/MgH_2 particles. Moreover, Mg-based materials with Nb_2O_5 additive were found to be more effective in terms of hydrolysis than with V_2O_5 or transition metal additives.

Hydrolysis behavior of core-shell structured Mg-MO_x (M=Al, Ti and Fe) nanocomposites prepared by arc plasma method and subsequent hydrogenation was studied in [30]. The synthesized and hydrogenated materials mostly contained MgH_2 with a low fraction of unreacted Mg and MgO, Fe, $MgAl_2O_4$ that formed during the arc plasma evaporation. The hydrogen yields by performing hydrolysis in 0.1M $MgCl_2$ aqueous solution of the hydrogenated and passivated Mg–Al_2O_3, Mg–TiO_2, Mg–Fe_2O_3 composites are 1503 mL/g (93.3%), 1525 mL/g (93.7%) and 1240

mL/g (85%), respectively, which are much higher than that for the passivated pure Mg (1167 mL/g, 77.7%). Thus, the hydrolysis reaction of core-shell nanostructured MgH_2–MO_x is dramatically facilitated. Among all studied composite powders, the passivated Mg–TiO_2 after the hydrogenation shows the best hydrolysis performances. This is due to the amphoteric nature of TiO_2 that locally at the surface of MgH_2 creates an acidic environment when it contacts with water (2). The formed acidic sites destroy the $Mg(OH)_2$ passive layer and, along with the created internal defects, promote the hydrolysis of MgH_2.

$$TiO_2 + 3H_2 \rightarrow Ti(OH)_5^- + H^+ \quad (2)$$

In the case of hydrogenated Mg–Fe_2O_3, the in-situ generated Fe during arc plasma evaporation forms micro galvanic cells, which accelerate the corrosion of MgH_2. However, the hydrogen yield of hydrogenated Mg–Fe_2O_3 is relatively low due to the fact that the addition of Fe_2O_3 reduces the hydrogen absorption content of Mg.

Yang et al. [31] studied the hydrolysis performance of MgH_2–5wt.%C and MgH_2–5wt.%C–5wt.Fe_2O_3 composites in municipal drinking water. After 5 min of hydrolysis at 353 K, the hydrogen yield of pure MgH_2, MgH_2–C, and MgH_2–C–Fe_2O_3 was found to be 202 mL/g, 416 mL/g, and 468 mL/g, while the conversion rate reached 19.3%, 52.5%, and 62.8%, respectively, after 60 min of reaction. It can be seen that addition of graphite and Fe_2O_3 significantly improved the hydrolysis performance of MgH_2. The authors attributed this synergistic effect to the lubricating properties of graphite that effectively reduces the agglomeration and size of magnesium particles, while Fe_2O_3 can further reduce the particle size of MgH_2 and may have a catalytic effect on the hydrolysis reaction.

Recently, Zhou et al. [32] systematically investigated the catalytic activity of typical oxides (MgO, Al_2O_3, CaO), hydroxides ($Mg(OH)_2$, $Al(OH)_3$, $Ca(OH)_2$) and chlorides on the hydrolysis reaction of MgH_2 with water. They found that MgH_2 –10 wt.%(MgO, Al_2O_3 or CaO) composites deliver only 433.0 mL/g, 432.4 mL/g and 421.0 mL/g hydrogen, respectively, within 60 min as compared to that of pure MgH_2 (377 mL/g). In this case oxides play the role of grinding aid that more

effectively reduces the particle size of MgH_2. However, such modification is limited by the milling efficiency. When 10 wt.% $Mg(OH)_2$, $Al(OH)_3$, and $Ca(OH)_2$ is introduced, the hydrogen generation performances are slightly decreased, delivering 407.2 mL/g, 357.3 mL/g, and 340.0 mL/g hydrogen, respectively. Here, the performance is influenced by the solubility of the hydroxides in water and the corresponding solutions produce more OH^- ions, which favors the formation of $Mg(OH)_2$ at the surface of MgH_2.

2.3. Hydrolysis of MgH_2-based materials with halide additives

Alternatively to the use of the acids, the chlorides are usually utilized as agents to create more aggressive medium to enhance the hydrolysis of MgH_2 and inhibit the formation of $Mg(OH)_2$. Recently, Zhou et al. [32] studied the effect of a series of 10 wt.% salt additives, including $CoCl_2$, $NiCl_2$, $CuCl_2$, $MgCl_2$, $CaCl_2$, NaCl, and KCl, on the hydrolysis reaction of MgH_2 with water. The 10 wt.% NaCl, KCl or $CaCl_2$ containing MgH_2 composites exhibit enhanced hydrolysis properties (540.1 mL/g, 590.2 mL/g and 604.5 mL/g H_2, respectively) compared to that of MgH_2 (377 mL/g). Both the hydrogen generation yield and hydrolysis kinetics of MgH_2 get further dramatically improved when catalyzed by $CoCl_2$, $NiCl_2$, $CuCl_2$ or $MgCl_2$, of which the solid-liquid systems deliver 1481.7 mL/g, 1496.1 mL/g, 1472.1 mL/g and 1554.6 mL/g H_2 in 60 min, respectively. The introduced chlorides show different catalytic properties due to their intrinsic physical characteristics. The aqueous solution has a neutral pH value when the neutral chloride (i.e. NaCl, KCl) is completely soluble in water. However, the cation ions from the acidic chloride (i.e. $CoCl_2$, $NiCl_2$, $CuCl_2$, $MgCl_2$) have a trend to dissociate water with the generation of more H^+, therefore making the corresponding aqueous solution weakly acidic. The authors state that Cl^- ions present in the aqueous solutions destroy the dense $Mg(OH)_2$ layer via a pitting corrosion, when introducing neutral chlorides only. However, both the anions (Cl^-) and cations (i.e. Co^{2+}, Ni^{2+}, Mg^{2+}, Cu^{2+}) derived from the acid chloride aqueous solution are able to attack the dense $Mg(OH)_2$ layer via pitting corrosion and H^+ corrosion, respectively. That is why the neutral chloride can promote the hydrolysis reaction at an early

stage only while the acidic chloride can increase the hydrolysis performance during the whole process.

In the same study [32] Zhou et al. investigated the effect of milling duration (0–5 h), amounts of additives (3–15 wt.% $CoCl_2$) and the way of introducing solute on the hydrolysis of MgH_2 – 10 wt.% $CoCl_2$. They found that 3–5 h-milled composites provide the highest hydrogen yield due to the reduced particle sizes, from 5.8 μm to 0.7–0.9 μm. The optimal amount of $CoCl_2$ was 10 wt.% as the hydrolysis performance at 15 wt.% $CoCl_2$ remained unchanged. Comparing the hydrolysis performance of MgH_2 – $CoCl_2$ and MgH_2 hydrolyzed in $CoCl_2$ aqueous solution, where $CoCl_2$ content in the two hydrolysis systems was kept at the same level, it was observed that the kinetics of hydrolysis improves with the increasing $CoCl_2$ concentration. However, the system demonstrated advanced hydrogen generation kinetics and capacity in the former case for the same amount of introduced $CoCl_2$. This is probably due to the higher local concentration of $CoCl_2$ around MgH_2 after the milling process. Authors concluded that the effect of the solution ions is proportional to the ions concentration in the solution, independently of the way of introducing a solute.

A systematic study of the effect of various halides on the hydrolysis of MgH_2 was performed by Sevastyanova et al. [33], who studied NH_4F, NH_4Cl, NH_4Br, NH_4I, NaCl, KCl, LiCl, $FeCl_3$, $MgBr_2$, $MgSO_4$, $MgCl_2{\cdot}6H_2O$, $CaCl_2{\cdot}2H_2O$, $CoCl_2{\cdot}2H_2O$, $NiCl_2{\cdot}6H_2O$, $CuCl_2{\cdot}2H_2O$ compounds to prepare aqueous solutions. They found that the hydrolysis process of MgH_2 accelerates in salt solutions, but the reaction rates depend more on the type of the salt rather than on the solution amount (see Table 1). Among tested salts, the most effective catalysts were ammonium chloride and bromide, as well as magnesium chloride, albeit with slightly different reaction rates, pointing out at the differences in the reaction mechanism. In the case of binary salt mixtures, the highest reaction rate and hydrogen yield were observed for $MgCl_2$+NH_4Cl. The authors emphasize that pH value is not the main factor determining the reaction, and ionic strength of the solution should also be considered since the combination of two various salts leads to a marked hydrolysis improvement.

Table 1 – Hydrogen yield in the MgH_2 hydrolysis reaction for the various salt solutions [33]

Salt	Salt concentration, mol/L (solution volume, mL)	Theoretical H_2 yield over 300 min, %	Theoretical maximum H_2 production, % (reaction completion time, h)
1	2	3	4
LiCl	0.85 (2)	57	78 (30)
NaCl	0.85 (2)	46	85 (57)
NaCl	0.85 (1)	49	100 (40)
KCl	0.85 (2)	66	94 (26)
NH_4F	0.85 (2)	16	21 (8)
NH_4Cl	0.85 (0.5)	100	100 (4)
NH_4Cl	0.85 (1)	100	100 (3)
NH_4Cl	0.85 (2)	100	100 (4)
NH_4Cl	0.85 (5)	82	82 (3)
NH_4Br	0.85 (2)	100	100 (4)
NH_4I	0.85 (2)	92	94 (6)
$MgCl_2$	0.45 (0.5)	99	99 (7)
$MgCl_2$	0.45 (1)	97	97 (6)
$MgCl_2$	0.45 (2)	90	90 (5)
$MgBr_2$	0.45 (2)	96	100 (9)
$CaCl_2$	0.45 (2)	40	79 (71)
$FeCl_3$	0.032 (1)	82	89 (9)
$CoCl_3$	0.032 (1)	73	78 (8)
$NiCl_2$	0.032 (1)	71	83 (8.5)
$CuCl_2$	0.032 (1)	86	100 (10)
$MgCl_2$+LiCl	0.45 (2) + 0.85 (2)	99	99 (6)
$MgCl_2$+NaCl	0.45 (2) + 0.85 (2)	82	93 (10)
$MgCl_2$+NaCl	0.45 (1) + 0.85 (1)	100	100 (9)
$MgCl_2$+KCl	0.45 (2) + 0.85 (2)	99	99 (5)
$MgCl_2$+NH_4Cl	0.45 (1) + 0.85 (1)	100	100 (2)

1	2	3	4
$MgCl_2$+$FeCl_3$	0.85 (2) + 0.032 (5)	65	83 (14)
$MgCl_2$+$CoCl_2$	0.85 (2) + 0.032 (5)	62	97 (24)
$MgCl_2$+$NiCl_2$	0.85 (2) + 0.032 (5)	67	95 (23)
$MgCl_2$+$CuCl_2$	0.85 (2) + 0.032 (5)	95	96 (6)
$MgCl_2$+$CuCl_2$	0.85 (1) + 0.032 (1)	100	100 (3.5)

Recently, $CoCl_2$ [34] and $AlCl_3$ [35] solutions were also tested as reaction mediums for hydrolysis of MgH_2. The increase in $CoCl_2$ and $AlCl_3$ concentration resulted in an improved reaction kinetics and the maximum generation performance was obtained by using 6.25 wt.% $CoCl_2$ and 0.5 M $AlCl_3$ concentrated solutions. The improved hydrolysis performance is attributed to the large amounts of H^+ produced by the Al^{3+} and Co^{2+} hydrolysis that along with the Cl^- pitting corrosion could contribute to destroying the $Mg(OH)_2$ layer wrapped on the surface of MgH_2.

The influence of $MgCl_2$ and $CaCl_2$ salts on the hydrolysis of the hydrogenated 30 wt.% Ca–Mg alloy was investigated in [36]. Composites with various $MgCl_2$ and $CaCl_2$ content were obtained by ball milling for 0.5 h and were composed of Mg, MgH_2, and $Ca_4Mg_3H_{14}$ phases, further to the chlorides. The hydrogen yields of the composites with $MgCl_2$ additive, in which the highest value is 1002 mL/g within 1 h, are lower than that of pure Ca–Mg alloy (1113 mL/g within 1 h). The authors attributed this effect to the displacement reaction and the common ion effect of Mg^{2+}. However, composites with $CaCl_2$ chloride showed better hydrogen generation performances during the hydrolysis process. Moreover, with the increase of $CaCl_2$ content, the conversion rates of the composites also become higher due to the leaching and exothermic dissolution of $CaCl_2$, which contributes to the formation of the fresh reactive material surfaces and disintegration of the passive layer. The hydrolysis performance of the hydrogenated 30 wt.% Ca–Mg alloy can be further improved by ball-milling with NH_4Cl, as it was shown by the same group of investigators [37]. The hydrogenated Ca–Mg /5 wt.% NH_4Cl composite has the best hydrolysis properties, generating 720 mL/g hydrogen in 1 min. The improved performance was explained by: (1) reduced particle size after the ball milling with NH_4Cl; (2) formation of a new reactive material surface during leaching of chlorides from the composite; (3) high affinity of NH_4^+ to OH^- and formation of soluble $NH_3 \cdot H_2O$.

The effect of additives of different nature, namely $AlCl_3$, ethylenediaminetetraacetic acid (EDTA), and TiC–$2TiB_2$, on the hydrolysis of MgH_2 was investigated in our earlier study [38]. It was found that MgH_2 + 5 wt.% EDTA unfortunately demonstrates the lowest reactivity among the tested materials and produces only 176 mL/g H_2 in 10 min. The most probable reason for such a decreased efficiency is an interaction of MgH_2 with EDTA during the ball milling, which leads to the formation of magnesium salts and reduces the amount of highly active MgH_2 nanoparticles. As the result, only a small volume of MgH_2 can generate hydrogen during the hydrolysis, while the formed salts do not contribute to the hydrogen yield. Pure MgH_2 and MgH_2 + 5 wt.% TiC–$2TiB_2$ composite demonstrate a much improved hydrolysis performance (309–317 mL/g of hydrogen yield and 16.8–17.2% of the conversion rate after 10 min). However, still poor hydrolysis kinetics is attributed to the formation of a poorly soluble in water $Mg(OH)_2$ layer on the surface of MgH_2 particles, while the addition of 5 wt.% TiC–$2TiB_2$ does not contribute to the hydrolysis reaction probably due to non-optimized synthesis parameters. The maximum hydrogen yield of 557 mL/g MgH_2 and conversion rate of 30.3% were observed for MgH_2 + 5 wt.% $AlCl_3$ composition after 10 min of hydrolysis, which can be attributed to the destabilization of the $Mg(OH)_2$ layer by chlorine ions.

2.4. Hydrolysis of MgH_2-based materials with surfactant additives

The hydrolysis efficiency can be improved not only by adding different catalysts (acids, halides, oxides, etc.) but also by adjusting reaction conditions such as temperature, precursor's size, stirring, ultrasonic irradiation, etc. Recently, Chen et al. [39] investigated the effect of various surfactants on the hydrogen generation by hydrolysis of MgH_2 in water. It is known that surfactants can change the surface energy by forming an adsorbed layer with a certain orientation at the solid-liquid interface, and thus can influence the reaction kinetics. It was found that the addition of surfactants reduces the surface tension of the liquid, improves the wetting effect of the liquid to the MgH_2, and increases the hydrogen yield. However, with the addition of surfactants, the reaction system is more prone to the formation of foam, limiting the release of hydrogen and thus reducing the efficiency of hydrogen generation. Moreover, different surfactants have variable effects on hydrogen generation. The hydrogen generation capacity from high to low is as

follows: tetrapropylammonium bromide (TPABr), sodium dodecyl benzene sulfonate (SDBS), Ecosol 507, octadecyl trimethyl ammonium chloride (OTAC), sodium alcohol ether sulfate (AES), and fatty methyl ester sulfonate (FMES-70). The best performance was observed when the ratio of MgH_2 to TPABr was 5:1, and in this case the hydrogen generation increased by 52% as compared to the one without surfactants (after hydrolysis for 100 s). Due to the adsorptive effect of TPABr, it inhibits the formation of a passivation layer and prolongs the time for $Mg(OH)_2$ to reach the critical in size volume. In addition, the reduced surface energy weakens the interaction among the particles and prevents their agglomeration. The surfactants can also change the morphology of $Mg(OH)_2$, which forms a three-dimensional stacking to produce a discontinuous layered structure that improves the continuity of the hydrolysis reaction.

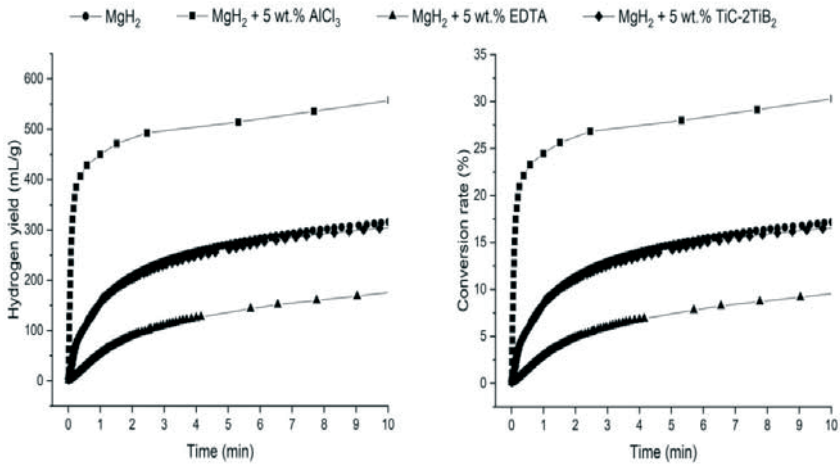

Fig. 1. Hydrogen yield (a) and conversion rate (b) for the MgH_2 composites [38].

2.5. Summary of the main observations and regularities of the hydrolysis of MgH_2-based materials

The main features of the hydrolysis performance of the MgH_2-based materials are summarized in Table 2.

Table 2 – Hydrolysis performance of MgH_2-based materials

Materials	Solution	Hydrogen conversion yield (%)	Hydrogen generation rate (mL/g) in 5 min	Activation energy (kJ/mol)	Ref.
1	2	3	4	5	6
MgH_2– 5 wt.%C	Water	52.5% in 60 min	416	43.4	[31]
MgH_2– 5 wt.%C– 5 wt.%Fe_2O_3	Water	62.8% in 60 min	468	36.92	
MgH_2– 5 wt.%Ge	30 wt.% acetic acid	100% in 1 min	-	-	[25]
H– 10 wt.% Mg– 10 wt.% TiO_2	0.1M $MgCl_2$	93.7% in 60 min	~400	45.14	[30]
H– 10 wt.% Mg– 10 wt.% Al_2O_3		93.3% in 60 min	~390	51.06	
H– 10 wt.% Mg– 10 wt.% Fe_2O_3		85.1% in 60 min	~470	47.62	
H–MgLi	Deionized water	-	734	-	[27]
	0.1M $MgCl_2$	-	1247	-	
	0.5M $MgCl_2$	-	1263	-	
	1M $MgCl_2$	90% in 30 min	1542	24.6	
MgH_2	0.1M $AlCl_3$	~60% in 60 min	~450	34.68	[35]
	0.5M $AlCl_3$	~100% in 60 min	~950	21.64	
H– 30wt.%Ca-Mg	Water	55.9% in 60 min	~540	-	[37]

1	2	3	4	5	6
H–30wt.%Ca-Mg–3% NH_4Cl	Water	61% in 60 min	~690	-	[37]
H–30wt.%Ca-Mg–5% NH_4Cl		67% in 60 min	~830	-	
H–30wt.%Ca-Mg–7% NH_4Cl		65.9% in 60 min	~820	-	
H–30wt.%Ca-Mg–10% NH_4Cl		66.5% in 60 min	~800	-	
MgH_2	0.1M $MgCl_2$	63.7% in 60 min	~400	54.1±2.5	[24]
H–Mg–10 wt.% In		92% in 60 min	~540	43.4±1.1	
H–Mg–5 wt.% Ag		90.7% in 60 min	~480	59.6±2.7	
MgH_2	Deionized water		377.0	-	[32]
MgH_2 + 10wt.% MgO			433.0	-	
MgH_2 + 10wt.% Al_2O_3			432.4	-	
MgH_2 + 10wt.% CaO			421.0	-	
MgH_2 + 10wt.% $Mg(OH)_2$			407.2	-	
MgH_2 + 10wt.% $Al(OH)_3$			357.3	-	
MgH_2 + 10wt.% $Ca(OH)_2$			340.0	-	
MgH_2 + 10wt.% $CoCl_2$		~88% in 60 min	1481.7	17.59	

1	2	3	4	5	6
MgH_2 + 10wt.% $NiCl_2$	Deionized water		1496.1	-	[32]
MgH_2 + 10wt.% $CuCl_2$			1472.1	-	
MgH_2 + 10wt.% $MgCl_2$			1554.6	-	
MgH_2 + 10wt.% NaCl			540.1	-	
MgH_2 + 10wt.% KCl			590.2	-	
MgH_2 + 10wt.% $CaCl_2$			604.5	-	
H-$CaMg_2$		~72% in 1 min	800	-	[26]
H-$CaMg_{1.9}Ni_{0.1}$		~87% in 5 min	968	32.9	
H–30wt.%Ca-Mg	Water	74.5% in 60 min	~600	-	[36]
H–30wt.%Ca-Mg –5% $MgCl_2$		77.4% in 60 min	~720	-	
H–30wt.%Ca-Mg –10% $MgCl_2$		70.8% in 60 min	~560	-	
H–30wt.%Ca-Mg –15% $MgCl_2$		69% in 60 min	~510	-	
H–30wt.%Ca-Mg –20% $MgCl_2$		70.3% in 60 min	~550	-	
H–30wt.%Ca-Mg –5% $CaCl_2$		83.2% in 60 min	~750	-	
H–30wt.%Ca-Mg –10% $CaCl_2$		81.8% in 60 min	~710	-	
H–30wt.%Ca-Mg –15% $CaCl_2$		81.4% in 60 min	~690	-	

1	2	3	4	5	6
H–30wt.%Ca-Mg–20% $CaCl_2$	Water	76.9% in 60 min	~580	-	[36]
H–Mg – 10 wt.% Ni	3.5 wt.% NaCl	97% in 30 min	-	30.19	[17]
H–Mg – 10 wt.% Fe		81% in 30 min	-	36.09	
H–Mg – 10 wt.% Al		45% in 30 min	-	-	
H–Mg – 10 wt.% Nb_2O_5		57.3% in 30 min	-	31.46	
H–Mg – 10 wt.% V_2O_5		52.5% in 30 min	-	-	
MgH_2	Distilled water	17.2% in 10 min	272	-	[38]
MgH_2 + 5 wt.% TiC–$2TiB_2$		16.8% in 10 min	260	-	
MgH_2 + 5 wt.% $AlCl_3$		30.3% in 10 min	512	-	
MgH_2 + 5 wt.% EDTA		9.6% in 10 min	140	-	
MgH_2		19% in 10 min	335	-	This study
MgH_2 + 5 wt.% $MgCl_2$		33.5% in 10 min	616	-	
MgH_2 + 5 wt.% $MgCl_2$ + 1 wt.% TiC–$2TiB_2$		34.4% in 10 min	633	-	

3. Experimental studies

The nanocrystalline magnesium hydride powder (sample S1) was prepared by a reactive ball milling of Mg powder (Fluka, 99.8%, grit, 50–150 mesh) in hydrogen gas. The milling was performed in a Retsch PM 100 ball mill using high-pressure milling vial commercialized by Evico-magnetics GmbH filled with hydrogen gas (P = 80 bar H_2) and stainless steel balls of 10 mm in diameter each, at a rotation speed of 400 rpm, with a ball-to-powder mass ratio of 65:1. The milling was conducted in two cycles, 90 min milling time and 90 min rest each, i.e. total milling

time of 180 min. The handling of the samples was carried out in a glove box filled with purified argon gas.

In order to study the effect of preparation procedures on the hydrolysis of MgH_2 – $MgCl_2$ composites, the samples were prepared in different ways:

1) mixing of preliminary synthesized MgH_2 with 5 wt.% $MgCl_2$ in an agate mortar for 30 min (sample S2);

2) simultaneous hydrogenation of Mg and its milling with 5 wt.% $MgCl_2$ in a ball mill for 180 min (sample S3);

3) milling of a preliminary synthesized MgH_2 with 5 wt.% $MgCl_2$ in a ball mill for 30 min (sample S4);

4) milling of a preliminary obtained MgH_2 with 5 wt.% $MgCl_2$ and 1 wt.% TiC–2TiB_2 in a ball mill for 30 min (sample S5).

Ball milling of preliminary synthesized MgH_2 with additives was performed in H_2 at 400 rpm for 30 min, while a hand milling in the agate mortar was conducted in a glove box filled with a purified Ar.

The hydrogen generation during the hydrolysis reaction was monitored by using a water replacement method, by using a homemade setup that consists of a reaction volume and gas collecting/measuring components. The reaction part is a 500 mL four-neck glass flask with openings for water addition, insertion of a thermometer, Ar purge gas, and H_2 removal. The reaction part is connected by a silicone tube to the collecting/measuring part, which consists of gas washing bottle, beaker, and electronic balance. The hydrogen drains the water from the gas washing bottle to the beaker placed on the electronic balance. The amount of hydrogen is estimated by the measurements of the mass of the replaced water.

The samples in a form of powders were placed into the flask with subsequent system sealing. After that, the apparatus was purged with argon gas for 5 min, and the flask was filled with distilled water from the pressure-equalizing funnel to start the hydrolysis reaction. All experiments were carried out at room temperature and atmospheric pressure.

The hydrogen generation or conversion yield (%) was defined as the ratio between the actual amount of the produced hydrogen and the theoretical amount that should be released, assuming a completeness of the reaction of the hydride with water.

X-ray powder diffraction (XRD) measurements were performed on a DRON-3 diffractometer with Cu Kα radiation (λ=1.5406 Å) in the 2θ range from 20° to 80° with a scanning rate of 0.15 °/min and a step size of 0,01°.

4. Results and discussion

The XRD analysis of magnesium hydride sample prepared by reactive ball milling of Mg powder under hydrogen pressure reveals that at the selected synthesis parameters a complete hydrogenation of magnesium occurs resulting in the formation of two polymorphic modifications of MgH_2, namely, β-MgH_2 and a high-pressure modification γ-MgH_2. The broad diffraction peaks of the synthesized hydride indicate that the material is nanocrystalline. No Mg peaks were observed in the XRD pattern of the prepared MgH_2.

The hydrogen generation properties by hydrolysis of all samples were studied at room temperature using a distilled water, and corresponding hydrogen generation and conversion rate curves are shown in Fig. 2. According to the Fig. 2a, the hydrolysis reaction of pure MgH_2 (sample S1) is rather sluggish, delivering only 335 mL/g and 419 mL/g hydrogen, while the conversion rate of the hydrolysis reaction reached ~19% and ~24% within 10 min and 20 min, respectively. This slow hydrogen generation rate is not surprising, since the reaction between MgH_2 and water is rapidly interrupted due to the formation of a passive $Mg(OH)_2$ layer on the surface of the MgH_2 particles. The formed $Mg(OH)_2$ layer has low solubility in water and prevents further contact between the water and the hydride.

The hydrolysis kinetics and hydrogen yield of MgH_2 can be increased by addition of the chloride salts, such as $MgCl_2$. $MgCl_2$ is an acidic chloride, and thus, it increases content of H^+, making the corresponding aqueous solution weakly acidic. A large amount of Cl^- and H^+ ions derived from the acid chloride aqueous solution can affect the

$Mg(OH)_2$ layer via both pitting and H^+ corrosion, therefore creating more channels for the reaction between MgH_2 and water [32]. In the case of the MgH_2 + 5 wt.% $MgCl_2$ composite that was prepared by hand mixing of the previously synthesized MgH_2 and $MgCl_2$ in an agate mortar for 30 min (sample S2), the hydrolysis performance improved for about 32% as compared to the individual MgH_2 (Fig. 2). The hydrogen yield of 512 mL/g and conversion rate of 28.8% were observed for the prepared sample after 20 min of hydrolysis (Fig. 2). The insignificant improvement of the hydrolysis performance can be attributed to the insufficient efficiency of the hand mixing by using a mortar. As the result, $MgCl_2$ was inhomogeneously distributed in the MgH_2 powder with only a small fraction of $MgCl_2$ having a good contact with the MgH_2 particles, and thus having a limited contribution to the destabilization of the $Mg(OH)_2$ layer.

Fig. 2. Kinetic curves of hydrogen yield (a) and conversion rate (b) for MgH_2 – $MgCl_2$ composites prepared by various techniques.

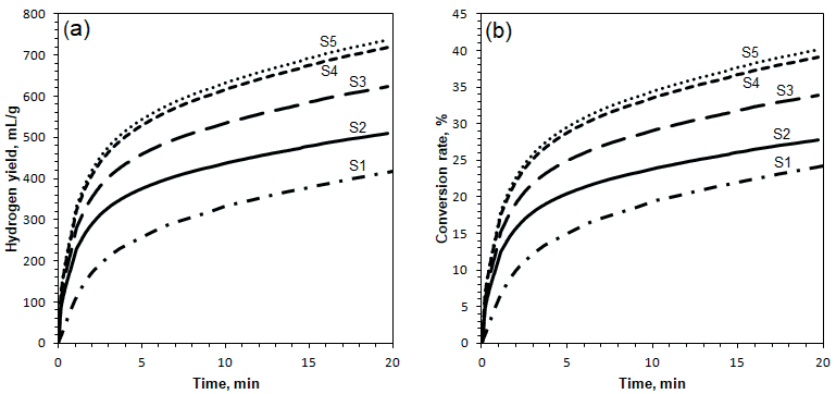

When the MgH_2 + 5 wt.% $MgCl_2$ composite (sample S3) was prepared by a simultaneous hydrogenation of Mg and its mixing with 5 wt.% $MgCl_2$ in a ball mill for 180 min, both hydrogen yield and conversion rate further increased, reaching about 623 mL/g H_2 and 34% in 20 min, respectively (Fig. 2). The enhanced hydrolysis performance is

attributed to the homogeneous distribution of $MgCl_2$ salt over the nanocrystalline MgH_2 particles after the reactive ball milling.

However, the MgH_2 + 5 wt.% $MgCl_2$ composite (sample S4) that was obtained by mixing a preliminary synthesized MgH_2 with 5 wt.% $MgCl_2$ in a planetary ball mill for 30 min showed a much higher hydrolysis efficiency, which was about 15% higher than that of the sample prepared by simultaneous hydrogenation of Mg and its milling with $MgCl_2$. In this case the hydrogen yield of 719 mL/g and a conversion rate of 39.1% were obtained after 20 min of hydrolysis (Fig. 2). In our opinion such improvement of the hydrolysis process can be a result of the "mild" conditions that were realized during the ball milling of preliminary synthesized MgH_2 and $MgCl_2$ powders, and can provide a homogeneous distribution of the materials after 30 min of the milling. In contrast, during the simultaneous hydrogenation of Mg and its milling with $MgCl_2$, the latter can affect the hydrogenation process and/or react with MgH_2 hydride, leading to the reduced hydrogen generation.

The reactivity of the MgH_2 particles with water can be increased by adding hard and brittle powdered materials that improve the efficiency of the ball milling process by decreasing the particle size and by creating more microstructural defects. In this respect, the TiC–$2TiB_2$ composite that was previously studied by us as an additive to MgH_2 [38], can be used for this purpose. However, since the TiC–$2TiB_2$ additive does not participate in the hydrolysis reaction either as a raw material or as a part of a micro-galvanic cell, its amount was limited to 1 wt.%. The hydrolysis performance of the MgH_2 + 5 wt.% $MgCl_2$ + 1 wt.% TiC–$2TiB_2$ composite (sample S5) prepared by mixing previously hydrogenated MgH_2 with 5 wt.% $MgCl_2$ + 1 wt.% TiC–$2TiB_2$ powders in a ball mill for 30 min, is shown in Fig. 2. From Fig. 2, it can be seen that prepared composite demonstrates the highest reactivity among the tested materials and produces 738 mL/g hydrogen in 20 min, which corresponds to the conversion rate of 40.2%. The hydrolysis performance improved by about 5% in comparison with that of the material without 1 wt.% TiC–$2TiB_2$ additive. Thus, the combined effect of the Cl^- and H^+ ions from chloride

aqueous solution and grinding additive is responsible for a significant enhancement of the hydrolysis reaction.

Conclusions

In the present work we have reviewed recent reference publications on the hydrolysis of MgH_2-based materials and current approaches to enhance the hydrolysis performance when utilizing metals, oxides, hydroxides and halides as additives, as well as surfactants. We summarized the recent advances in the work on the hydrolysis of the composites based on magnesium hydride where the most distinct improvements were observed for the various salt additives while the reaction rate appears to depend more on the additive type rather than its concentration. In this study we explored the influence of the preparation procedures on the hydrolysis of MgH_2 – $MgCl_2$ composites, which suggests that milling of MgH_2, preliminary obtained by mechano-chemical synthesis, with the addition of $MgCl_2$ is as a preferred route to achieve advanced hydrolysis performance of the composite.

Acknowledgments

This work was supported by the NATO Programme "Science for Peace and Security" (Project G5233 "Portable Energy Supply").

References

[1] Marbán G., Valdés-Solís T. Towards the hydrogen economy? *Int. J. Hydrogen Energy,* 2007, vol. 32, Issue 12, pp. 1625–1637. https://doi.org/10.1016/j.ijhydene.2006.12.017.

[2] Abdin Z., Zafaranloo A., A. Rafiee, Merida W., Lipinski W., Khalilpour K.R. Hydrogen as an energy vector, *Renew. Sustain. Energy Rev,* 2020, vol. 120, pp. 109620. https://doi.org/10.1016/j.rser.2019.109620.

[3] Eberle U., Felderhoff M., Schuth F. Chemical and physical solutions for hydrogen storage, *Angew. Chem. Int. Ed,* 2009. vol. 48, pp. 6608–6630.

https://doi.org/10.1002/anie.200806293.
[4] Bellosta von Colbe J., Ares J.-R., Barale J., Baricco M., Buckley C., Capurso G., Gallandat N., Grant D.M., Guzik M.N., Jacob I., Jensen E.H., Jensen T., Jepsen J., Klassen T., Lototskyy M.V., Manickam K., Montone A., Puszkiel J., Sartori S., Sheppard D.A., Stuart A., Walker G., Webb C.J., Yang H., Yartys V., Züttel A., Dornheim M. Application of hydrides in hydrogen storage and compression: Achievements, outlook and perspectives, *Int. J. Hydrogen Energy,* 2019, vol. 44, Issue 15, pp. 7780–7808.
https://doi.org/10.1016/j.ijhydene.2019.01.104.
[5] Tegel M., Schone S., Kieback B., Röntzsch L. An efficient hydrolysis of MgH_2-based materials, *Int. J. Hydrogen Energy,* 2017, vol. 42, Issue 4, pp. 2167–2176.
https://doi.org/10.1016/j.ijhydene.2016.09.084.
[6] Ropp R.C. *Encyclopedia of the Alkaline Earth Compounds*, Elsevier, 2013. 1216 p.
[7] Hirscher M., Yartys V.A., Baricco M. *et.al*., Materials for hydrogen-based energy storage – past, recent progress and future outlook, *J. Alloys Compd.,* 2020, vol. 827, pp. 153548.
https://doi.org/10.1016/j.jallcom.2019.153548.
[8] Yartys V.A., Lototskyy M.V., Akiba E. *et.al*., Magnesium based materials for hydrogen based energy storage: Past, present and future. *Int. J. Hydrogen Energy,* 2019, vol. 44, Issue 15, pp. 7809–7859. https://doi.org/10.1016/j.ijhydene.2018.12.212.
[9] Crivello J.-C., Dam B., Denys R.V. *et.al*. Review of magnesium hydride-based materials: development and optimization, *Appl. Phys. A,* 2016, vol. 122, No. 97, pp. 1–20.
https://doi.org/10.1007/s00339-016-9602-0.
[10] Sadhasivam T., Kim H.-T., Jung S., Roh S.-H., Park J.-H., Jung H.-Y. Dimensional effects of nanostructured Mg/MgH_2 for hydrogen storage applications: A review. *Renewable Sustainable Energy Rev.,* 2017, vol. 27, pp. 523–534.
https://doi.org/10.1016/j.rser.2017.01.107.
[11] Wang Y., Wang Y. Recent advances in additive-enhanced magnesium hydride for hydrogen storage, *Prog. Nat. Sci.,* 2017, vol. 27,

Issue 1, pp. 41–49. https://doi.org/10.1016/j.pnsc.2016.12.016.
[12] Sun Y., Shen C., Lai Q., Liu W., Wang D.-W., Aguey-Zinsou K.-F. Tailoring magnesium based materials for hydrogen storage through synthesis: Current state of the art. *Energy Storage Mater.,* 2018, vol. 10, pp. 168–198. https://doi.org/10.1016/j.ensm.2017.01.010.
[13] Manilevich F.D., Pirskyy Yu.K., Danil'tsev B.I., Kutsyi A.V., Yartys V.A. Studies of the hydrolysis of aluminum activated by additions of Ga–In–Sn eutectic alloy, bismuth, or antimony, *Mater. Sci.,* 2020, vol. 55, No. 4, pp. 536–547. https://doi.org/10.1007/s11003-020-00336-x.
[14] Hong S.-H., Kim H.-J., Song M.Y. Rate enhancement of hydrogen generation through the reaction of magnesium hydride with water by MgO addition and ball milling, *J. Ind. Eng. Chem.,* 2012, vol. 18, Issue 1, pp. 405–408. https://doi.org/10.1016/j.jiec.2011.11.104.
[15] Laversenne L., Goutaudier C., Chiriac R., Sigala C., Bonnetot B. Hydrogen storage in borohydrides: Comparison of hydrolysis conditions of $LiBH_4$, $NaBH_4$ and KBH_4. *J. Therm. Anal. Calorim.,* 2008, vol. 94, pp. 785–790. https://doi.org/10.1007/s10973-008-9073-4.
[16] Tayeh T., Awad A.S., Nakhl M., Zakhour M., Silvain J.-F., Bobet J.-L. Production of hydrogen from magnesium hydrides hydrolysis, *Int. J. Hydrogen Energy*, 2014, vol. 39. pp. 3109–3117. https://doi.org/10.1016/j.ijhydene.2013.12.082.
[17] Awad A.S., El-Asmar E., Tayeh T., Mauvy F., Nakhl M., Zakhour M., Bobet J.L. Effect of carbons (G and CFs), TM (Ni, Fe, and Al) and oxides (Nb_2O_5 and V_2O_5) on hydrogen generation from ball milled Mg-based hydrolysis reaction for fuel cell, *Energy,* 2016, vol. 95, pp. 175–186. https://doi.org/10.1016/j.energy.2015.12.004.
[18] Zou M.S., Yang R.J., Guo X.Y., Huang H.T., He J.Y., Zhang P. The preparation of Mg-based hydro-reactive materials and their reactive properties in seawater, *Int. J. Hydrogen Energy,*2011, vol. 36, Issue 11, pp. 6478–6483. https://doi.org/10.1016/j.ijhydene.2011.02.108.
[19] Li S., Gan D.-Y., Zhu Y.-F., Liu Y.-N., Zhang G., Li L.-Q. Influence of chloride salts on hydrogen generation via hydrolysis of MgH_2 prepared by hydriding combustion synthesis and mechanical milling, *Trans. Nonferrous Met. Soc. China,* 2017, vol. 27, pp. 562–568.

https://doi.org/10.1016/S1003-6326(17)60062-1.
[20] Huang J.M., Duan R.M., Ouyang L.Z., Wen Y.J., Wang H., Zhu M. The effect of particle size on hydrolysis properties of Mg_3La hydrides, *Int. J. Hydrogen Energy,* 2014, vol. 39, Issue 25, pp. 13564–13568. https://doi.org/10.1016/j.ijhydene.2014.04.024.
[21] Huang J.M., Ouyang L.Z., Wen Y.J., Wang H., Liu J.W., Chen Z.L., Zhu M. Improved hydrolysis properties of Mg_3RE hydrides alloyed with Ni. *Int. J. Hydrogen Energy,* 2014, vol. 39, Issue 13, pp. 6813–6818. https://doi.org/10.1016/j.ijhydene.2014.02.155.
[22] Xiao Y., Wu C.L., Wu H.W., Chen Y.G. Hydrogen generation by CaH_2-induced hydrolysis of $Mg_{17}Al_{12}$ hydride, *Int. J. Hydrogen Energy,* 2011, vol. 36, Issue 24. pp. 15698–15703.
https://doi.org/10.1016/j.ijhydene.2011.09.022.
[23] Liu P.P., Wu H.W., Wu C.L., Chen Y.G., Xu Y.M., Wang X.L., Zhang Y.B. Microstructure characteristics and hydrolysis mechanism of Mg-Ca alloy hydrides for hydrogen generation, *Int. J. Hydrogen Energy,* 2015, vol. 40, Issue 10, pp. 3806–3812.
https://doi.org/10.1016/j.ijhydene.2015.01.105.
[24] Mao J.W., Huang T.P., Panda S., Zou J.X., Ding W.J. Direct observations of diffusion controlled microstructure transition in Mg-In/Mg-Ag ultrafine particles with enhanced hydrogen storage and hydrolysis properties, *Chem. Eng. J.,* 2021, vol. 418, pp. 129301. https://doi.org/10.1016/j.cej.2021.129301.
[25] Adeniran J.A., Akbarzadeh R., Lototskyy M., Nyallang Nyamsi S., Olorundare O.F., Akinlabi E.T., Jen T.C. Phase-structural and morphological features, dehydrogenation/re-hydrogenation performance and hydrolysis of nanocomposites prepared by ball milling of MgH_2 with germanium, *Int. J. Hydrogen Energy,* 2019, vol. 44, Issue 41, pp. 23160–23171. https://doi.org/10.1016/j.ijhydene.2019.06.119.
[26] Ma M.L., Duan R.M., Ouyang L.Z. Zhu X.K., Peng C.H., Zhu M. Hydrogen generation via hydrolysis of H-$CaMg_2$ and H-$CaMg_{1.9}Ni_{0.1,}$ *Int. J. Hydrogen Energy,* 2017, vol. 42, Issue 35. P. 22312–22317. https://doi.org/10.1016/j.ijhydene.2017.05.159.

[27] Jiang J., Ouyang L.Z,, Wang H., Liu J.W., Shao H.Y., Zhu M. Controllable hydrolysis performance of MgLi alloys and the hydrides, *ChemPhysChem*., 2019, vol. 20, Issue 10, pp. 1316–1324. https://doi.org/10.1002/cphc.201900058.

[28] Naseem K., Zhong H., Wang H., Ouyang L.Z., Zhu M. Promoting hydrogen generation via co-hydrolysis of Al and MgH_2 catalyzed by Mo and B_2O_3, *J. Alloys Compd.,* 2021, vol. 888, pp. 161485. https://doi.org/10.1016/j.jallcom.2021.161485.

[29] Hong S.H., Kim H.J., Song M.Y. Rate enhancement of hydrogen generation through the reaction of magnesium hydride with water by MgO addition and ball milling, *J. Ind. Eng. Chem*., 2012, vol. 18, Issue 1. pp. 405–408. https://doi.org/10.1016/j.jiec.2011.11.104.

[30] Yang B., Zou J.X, Huang T.P., Mao J.F., Zeng X.Q., Ding W.J. Enhanced hydrogenation and hydrolysis properties of core-shell structured Mg-MO_x (M=Al, Ti and Fe) nanocomposites prepared by arc plasma method, *Chem. Eng. J.,* 2019, vol. 371, pp. 233–243. https://doi.org/10.1016/j.cej.2019.04.046.

[31] Yang K., Qin H.Y., Lv J.N., Yu R.J, Chen X., Zhao Z.D., Li Y.J., Zhang F., Xia X.C., Fu Q., Wang M. The effect of graphite and Fe_2O_3 addition on hydrolysis kinetics of Mg-based hydrogen storage materials, *Int. J. Photoenergy.,* 2021, vol. 2021, pp. 6651541.
https://doi.org/10.1155/2021/6651541.

[32] Zhou C., Zhang J.G., Zhu Y.F., Liu Y., Li L.Q. Controllable hydrogen generation behavior by hydrolysis of MgH_2-based materials, *J. Power Sources,* 2021, vol. 494, pp. 229726.
https://doi.org/10.1016/j.jpowsour.2021.229726.

[33] Sevastyanova L.G., Klyamkin S.N., Bulychev B.M. Generation of hydrogen from magnesium hydride oxidation in water in presence of halides. *Int. J. Hydrogen Energy,* 2020, vol. 45, Issue 4, pp. 3046– 3052. https://doi.org/10.1016/j.ijhydene.2019.11.226.

[34] Coşkuner Filiz B. Investigation of the reaction mechanism of the hydrolysis of MgH_2 in $CoCl_2$ solutions under various kinetic conditions, *Reac. Kinet. Mech. Cat.,* 2021, vol. 132, pp. 93–109.

https://doi.org/10.1007/s11144-020-01923-4.
[35] Gan D.Y., Liu Y., Zhang J.G., Zhang Y., Cao. C.T., Zhu Y.F., Li L.Q. Kinetic performance of hydrogen generation enhanced by $AlCl_3$ via hydrolysis of MgH_2 prepared by hydriding combustion synthesis, *Int. J. Hydrogen Energy,* 2018, vol. 43, Issue 22, pp. 10232– 10239. https://doi.org/10.1016/j.ijhydene.2018.04.119.
[36] Li J.F., Liu P.P., Wu C.L., Chen Y.G. Common ion effect in the hydrolysis reaction of Mg–Ca alloy hydride-salt composites, *Int. J. Hydrogen Energy,* 2017, vol. 42, Issue 2, pp. 1429– 1435. https://doi.org/10.1016/j.ijhydene.2016.06.006.
37] Zhong S.A., Wu C.L., ChenY.G., Feng Z., ZhaoY., Xia Y.T. Enhanced hydrolysis performance and the air-stability of Mg-Ca hydride-chloride composites, *J. Alloys Compd.*, 2019, vol. 792, pp. 869–877. https://doi.org/10.1016/j.jallcom.2019.03.394.
[38] Korablov D.S., Bezdorozhev O.V., Gierlotka S., Yartys V.A., Solonin Yu.M. Effect of various additives on the hydrolysis performance of nanostructured MgH_2 synthesized by high-energy ball milling in hydrogen, *Powder Metall. Met. Ceram.,* 2021, vol. 59, pp. 483–490. https://doi.org/10.1007/s11106-021-00193-6.
[39] Chen et al. Chen Y.Y., Wang M., Guan F.G., Yu R.J., Zhang Y.Y., Qin H.Y., Chen X., Fu Q., Wang Z.Y. Study on hydrolysis of magnesium hydride by interface control, *Int. J. Photoenergy,* 2020, vol. 2020, pp. 8859770.
https://doi.org/10.1155/2020/8859770.

Activated aluminum for hydrogen generation from water

F. Manilevich[1], Yu. Pirskyy[1], A. Kutsyi[1], V. Berezovets[2], V. Yartys[3]

[1]*Vernadsky Institute of General & Inorganic Chemistry, NASU, Kyiv, Ukraine*
[2]*Karpenko Physico-Mechanical Institute, NASU, Lviv, Ukraine,*
[3]*Institute for Energy Technology, Kjeller, Norway*

Al-based alloys and mechanochemically activated aluminum powders were prepared in this study, and the regularities of their hydrolysis reaction with water were studied. Aluminum alloys were prepared by melting aluminum with additions of Ga–In–Sn eutectic (5 wt.%), bismuth (3 wt.%), antimony (3 wt.%), or zinc (3 wt.%). The temperature-dependent kinetics of their hydrolysis in a temperature range 25–70 °C was studied by using a volumetric technique. The most efficient activation of the hydrolysis process was achieved for the Al–Ga–In–Sn-Zn alloy, particularly at low temperatures (5 and 25° C). The addition of bismuth to the Al–Ga–In–Sn alloy significantly decreases the hydrolysis rate, whereas the addition of antimony has only a weak effect on the process, despite the fact that the standard electrode potentials of bismuth and antimony have rather close values.

Commercially available aluminum PA-4 and ASD-1 powders were mechanochemically activated by Ga–In–Sn or Ga–In–Sn–Zn eutectic alloys (5 wt.%) and graphite (1–3 wt.%) in a mixer type ball mill. Subsequently, they were pressed (P = 4 MPa) into the pellets, which were used to generate hydrogen from water via the hydrolysis process. X-ray diffraction study of the milled PA-4 powder revealed the presence of four phases, including aluminum, graphite, and two In–Sn intermetallic compounds (In_3Sn and $In_{1-x}Sn_x$, were $x \approx 0.04$). The quantitative analysis by EDX showed a uniform distribution of the activating additives over the pellet surface, while the graphite was partly aggregated. Studies on the hydrolysis kinetics when utilizing Al-based pellets demonstrated that the process readily proceeds at temperatures ≥ 5° C. At the same time, the efficiency of hydrogen generation depends on the amount of the added graphite, particle size of aluminum powders, duration and medium of their mechanochemical treatment, and the hydrolysis temperature.

Keywords: *Aluminum alloys, Activated aluminum powders, Hydrolysis, Hydrogen generation.*

Introduction

During the past decades, hydrogen power industry, which is aimed on the use of hydrogen as an energy carrier and as a fuel, has been actively developing [1-3]. Particularly, the demand for fuel cells for various purposes, when electric current is generated as a result of the anodic oxidation of hydrogen and corresponding cathodic process, has been greatly increased. Broadening of the application scopes and increasing of the used amount of hydrogen call for improving technologies of its production, transportation and storage. Despite free hydrogen is not naturally available, it is however obtained from a variety of its compounds, first of all from water and hydrocarbons.

Among the known methods of hydrogen production, hydrolysis of so-called energy-storage substances (ESSs) [4] deserves special attention because the obtaining of hydrogen from water using ESSs can be carried out directly at the place of its use, which allows avoiding challenges associated with its accumulation, storage and transportation. The most efficient ESSs are binary and complex metal hydrides (MgH_2, $NaBH_4$, $LiBH_4$ etc.) and light metals (Al, Mg etc.) or their alloys.

Aluminum has a number of obvious advantages for use as an ESS, however, it must be activated in order to destroy the integrity of the protective oxide film on its surface. Depending on conditions, the unoxidized aluminum readily and rapidly reacts with water according to the following equations:

$$2Al + 3H_2O = Al_2O_3 \text{ (oxide)} + 3H_2 + 15.1 \text{ MJ/kg Al}, \quad (1)$$

$$2Al + 4H_2O = 2AlOOH \text{ (boehmite)} + 3H_2 + 15.5 \text{ MJ/kg Al}, \quad (2)$$

$$2Al + 6H_2O = 2Al(OH)_3 \text{ (bayerite)} + 3H_2 + 16.3 \text{ MJ/kg Al}. \quad (3)$$

All these reactions are exothemic. The amount of hydrogen evolving from water is 1244 L H_2/kg Al or equivalently 0.111 kg H_2/kg Al.

Various mechanical, mechanochemical and chemical methods of activating aluminum are broadly utilized [5, 6]. In our studies, the alloys of aluminum with low-melting and electropositive metals, as well as pellets made from aluminum powders, mechanochemically activated by low-melting metals and graphite were prepared, and regularities of their hydrolysis were studied.

Materials and Experimental procedures

Aluminum alloys with the additives of activating metals (eutectic Ga-In-Sn alloy, Bi, Sb, Zn) were prepared in a resistance electric furnace in an argon atmosphere with mechanical stirring. All used metals were of high purity (≥ 99.9 wt.%). The eutectic Ga-In-Sn alloy with mass fractions of the components of 67/22/11 % has a melting point of 10.7 ± 0.3 °C [7]. The regularities of hydrogen evolution during the interaction of the obtained alloys (1 g samples) with water were studied by periodically measuring the volume of hydrogen formed using a volumetric unit, which consisted of a thermostated reactor containing 100 mL of distilled water, an eudiometer and a connecting tube. The measured values of the volume of the released hydrogen gas were normalized to the normal conditions.

Mechanochemical activation of aluminum powders PA-4 (grain size ≤ 100 μm) and ASD-1 (grain size < 30 μm) by Ga-In-Sn or Ga–In–Sn–Zn eutectic alloys and graphite was performed in a SPEX SamplePrep 8000D® mixer ball mill (2 hardened steel vials, 2 steel balls in each vial, mass of one ball of 1 g, ball-to-mixture mass ratio of 1 : 1) in an argon atmosphere for 1, 2 or 4 hours. The melting point of eutectic Ga–In–Sn-Zn alloy with mass fractions of the components of 61/25/13/1 % is ≈ 3 °C [8].

X-ray diffraction patterns of activated Al powders were obtained using a powder X-ray diffractometer DRON-3.0 with Cu-K_α radiation. A full-profile refinement of lattice parameters was performed by the Rietveld method using the Fullprof software package [9, 10]. The surface morphology and composition of prepared pellets were studied using a Zeiss EVO 40XVP scanning electron microscope with an INCA Energy microanalysis system.

The obtained powders were compressed into the pellets (P = 4 MPa, ⌀ = 1 cm, m = 0.2 or 0.3 g) in a protective atmosphere of argon gas. The main elements of volumetric unit, used to control the volume of hydrogen released during the hydrolysis of aluminum, included a thermostated reactor with distilled water and a flowmeter SmartTrak® M100L.

Results and Discussion

Aluminum alloys, containing 3-10 wt.% of eutectic Ga-In-Sn alloy, started the hydrolysis reaction already at a temperature of 25 °C. The increase in the mass fraction of Ga-In-Sn eutectic in the aluminum alloy from 3 to 10 % led to a significant acceleration of the hydrolysis of aluminum (see Fig. 1). During the first minutes of the reaction, active cracking and grinding of the alloys took place, after which the hydrolysis of aluminum proceeded almost to the end, while its rates accelerated for the alloy samples containing a higher eutectic content. The metals of the activating eutectic did not participate in the hydrolysis reaction [11].

Therefore, doping aluminum by small amounts of Ga, In and Sn, forming the eutectic alloy, provides an efficient ESSs that can be widely used to release hydrogen from water under ambient conditions. However, hydrogen evolution rate varies greatly during the hydrolysis of aluminum based alloys, and the hydrolysis is accompanied by a significant heating of the reaction mixture when there is no external cooling.

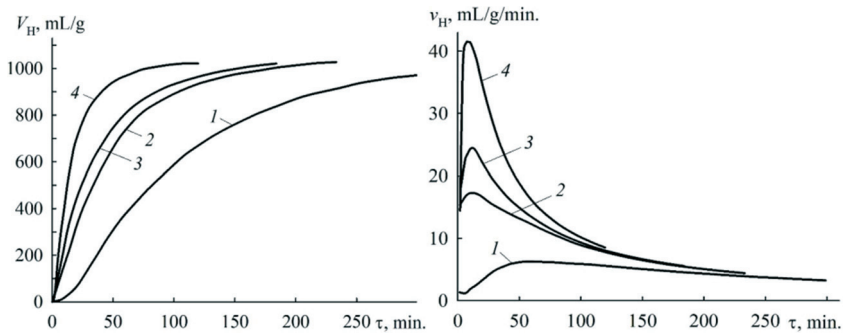

Fig. 1. Time dependencies of the volume of the evolved hydrogen (a) and average hydrogen evolution rate (b) during the hydrolysis at 25 °C of the aluminum alloys with mass fractions of eutectic Ga-In-Sn alloy (%): 3 (1); 5 (2); 7 (3); 10 (4)

The introduction of the Bi or Sb additives (3 wt.%) into the alloy of aluminum with the Ga-In-Sn eutectic (5 wt.%) differently affected the course of the hydrolysis of aluminum. In the presence of bismuth in the aluminum based alloy, the rate of hydrolysis decreased significantly,

while the presence of antimony did not significantly affect its course, although the standard electrode potentials of bismuth and antimony have similar values (see Fig. 2). Obviously, the electrochemical properties of the Bi or Sb additives do not have a significant influence on the regularities of interaction of aluminum with water. The increase in temperature from 25 to 70 °C led to a significant increase in the rate of hydrolysis of aluminum for all investigated alloys [12].

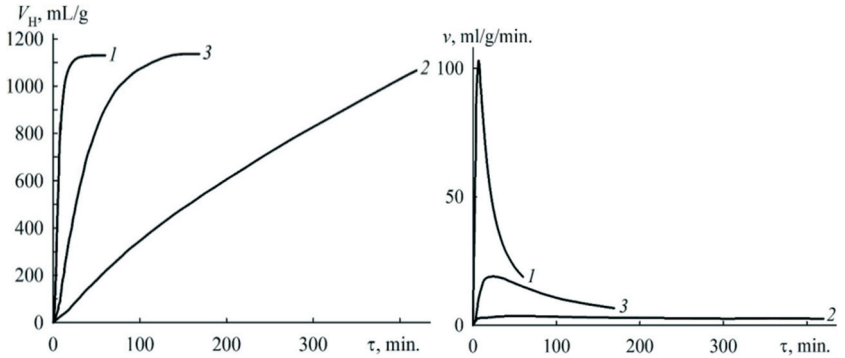

Fig. 2. Time dependencies of the volume of the evolved hydrogen (*a*) and average hydrogen evolution rate (*b*) during the hydrolysis at 55 °C of the aluminum alloys with 5 wt.% of eutectic Ga-In-Sn alloy (*1*) and 3 wt.% of Bi (2) or Sb (3)

It should be noted that during the hydrolysis of aluminum, doped with the Ga-In-Sn eutectic and bismuth, the generation of hydrogen occurred at almost constant rates for a long period of time, which is important to achieve a stable hydrogen supply to a fuel cell.

When zinc (3 wt.%) was used as an additional additive to the aluminum alloy with the Ga-In-Sn eutectic (5 wt.%), the rate of hydrogen evolution from water significantly increased, particularly at low hydrolysis temperatures (25 and 40 °C) (see Fig. 3) [13]. Thus, the change in the composition of the alloying additives to the aluminum-based alloys allows one to significantly change the regularities of aluminum hydrolysis and the productivity of hydrogen generation. According to the results of the X-ray diffraction phase analysis, the main component of the hydrolysis products of the investigated Al-based ESS is

boehmite. In addition, the products include bayerite and small amounts of alloying metals, which do not participate in the hydrolysis reaction [13].

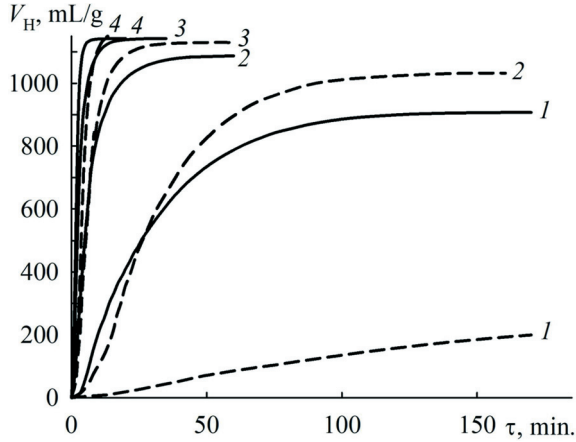

Fig. 3. Time dependencies of the volume of the evolved hydrogen during the hydrolysis of the aluminum alloys with 5 wt.% of eutectic Ga-In-Sn alloy (---) and 3 wt.% of Zn (—) at temperatures (°C): 25 (1); 40 (2); 55 (3); 70 (4)

The hydrolysis of aluminum is a heterogeneous reaction, and its rate depends on the interface area between the reagents. Therefore, an obvious way to achieve a high rate of hydrogen generation is by using the pre-activated fine powders of aluminum. Analysis of the published reference data shows that the kinetics of interaction of the activated aluminum powders with water depends on the activation method, the amount and composition of the activating substances used, size and morphology of the powders and the temperature of the process, further to the amount of the reagents, in particular, water. In our studies, aluminum powders PA-4 and ASD-1 were mechanochemically activated by the eutectic Ga-In-Sn or Ga-In-Sn-Zn alloys (5 wt.%) and graphite (1-3 wt.%), then compressed into the pellets. X-ray phase analysis of the non-pressed activated PA-4 powder showed presence of the phases of aluminum and graphite as well as intermetallic compounds of indium and tin (In_3Sn and $In_{1-x}Sn_x$ ($x \approx 0.04$)). SEM micrographs of the pellet surface showed the well developed interfaces between the compressed aluminum

grains. According to the energy dispersive X-ray analysis, the distribution of activating elements in the pellet surface was very uniform, but the graphite was partially aggregated [14].

The kinetics studies of the hydrolysis of activated aluminum powders used in the form of the pellets showed that the use of graphite as an additional activating additive led to an increase in the rate of the hydrolysis for more than an order of magnitude (see Fig. 4).

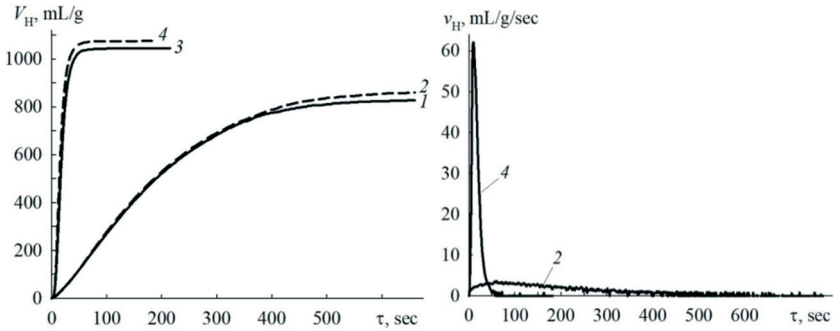

a b

Fig. 4. Time dependencies of the volume of the evolved hydrogen (*a*) and average hydrogen evolution rate (*b*) during the hydrolysis of the pellets from PA-4 powder activated during 4 h with following additives: Ga–In–Sn (5 wt.%) (*1*, *2*); Ga–In–Sn (5 wt.%) + graphite (3 wt.%) (*3*, *4*); hydrolysis temperature 25 °C, m_{pellet} = 0.2 (*1*, *3*) and 0.3 g (*2*, *4*)

Based on the data presented in Fig. 4*a*, the values of the hydrogen yield were calculated as related to the theoretically limiting volumes of the evolved hydrogen. The reached values of the hydrogen yield were: 70 % (1); 73 % (2); 91 % (3); 94 % (4) (see Fig 4*a*). From Fig. 6*a* it is also clear that an increase in the weight of the pellets from 0.2 g to 0.3 g led to a slight increase in the hydrolysis rate and hydrogen yield.

The difference in the values of the melting point of eutectic alloys Ga-In-Sn and Ga-In-Sn-Zn is about 8 °C, but the replacement of one alloy with another one during the mechanochemical activation of aluminum powders together with graphite did not lead to a considerable change in the rate of the hydrolysis of aluminum from activated and compressed

powders as well as the hydrogen yield. Apparently, the amounts of the used eutectic alloys (5 wt.%) were too small to identify the effect of the difference in their melting points on the regularities of the hydrolysis of aluminum from the prepared pellets [14].

The influence of the amount of graphite in the prepared pellets and the temperature of their hydrolysis on the rate of hydrogen evolution can be estimated from the dependencies shown in Fig. 5. It is seen that the evolution of hydrogen during the active stage of aluminum hydrolysis from pellets of PA-4 powder mechanochemically activated by Ga-In-Sn eutectic is accelerated with an increase in the amount of graphite and temperature.

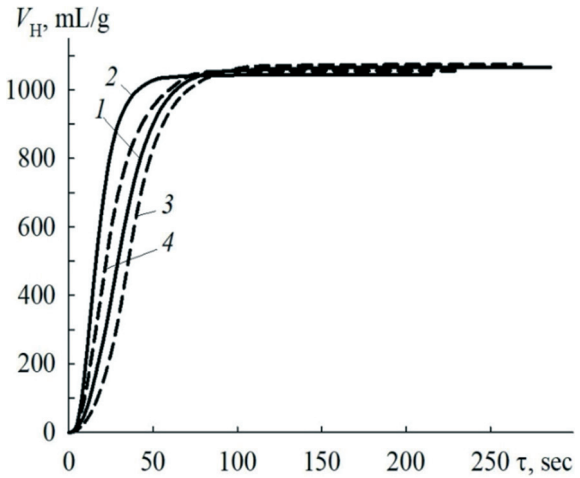

Fig. 5. Time dependencies of the volume of the evolved hydrogen during the hydrolysis of the pellets from PA-4 activated for 4 h using Ga–In–Sn eutectic alloy (5 wt.%) with 3 (1, 2) and 1 wt.% of graphite (3, 4); hydrolysis temperature 5° C (1, 3) and 25° C (2, 4), m_{pellet} = 0.2 g

It should be noted that PA-4, activated and compressed as described above, actively reacts with water already at a temperature of 5 °C. The effect of the grain size of the aluminum powders on the performance of the hydrogen evolution during hydrolysis of the pellets prepared from the both powders, which were mechanochemically activated by 5 wt.% of Ga-In-Sn-Zn eutectic and 3 wt.% of graphite, is

shown in Fig. 6. It can be seen that replacing a coarser PA-4 powder with a finer ASD-1 powder led to the higher rate of the hydrogen evolution and hydrogen yield.

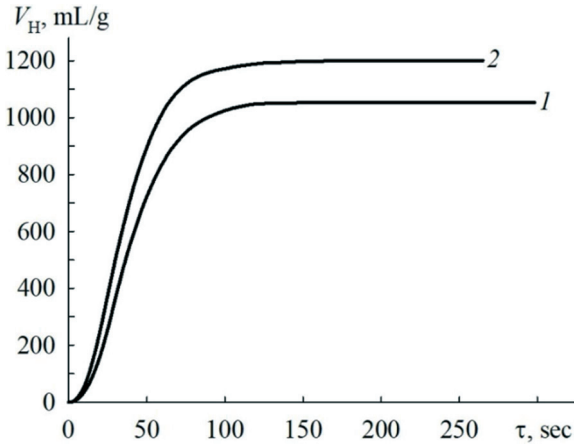

Fig. 6. Time dependencies of the volume of the evolved hydrogen during the hydrolysis of the pellets from PA-4 (1) and ASD-1 (2) powders activated by Ga–In–Sn–Zn (5 wt.%) + graphite (3 wt.%) during 4 h; hydrolysis temperature 5° C, m_{pellet} = 0,3 g

Our studies have shown that the duration of mechanochemical activation of aluminum powders also affects their activity in the hydrolysis process. As it follows from the Fig. 7, increasing the duration of the treatment of the ASD-1 powder together with 5 wt.% of Ga-In-Sn eutectic and 3 wt.% of graphite in the mill from 1 to 4 hours resulted in a significant increase in the rate of the hydrolysis of the aluminum from the prepared pellets and the hydrogen yield [14].

A medium, in which the powders were treated, also influenced their activity during hydrolysis. According to Fig. 8, the rate of hydrogen evolution and its yield during hydrolysis of PA-4 powder mechanochemically activated by Ga-In-Sn-Zn eutectic (5 wt.%) and graphite (3 wt.%) in air were lower, than during the hydrolysis of the same powder activated in an argon atmosphere.

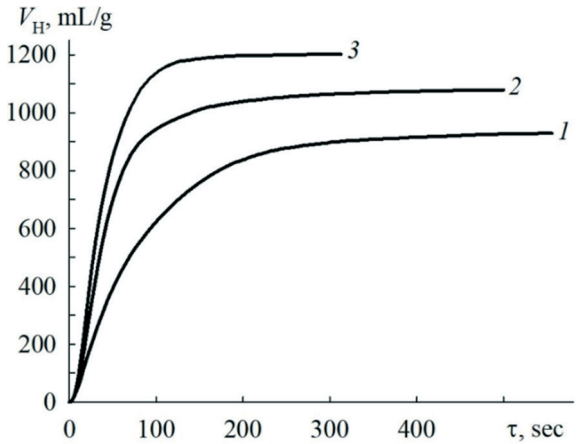

Fig. 7. Time dependencies of the volume of the evolved hydrogen during the hydrolysis of the pellets from ASD-1 activated by Ga–In–Sn (5 wt.%) + graphite (3 wt.%) during 1 (*1*), 2 (*2*), and 4 h (*3*); hydrolysis temperature 5 °C, m_{pellet} = 0.2 g

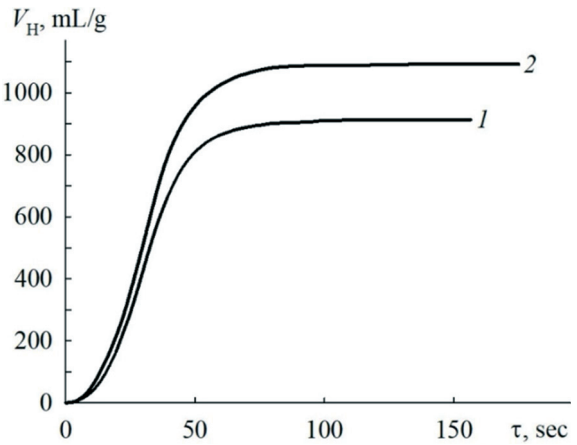

Fig. 8. Time dependencies of the volume of the evolved hydrogen during the hydrolysis of the pellets from PA-4 activated by Ga–In–Sn-Zn (5 wt.%) + graphite (3 wt.%) during 4 h in air (*1*) and in argon (*2*); hydrolysis temperature 5 °C, m_{pellet} = 0.2 g

Thus, hydrogen evolution during the hydrolysis of the pellets prepared from the aluminum powders mechanochemically activated by low-melting metals and graphite depends on many parameters. It is important that such materials actively release hydrogen from water at temperatures of ≥ 5 °C and can be used in autonomous hydrogen generators of hydrolysis type for various purposes.

Conclusions

The activation of aluminum by the alloying with small quantities of the Ga–In–Sn eutectic alloy, bismuth, antimony, or zinc dramatically improves the performance of the individual Al metal used for generating gaseous hydrogen as a result of the hydrolysis process at temperatures of ≥ 25 °C. The variations in the qualitative and quantitative composition of the alloying additives to the aluminum-based alloys allows to significantly change the regularities of aluminum hydrolysis and the productivity of hydrogen generation.

Mechanical grinding of PA-4 and ASD-1 aluminum powders with additions of Ga-In-Sn or Ga-In-Sn-Zn eutectic alloys and graphite, followed by pressing the obtained activated powders into pellets, makes it possible to obtain materials capable of intensively evolving hydrogen from water at temperatures down to 5 °C. The hydrolysis of the aluminum powders, treated in such a way, occurs quickly and almost completely. The performance of aluminum pellets during their hydrolysis and hydrogen generation becomes significantly more efficient with increasing graphite content in the pellets and duration of the mechanochemical treatment of the powders in argon atmosphere as well as with decreasing grain size of the aluminum powders and increasing the hydrolysis temperature.

The investigated Al-based ESSs are promising for use in hydrolysis-type hydrogen generators of various performance parameters and purposes without an additional heating of the reaction mixture. Taking into account the peculiarities of the hydrolysis of such ESSs, it is possible to use aluminum alloys in hydrogen generators as disposable cartridges, for example, when charging batteries of mobile electronic devices, while dosing of the pellets made from activated aluminum

powders can provide long-term operation of autonomous current sources based on fuel cells and hydrogen generators of hydrolysis type.

Acknowledgment

This work was supported by the NATO Programme "Science for Peace and Security" (Project G5233 "Portable Energy Supply").

References

[1] Kozin L.H., Volkov S.V., Skryptun I.N. Modern Hydrogen Energetics and Ecology. K.: Akademperiodyka, 2019. 364 p.
[2] Tarasov B.P. and Lototskyi M. V. Hydrogen energetics: past, present, and prospects. *Russ. Khim. Zh*., 2006, vol. 50, No. 6, pp. 5-18.
[3] Goltsov V. A. Veziroglu T. N., Goltsova L. F. Hydrogen civilization of the future - A new conception of the IAHE. *Int. J. Hydrogen Energy,* 2006, vol. 31, No. 2, pp. 153-159.
[4] Varshavskyi I.L. *Energy-Accumulating Substances and Their Applications* [in Russian]. K.: Nauk. Dumka, 1980. 240 p.
[5] Ziebarth J.T., Woodall J.M., Kramer R.A., Choi G. Liquid phase-enabled reaction of Al-Ga and Al-Ga-In-Sn alloys with water. *Int. J. Hydrogen Energy,* 2011, vol. 36, No 9, pp. 5271-5279.
[6] Shkolnikov E.I., Zhuk A.Z., Vlaskin M.S. Aluminum as energy carrier: Feasibility analysis and current technologies overview, *Renewable and Sustainable Energy Reviews,* 2011, vol. 15, No 9, pp. 4611-4623.
[7] Plevachuk Yu., Sklyarchuk V., Eckert Sv., Gerbeth G., Novakovic R. Thermophysical Properties of the Liquid Ga−In−Sn Eutectic Alloy, *J. Chem. Eng. Data,* 2014. vol. 59, No 3, pp. 757-763.
[8] Grin Yu.N., Gladyshevskij R.E. *Gallides* [in Russian]. M.: Metallurgiya, 1989. 304 p.
[9] Rietveld H.M. A profile refinement method for nuclear and magnetic structures. *J. Appl. Crystallogr,* 1969, vol. 2, No. 2, pp. 65−71.
[10] Rodriguez-Carvajal J. Recent advances in magnetic structure determination by neutron powder diffraction, *Physica B: Condensed Matter.,* 1993, vol. 192, No. 1–2, pp. 55–69.
[11] Manilevich F.D., Kozin L.Kh., Danil'tsev B.I., Kutsyi A.V., Pirskyy Yu. K. Regularities of the hydrolysis of aluminum activated with the

eutectic alloy of gallium, indium, and tin. *Ukr. Khim. Zh,.* 2017, vol. 83, No. 7, pp. 51-59 [in Ukrainian].
[12] Manilevich F.D., Pirskyy Yu.K., Danil'tsev B.I., Kutsyi A.V., Yartys V.A. Studies of the hydrolysis of aluminum activated by additions of Ga–In–Sn eutectic alloy, bismuth or antimony, *Mater. Sci*., 2020, vol. 55, No. 4, pp. 536–547.
[13] Manilevich F.D., Pirskyy Yu.K., Kutsyi A.V., Danil'tsev B.I. Regularities of hydrolysis of aluminum activated by Ga-In-Sn eutectic alloy and zinc, *Ukr. Khim. Zh.,* 2020, vol. 86, No. 2, pp. 63-77 [in Ukrainian].
[14] Manilevich F.D., Pirskyy Yu.K., Kutsyi A.V., Berezovets V.V., Yartys V.A. Studies of mechanochemically activated aluminum powders for generating hydrogen from water. *Powder Metallurgy,* 2021, No. 5/6, pp. 14-24.

Ni-, Co- and Pt-based nanocatalysts for hydrogen generation via hydrolysis of $NaBH_4$

V. Yartys[1], I. Zavaliy[2], A. Kytsya[2,3], V. Berezovets[2], Yu. Pirskyy[4], F. Manilevich[4], Yu. Verbovytskyy[2], P. Lyutyy[2]

[1]*Institute for Energy Technology, Kjeller, Norway*

[2]*Karpenko Physico-Mechanical Institute NASU, Lviv, Ukraine*

[3]*Department of Physical Chemistry of Fossil Fuels InPOCC, NASU, Lviv, Ukraine*

[4] *Vernadsky Institute of General & Inorganic Chemistry, NASU, Kyiv, Ukraine*

Ni-, Co- and Pt-based nanostructures were prepared via different physical-chemical methods and tested as the catalysts of hydrolysis of $NaBH_4$. Ni-Co bimetallic nanoparticles with different Ni-Co ratios were synthesized by the modified polyol method via the reduction of in situ precipitated slurries of Ni and Co hydroxides by hydrazine in ethylene glycol solutions. It was found that a Ni-Co nanoparticles with the equal Ni/Co content and mean size of 130 nm are a more active catalyst as compared to $Ni_{75}Co_{25}$ and $Ni_{25}Co_{75}$ nanopowders and provide a constant rate of hydrogen evolution up to the full conversion of $NaBH_4$. Zeolite supported Ni- and Co-based nanostructures (Ni-Z and Co-Z) as a convenient in use alternative to the metallic nanoparticles were synthesized via two-stage procedure consisted of adsorption of Ni^{2+} or Co^{2+} ions by zeolite from the aqueous solutions followed by the reduction of the adsorbed cations by $NaBH_4$. Using SEM and EDX it was found that such method of synthesis provide the uniform distribution of 50 – 100 nm metallic nanopaticles both on the surface and in the bulk of the carrier due to the high cation-exchange capacity of the aluminosilicates. It was found that Co-Z catalyst is more active compared to Ni-Z and in studied conditions provides the H_2 evolution rate close to 1450 mL/min per 1 g of precipitated metal. Various Pt-based nanocomposites were obtained by polyol synthesis and subsequently deposited on the carriers (carbon cloth or cordierite) as well as via a platinum electrodeposition on the titanium crump. It was found that the most efficient catalyst of the hydrolysis of $NaBH_4$ is a cordierite-supported nanodispersed Pt which is able to maintain operation of a 30 W battery of fuel cells for 9-10 hours when using for the hydrolysis 1.1 L of 10 % $NaBH_4$ solution.

***Keywords**: $NaBH_4$ hydrolysis, nanocatalysts; Pt nanoparticles; Ni nanoparticles; Co nanoparticles; Zeolite.*

Introduction

Using hydrogen as an energy carrier allows to develop portable energy systems offering benefits of application in autonomous and compact energy sources. In such systems hydrogen is obtained directly at the place of its use, which eliminates the need for its storage and transportation. In recent years, special attention has been paid to the hydrides as a compact and efficient form of hydrogen storage [1]. Among them, sodium borohydride ($NaBH_4$) occupies a special place due to the high content of hydrogen (10.8 wt.% H), reasonable price, stability in alkaline solutions. Like many metal hydrides, it undergoes hydrolysis reaction in presence of water, releasing hydrogen and forming sodium metaborate $NaBO_2$ as a product. The use of catalysts maintains a controlled generation of hydrogen at room temperature.

Several reviews were devoted to a description of different classes of catalysts where their feasibility and conditions of use was systematically analyzed [2-7]. The largest group of catalysts is heterogeneous catalysts containing transition metals. Transition metals include more than 20 elements, among which a significant attention is paid to cobalt, nickel, ruthenium and platinum. Elementary catalysts are the most studied ones; binary and ternary catalysts have become increasingly in focus of the research in recent years. Among them, Al, Ag, Ca, Cr, Cs, In, La, Mg, Mn, Mo, Sb, Sn, W, Zr are the alloying additives. Catalysts with boron and phosphorus (for example, Co-B, Ni-B, Co-P systems, etc.) can be separated into an individual group. These catalysts can be synthesized "in situ" by addition of the metal salts directly in the working solution of $NaBH_4$. When considering efficiency and convenience of use, the catalysts, immobilized on the carriers, are frequently used. They can be in a form of metal films, foams or nanoparticles deposited on the surface of activated carbon, carbon nanotubes, graphene, oxides ($LiCoO_2$, TiO_2, Al_2O_3, etc.), clays, polymers, rubber, etc. From the point of view of practical use, special attention is paid to the different alumosilicates, both synthetic and of a natural origin as carriers for catalysts [8,9]. They are chemically and thermally stable and capable of ion exchange involving *d*-metal ions. Such cation exchange reactions allow obtaining nanostructured catalysts with uniformly distributed catalytic elements both on the surface of the granules

(or powders) and in the bulk while using such specific type of the carrier leads to the increased resistance to the oxidation of the supported *d*-elements.

In this study we present the data of the studies of the kinetics of hydrolysis of $NaBH_4$ catalyzed by amorphous Ni-B and Co-B catalysts, the method of synthesis of zeolite-supported Ni and Co catalysts as well as a comparison of the catalytic activity of the amorphous and zeolite-supported nanocatalysts in the hydrogen generation process.

Decomposition of an aqueous solution of sodium borohydride is one of the most productive methods of hydrogen production by hydrolysis. In alkaline solutions, the interaction of $NaBH_4$ with water practically does not occur, which makes it possible to store such solutions for a long time. However, when more than catalysts of various types are used (300 homogeneous and heterogeneous catalyzers are known), sodium borohydride becomes able to react with water at ambient temperature. The most active catalysts of this reaction are rhodium, ruthenium and platinum [3,4,7,10]. In our studies, we used nanodispersed platinum immobilized on various substrates as a catalyst for $NaBH_4$ hydrolysis. Flat and cylindrical flow reactors were designed and manufactured. Furthermore, we have developed and tested Ni- and Co-based catalysts of the process.

Materials and Experimental details

For the preparation of Ni and Co based catalysts, acetates $Ni(CH_3COO)_2 \cdot 4H_2O$, $Co(CH_3COO)_2 \cdot 4H_2O$ and zeolite Na-A were used. As a reducing agent for the Ni-Co-NPs preparation N_2H_4 was used. All used reagents were purchased from Sfera Sim (Lviv, Ukraine, 99+% grade). For the regulation of the pH of the working solutions, NaOH (titrant, Kharkovreachem, Ukraine) was used.

The XRD patterns of the samples were measured at a diffractometer DRON-3.0 using Fe-Kα radiation. Investigations of the morphology, quantitative elemental analysis and elemental mapping of the obtained catalysts were performed by using EVO-40 XVP (Carl Zeiss) scanning electron microscope equipped with Inca Energy 350 (Oxford Instruments) microprobe analysis system. Ion exchange capacity of zeolite as related to Ni^{2+} and Co^{2+} ions was evaluated by photocolorimetry by using Shimadzu Uvmini spectrophotometer.

Kinetics of hydrolysis of $NaBH_4$ in the presence of Ni- and Co-based catalysts was investigated at 20 °C when applying pseudo-isothermal conditions in a setup similar to the one described in [11] and consisting of a two-neck glass vessel immersed into a water bath equipped with a magnetic stirrer and injector of the solutions of $NaBH_4$ (5 mL, 1M) The generated hydrogen was released through an Allihn-type fluid-cooled condenser which was connected to a filled with water bottle. Then, H_2 was collected at room temperatures by replacing the water in a beaker.

The Pt catalyst, used in the flat flow reactor, consisted of nanodispersed platinum (up to 40 wt.%) deposited on carbon black (XC-72), which, in turn, was immobilized on the surface of carbon cloth (1-2 mg/cm^2).

For the cylindrical reactor, platinum catalysts were prepared by their deposition on various substrates:

1) 100 mg of the platinum catalyst (40 %) on carbon black XC-72 was applied on a carbon cloth (50 cm^2) which was then rolled with a 4 mesh polyamide net and packed into a reactor;

2) 150 mg of platinum was applied on the 2 g of activated granular carbon AG-3 by polyol-synthesis with reduction with $NaBH_4$ and placed in a reactor;

3) Platinum was electrochemically deposited on porous defatted and pickled titanium crump from the electrolyte 25 g/l of K_2PtCl_6, 100 g/l of $NaNO_2$ and 20 ml/l of ammonia solution (0.915 g/cm^3) at a temperature of 70ºC and a cathode current density of 20 mA/cm^2. Under these conditions, the yield of platinum was about 30 %. The weight of precipitated platinum was monitored gravimetrically. The surface density of platinum was 1-4 mg/cm^2.

Very promising for catalytic hydrolysis of $NaBH_4$ is the nanodispersed platinum catalyst immobilized on cordierite of honeycomb structure with surface, previously modified by alumina. We used the synthetic cordierite (general formula $2MgO \cdot 2Al_2O_3 \cdot 5SiO_2$) with a square canal density of 400 canals per square inch and canal cross-sectional area of 1 mm^2. After the modification of cordierite surface by Al_2O_3 sol, the carrier was impregnated with the H_2PtCl_6 solution. Reduction of platinum was carried out by a 10 % solution of sodium borohydride. Content of platinum in the prepared composite catalyst was 27.9 mg/g. Such monolithic catalyst was placed into the flat or cylindrical flow reactors for the testing.

Results and Discussion

Catalytic Activity of Ni-Co NPs for hydrolysis of $NaBH_4$.

Ni-Co-NPs were synthesized via the reduction of the mixtures of Ni^{2+} and Co^{2+} by hydrazine in alkaline water/ethylene glycol solutions. Obtained precipitates were washed by deionized water and studied using XRD and SEM. It was found that 1) the samples do not contain any unreacted hydroxides (Fig. 1) and their composition is equal to the ratio of Ni/Co in the reaction mixture; 2) the mean size of Ni-Co-NPs slightly decreased with the decrease of Ni content increasing up to 50 % (Fig. 2).

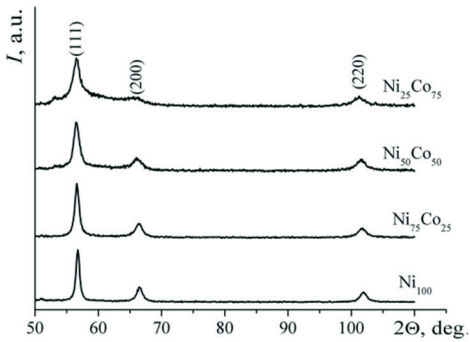

Fig. 1. XRD-patterns of Ni-Co-NPs (Fe-K_α).

Obtained Ni-Co-NPs were tested as catalysts of the hydrolysis of alkaline (pH = 9) solution of $NaBH_4$. It was found that 1) Ni-Co-NPs provide a constant rate of hydrogen evolution up to the full conversion of $NaBH_4$ (see Fig. 3); 2) $Ni_{50}Co_{50}$ nanoparticles show the best catalytic activity providing the H_2 evolution rate close to 300 mL/min per 1 g of catalyst; 3) the increase of Co content in the Ni-Co-NPs up to 25 % leads to a sharp decrease of the rate of H_2 evolution. The decreasing rate of $NaBH_4$ hydrolysis observed for $Ni_{25}Co_{75}$ may be caused by the morphological peculiarities of the obtained samples.

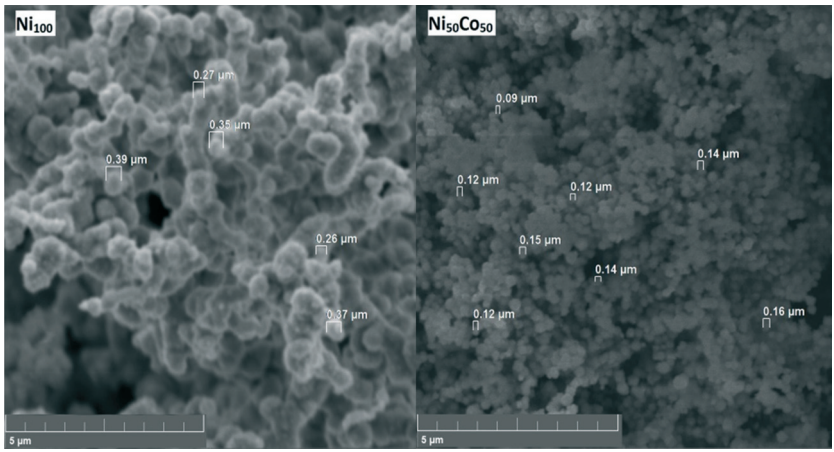

Fig. 2. SEM-images of Ni_{100} and $Ni_{50}Co_{50}$ samples.

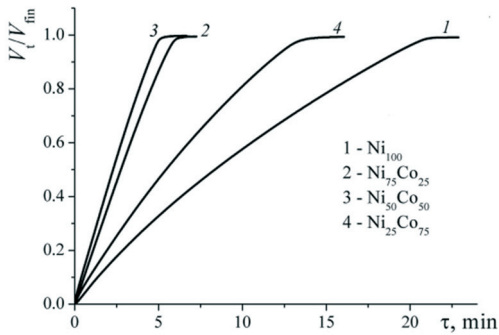

Fig. 3. The kinetic curves of H_2 evolution catalyzed by Ni-Co-NPs.

Zeolite-supported Ni/Co catalysts for hydrolysis of $NaBH_4$.

Ni-Co-NPs appear to be efficient catalysts of the hydrolysis of $NaBH_4$. At the same time, the usability of such types of catalysts is insufficient for their use in the systems for hydrogen generation due to their low stability to oxidation by atmospheric oxygen at ambient

conditions. That is why the complex nanostructured catalysts based on zeolite and Ni and Co were studied. As it was mentioned in the Introduction, alumosilicates in general and zeolites in particular show the ability to participate in the process of cation exchange and this feature was used to synthesize nanostructured catalysts. The synthesis procedure included two stages, namely adsorption of Ni^{2+} or Co^{2+} by zeolite from an aqueous solution followed by a reduction of the adsorbed cations by $NaBH_4$. It was found that cation exchange capacities of zeolite for Ni^{2+} and Co^{2+} are high and equal to 2.6 and 2.4 % by weight respectively. Obtained catalysts were studied using SEM and it was found that metals are evenly distributed on the surface of the zeolite granules (Fig. 4).

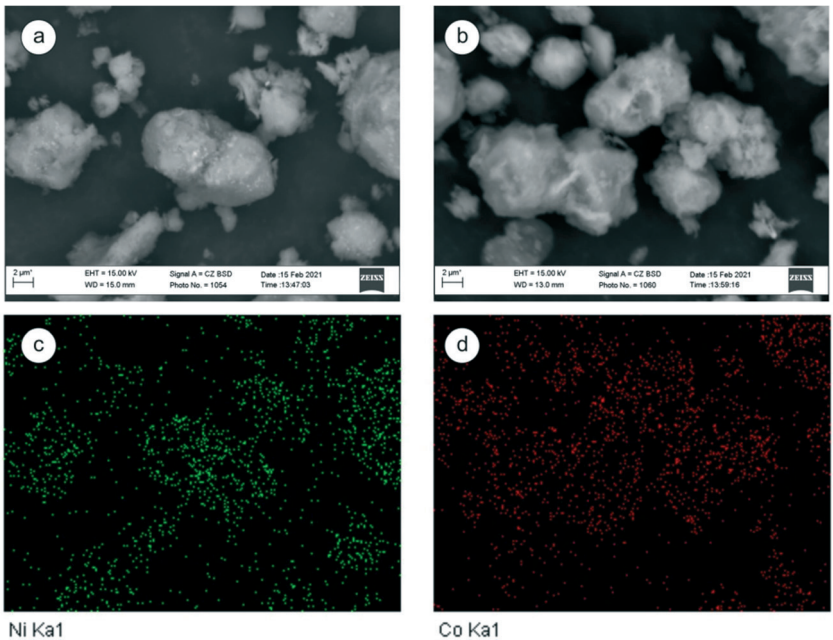

Fig. 4. SEM images of Ni-Z (a) and Co-Z (b) and the distribution of Ni (c) and Co (d).

Synthesized samples were tested as catalysts of the hydrolysis of $NaBH_4$. For the hydrolysis experiment 0.5 g of catalyst and 5 mL of 1 mol/L $NaBH_4$ solution (5 wt. % NaOH) were used. As it was expected, catalytic activity of Co-Z is higher than that for the Ni-Z (Fig. 5) and promotes the H_2 evolution with a rate close to 1450 mL/min per 1 g of the precipitated metal.

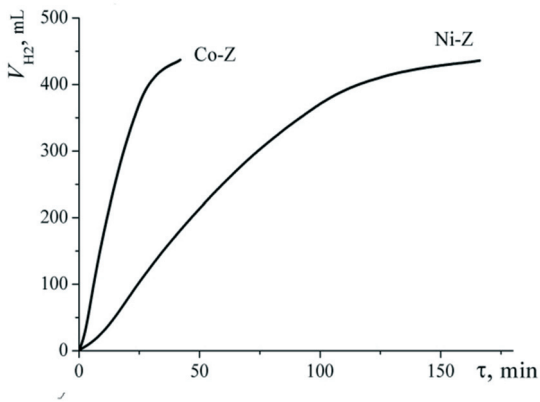

Fig. 5. Kinetic curves of H_2 evolution catalyzed by Ni-Z and Co-Z.

Thus, a high catalytic activity of the synthesized zeolite-supported Ni and Co nanocatalysts, as well as their stability at ambient conditions make such catalysts attractive from the point of view of their practical application for promoting an efficient generation of hydrogen gas.

Hydrogen generation by hydrolysis of $NaBH_4$ using supported Pt catalysts.

At 24 °C, the measured rate of hydrogen evolution during the hydrolysis of 10 % $NaBH_4$ + 5 % NaOH solution in a flat flow reactor with nanodispersed Pt catalyst immobilized on the carbon cloth was directly proportional to the solution pumping rate and reached 400 ml/min. at a flow rate of sodium borohydride solution of 7.8 ml/min. This is sufficient for a stable supply by hydrogen fuel of a 30 W hydrogen-

oxygen fuel cell. The decomposition degree of sodium borohydride decreases with increasing rate of pumping the solution through the generator.

It was shown that the platinized titanium is less active than the catalyst obtained by the polyol method. During the formation of a roll from the carbon cloth with applied platinum catalyst, the latter peeled off. That is why its activity was lower than that for the flat reactor.

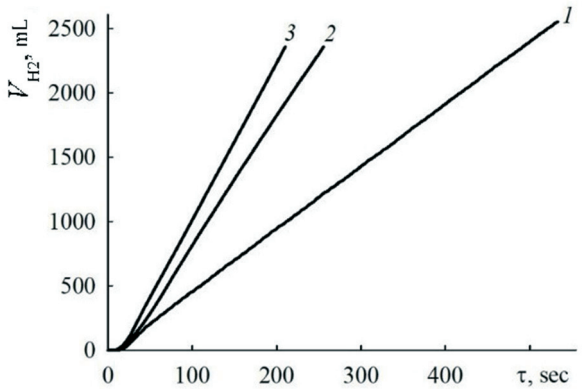

Fig. 6. Time dependencies of the volumes of the evolved hydrogen during the hydrolysis of 10 mL of the 10 % $NaBH_4$ + 5 % NaOH solution in the 5 mL cylindrical flow reactor with Pt/Al_2O_3/cordierite catalyst at the following rates of the solution flow (mL/min): 1.1 (*1*), 2.4 (*2*) and 2.75 (*3*)

According to the Fig. 6, the rate of hydrogen evolution from the alkaline 10 % $NaBH_4$ solution during its hydrolysis when using Pt catalyst immobilized on cordierite superficially modified by Al_2O_3 is practically constant if the rate of solution flow and $NaBH_4$ concentration are constant. When the rate of the solution flow increased, the hydrogen evolution accelerated. As it follows from Fig. 6, the hydrolysis of 1.1 liters of such a solution will ensure the operation of a 30 W battery of fuel cells for 9-10 hours. This catalyst provides a high and stable rate of hydrogen generation at a moderate $NaBH_4$ solution temperature of 60 ± 5°C.

Conclusions

Ni-Co-NPs with different Ni/Co ratios were synthesized via the reduction of the mixtures of Ni^{2+} and Co^{2+} precursors by hydrazine in alkaline water/ethylene glycol solutions and tested as the catalysts of the hydrolysis of alkaline solutions of $NaBH_4$. It was found that the rate of the hydrolysis reaction non-monotonically changes as related to the Co content in the Ni-Co-NPs, while the highest H_2 evolution rate was observed for $Ni_{50}Co_{50}$. A simple and reproducible method of synthesis of the stable zeolite-based nanostructured Ni and Co containing catalysts of the hydrolysis of $NaBH_4$ was developed. The optimized catalyst provides high (1450 mL/min per 1 g of the precipitated metal at maximum) H_2 evolution rate. Different chemical and electrochemical techniques of the preparation of Pt-based nanocomposite catalysts were tested. It was established that the most efficient catalytic system is PtNPs immobilized on a superficially modified cordierite with honeycomb structure. When 1.1 L of $NaBH_4$ solution is subjected to the hydrolysis process, an application of the mentioned catalyst in a cylindrical flow reactor generates a sufficient amount of hydrogen gas allowing to operate a 30 W battery of the fuel cells for 9-10 hours.

Acknowledgment

This work was supported by the NATO Programme "Science for Peace and Security" (Project G5233 "Portable Energy Supply").

References

[1] Hirscher M., Yartys V.A. *et al.* Materials for hydrogen-based energy storage–past, recent progress and future outlook, *J. Alloy. Compd*., 2020, vol. 827, pp. 153548.

[2] Liu B.H., Li Z.P. A review: Hydrogen generation from borohydride hydrolysis reaction, *J. Power Sources*, 2009, vol. 187, pp. 527-534.

[3] Muir S.S., Yao X. Progress in sodium borohydride as a hydrogen storage material: Development of hydrolysis catalysts and reaction systems, *Int. J. Hydrog. Energy*, 2011, vol. 36, pp. 5983-5997.

4] Simagina V.I., Netskina O.V., Komova O.V., Ozerova A.M. Progress in the catalysts for H_2 generation from $NaBH_4$ fuel, *Current Topics in Catalysis*, 2012, vol. 10, pp. 147-165.
[5] Patel N., Miotello A. Progress in Co-B related catalyst for hydrogen production by hydrolysis of boron-hydrides: A review and the perspectives to substitute noble metals, *Int. J. Hydrog. Energy*, 2015, vol. 40, pp. 1429-1464.
[6] Demirci U.B. The hydrogen cycle with the hydrolysis of sodium borohydride: A statistical approach for highlighting the scientific/technical issues to prioritize in the field, *Int. J. Hydrog. Energy*, 2015, vol. 40, pp. 2673-2691.
[7] Abdelhamid H.N. A review on hydrogen generation from the hydrolysis of sodium borohydride, *Int. J. Hydrog. Energy*, 2021, vol. 46, pp. 726-765.
[8] Rakap M., Özkar S. Intrazeolite cobalt (0) nanoclusters as low-cost and reusable catalyst for hydrogen generation from the hydrolysis of sodium borohydride, *Appl. Catal*. B, 2009, vol., 91(1-2), pp. 21-29.
[9] Joydev M., Binayak R., Pratibha S. Zeolite supported cobalt catalysts for sodium borohydride hydrolysis, *App. Mech. Mater.*, 2014, vol. 490, pp. 213-217.
[10] Liu B., Li Z. A review: Hydrogen generation from borohydride hydrolysis reaction. *J. Power Sources*. 2009. Vol. 187, No 2. P. 527-534.
[11] Ouyang L., Ma M., Huang M. *et al*. Enhanced hydrogen generation properties of MgH_2-based hydrides by breaking the magnesium hydroxide passivation layer, *Energies*, 2015, vol. 8(5), pp. 4237-4252.

CHAPTER 2

Overview of the results of the research Programme "Development of scientific principles for hydrogen production, storage and use in autonomous energy supply systems" (2019-2021) supported by the National Academy of Sciences of Ukraine

Obtaining of fermentation parameters of experimental-industrial technology for synthesis of biohydrogen

O. Tashyrev , V. Hovorukha, O.Havryliuk , G. Gladka,
I. Bida , Ya. Danko , O. Shabliy

Zabolotny Institute of Microbiology and Virology, NASU, Kyiv, Ukraine

Environment pollution by man-made organic waste is one of the most urgent problems nowadays. Solid and liquid organic waste produced in megacities and suburb area is the greatest threat. Despite some achievements in the direction of their degradation and bioremediation, the number of landfills is constantly growing all over the world. None of the modern technologies provides their efficient treatment: the rate of waste generation is higher than the rate of their processing.

Biodegradable organic waste of plant and animal origin (food, etc.) and toxic leachate are the most hazardous. Concentrated organic polymers of natural origin (vegetables, fruits, meat and other food waste) are very quickly degraded by microorganisms with the formation of also concentrated toxic compounds such as fatty acids (acetic, propionic, etc.), alcohols (methanol, ethanol, etc.) and gases (hydrogen sulfide, ammonia, etc.). That is why the environment suffers from multilevel pollution with a wide range of toxic gaseous and liquid compounds (Fig. 1, A). That is why the development of the novel universal biotechnologies for fast and efficient treatment of solid and liquid organic waste is a relevant area for the whole world.

The goal of the work was to increase the efficiency of molecular hydrogen synthesis by optimizing the fermentation process of environmentally hazardous multicomponent food waste, as well as purification of associated toxic filtrate with methane obtaining via the application of granular microbial preparation (GMP).

To solve these problems, we have created novel universal microbial biotechnology using the thermodynamic prognosis. It allows applying the GMP for quick and effective degradation of multicomponent solid and liquid organic waste as well as for obtaining commercial volumes of energy carriers: hydrogen and methane.

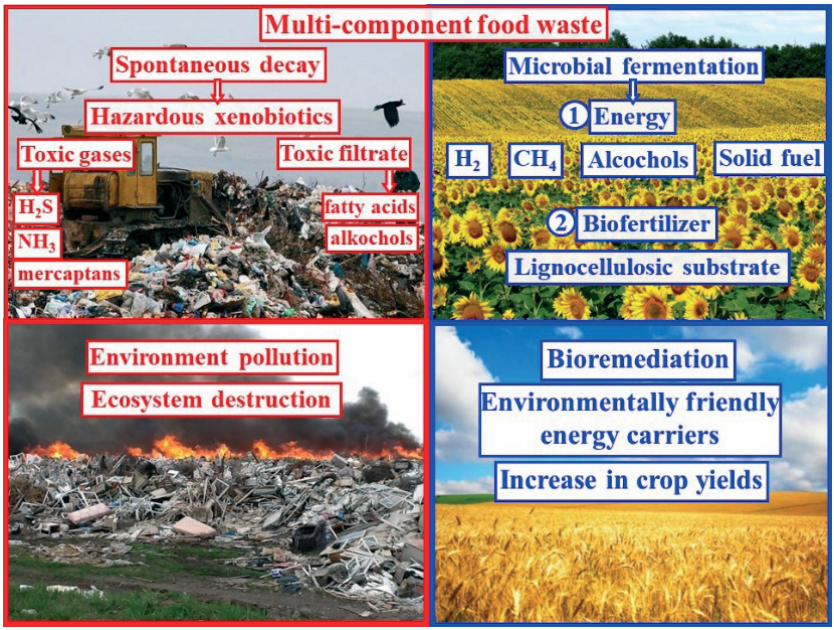

A B

Fig. 1. Negative consequences of environment pollution (A) and the prospects for the implementation of bioremediation biotechnologies (B)

To obtain energy from organic waste efficiently, we have created new bioreactors 10-fold reducing the fermentation time and 2-3-fold increasing the yield of energy carriers (H_2 and CH_4).

Thanks to our versatile biotechnology, huge volumes of environmentally hazardous solid and liquid organic waste serve as unlimited, constantly renewable raw material for energy carrier production.

Optimization of biotechnology and structural refinement of the bioreactor creates the prerequisites for large scale industrial implementation.

Applying the method of thermodynamic prognosis, we have developed a theoretical model of optimal pathways for degradation of solid and liquid organic waste by microbial communities. Anaerobic hydrolysis of organic compounds with the synthesis of hydrogen was

established to occur the most efficiently under neutral conditions and low redox potential Eh, i.e., at pH = 7.0 and Eh = – 414 mV (Fig. 2). In our opinion, the development and implementation of such approach will save the environment and ensure the possibility of useful product manufacturing (Fig. 1, B).Obtaining of fermentation parameters of experimental-industrial techn...

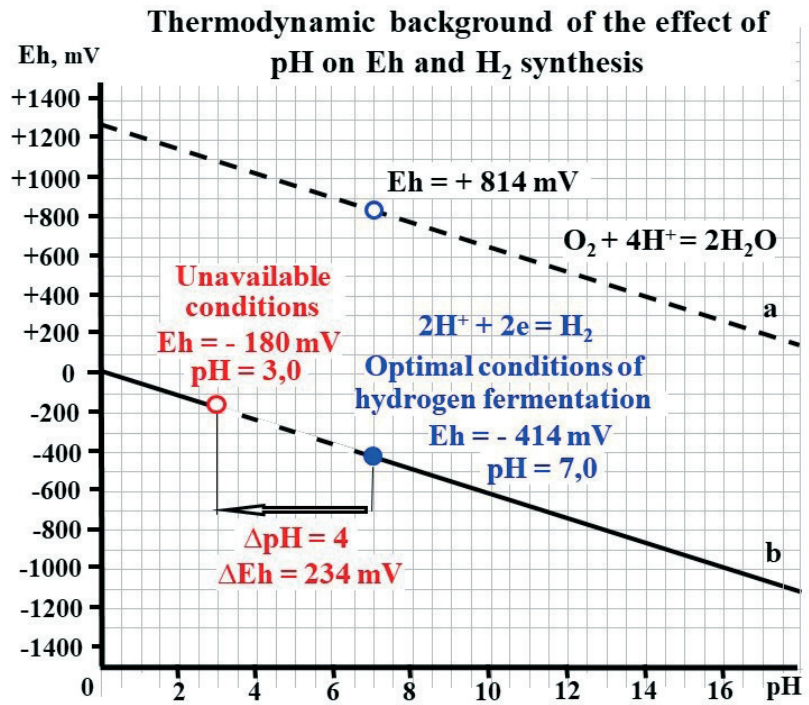

Fig. 2. Thermodynamic basis for optimal conditions of degradation of organic waste via hydrogen dark fermentation

We have developed a universal granular microbial preparation (GMP) for effective degradation of organic waste (Fig. 3). It contains concentrated living microorganisms, starting substrates and regulators of microbial metabolism. GMP is environmentally friendly and can increase the efficiency of organic waste degradation and energy carrier production (either H_2 or CH_4).

Fig. 3. Modifications of GMP (granular microbial preparation) for the degradation of solid and liquid organic waste and the production of useful products: energy carriers (H_2 or CH_4), biofertilizers and pure water

We have developed and tested an experimental industrial horizontal Bioreactor-1 for the degradation of concentrated solid food waste using GMP (Fig. 4).

Modern experimental and industrial biogas plants provide the duration of fermentation (T) about 30 days, the coefficient of waste degradation (multiplicity of waste reduction, Kd) about 5-10, and the yield of hydrogen in the range of 30L-40 L/kg of waste. Application of our Bioreactor-1 improved corresponding indicators several times. In particular, T was only 4 days, which is 7 times less, Kd was equal 140, which is 14 times higher, and hydrogen yield was equal 90 L/kg of waste, which at least 2 times more.

However, during the degradation of multicomponent solid waste, an acidic filtrate is formed, in which low molecular fatty acids and alcohols are present in high concentrations. The concentrated filtrate is extremely toxic to all parts of the food chain in the environment. In addition, it almost completely inhibits the further degradation of natural organic polymers in landfills. That is why such solid waste in landfills rots very slowly, for decades.

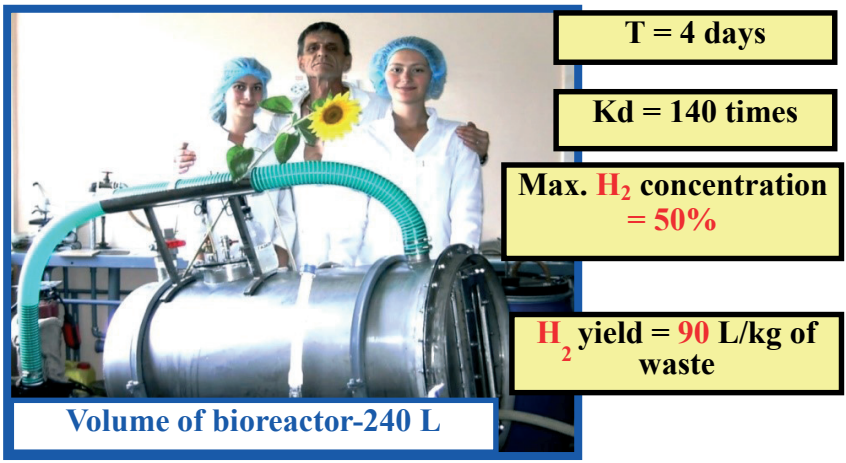

Fig. 4. Horizontal Bioreactor-1 for rapid fermentation of solid organic waste and obtaining of environmentally friendly energy carrier H_2

Therefore, the development of novel biotechnologies for the purification of the filtrate from toxic components that inhibit the growth of microorganisms and poison the environment is an urgent task.

We have developed Bioreactor-2, which allows effective purification of the toxic filtrate in both aerobic and anaerobic conditions (Fig. 5).

For the anaerobic purification, the methanogenic modification of GMP was added into Bioreactor-2 (Fig. 5, A). For the aerobic treatment modification of GMP containing aerobic microorganisms was added into Bioreactor-2 (Fig. 5, B). Air was supplied in a continuous stream through the filtrate to Biofermenter-2 (Fig. 5, B) to provide aerobic conditions.

Within 3 weeks, the microorganisms of GMP modifications adapted to the filtrate and started degradation of the organic compounds of the filtrate. In general, during 3.8 months (115 days) the concentration of organic compounds decreased from 1071 mg/L (of total Carbon) to 106 mg/L via anaerobic methanogenic fermentation, and to 56 mg/L via aerobic oxidation. Therefore, the efficiency of aerobic purification was 1.9 times higher than anaerobic one. However, 1 L of methane was obtained from each liter of filtrate by anaerobic fermentation.

A B

Fig. 5. Bioreactor-2 for purification of filtrate from fatty acids and alcohols: A- purification in anaerobic mode with CH_4 synthesis; B - purification in aerobic mode

Thus, the two microbial metabolic pathways were established to be promising for the purification of filtrate after fermentation. Aerobic oxidation was shown to be more effective. It provided 19-fold decrease in soluble organic compound concentration in terms of total carbon (from 1071 mg/L to 56 mg/L) in comparison with methanogenic fermentation with 10-fold reduction of carbon concentration (from 1071 mg/L to 105 mg/L) providing synthesis of CH_4 in amount 1 L/L of filtrate. However, the duration of the process was long - up to 115 days. So, the optimization of the process was required. The regulation of the pH equal to 7.0 provided accelerated the oxidation of soluble organics (from 210 to 34 mg/L) reducing the concentration 6.1 times during 41 days. Methane fermentation required longer adaptation period resulting in the 2.6-fold decrease in the carbon concentration from 210 mg/L to 80 mg/L during this period.

In general, the results are very promising. Thus microorganisms of the both modifications provided the degradation of the liquid organic waste filtrate, which usually slowly decomposes for decades in the collectors and in the body of landfills, during 4 months with 10-20 fold reduction of the content of fatty acids and alcohols. The content of

organic compounds in the concentration range of 50 mg/L-100 mg/L is environmentally friendly, and in the future such purified filtrate can be used for irrigation without harming the environment.

Thus, we have developed the approach providing the solution of the problems of environmental protection, energy carrier production (H_2 or CH_4) and water purification. It provides the degradation of multicomponent solid food waste to obtain energy carriers (hydrogen or methane) as well as the purification the toxic filtrate from fatty acids and alcohols to obtain pure water and methane. The biotechnology is ready for the implementation and industrial scaling. It will be useful for both small households, farms, cottages, restaurants as well as for large scale agro-industrial complexes, canneries, landfills, etc.

For more information, visit our YouTube channel tash2232:

https://www.youtube.com/watch?v=FB7qjdL-Ejg&t=2s;

https://www.youtube.com/watch?v=2br_2zUV70I&t=10s.

The main publications in the frame of the project “Obtaining of fermentation parameters of experimental-industrial technology for synthesis of biohydrogen”

1. V.M. Hovorukha, O.B. Tashyrev, O.A. Havryliuk, L.S. Iastremska. High Efficiency of Food Waste Fermentation and Biohydrogen Production in Experimental-industrial Anaerobic Batch Reactor. *Open Agriculture Journal*, 2020, vol.14, pp. 174-186. https://benthamopen.com/EPUB/BMS-TOASJ-2019-HT1-1140-2.

2. V.M. Hovorukha, O.A. Havryliuk, I.O. Bida, Ya.P. Danko, O.V. Shabliy, G.V. Gladka, L.S. Yastremska, O.B. Tashyrev. Two-stage degradation of solid organic waste and liquid filtrate. *Biotechnologia Acta*, 2021, vol.14, No.4, pp. 70-79.

High pressure membraneless electrolyser for helio-hydrogen power plants

V. Solovey, M. Zipunnikov, V. Semikin, I. Vorobjova

Pidhornyi Institute of Mechanical Engineering Problems, NASU, Kharkov, Ukraine

The new generation electrolysis equipment has got the ability to be adapted to the operating conditions of the systems that use renewable energy sources. The energy- technological complexes for green hydrogen electrolytic production in combination with the Solar PhotoVoltaic Converters (SPVC) are of special practical interest. They allow elimination of the carbon dioxide emissions. While the solar energy is used as the base load due to its wide availability, the direct use of the renewable energy sources by the power system is complicated due to mismatch between energy consumption and its production. Therefore, the urgent task is to develop electrochemical technologies for hydrogen generation with minimal electricity consumption, which can be integrated into the autonomous energy complexes using renewable energy sources (sun, wind).

The main idea, which is the basis of research - is the ability to consume and convert the renewable solar energy using the electrochemical plants created at Pidhornyi Institute of Mechanical Engineering Problems of NASU (IPMach). They give the possibility for hydrogen generating and accumulating in the high pressure systems directly in the conditions of the autonomous power plants. Irregular primary flow of solar energy, i.e. the volatility of SPVC power generation, is compensated in the developed electrolysis systems, which are not sensitive to the power supply quality. So, there is no need in the inverter systems, which are designed to bring the parameters of the SPVC generated electricity in accordance with the requirements of the electrolyzer power supply that results in increasing the efficiency of operation and in reducing the equipment cost. This approach is appropriate for the green hydrogen generation when creating the autonomous power plants of small and medium capacity.

The electrochemical method of water decomposition developed by IPMach uses a gas-absorbing electrode [1]. The process of water decomposition is cyclic and provides the hydrogen and oxygen evolution alternate in time. The operating temperature range of the aqueous alkali

solution (KOH) electrolysis process is from 280 K to 358 K, and the pressure range is of 0.1 MPa-70 MPa. The decomposition reaction of water occurs continuously with the alternating release of hydrogen and oxygen in the Electrolysis Cell (EC). In the first half-cycle, hydrogen is released on the passive electrode and fed into the high-pressure line, and oxygen is chemically bound by the active electrode (forming a chemical compound). In the second half-cycle, the electrochemical reduction of the active electrode by hydrogen is carried out, which is accompanied by the release of oxygen at the passive electrode and its selection into the high-pressure oxygen line.

Studies of the electrolysis process and testing of the common modes of operation of the primary source of renewable energy (SPVC) and a membrane-less high-pressure electrolyzer were performed using a developed mock-up power plant, which reproduces the processes in the non-network helio-hydrogen autonomous power plants.

The studies were performed under electrolyzer direct feeding from SPVC (TOPRAY SOLAR) without secondary converters. They were conducted in the real climatic conditions (Fig. 1).

Fig. 1 The experimental laboratory installation with SPVC (TOPRAY SOLAR) in the real climatic conditions.

The experimental data were obtained when the electrolyzer was directly connected with the ESPVC (TOPRAY SOLAR) having a total working surface area of S = 0.288 m^2; short circuit current I_{sc} = 1.07 A; no-load voltage U_{nl} = 22.4 V. The volt-ampere characteristics of the SPVC and membrane-less alkaline electrolyzer at different levels of solar radiation are presented on Fig. 2 (curves 1–5 are the SPVC characteristics).

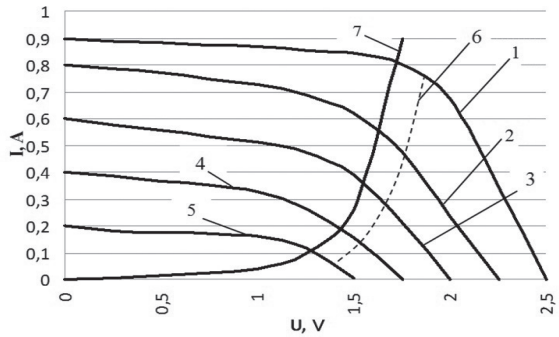

1 - June (47.2 kW·h); 2 - September (30.2 kW·h); 3 - March (26.35 kW·h); 4 - November (10.28 kW·h); 5 - December (7.77 kW·h); 6 - maximum power of the solar panel; 7 - volt-ampere characteristic of the alkaline electrolyzer.

Fig. 2 Volt-ampere characteristics of SPVC and membrane-less alkaline electrolyzer at different levels of solar radiation

It is experimentally proven that the operating power range of the alkaline electrolyzer (curve 7) is less than the maximum power of the solar panel (curve 6). Therefore, the used SPVC fully provides the limits of the electrolyzer working capacity. However, the compatibility of the SPVC and the alkaline electrolysis system must be adjusted to ensure the maximum output performance. The intersections of curve 7 with curves 1-5 determine the possible operating points of the electrolyzer with SPVC. To provide the efficient electrolyzer operation, the distance from curve 7 to curve 6 (SPVC maximum power) must be minimal, i.e. the electrolyzer operates under highest consumption of electricity generated by SPVC. At the same time, the guaranteed excess stock of the electric

power from SPVC provides reliable work of the electrolysis system. The obtained data testify the ability of join operating the solar power plant and the membrane-less electrolyzer without any intermediate inverter equipment.

The average monthly specific volume of hydrogen generated by the electrolyzer fed from SPVC (TOPRAY SOLAR) is presented at Figure 3. The electrolyzer was connected to the SPVC without secondary converters.

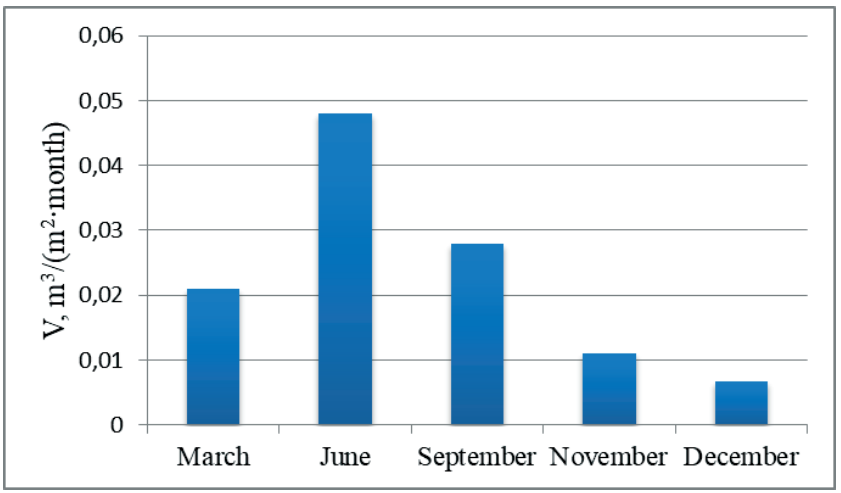

Fig. 3 The average monthly specific volume of hydrogen generated by the electrolyzer fed from SPVC for different seasons (different levels of the solar radiation).

The largest increase of hydrogen generation by the electrolyzer is observed in the period from May to August, i.e. in the summer period that is about 7 times more than in winter one (January-February).

To work out the modes of joint operation of a membrane-less high-pressure electrolyzer and a plant powered from the renewable energy source, the solar photovoltaic module JAM60S10-330/PR, “JA SOLAR Technology” firm was used. Its working surface area is of

$S = 1.5\ m^2$ (Fig. 4).

Fig. 4 The JAM60S10-330/PR solar photovoltaic module.

The results of experimental studies of the electrochemical activity for the 08H18N10T-Fe_p electrode twin of the membrane-less alkaline electrolyzer depending on the current density for different levels of insolation when the electrolyzer is powered by a JAM60S10-330 / PR solar photovoltaic module are presented in Table 1.

Table 1 - Electrochemical activity of the 08X18H10T-Fe_p electrode twin depending on the current density (different levels of insolation)

Electrode material	Current density, A/m^2	The electrolyzer specific capacity for hydrogen, $m^3/(m^2 \cdot h)$	Specific electricity consumption, $kW \cdot h/m^3$	Active electrode area, m^2
08X18H10T-Fe_p	60	$7.7 \cdot 10^{-3}$	4.1	0.066
	91	$16.2 \cdot 10^{-3}$	4.02	
	106	$21.4 \cdot 10^{-3}$	3.96	
	136	$25.8 \cdot 10^{-3}$	4.0	

The current density level is provided by the SPVC (JAM60S10-330/PR) power generation and depends on the level of insolation. The electrolyzer provides the highest hydrogen generation at current density of 136 A/m^2, i.e. at maximum power generation current of 9 A. The specific consumption of electricity is practically unchanged under all operating

modes. That confirms the efficiency of the electrolysis process along the entire range of insolation changes.

As a result of the conducted research, we have tested the joint modes of operation of the photoelectric converter with the membrane-less high-pressure electrolyzer that were combined in a model sample of the power plant. The modes of operation were tested depending on changes of solar insolation. The obtained experimental data as to adapting the electrolyzer to SPVC give the possibility for developing the original algorithms for automatic control of the main elements of the helio-hydrogen autonomous power supply units and for creating a technical basis for such unit implementation.

The helio-hydrogen power plants can be used for creating the hydrogen gas stations, on farms, livestock complexes, communications companies, health resorts and other facilities that require a reliable autonomous power supply. It is possible to implement the proposed development in the installations that use solar energy for smoothing out the unevenness between energy supply and consumption in the utilities sector.

Cooperation of Ukraine with the European Clean Hydrogen Alliance is aimed at the development of efficient hydrogen technologies. Providing the alkaline water electrolysis under using the renewable energy sources to generate the green hydrogen is an important step towards the decarbonization of industrial processes and the transport sector. While the process of water electrolysis alkaline can be determined by the electrolyzer properties, the photovoltaic panels must operate at the point of maximum power. The combination of electrolyzer and a plant powering from the renewable energy sources ensures sustainable hydrogen production without significant carbon dioxide emissions.

The level of technological readiness is a prototype.

The development is protected by 15 patents.

The main publications in the frame of the project “Study of the processes and optimization of design and technological parameters for the high pressure electrolysis systems used at the autonomous helio-hydrogen energy supply plants”:

1. M.M. Zipunnikov. Formation of potassium ferrate in a membrane-less electrolysis process of water decomposition, *Voprosy*

khimii i khimicheskoi tekhnologii, 2019, No. 5, pp. 42–47. http://doi.org/10.32434/0321-4095-2020-131-4-148-156

2. V.V. Solovei, A.M. Avramenko, K.R. Umerenkova An analysis of thermodynamic characteristics of metal-hydride systems for hydrogen storage, using a modified scheme of the perturbation theory. *Problemy Mashynobuduvannia*, 2019, vol. 22, No.3, pp. 44–49. https://doi.org/10.15407/pmach2019.03.044

3. V.V. Solovey , M.M. Zipunnikov, V.B. Poda , I.O. Vorobjova Hydrogen generation from water by using alloys based on silicon and aluminium. *Voprosy khimii i khimicheskoi tekhnologii*, 2020, No.4, pp. 148-156.
http://doi.org/10.32434/0321-4095-2020-131-4-148-156.

4. A.V.Rusanov ,V.V.Solovey, M.V. Lototskyy. Thermodynamic features of metal hy-dride thermal sorption compressors and perspectives of their application in hydrogen liquefac-tion systems, *Journal of Physics: Energ*, 2020, No.2(2), pp. 1-10.
https://doi.org/10.1088/2515-7655/ab7bf4.

5 V.V.Solovey, Zipunnikov M.M., V.M.Semikin . Method for Calculating the Feed Wa-ter Replenishment Parameters under Electrolysis Process in Electrolyzer, *French-Ukrainian Journal of Chemistry*, 2020, vol. 8, No. 2, pp. 168-175.
https://doi.org/10.17721/fujcV8I2P168-175

6. A.A.Shevchenko , M.M. Zipunnikov , A.L. Kotenko , N.A. Chorna . Investigation of the Electrolysis Process of Obtaining Hydrogen and Oxygen with Serial and Parallel Connection of Electrons. *Journal of mechanical engineering*, 2020, vol.23, No. 4, pp. 63-71. https://doi.org/10.15407/pmach2020.04.063.

7. A.A. Shevchenko, M.M. Zipunnikov, A.L.Kotenko . Adaptation of the high-pressure electrolyzer In the conditions of joint operation with TPP and NPP power-generating units. *Naukovyi visnyk Natsionalnoho Hirnychoho Universytetu*, 2020, No. 6, pp. 76–82. https://doi.org/10.33271/nvngu/2020-6/076.

8. A.V. Rusanov, V.V. Solovey , M.M.Zipunnikov. Thermochemical activation of hy-drogen in the process of desorption from metal hydride. *French-Ukrainian Journal of Chemistry*, 2020, vol. 8, No. 2, pp. 60-72.

https://doi.org/10.17721/fujcV8I2P60-72

9. V.V.Solovey , A.A.Shevchenko , M.M. Zipunnikov, A.L.Kotenko , Nguyen Tien Khi-em, Bui Dinh Tri, Tran Thanh Hai. Development of high pressure membraneless alkaline elec-trolyzer, *International Journal of Hydrogen Energy*, 2021. p 11.
https://doi.org/10.1016/j.ijhydene.2021.01.209

10. A.V.Rusanov, V.V. Solovey, M.M.Zipunnikov . Improvement of the membrane-free electrolysis process of hydrogen and oxygen production. *Naukovyi visnyk Natsionalnoho Hirn-ychoho Universytetu*, 2021, No. 1, pp. 117-122.
https://doi.org/10.33271/nvngu/2021-1/117

References

[1] Solovey V.V., Shevchenko A.A., Kotenko A.L., Zipunnikov M.M., Nguyen Tien Khiem, Bui Dinh Tri, Tran Thanh Hai. Development of high pressure membraneless alkaline electrolyzer, *International Journal of Hydrogen Energy*, 2021, p. 11.
https://doi.org/10.1016/j.ijhydene.2021.01.209

Development of autonomous cogeneration hydrogen power plants with solid organic waste conversion

O. Dudnyk, I. Sokolovska

Thermal Energy Technology Institute, NASU, Kyiv, Ukraine

Hydrogen-rich synthesis gas and, if it is necessary, pure hydrogen are produced in the Thermal Energy Technology Institute (TETI) gasifier, which can be transformed for the various solid organic waste conversion in the different modifications of moving and fluidized beds. The gasifier start is carried out using plasma torches (steam or air). The gasifier can operate both with and without plasma torches depending on the solid organic waste properties.

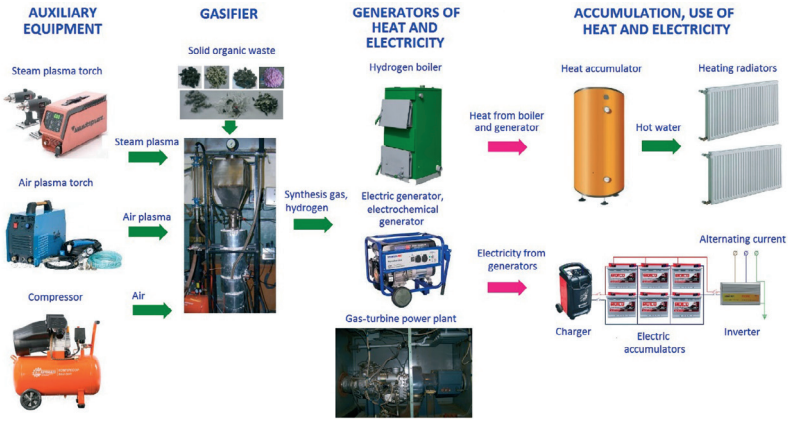

The principle of autonomous operation of cogeneration plants with solid organic waste conversion using equipment of Thermal Energy Technology Institute (former Coal Energy Technology Institute) of the National Academy of Sciences of Ukraine

A parallel-series circuit of heat and electricity generation units was used for the construction of cogeneration power plants. Depending on the needs in the cold season, only heat can be produced in the boiler using hydrogen-rich synthesis gas or pure hydrogen. In order to achieve autonomy, energy efficiency improvement, and the plant operation in the mode of heat load change, the hot water obtained in the boiler is fed into

the heat accumulator that provides the possibility of boiler periodic operation with continuous independent heat supply from heat accumulator for heating.

In the case of heat and electricity generation, the heat from an electric generator with an Internal Combustion Engine (ICE), Fuel Cell Electrochemical Generator (FC ECG) or a Gas Turbine Unit (GTU) is fed into the heat recovery unit. In the cogeneration power plant circuits, FC ECG can be involved, for example, with Bloom Energy or Rolls Royce planar solid oxide fuel cells; Mitsubishi Hitachi Heavy Industries, Bosch Thermotechnology/Aisin Seiki tubular solid oxide fuel cells or others.

In order to achieve autonomy, energy efficiency improvement, and the plant operation in the mode of electrical load change, electricity generated by power generators is fed through the charger to the electric accumulators, from which electricity is fed through the inverter to the consumer. Thus, cogeneration plants are hybrids for generating both electricity and heat using accumulators. In these plants, both periodically operating power units and batteries are used to achieve autonomy. This is done to reduce the load on the main equipment (gasifier, plasma torches, boiler, electric generators, and fuel cells) and to increase the life time of power plants, which operate intermittently with continuous supply of electricity and heat from batteries to the consumer.
For further energy efficiency improvement, cogeneration plants may contain metal hydride hydrogen accumulators (to store hydrogen in the warm season and to use it in the cold season in a hydrogen boiler), solar cell panels without electrolyzers and with the use of electric accumulators for power supply and for the operation of electric heaters built into the heat accumulator, and with electrolyzers (with the production of hydrogen for the FC ECG operation and oxygen for the gasifier operation), as well as heat pumps. Solar and wind power plants with reversible electrolyzers can be added to the existing hydrogen utilization circuit for increasing efficiency of this plants in reverse mode using cogeneration, trigeneration, and polygeneration units.

The gasifier-transformer was developed for the use as part of cogeneration power plants. The gasifier was tested on different types of

Solid Organic Waste (SOW). The main equipment for the operation of the cogeneration plant (a boiler and electric generators) was identified, selected, and purchased. The boiler is Kolvi Euroterm KTK standard solid fuel-fired boiler with thermal capacity up to 18 kW with anthracite, coal, briquettes, and wood combustion for autonomous heating of rooms up to 200 m^2. The boiler was transformed for combustion of synthesis gas and hydrogen obtained in the gasifier (the way from carbonization to decarbonization). The electric generator with ICE Endress ESE 3200P with nominal electric power of 2.35 kW, which was modified to operate on hydrogen-rich synthesis gas, was used in the power supply circuit. The electric generator with different carburetors can also operate autonomously on gasoline, propane-butane, and natural gas.

Optimization of the operation of the gasifier, boiler, and electric generator with internal combustion engine for heat and electricity production has been started. There were determined optimal parameters of gasification for different SOWs depending on their composition and consumption of oxidants (air and steam) in order to use the obtained gas for the operation of cogeneration and trigeneration power plants. Tangential two-stage air supply to the zones of partial oxidation and carbonization of the gasifier was used to increase the gasification efficiency. There were determined the regularities of increasing the molar ratio of H_2/CO compounds in the gas obtained after gasification due to the use of high-temperature steam. The temperature of gases at the outlet of the carbonization zone depends on the type of SOW and, for their effective conversion, should be 300 °C to 500 °C, and the temperature of gases at the outlet of the gasifier should be more than 600 °C - 650 °C. It was found that the use of a reactor with a regenerated Ni-catalyst is the best option for use in cogeneration plants to reduce the content of high-molecular compounds in the gas before electric generators.

It is determined that the use of autonomous trigeneration power plants for the production of electricity, heat, and cold is necessary for full autonomous climate control in rooms. In this case, the maximum energy efficiency of the SOW energy use is achieved when changing both the daily load and the load at different times of the year. The use of the

trigeneration principle provides the highest fuel efficiency at different times of the year. The principle circuit of the installation for obtaining cold using of solid organic waste has been developed. The principle circuit of a hybrid power plant with an electric power of 250 kW with pressurized gasifier, 9I120 gas turbine unit, and electrochemical generator on solid oxide fuel cells has been developed.

The possibility of obtaining carbon-free gas from gas at the outlet of the gasifier-transformer using of a high-temperature reactor for conversion of macromolecular compounds, a water shift catalytic reactor, and a low-temperature carbon dioxide sorption reactor were tested.

It is established that the use of SOW as a fuel in cogeneration and trigeneration power plants reduces the cost of the obtained products in comparison with the use of traditional fuels by 1.5-2.0 times.

The analysis was carried out and proposals were prepared on the possibility of using the by-product of SOW conversion – carbon dioxide for the operation of polygeneration cogeneration hydrogen power plants for the production of electricity, fertilizers, plastics, third generation biofuels, construction materials, nanocarbon, etc.

Area of application of autonomous plants for heat and electricity production with solid organic waste conversion can be used for independent energy supply in the municipal power and chemical industries, hospitals, food industry, educational institutions, farms, private houses, shops, hotels, mobile houses, power systems of special devices and tools, etc. It is possible the use of green hydrogen utilization equipment of TETI NASU for the improvement of the efficiency of solar and wind power systems with reversible system of hydrogen production and utilization. Scope of commercial capacity application of such systems is on level up to 10 GW_{th}.

Advantages of TETI NASU technologies and approaches are the following: improvement of the efficiency of the use of solid organic waste due to the simultaneous generation of electricity and heat, the use of heat and electricity accumulators and fuel cell electrochemical generators; an increase in the life time of plants due to a decrease in the load on the main equipment, the mobility of the plants due to the use of

heat and electricity accumulators, and possibility to work on different types of solid organic waste; a decrease in the cost of electricity and heat generated due to the use of cheap organic raw materials (solid organic waste) and power equipment. Hydrogen cost in case of solid organic waste utilization is in two-three time less than hydrogen cost after conventional water electrolysis.

The basic equipment of the TETI autonomous cogeneration power plant was tested in operation up to output of 18 kW_{th}.

Potential partners for future developments of Thermal Energy Technology Institute of NAS of Ukraine (TETI of NASU) are participants of Implementation of Federal Government's National Hydrogen Strategy of Germany. In 2021, TETI of NASU under support of German-Ukrainian Chamber of Commerce and Industry held the seminars in field of green hydrogen with Fraunhofer Institute for Environmental, Safety, and Energy Technology (Branch Sulzbach-Rosenberg) and Institute of Energy and Climate Research (Forschungszentrum Jülich GmbH).

Competitors are TDA Research Inc., Off Grid Pro Inc. and Utrecht University.

The results of the development of cogeneration power plants on solid organic waste are the intellectual property of the Thermal Energy Technology Institute of NAS of Ukraine.

The main publications in the frame of the project "Development of autonomous cogeneration hydrogen power plants with solid organic waste conversion":

1. O.M. Dudnyk. Development of hydrogen production systems with biomethane and solid renewable feedstock conversion for operation of electrochemical generators on fuel cells with protone exchange membrane. Proceedings of the 22th International Scientific and Practical Conference *«Renewable Energy and Energy Efficiency in the XXI Century»,* May 20, 2021, Kyiv. pp. 364-367.
https://www.ive.org.ua/wp-content/uploads/tezi2021.pdf#page=364
2. O.M. Dudnyk. Hydrogen economics and energy. Proceedings of the 17th International Scientific and Practical Conference "Coal heat power

generation: Ways of reconstruction and development". Kyiv: Gnozis, October 19-20, 2021, pp. 66-74.
https://doi.org/10.48126/conf2021#page=67
3. O.M. Dudnyk, I.S. Sokolovska, V.G. Borisevich. Optimization of circuits of cogeneration and trigeneration power plants operation with solid organic waste gasification. Proceedings of the 16th International Scientific and Practical Conference *"Coal heat power generation: Ways of reconstruction and development",* Kyiv: Gnozis, November 13, 2020, pp. 110-115.
https://doi.org/10.48126/conf2020#page=111
4. O.V.Dudnyk, N.I. Dunaevska, I.S. Sokolovska, A.I. Tripol’skii, P.E. Stryzhak. CO_2 production, purification and utilization in the processes of power generation and chemical production. Proceedings of the 16th International Scientific and Practical Conference *"Coal heat power generation: Ways of reconstruction and development"***.** Kyiv:
Gnozis. November 13, 2020, pp. 46-55.
https://doi.org/10.48126/conf2020#page=47
5. O.M. Dudnyk, N.I. Dunaevska, I.S. Sokolovska. Development of the world market of fuel-cell power plants. Creation of normative base for hydrogen power, *The Problems of General Energy,* 2020, 1(60). pp. 66-73. https://doi.org/10.15407/pge2020.01.066
6. H. Singh, R. Yadav, S.A.Farooqui, O. Dudnyk , A.K. Sinha. Nanoporous nickel oxide catalyst with uniform Ni dispersion for enhanced hydrogen production from organic waste. *Int. J. Hydrogen Energy,* 2019, vol.44, pp. 19573-19584.
https://doi.org/10.1016/j.ijhydene.2019.05.203
7. O.M. Dudnyk, N.I. Dunaevska, I.S. Sokolovska. Application of the technologies of combined-cycle power plants with the integrated gasification of solid and liquid fuel in the global energy industry and prospects for their introduction in Ukraine, *The Problems of General Energy,* 2019, 3(58). pp. 32-39.
https://doi.org/10.15407/pge2019.03.037
8. O.M. Dudnyk Development of biogas power technologies in PRC and Ukraine. *Energy news*. 2019. No.1, pp.23-26.

9. O.M. Dudnyk, I.S. Sokolovska. Autonomous cogeneration power plant using energy of solid organic fuels and hydrogen. Proceedings of the 15th International Scientific and Practical Conference *"Coal heat power generation: Ways of reconstruction and development"***,** Kyiv: Gnozis, October 1-2, 2019, pp. 46-49.

10. O.M. Dudnyk. New Fuel Cell Combined Cycle and Hybrid Power Plants. Proceedings of the 15th International Scientific and Practical Conference *"Coal heat power generation: Ways of reconstruction and development"***,** Kyiv: Gnozis. October 1-2, 2019, pp. 40-43.

11. Ye.Yu. Kalishyn, A.I. Trypolsky, O.M. Dudnyk, I.B. Bychko, I.S. Sokolovska, P.E. Stryzhak. Fuel briquett for hydrogen production, UA utility patent No.106501, published Apr.25, 2016.

12. I.B. Bychko, Ye.Yu. Kalishyn, A.I. Trypolsky, L.Yu. Dolgikh, I.V. Deynega, P.E. Stryzhak, O.M. Dudnyk, I.S. Sokolovska. The catalyst of carbon monoxide conversion. UA utility patent No. 60805, published June 25, 2011.

13. Ye.Yu. Kalishyn, A.I. Trypolsky, L.Yu. Dolgikh, I.V. Deynega, P.E. Stryzhak, O.M. Dudnyk, I.S. Sokolovska. A method for hydrogen production, UA utility patent No. 60806, published June 25, 2011.

Development of the methods of hydrogen production in autonomous power supply systems using renewable energy sources

S. Kudrya, Yu. Morozov, M. Kuznetsov

Institute of Renewable Energy, NASU, Kyiv, Ukraine

Methodological foundations of energy indicator calculations for solar and wind power plants based on actual data of solar radiation and wind speed in their locations (Lviv, Zaporizhia and Kyiv regions) are developed.

Meteorological data of solar radiation and wind power in the areas of the above stations are analyzed and used for calculation of electricity production of solar and wind power plants to obtain technical and economic indicators for appropriate technological schemes.

On the territory of the above-mentioned wind and photovoltaic stations the technological parameters of operation of these power plants are determined and the scheme decision for application of electrolyzers for hydrogen production is developed.

The data of hydrogeological conditions of geothermal deposits of Kharkiv, Poltava, Lviv and Zakarpattia regions of Ukraine are generalized.

The use of geothermal energy sources is envisaged in two main directions. The first direction involves the use of existing wells with a depth of more than 3000 m to generate electricity through the use of heat generators and downhole electrolyzers. The second direction involves the use of thermal energy of underground permeable layers by creating a geothermal circulation system. To increase the flow rate of geothermal wells, the use of a high-pressure electrolyzers is envisaged. In this case for increasing of energy properties not only hydrogen obtained by electrolysis of water is used, but also oxygen is used too.

The production of electricity under meteorological conditions of the wind power plant in Stary Sambir, with a capacity of 13.2 kW, located in the Lviv region, has been determined. Annual electricity production is 35 million kWh. The wind rose and the average annual wind speed were determined, the analysis of hydrogeological data in the

areas of construction of the wind power plant and the generalization of data on their electricity generation have been performed.

Technological schemes of hydrogen production in the construction sites of solar, wind and geothermal power plants have been developed. The combined schemes of hydrogen production are developed, and the priority objects of construction of research and industrial installations are substantiated, in particular, schematic diagram of an underground gas reservoir in an aquifer using a solar power plant, and also schematic diagram of an underground gas reservoir in an aquifer using a wind farm. According to the developed technological schemes, the cooling of hydrogen after its compression to a pressure value equal to 1.3 values from the initial hydrostatic pressure in the underground permeable layers occurs due to heat exchange with water coming from the upper permeable layers and corresponding temperature is equal 10^0 C-15^0 C. This allows not only to cool hydrogen for storage in aquifers, but also at least 2 times to increase its share.

Hydrogeological conditions of Ukraine in the locations of existing solar and wind power plants allow us to raise the question about construction of underground hydrogen storage facilities in aquifers.

Existing gas storage facilities cannot be used to accumulate hydrogen because they mostly use depleted gas fields. So, when hydrogen is injected to existing gas storage facilities a mixture of hydrogen with natural gas of uncertain proportions may be created. Furthermore, the existing gas storage facilities are located relatively far (at a great distance) from the built solar and wind power plants.

The objects of priority construction of research and industrial installations for hydrogen production and storage have been identified, namely locations in Ivano-Frankivsk, Mykolaiv, and Kherson regions.

A system of hydrogen and oxygen utilization has been developed to increase the energy efficiency of geothermal power plants that use associated fuel gas from geothermal fields.

The analysis of hydrogeological data of separate regions of Ukraine has been carried out for the purpose of substantiation of locations of underground reservoirs of hydrogen.

Technological schemes of hydrogen production and underground storage with the use of solar and wind energy have been developed. The

mathematical model of underground hydrogen storages is substantiated and developed, and technological indicators of construction and operation of research and industrial installations with use of wind, solar and geothermal energy are defined.

Proposed method for creating of underground storage of hydrogen in aquifers allows to reduce energy costs for its injection into aquifers and ensures hydrogen cooling in a continious mode (Fig. 1).

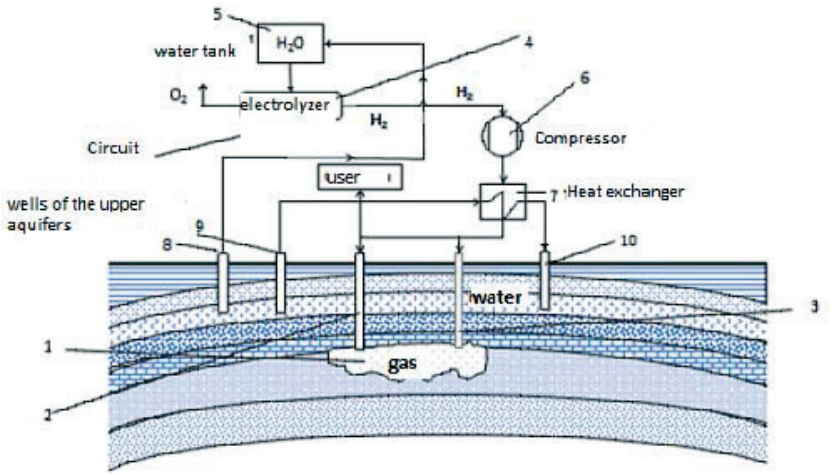

Fig. 1 The method for creating of underground hydrogen storage in aquifers.

When method of creating underground storage of hydrogen in aquifers, which includes drilling injection or production-injection wells is applied, water from the upper layers of the earth, which at a depth of 20-50 meters (according to the Geological Survey) has the temperature 8 ^{0}C - 12 ^{0}C is used for gas cooling (hydrogen). According to the proposed invention pumping of groundwater and injection of heated water is carried out in the same aquifers, or another aquifer, depending on the filtration capacity of the reservoir to receive this water. In the case of injection of heated water into the same formation as the selection of cooling water, the distance between the production and injection wells

must ensure the impossibility of thermal exposure to water in the underground horizon, which is used to cool hydrogen.

The method of installing of a filter with gravel packing in wells with weakly cemented reservoirs have been proposed. Due to new technological operations and changing the ratio of process parameters it provides an increase in the density of gravel packing filter and, accordingly, improve the quality and durability of downhole filter.

Intellectual Property:

UA patent for a utility model No. 145063 "Hydrogen and oxygen utilization system to increase the energy performance of geothermal power plants that use associated fuel gas from geothermal fields", published Nov 25, 2020, bull. No. 22 had been received.

Two applications for utility model have been submitted:

1. A method of creating underground storage of hydrogen in aquifers;
2. The method of installing a filter with gravel packing in wells with poorly cemented reservoirs.

Some project results are presented in monograph “Renewable energy sources”, edited by S.O. Kudrya, 2020, Kyiv, IRE, 392p.

Technological readiness for the construction of underground hydrogen storage facilities is evaluated as sufficient for implementation. Such conclusion based on many years’ experience in the construction of such natural gas storage facilities in porous underground structures, both in aquifers and depleted gas fields.

Development of scientific bases for the establishment of the hydrogen production technologies using renewable energy sources and prospects of its further usage for energy supply in Ukraine

S. Kudrya, M. Kuznietsov, K. Petrenko

Institute of Renewable Energy, NASU, Kyiv, Ukraine

The paper presents a justification of the possible ways, stages and quantitative indicators of the use of hydrogen obtained with the renewable energy sources, in particular wind and solar energy. The aim of the project is the study of the possibility of hydrogen use as an energy source in power systems of different levels of localization, as well as in other industries, such as an autonomous energy source in vehicles and heat supply systems. In addition to a stable supply of energy needs, the use of hydrogen minimizes environmental damage. The potential opportunities and achievable volumes of hydrogen production by solar and wind power plants in the natural conditions for different regions of Ukraine have been studied the possibilities of hydrogen use have been determined.

In Ukraine, the state of energy system is characterized by the deterioration of infrastructure, electricity networks, and by the exhaustion of the service life for traditional generating stations. There is a significant deficit of shunting and regulating capacities in the balance of power system capacities: the available amount of shunting capacities is less than 10% with an estimated need of more than 15%, while electricity losses in the networks are almost 12%. Balancing is complicated by the growth of non-guaranteed generation capacity. The total wind and solar installed capacities have already exceeded 6 GW. Furthermore, there are projects for expanding installed capacity up to 10 GW and more. Since these capacities are concentrated in the southern regions, the current power system is not able to operate adequately with such volumes of variable generation. Localization of power systems, in particular with hydrogen-based balancing, reduces the need for interregional electricity flows and overall shunting capacity. A rational solution is the energy storage to ensure energy balance. Another possibility of excess renewable energy

storage is the production of hydrogen with its subsequent supply to the natural gas pipeline. Hydrogen from renewable electricity allows large amounts of RES to be directed from one the energy sector to other ones where the further electrification (and, consequently, decarbonization) is difficult. Thus, hydrogen promotes closer links between the electricity system and industry, utilities and transport, increasing the flexibility of the energy system while promoting the integration of RES.

Ukraine has a significant potential for the use of hydrogen not only in energy (as a means of energy storage), but also in other industries. The possibility of hydrogen long-term storage as an intermediate energy source is the advantage, that makes it attractive for autonomous power systems. The cost of hydrogen depends on the technology of its production, and in the case of the renewable energy sources using - on their natural potential. The cost of "green" hydrogen is equal to traditional technologies in some cases, mostly at the areas with high wind and solar potential.

Scenarios for obtaining of a "green" hydrogen from RES (wind, sun) are based on the studies of the natural potential of Ukraine. The potential of wind and solar energy has been studied for all the regions of Ukraine. For this purpose, various sources of information about meteorological factors were used (data from state meteorological stations, operating wind and solar stations, loggers’ data and satellite data). There are opportunities for implementation 500 GW -700 GW installed capacity of RES in Ukraine (including offshore wind farms) and for average annual electricity production of more than 1.5 billion MWh that is 10 times higher than annual consumption in Ukraine. The largest capacities are available in Dnipro, Zaporizhzhia, Odessa, Kherson regions, and it applies to both wind and solar energy. If we direct the entire potential of RES on hydrogen production, it is possible to obtain up to 500 billion nm^3 per year. Thus, significant amounts of "green" hydrogen can be used for decarbonization in energy, transport, industry sectors or export.

The needs in hydrogen for the transport industry can be estimated by the volume of passenger and freight traffic. In Ukraine, more than a half of the passenger traffic was traditionally operated by buses. The railway carries about 500 million passengers a year, while road transport carries more than 3 billion passengers, and this value will exceed 5 billions

passengers if private transport will be included. Most of the large public buses (about 90%) are overworn and need to be replaced with more comfortable and environmentally friendly ones. The same applies to minibuses in cities. In railway transport, Ukraine has about half of the electrified tracks with a total length of tracks up to 20 thousand km. Transport consumes up to 7 billion kWh of electricity per year. This determines the potential market for hydrogen transport. In the naval sector, ships with fuel cells are mainly at the stage of demonstration projects. In Ukraine, the use of hydrogen in water transport has its own prospects. In particular, over the last 5 years there has been an increase in the volume of transportation of goods by river transport, its potential has been mastered by only a third. There is a background for increasing the volume of that traffic, as the cost of transportation by river is more profitable than by road and rail.

In the gas industry, hydrogen can be used for the substitution of the natural gas, currently mainly in the form of additives or mixtures. Pipelines seem to be the main way of hydrogen transportation in Ukraine, and underground gas storage facilities can serve as storage tanks. In addition to its main purpose as a mechanism for transporting hydrogen, the use of pipelines can provide a number of additional benefits: improved gas supply; convergence of electricity and gas network ("power-to-gas"); energy storage ("energy transfer over time"); decarbonization of the gas network. The main problem at the moment is the prospects of the Ukrainian gas transportation system after the expected reduction in the transit of Russian natural gas. Even now, gas pipelines are not fully used. However, there is a possibility of their modernization for alternative usage related to the supply of hydrogen or mixtures to both the national market and for export to EU countries. It is also possible to implement investment projects for the construction of new special pipelines for hydrogen transportation. According to “Ukrtransgaz” company information, the total length of gas pipelines in Ukraine is 39 thousand km, including 22 thousand km of main pipelines, and their capacity at the exit to the EU is almost 150 billion m^3 per year.

The potential for hydrogen storage capacity in Ukraine requires further research; it also applies to the capacity of underground gas storage

facilities, that are concentrated mainly in the western regions of the country. The total capacity of 12 underground gas storage facilities reaches 30 billion m^3, and they are currently used by 50-60%.

An important component of assessing the possibilities of obtaining hydrogen by electrolysis is the analysis of water resources of Ukraine, because electrolysis of water is currently considered the most optimal technology for obtaining stable hydrogen. The purpose of the analysis of Ukraine's water resources is to evaluate the water resources of Ukraine and find out the possibility of using them to obtain "green" hydrogen. The potentially possible volume of "green" hydrogen production in Ukraine by electrolysis is calculated based on the results of scientific research of the potential of electricity generation by wind and solar plants. For the calculation of the potential "green" hydrogen output via electrolysis it was provided specific power consumption of 4.5 kWh /nm^3 H_2. 750 million m^3 of water is required to use the annual potential of “green” hydrogen per year (500 million nm^3). The expected reduction of water losses by 2030 due to the improvement of technological processes of lifting, production and transportation of water as a result of the introduction of energy efficient technologies, allows to meet 70% of water demand to use all available average annual production potential of "green" hydrogen per year. Analysis of stocks of normatively treated and normatively pure without wastewater treatment (4,5 billion m^3) showed a 6-fold excess of water demand for the realization of the full potential of "green" hydrogen. Seawater can also be used to produce hydrogen. Thus, the available water resources of Ukraine are quite sufficient to fully realize the potential of green hydrogen production without increasing the water intake.

Energy sector should be the most important consumer of hydrogen at the moment. The use of "green" hydrogen as an intermediate energy source is quite favorable for the power system. Electrolyzers are able to provide flexibility of the power system on several time measurements. Electrolyzers to be the devices for ballancing changes in electricity consumption, can manage energy flows in the common network. A key factor is the unique ability to locate electrolysis facilities to provide seasonal power system flexibility, that no other resource can effectively provide. It plays a significant role in balancing the energy system with

high proportions of solar and wind energy. To be able to provide such services, electrolyzers must not be designed to operate at full capacity throughout the year, but to use available environmentally friendly electricity. According to the optimistic scenario of Ukraine's energy development, part of RES energy (30-35 billion kWh) is used directly for the needs of the power system, and the surplus (10-12 billion kWh) goes to the production of "green" hydrogen, which is then used for production electricity ("Power to Gas" technology). The volume of hydrogen obtained in this case is about 2.5 billion nm^3, and the losses of RES production due to artificial power limitations are insignificant.

The share of RES in the generation of electricity may eventually exceed this scenario, replacing fossil fuels; the share of "green" hydrogen will increase proportionally to ensure the flexibility of the RES. RES capacity that exceeds the needs of the power system can work for the technology "Power to X" (including "Power to Gas"), to obtain commercial hydrogen as a raw material for the chemical industry, metallurgy, transport, utilities, as export products.

The assessment of the renewable energy potential for the needs of the hydrogen economy, performed at the Institute of Renewable Energy of the National Academy of Sciences of Ukraine, was used in the development of a number of programs and draft strategies. An example of such developments is the Draft Roadmap for Hydrogen Production and Use in Ukraine (2021), performed at the request of the Ministry of Energy of Ukraine with the support of the United Nations Economic Commission for Europe and funded by the Regular Technical Cooperation Program (RPTC). The use of hydrogen in transport is considered in the Draft Roadmap for the use of hydrogen in Ukraine in the field of road transport (2021), in the framework of the RPTC. Much of the research in the field of "green" hydrogen was performed by the International Renewable Energy Agency (IRENA), the Ukrainian Hydrogen Council. Problems of balancing the power system of Ukraine and the possibility of using hydrogen are contained in the "Report on the assessment of compliance (sufficiency) of generating capacity to cover projected electricity demand and provide the necessary reserve in 2020" (2021), performed by the transmission system operator NEC Ukrenergo.

According to the research, the problem of using hydrogen obtained from renewable energy sources needs a comprehensive solution. Scientific, design, financial institutions should be involved in development of such complex solutions. State support should be provided by state-level agencies: the Ministry of Energy, the Ministry of Ecology and Natural Resources, the Ministry of Finance, the Ministry of Development of Communities and Territories of Ukraine, the State Agency for Energy Efficiency and Energy Saving, the Antimonopoly Committee of Ukraine, the State Nuclear Regulatory Inspectorate. The obligatory components of the hydrogen strategy should be: assessment of the available natural and technical potential of renewable energy sources, especially wind and solar, diversified by regions of Ukraine; analysis of the opportunities for energy and gas transport infrastructure; evaluation of the technical capabilities for the production of appropriate equipment; determination of the various industries demand in hydrogen both energy and raw materials; estimation of the possibiliities for storage, transportation, export of hydrogen.

The transition to hydrogen energy as carbon-free technology requires certain stages where scientific, technical, organizational, financial and commercial issues should be solved. The presence of a comprehensive issue and assessment of the main problems are the advantages of this study, especially the developed methodology and the results obtained in assessing the potential of RES. However, the development of a detailed strategy and action plan requires further concerted work of the above-mentioned stakeholders.

The main research results on the project “Development of scientific bases for the establishment of the hydrogen production technologies using renewable energy sources and prospects of its further usage for energy demands in Ukraine” are published in the following publications

1. S.Kudria, I. Ivanchenko, B.Tuchynskyi, K. Petrenko, O. Karmazina, O. Riepkin. Resource potential for wind-hydrogen power in Ukraine, *Int. J. of Hydrogen Energy*, 2021, vol.46, pp.157-168

2. S.Kudria. Atlas of Energy Potential of Renewable Energy Sources of Ukraine, 2020, IRE, Kyiv, 45p.
https://www.ive.org.ua/wp-content/uploads/atlas.pdf

3. Renewable energy sources, monograph, edited by S. Kudria, IRE, Kyiv, 392 p.
https://www.ive.org.ua/?page_id=953
4. K.Petrenko, I.Ivanchenko, O.Karmazin. Analysis of Ukraine's water resources in the context of their use possibility for the production of "green" hydrogen, *Vidnovluvana energetika,* 2021, No.2, pp.19-28. (in Ukrainian).
https://doi.org/10.36296/1819-8058.2021.2(65).19-28).

Autonomous catalytic hydrogen generator from raw bio-materials

L. Dolgikh, A. Trypolskyi, I. Stolyarchuk, L. Stara, Y. Pyatnitsky, P. Strizhak

Pisarzhevsky Institute of Physical Chemistry, NASU, Kyiv, Ukraine

Introduction

Ethanol steam reforming (ESR) is a promising process for hydrogen production from liquid biomaterials: $C_2H_5OH + 3H_2O \rightarrow 6H_2 + 2CO_2$. Theoretically, it allows obtaining 50% of hydrogen from ethanol and 50% of hydrogen from water. Moreover, hydrogen production from bioethanol by ESR reaction does not affect the concentration of carbon dioxide in the atmosphere because the carbon dioxide produced by ESR is consumed during biomass growth. Bioethanol (aqueous solution of 10-18 wt % of ethanol) can be directly employed for steam reforming, thus avoiding the expensive costs for water separation, and increasing the overall energy efficiency of the process. Taking into account the increasing demand for renewable energy, the industrial implementation of bioethanol steam reforming as an alternative source of hydrogen is highly realistic [1]. Hydrogen produced via steam reforming from the renewable sources may be efficiently utilized for electric energy production, especially for small-scale electricity supply. Combining of the steam reforming with a fuel cell establishes a new kind of technology for power generation. Using of the portable power systems based on fuel cell application simultaneously resolves the two issues of hydrogen use, in particular, hydrogen storage and its transportation [2].

The project aims to develop catalysts and a portable reactor for heterogeneous-catalytic conversion of bioethanol for its use as an autonomous hydrogen generator for the operation of hydrogen fuel cells.

Testing of the mixed oxide catalysts for the ESR reaction

To ensure compliance with the specifications of fuel cells, hydrogen production processes are aimed at increasing the yield of H_2, reducing the CO content, and limiting the formation of carbon deposits. In the ESR process, the choice of the appropriate catalyst is a key factor

for ethanol conversion and high hydrogen selectivity. A very wide range of catalysts was explored to obtain the optimum conditions for the ESR reaction, in the overwhelming majority, they were supported metals, including Ni, Co, Cu, Rh, Ru, Pd, Ir, and Pt [3-6]. Only a limited number of other types of catalysts have been employed for this reaction, in particular, simple and complex oxides [7, 8].

In this work, an experimental evaluation of the possibility for obtaining of hydrogen with the required purity for the operation of fuel cells by steam reforming of bioethanol on iron-containing oxide catalysts supported on oxide (ZrO_2) and carbon (CNT) carriers, as well as on massive ferrites MFe_2O_4, (M = Fe, Co, Ni, Cu, Zn) with a spinel structure was performed. To optimize the method of preparation, the catalytic properties of iron-containing catalysts prepared by methods of impregnation (the obtained samples were denoted as Fe/ZrO_2 and Fe/CNT), coprecipitation (the catalyst was denoted as MFe_2O_4-CP), and solvothermal decomposition (the catalyst was denoted as MFe_2O_4-HC) were studied. To investigate the optimal parameters for the design of the autonomous catalytic hydrogen generator, the process of the steam reforming of either diluted $C_2 - C_4$ alcohols or ethanol/higher alcohols mixtures which reflect the composition of the raw bioethanol is studied.

Fe/CNT exhibits increased activity and productivity to hydrogen at relatively low temperatures. Over this catalyst, high ethanol conversion (94%) and hydrogen selectivity (50%) was achieved at 400 °C. The catalyst supported on ZrO_2 and massive samples show similar performance at 450-550 ° C with H_2 selectivity up to 75%. Under these conditions, the Fe/CNT catalyst tends to agglomerate and gasify with hydrogen, which is formed during ESR. Using ferrites $MgFe_2O_4$, $MnFe_2O_4$, $FeFe_2O_4$ 98 – 100% ethanol conversion is achieved in the temperature range between 550 and 650 ºC, whereas hydrogen yield reaches 82-94 % (WHSV = 4000 h^{-1}, 2,7 mol % C_2H_5OH, 50 mol % H_2O, N_2 - balance). It is shown that the formation of carbon monoxide was not observed up to a temperature of 500 °C. At elevated temperatures, CO was recorded on $NiFe_2O_4$ (550-700 °C), $CoFe_2O_4$ (600-700 °C), and $MnFe_2O_4$ (700 °C). For the ethanol/higher alcohols mixture (propan-1-ol, propan-2-ol, butan-1-ol, butan-2-ol, pentan-1-ol (1 mol % of each alcohol), and 4.75 mol % of ethanol), ethanol conversion and higher

alcohols conversion at 500 ºC are 97% and 83 – 90%, respectively. Selectivity toward hydrogen is ~80%. $MnFe_2O_4$-CP catalyst exhibits higher hydrogen yield in the temperature range between 450 ºC and 550 ºC compared to $MnFe_2O_4$-HP catalyst. In contrast, a higher hydrogen yield is observed on the $MnFe_2O_4$-HP catalyst for T > 600 °C. At 500 ºC, productivity toward hydrogen of the steam reforming process is higher for alcohol mixture in contrast to the water-ethanol mixture without higher alcohols. This difference in productivity is regulated by an effective steam reforming of higher alcohols with the utilization of the water vapor on the developed catalyst.

The obtained results for of $MnFe_2O_4$ catalysts stability assessment by their using in the reforming process for 30-40 hours demonstrated that the ethanol conversion and hydrogen yield remain stable at 550-650 °C using water-ethanol mixtures containing 12 - 24 % (wt.) of ethanol.

Technological design of the catalytic generator of hydrogen

Various hydrogen generators, including portable devices, have been introduced in recent years. A small-size generator based on n-dodecane steam reforming for naval use with the hydrogen productivity of 1.5 Nm^3/h has been reported [9]. A combined all-in-one portable generator with a PEMFC has been developed using sodium borohydride as a source of hydrogen [10]. An autonomous setup for hydrogen production by methane steam reforming coupled to a catalytic methane combustor has been developed [11]. However, the reported devices imply the use of chemical hydrides, ammonia borane, and hydrocarbons as a source for H_2 generation [12].

The portable autonomous hydrogen generator requires a simple technological scheme and should be easy for exploitation in contrast with large stationary generators. The autonomous catalytic hydrogen generator was developed under ISO 16110 Hydrogen generators using fuel processing technologies and IEC 62282-5-100 Portable fuel cell power systems requirements. In general, the essential parts of a portable hydrogen generator are fuel processing system, fuel cell module, fuel supply system, onboard energy storage system, and water treatment system. The fuel processing system provides fuel conversion into hydrogen. In the fuel cell module, hydrogen is converted into electric

energy in an electrochemical way. The obtained electricity is further integrated into the energy generation system.

Small power plants are typically based on proton-exchange membrane fuel cells (PEMFC) and solid oxide fuel cells (SOFC). In this project, we used the PEMFC. This cell works at low temperature (< 80°C) and is not sensitive to hydrogen purity, e.g., CO_2 additives. For the calculations of the generator efficiency, we use the characteristics of the commercially available PEMFC produced by Horizon Fuel Cell Technologies Company.

We propose an approach to carry out ESR reactions in a single fixed bed reactor using the patented catalyst. A principal scheme of the hydrogen generator is shown in the figure.

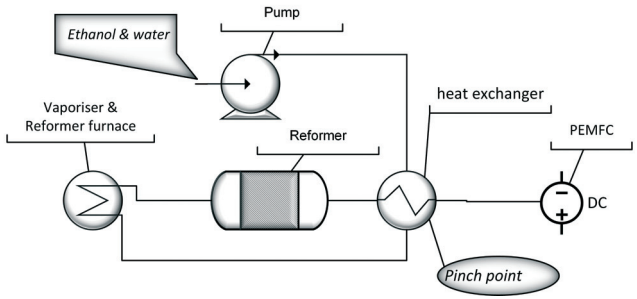

The applicability of a single-reactor scheme is governed by the developed $MnFe_2O_4$ catalyst. Using this catalyst in the ESR reaction almost 100% bioethanol conversion may be achieved at relatively low reaction temperature (650 °C). Moreover, small amounts of the reaction byproducts, e.g., oxygenates and CO, are obtained. The amount of CO is only 50 – 60 ppm, which is suitable for PEMFC stable functioning. The unreacted bioethanol and reaction byproducts (oxygenates) do not effect on the PEMFC operation. Carbon dioxide does not poise the Pt-Ru catalyst in the fuel cell, whereas water is required for stable fuel cell functioning.

The presented scheme admits the utilization of thermal energy of the reaction mixture for vaporization and heating the input water-alcohol mixture. According to this scheme, the heat exchanger is placed between

the reactor and fuel cell module and serves as a pinch zone. Also, the pinch zone provides the flexibility of the water/alcohol ratio in the input mixture. The role of the water/alcohol ratio is crucial because this ratio significantly affects the alcohol conversion, hydrogen yield, as well as catalyst lifetime. The generator is capable to produce 1 kW/h electricity with 0.63 kg/h water/alcohol mixture (50 % ethanol) consumption. The energy conversion efficiency of the developed generator is 44%.

Area of application

The proposed hydrogen generator is suitable for various applications related to in-field hydrogen production.

Comparative evaluation of the results

The process of ethanol steam reforming is not commercialized today. Investigations in this area are carried out in scientific centers of several European countries (France, Italy, Spain, Greece, Hungary), the USA, Brazil, China, and Japan.

An autonomous catalytic hydrogen generator provides the possibility of hydrogen production based on renewable raw materials (bioethanol) as an alternative to the processes using fossil fuels, in particular methane. The generator allows the utilization of thermal energy of the reaction mixture for vaporization and heating the input water-alcohol mixture. The generator is characterized by a simple single-stage design without a stage for hydrogen purification. The proposed catalysts can provide a high degree of ethanol conversion and selectivity for hydrogen production, contain no noble and/or rare earth metals, have a carbonization resistance, and do not require additional hydrogen costs for the reduction of the active metal phase. We believe that the development of the autonomous power plant consisting of the catalytic hydrogen generator based on bioethanol steam reforming and fuel cells allows eliminating the issues concerning hydrogen transportation and storage.

Level of technology readiness

TRL 4 – Technology validated in lab. A working laboratory model of a portable autonomous catalytic hydrogen generator has been developed. The possibility of its use for testing the technological

parameters of the process of obtaining hydrogen from bioethanol on the developed catalysts is shown. There were developed the perspective initial catalytic systems based on ferrites Mn and Fe, which were characterized by the thermal stability of the oxide phase, demonstrated significant catalytic activity and selectivity in the process of hydrogen production by steam reforming of liquid oxygenates derived from biomass.

Intellectual property

Method for obtaining hydrogen. UA patent No,60806, published June 25, 2011, bull. No. 12..

Catalyst for the obtaining of hydrogen by steam reforming of ethanol. UA patent No. 115288, published Apr. 10, 2017, bull. No. 7

The main publications in the frame of the project “Autonomous catalytic generator of hydrogen from biological raw materials”:

1. L.Yu. Dolgikh, L.O. Staraya, I.L. Stolyarchuk, Yu.I. Pyathitsky. Low-temperature steam reforming of ethanol over iron catalysts on oxide and carbon supports , *Theor. Exp. Chem*., 2020, vol. 56. No 3. pp.192-196. https://doi.org/10.1007/s11237-020-09651-5

2. L.Yu. Dolgikh, I.L. Stolyarchuk, L.A. Staraya, I.V. Vasylenko, Y.I. Pyatnitsky, P.E. Strizhak. Efficient hydrogen production by steam reforming of ethanol over ferrite catalysts, *Kataliz ta naftohimia*, 2020, No.29. pp.1-10.
https://doi.org/10.15407/kataliz2020.29.001

3. Y.I. Pyatnitsky, L.Y. Dolgikh, L.Y., P.E. Strizhak. Hydrogen Selectivity in the Steam Reforming of Alcohols, *Theor. Exp. Chem.*, 2021, vol. 57, pp. 71–76.
https://doi.org/10.1007/s11237-021-09676-4

4. Y. Pyatnitsky, L. Dolgikh, L. Senchylo, L. Stara, P. Strizhak. A two-step strategy for the selective conversion of ethanol to propene and hydrogen, *Chemical Papers,* 2021, vol. 75, pp.5773–5779. https:// doi.org/10.1007/s11696-021-01758-w

5. L.Y. Dolgikh, A.I. Trypolskyi, I.L. Stolyarchuk, Y.I. Pyatnitsky, P.E. Strizhak Autonomous catalytic hydrogen generator based on bioethanol steam reforming, Proceedings of 3rd International Scientific Conference

"*Chemical Technology and Engineering",* Ukraine, Lviv, June 21-24th, 2021, pp. 67-69.

6. I.L. Stoliarchyk (2019). Catalytic properties of nanosized ferrites $MIIFeIII_2O_4$ in the process of ethanol steam reforming. *PhD thesis in Chemistry 02.00.15* / Pisarzhevskii Institute of Physical Chemistry, NASU, Kyiv, Ukraine, 2019, 143 p.

References

[1] Lazar M.D, Senila L, Dan M, Mihet M. Crude Bioethanol Reforming Process, *Ethanol*, Elsevier; 2019, pp. 257–288.

[2] Ni M, Leung DYC, Leung MKH. A review on reforming bio-ethanol for hydrogen production, *Int. J. Hydrogen Energy*, 2007,vol.32, pp.3238–3247.

[3] Contreras J.L., Salmones J, Colín-Luna J.A., Nuño L, Quintana B, Córdova I, Zeifert B, Tapia C, Fuentes GA. Catalysts for H_2 production using the ethanol steam reforming (a review). *Int. J. Hydrogen Energy,* 2014, vol. 39, pp.18835–18853.

[4] Haryanto A, Fernando S, Murali N, Adhikari S. Current Status of Hydrogen Production Techniques by Steam Reforming of Ethanol: A Review, *Energy & Fuels*, 2005, vol.19, pp.2098–2106.

[5] Vaidya P.D., Rodrigues A.E., Insight into steam reforming of ethanol to produce hydrogen for fuel cells, *Chem. Eng. J.,* 2006, vol.117,pp.39–49.

[6] Mattos L.V, Jacobs G, Davis B.H, Noronha F.B. Production of Hydrogen from Ethanol: Review of Reaction Mechanism and Catalyst Deactivation. *Chem. Rev.* 2012,vol. 112, pp.4094–4123.

[7] Dolgikh L.Y, Pyatnitsky Y.I, Strizhak P.E. Hydrogen production from bioethanol on mixed oxide catalysts. In M. Brenzo (Ed.), *Bioethanol and Beyond: Advances in Production Process and Future Directions*, New-York: Nova Science Publishers, Inc.; 2018, p. 381-428.

[8] Ogo S; Sekine Y. Recent progress in ethanol steam reforming using non-noble transition metal catalysts: A review, *Fuel Proces. Technol.,* 2020, vol.199, 106238.

[9] Fabiano C, Italiano C, Vita A, Pino L, Laganà M, Recupero V. Performance of 1.5 Nm^3/h hydrogen generator by steam reforming of n-

dodecane for naval applications. *Int. J. Hydrogen Energy,* 2016, vol.41, pp.19475–19483.
[10] Kim J, Kim T. Compact PEM fuel cell system combined with all-in-one hydrogen generator using chemical hydride as a hydrogen source, *Appl. Energy,* 2015, vol.160, pp.945–953.
[11] Simakov D.S., Sheintuch M. Experimental optimization of an autonomous scaled-down methane membrane reformer for hydrogen generation, *Ind. Eng. Chem Res.,* 2010, vol.49, pp.1123–1129.
[12] Zhu L, Kroodsma N, Yeom J, Haan J.L, Shannon M.A, .Meng D.D. An on-demand microfluidic hydrogen generator with self-regulated gas generation and self-circulated reactant exchange with a rechargeable reservoir. *Microfluid Nanofluidics*, 2011, vol.11, pp.569–578.

Portable photoelectrochemical cells integrated with hydrogen storage in the metal hydride electrodes

I. Rusetskyi[1], M.Danilov[1], S. Fomanyuk[1], V. Smilyk[1], G. Kolbasov[1], L. Scherbakova[2], A. Krapivka[2], K. Graivoronskaya[2], Yu. Solonin[2]

[1]*Vernadsky Institute of General and Inorganic Chemistry, NASU, Kyiv, Ukraine*
[2]*Frantsevich Institute for Problems of Materials Science, NASU, Kyiv, Ukraine*

Development of the efficient systems for the production, storage and use of hydrogen, as one of the most environmentally friendly fuel, is one of the urgent tasks of modern power engineering. Photoelectrochemical systems with photosensitive semiconductors can be used for the hydrogen production and storage. To ensure the high efficiency of the photoelectrochemical system for hydrogen production, it was developed a photoelectrochemical cell (PEC) with anode and cathode chambers separated by an ion-exchange membrane, containing an electrolyte with different compositions. In this case it is possible to use photosensitive materials with a small band gap as a photoanode. Such materials, for example, $A^{II}B^{VI}$ type semiconductor compounds, etc. can absorb visible light well. And hydrogen storage alloys (metal hydrides) have been used as a cathode.

Improved electrochemical and chemical methods for the synthesis of photosensitive electrodes for photoelectrochemical cells with hydrogen storage have been developed. By simple pyrolysis of urea and melamine foam photosensitive porous carbon nitride (g-C_3N_4) has been obtained. Photosensitive nanocomposites TiO_2/C_3N_4 and SnO_2/C_3N_4 were obtained from an emulsion of methyl alcohol and C_3N_4. The samples annealed at 300° C in air or in argon environment had high photosensitivity when they were used in photoelectrochemical cell. It was shown that at the g-C_3N_4/TiO_2 nanotube heterojunction, the absorption of visible light was significantly enhanced and, at the same time, charge separation between nanotubes TiO_2 and g-C_3N_4 was accelerated, which led to an improvement in the loading characteristics of the photoelectrochemical cell. Nanocomposites and heterostructures based on semiconducting metal oxides, sulfides and selenides (Ti, Zn, Cd), partially unzipped carbon

nanotubes, bismuth and copper vanadates and multilayer heterostructures based on them have been synthesized. It was shown that the electrochemical synthesis of semiconductor films based on the SnO_2/BiVO4/WO_3 and SnO_2/Cu_3VO_4/Cu_2O heterostructures allowed to produce materials with high physicochemical characteristics by controlling such parameters as the electrolyte composition and conditions of film annealing. Furthermore, it ensured decreasing of recombination losses and increasing for the efficiency of converting of sunlight energy into chemical energy of the hydrogen. The thermochemical synthesis of a hybrid nanocomposite with partially unzipped carbon nanotubes and C_3N_4 has been developed for the first time. Methods for modifying of the photoanode surface with semiconductor nanoparticles (quantum dots) (ZnSe, PbI_2, etc.) to reduce recombination losses and to increase the photo potential of photoelectrodes have been developed. It was shown that the formation of the NT-TiO_2/CdSe/ZnSe heterostructure led to an increase in the photosensitivity of the electrodes. The optimal annealing temperature (550 °C -600 °C) for obtaining of the electrode maximum efficiency has been determined. Using physicochemical research methods, it was found that during heat treatment an increase and ordering of the ZnSe crystals have been observed, and excess of selenium and other impurities has been removed from the film. And as a result the lifetime of the charge carrier's has been increased and the rate of their recombination has been decreased. It was found that heterostructures based on NT-TiO_2/CdSe/ZnSe had significantly better loading characteristics and quantum yield in comparison with CdSe and ZnSe, which used a small part of the visible light spectrum. In this case, the photopotential of the modified samples, when used as photoanodes, reached values of -1.2 V, which made it possible to use these electrodes together with MH cathodes in a photoelectrochemical cell for obtaining of hydrogen.

The investigated photoanodes were tested in developed photoelectrochemical cell with hydrogen accumulation. As MH cathodes there were used multicomponent alloys similar in composition to the industrial alloy $MmNi_{3,5}Co_{0,8}Mn_{0,4}Al_{0,3}$, which was recommended for use as a standard for further optimization of electrode characteristics (table 1). The structure and phase composition of $MmNi_{5-x-y-z}Co_xAl_yMn_z$ AB_5- type alloys obtained by gas sputtering (GS) have been studied. Dependence of

their electrochemical and sorption characteristics on the size of the alloy particle and electrode activation has been investigated.

Table 1 The characteristics of $Mm(NiCoMnAl)_5$ alloys.

Alloy	V, A^3	i_o, $mA \cdot cm^{-2}$	C_{max}, $mA \cdot hour \cdot g^{-1}$	Eeq / Peq V/Bar
$MmNi_{3.6}Co_{0.7}Al_{0.4}\ Mn_{0.3}$ - melt	87.775	0.18	293	-0.921/0.82
$MmNi_{3.6}Co_{0.7}Al_{0.4}\ Mn_{0.3}$- GS	89.468	0.10	288	-0.921/0.82
$(Mm+La)Ni_{3.68}Co_{0.7}Al_{0.3}\ Mn_{0.4}\ Zr_{0,03}$ - GS	88.615	0.36	287	-0.895/0.28
$MmNi_{3,7}Fe_{0,7}Al_{0,5}Cu_{0,1}$- GS	88.282	0.15	225	0.912/0.543

It was established that the process of electrochemical absorption of hydrogen for all investigated alloys was limited by the one-electron stage of charge transfer, and the discharge (hydrogen desorption) has been controlled by mixed diffusion-kinetic process. All studied alloys were easily activated (3-8 cycles) and created stable hydride (Peq.< 1 bar). Cobalt-containing alloy electrodes demonstrated high discharge capacity (C_{max} = 290 mA×h/g) and good stability of the cycles. Complete change in the composition of the alloy from Co to Fe ($MmNi_{3,7}Fe_{0,7}Al_{0,5}Cu_{0,1}$) led to a decrease in the maximum discharge capacity by 20% (225 mA×h/g). It was found that alloys of $LaNi_5$-$xM_{0.5}$ type containing Al and Mn were characterized by the good kinetics of reversible hydrogen absorption, by the high hydrogen capacity (about 300 mA×h/g), created stable hydrides, effectively absorbed hydrogen at charge currents up to $2C_{max}$ and were capable to give up to 90% of hydrogen when discharged with a currents up to 6 C_{max}.

For the first time it was shown that the ability of alloys to high-speed discharge was largely determined by the content of cobalt in its composition. Increasing the cobalt content from 6.4 wt. % ($LaNi_{4,5}Co_{0,5}$) to 13,6 wt. % ($LaNi_4Co$ $LaNi_4Co$) led to a sharp decrease in the discharge efficiency with currents ≥1000 mA/g from 88% to 10%, respectively. Electrodes made of $La_{0,7}Nd_{0,3}Ni_{2,3}Co_{2.4}Al_{0,1}$ alloy with a higher Co content (30 wt.%) were not discharged by such currents.

Alloys of the $La_3Ni_{9.7}Mn_{0.5}Al_{0.3}Co_x$ composition (where x = 0; 0,7; 1,9) were obtained by the method of electric arc melting in a protective atmosphere of argon. XRD data for studied alloy samples showed that all alloys had 2-phase structure, they contained phases of AB_3 type (spatial group $R\bar{3}m$) and AB_5 (P6 \ mmm), but the phase content and phase ratio in the alloy strongly depended on the composition of the alloy and its crystallization temperature. It was established that the electrodes from $La_3Ni_{9.7}Mn_{0.5}Al_{0.3}Co_x$ alloys were easily activated and reached the maximum value of the discharge capacity (C_{max}) within 3-7 cycles. All alloys, except $AB_{3,73}$ formed stable hydrides in open systems (Equ. <1 atm). With an increase in the stoichiometric index (x) and a decrease in the content in the alloys of the AB_3 phase, it was observed the increase in cyclostability and in the discharge capacity to 309 mA×h/g, the best results were obtained on the electrodes of alloys $AB_{4.12}$ (AB_3, 40,0 - AB_5, 60,0) and $LaNi_{3,9}Co_{0,7}$ ($AB_{4.6}$). As alloy Co content increased, the efficiency of high-velocity discharge with currents ≥ 1000 mA/g decreased sharply, but the activation process by cycling allowed to reach to the value of C max significantly quicker and improved it.

Solar cells where the chemical energy of accumulated hydrogen has been converted into electricity by the metal hydride cathode, hydrogen accumulation has been performed under the action of sunlight and discharge process has been ensured by a third electrode placed in the anode or cathode chamber have been developed.

The design of a photoelectrochemical solar cell based on the MH/air electrode system is shown in Fig. 1.

The cell includes three electrodes: a photoanode, an MH cathode, and an air electrode. The working chamber of the photoanode, filled with a sulfide solution is separated by the MF-4SK membrane from the working chamber filled with the KOH which contain the MH cathode and the air electrode (Fig. 1 b). From the discharge curves obtained on the MH-air cell, it was found that the voltage across the cell was ~ 0.85 V when discharging with a current of 20 mA in a 6M KOH solution using an air electrode took place.

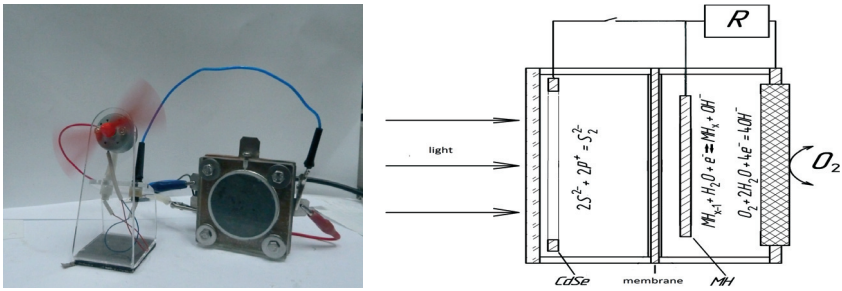

a b

Fig. 1 Photoelectrochemical cell (a) and its scheme (b) with the MH/air electrode system.

Thus, one of the possible solutions for rapid progress in the field of green energy is photoelectrochemical (photovoltaic) cells with energy storage integrated directly into the solar cell. In this case, we used the chemical energy of bound hydrogen, which should provide uninterrupted power supply, even when there was no illumination.

The results obtained may be interesting for the companies engaged in research in the field of hydrogen energy. These are companies and organizations such as MER (Material and Electrochemical Research) Corporation (US), MV Systems, General Electric, SRI International (Menlo Park, US), Japanese New Energy and Industrial Technology Development Organization (NEDO), Siemens (Germany), Hydrogenics (Canada), BP plc, Chevron Texaco, Praxair, Iwatani International (Japan) and others. Authors have following three patents of Ukraine:

1. G.Ya.Kolbasov, Yu.M.Solonin, I.A.Rusetskyi, D.B.Danko. Photoelectrochemical element with hydrogen storage, UA Patent No. 75975, published June 15, 2006, bull. No.6.
2. I.O. Slobodyanyuk, I.A. Rusetskyi, G.Ya. Kolbasov, S.D. Kobylianska, A.G. Bilous, Photoelectrochemical cell for hydrogen extraction with Li conductive membrane, UA Utility model patent No. 73554, published, Sep. 25, 2012, bull. No. 18.
3. M.O. Danilov, I.O. Slobodyanyuk, I.A. Rusetsky, G.Ya. Kolbasov, Oxygen electrode for current sources based on reduced graphene oxide, UA Utility model patent No. 78047, published March 11, 2013, bull. No. 5.

The results obtained within the framework of the project may be the basis for the creation of an experimental commercial installation for the production and use of hydrogen by the PEC method.

The main publications in the frame of the project "Portable photoelectrochemical cells with hydrogen accumulation":

1. I.A. Rusetskyi, M.O. Danilov, S.S. Fomanyuk, I.A. Slobodyanyuk, V.S. Vorobets, G.Ya. Kolbasov. Photoelectrochemical properties of the composites based on TiO_2 nanotubes, CdSe and graphene oxide, *Research on Chemical Intermediates*, 2019, vol. 45, pp. 4121–4132. https://doi.org/10.1007/s11164-019-03895-0

2. V.O. Smilyk, S.S. Fomanyuk, G.Ya. Kolbasov, I.A. Rusetskyi, V.S. Vorobets. Electrodeposition, optical and photoelectrochemical properties of $BiVO_4$ and $BiVO_4/WO_3$ films. *Research on Chemical Intermediates*, 2019, vol.45, pp. 4149–4161
https://doi.org/10.1007/s11164-019-03897-y

3. A. Rusetskyi, L. L. Kovalenko, I. A. Slobodyanyuk, M. O. Danilov, S. S. Fomanyuk, V. O. Smilyk, A. G. Belous, G.Ya. Kolbasov. Photoelectrochemical systems for hydrogen evolution using ion-conducting membranes, *ECS Trans.,* 2020, vol. 99, pp. 221-230. https:// doi.org/10.1149/09901.0221ecst

4. M.O. Danilov, S.S. Fomanyuk, G.I. Dovbeshko, O.P. Gnatyuk, I.A. Rusetskyi, G.Y. Kolbasov. Graphene Quantum Dots from Partially Unzipped Multi-Walled Carbon Nanotubes: Promising Materials for Oxygen Electrodes, *Journal of the Electrochemical Society*, 2021, vol. 168, No. 044514
https://doi.org/10.1149/1945-7111/abf4b3

5. M.O. Danilov, G.I. Dovbeshko, I.A. Rusetskyi, V.I. Pekhnyo, A.S. Nikolenko, G.Ya. Kolbasov. Partially unzipped multi-walled carbon nanotubes—promising material for oxygen electrodes of fuel cells, *Applied Physics A*, 2020, vol. 126, article id.764. https://doi.org/10.1007/s00339-020-03951-2

6. O.V. Perlova, Yu.S. Dzyazko, A.V. Palchik, I.S. Ivanova, N.O. Perlova, M.O. Danilov, I.A. Rusetskii, G.Ya. Kolbasov, A. G. Dzyazko Composites based on zirconium dioxide and zirconium hydrophosphate containing graphene-like additions for removal of U(VI) compounds

from water, *Applied Nanoscience,* 2020, vol.10, pp.4591-4602, https://doi.org/10.1007/s13204-020-01313-1

7. S.S. Fomanyuk, Kolbasov G.Ya., T.A. Mirnaya, G.G. Yaremchuk, Rusetskyi I.A. Electrosynthesis of colloid solutions of CdTe and ZnSe nanoparticles and their optical properties, *Chemical Problems,* 2020, vol.2, pp. 133-144.

Optimized production of synthesis gas from a mixture of hazardous organic waste

V. Zhovtyansky, E. Kolesnikova, M. Ostapchuk

Institute of Gas, NASU, Kyiv, Ukraine

1. Brief description

Processing of sewage sludge obtained from municipal treatment plants as well as worn-out tires, unsorted solid waste including those already accumulated in landfills and persistent organic pollutants is the subject of this study.

The purpose of the work is to develop the scientific foundations of modern technology for hydrogen production based on plasma-steam-oxygen gasification from hazardous renewable raw materials, in particular, mixture of sewage sludge from aeration stations contaminated with toxic heavy metals and rubber crumbs of worn tires (Fig. 1).

An exceptional advantage of plasma technologies used for gasification of waste is the high thermodynamic parameters of the process. That is why it has no restrictions on the quality of carbonaceous raw materials to be gasified. This advantage allows also converting even the most hazardous chlorine-containing waste. In the case of sewage sludge processing, they additionally provide vitrification (encapsulation in the glass mass of molten slag) of heavy metals. The absence of this operation creates significant environmental risks because in that case heavy metals are the part of dry ash residue compounds.

The key issue explored in this project is the achievement of maximum energy efficiency of the process of gasification of mixed raw organic waste. The idea of joint gasification of waste is the key element for solving the problem. Joint gasification or total energy gasification process allows the compensation of the high ash content of one type of raw material by high calorific value of another one. It is necessary to underline that the energy efficiency of the gasification process, and also the final cost of one of the components of syngas – hydrogen to be the target product of hydrogen energy, is fully consistent with the activity of new global coalition Clean Hydrogen Mission created by 22 countries and the European Commission in June 2021 to support a clean hydrogen economy [1].

Fig. 1. Hydrogen production based on plasma-steam-oxygen gasification of hazardous renewable raw materials

However, for specialists in hydrocarbons gasification, this area of research has a long history [2]. It should be underlined that abovementioned publication of project manager for today has more than 1500 downloads according to the information of world's leading publishing house InTechOpen (London), more than half downloads had been performed from USA (Fig.2). Later, the conclusions of the publication [2] were clarified and specified in the monograph [3] during the project activity.

2. The results obtained

Experimental studies and thermodynamic calculations on the efficiency of gasification process for a mixture of sewage sludge (SS) and rubber roof of worn tires (RRWT) were performed in the process of implementation of this project as the development of the basic publication [2].

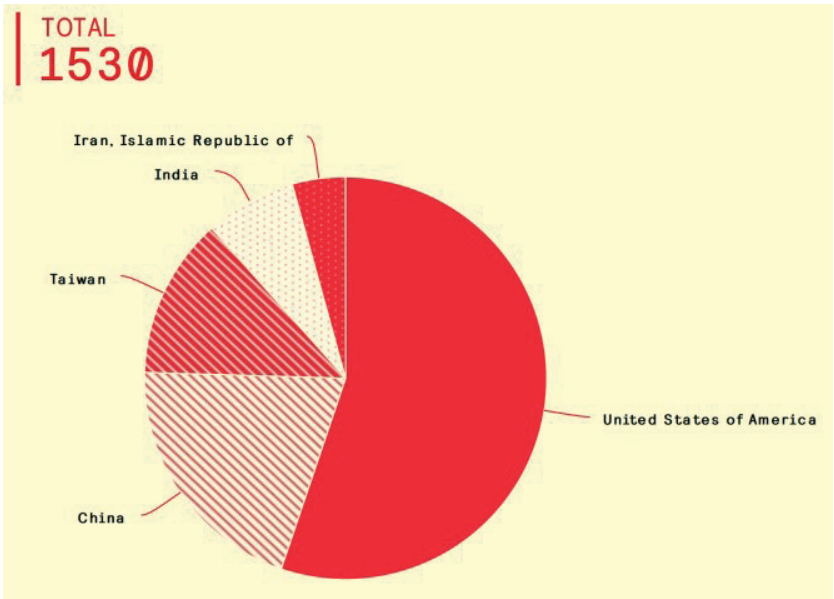

Fig. 2. Distribution of the basic publication [2] downloads by countries according to data of the publishing house InTechOpen, London (beginning of August 2021)

At a qualitative level, the positive effect of mixing RRWT with SS in terms of the gasification process can be shown by comparing the appearance of slag, which is formed as a result of plasma-air gasification of sewage sludge (Fig. 3) and a mixture of this raw material with RRWT (Fig. 4) under the conditions of laboratory experiment in the gasifier of small volume ~ 1 *l*. At the same time, these figures illustrate the exceptional advantage of abovementioned plasma technologies, which provide high parameters of thermodynamic processes and allow vitrification of heavy metals of SS, despite the high ash content of 50-60% (Fig. 3). However, the RRWT impurity further improves the quality of the vitrification process, as confirmed by the homogeneity of the slag melt in this case (Fig. 4).

In the thermodynamic modeling for the processes of joint gasification of SS and RRWT, the basic thermochemical equation for plasma-vapor-oxygen conversion of carbon-containing waste was used,

presented by the authors in [2, 3]. In abovementioned case it is generalized for the variant of mixed raw materials processing. A positive effect was quantified in terms of improving the energy efficiency of the gasification $\eta = (P_{PL}^{J} + P_{O2})/ \eta_{EE} W_{SG}$, which takes into account the cost of electrical energy P_{PL}^{J} for the production of plasma jet with plasma torch efficiency at ~ 0.8, ie: $P_{PL}^{J} = \Delta Q_{PL}/0{,}8$, P_{O2} – energy consumption for oxygen production, η_{EE} ~ 0,3 – efficiency of electricity production, W_{SG} – energy of synthesis gas production.

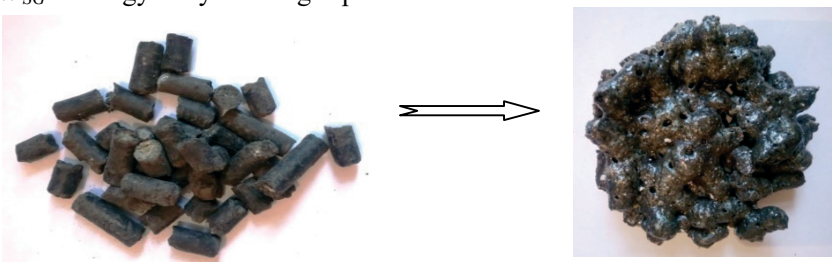

Fig. 3. Melt of slag (right), formed as a result of plasma-air gasification of sewage sludge (left)

Fig. 4. Melt of slag (right), formed as a result of plasma-air gasification of sewage sludge (left) in a mixture with rubber roof of worn tires (middle)

3. Possible areas of application and prospects for implementation

The project "Development of scientific and technological bases for synthesis gas production from a mixture of hazardous organic waste" is part of a more general project aimed for creating of full technological line of hazardous waste processing using plasma technologies with a capacity of 200 kg per hour at the Gas Institute of NAS of Ukraine (Fig. 5). The end result of these studies should be the production of electricity based on

the combustion of synthesis gas H_2 + CO, which is obtained as a result of waste processing. This electricity should be distributed both to meet the technological line's own energy needs and to external consumers, which will facilitate the commercialization of results. For the production of electricity, the use of a gas-diesel power plant or turbine is envisaged, depending on the specific conditions of the potential user of this technology. Modern fuel cells can also use synthesis gas for direct conversion of chemical energy into electricity. If necessary, membrane technologies can be used to extract hydrogen directly from the synthesis gas mixture – similar to what was done in development [4].

An agreement has been signed with one of the production companies in Sofia (Bulgaria) on the development of these studies in the field of processing of carbon-containing waste using plasma technologies and their practical implementation based on international cooperation for their application, search for potential partners, investors and customers in Bulgaria, Ukraine and third countries.

a b

Fig. 5. Technological line for hazardous waste processing: control panel (a), the system of gasification products cleaning (b)

4. Comparison with high-tech countries

The authors of a similar development using plasma technology [5] from company SGH2 (Washington, DC, USA) emphasize that the hydrogen produced in this process is "greener than green." The company plans to produce carbon-negative hydrogen from biogenic waste and biomass in the city of Lancaster, north of Los Angeles (USA). The hydrogen is titled carbon-negative because the waste would otherwise rot

in landfills and emit methane. For 20 years period of time greenhouse gas is 84 times more potent than CO_2. It thus calculates its carbon intensity as negative 188kg of CO_2 equivalent per megajoule, compared to 20kg for coal-derived H_2 and zero for standard green hydrogen.

Another close analogue is a design solution using plasma technology, which is implemented in a joint project of the company for the production of renewable hydrogen systems Ways2H Inc. (Long Beach, CA, USA) and its shareholder and technical partner Japan Blue Energy Co. (Tokyo, Japan) [4]. It is focused, as in our case, on the processing of bottom sludge, with the main difference that membrane technology is used to extract hydrogen from synthesis gas, and the residual CO is used to the production of thermal energy, which is returned to the process. This mini-plant with a capacity of 1 ton of dried sewage sludge per day was built in 2021 in partnership with the government of Tokyo, corporations TODA, TOKYU Construction, CHIYODA Kenko and researchers at Tokyo University of Science to help Japan meet the growing demand for renewable hydrogen while demonstrating a new path to sustainable waste disposal. It converts the mentioned amount of sewage sludge into 40-50 kg of pure hydrogen fuel for cars with fuel cells.

5. The level of technological readiness

The above-mentioned technological line for hazardous waste processing is fully equipped with plasma equipment, a reactor unit with high-quality thermal insulation and units for loading raw materials and unloading the ash residue, a system for cleaning gasification products. At the stage of completion is a system of mechanized loading of raw materials into the reactor.

6. Intellectual property

1. S.V. Petrov, S.G Bondarenko, V.A. Zhovtyansky, V.M. Korzhyk, V.V. Popov. Electric arc plasmatron, UA patent No. 98271, published April 25, 2012, bull. No. 8.

2. S.V.Petrov, S.G Bondarenko, V.A. Zhovtyansky, O.S. Zholudeva. Device for steam plasma gasification of solid carbonaceous materials, UA patent No. 111691, published March 25, 2016, bull. No.6, published May 25, 2016, bull. No.10.

3. Know-how for production experience in creating a technological line for hazardous waste processing.

The main publications in the frame of project “Development of scientific and technological fundamentals of synthesis gas production from a mixture of hazardous organic waste”:

1. S.V. Petrov, V.A. Zhovtyansky. Energy Efficient Steam Plasma Waste Recycling Technologies, - K.: Naukova Dumka, 2019. - 559 p. ISBN 978-966-00-1683-5

2. V. Zhovtyansky, E. Kolesnikova, Yu. Lelyukh1, Ya. Tkachenko. Non-monotony of the volt-ampere characteristics of the arc discharge caused by effects of heat conductivity, Tekhnichna elektrodynamika, 2019, No.3, pp.12-22.
https://doi.org/10.15407/techned2019.03.012

References

[1] Mission Innovation launches a new global coalition to support the clean hydrogen economy, electronic resource, https://ec.europa.eu/info/news/

[2] Zhovtyansky V., Valinčius V. Efficiency of plasma gasification technologies for hazardous waste treatment., Gasification for Low-grade Feedstock (ISBN 978-1-78923-289-9) , Ed. Yongseung Yun. – London: InTechOpen, 2018,pp. 165 - 189.
https://www.intechopen.com/chapters/59776

[3] Petrov S.V., Zhovtyansky V.A. Energy-efficient steam-plasma technologies for waste processing. - Kyiv: Naukova Dumka, 2019. 559 pp.. ISBN 978-966-00-1683-5.

[4] Ways2H Shareholder Japan Blue Energy Launches Tokyo Renewable Hydrogen Production Facility , electronic resource, https://www.prnewswire.com/news-releases

[5] World's largest 'green hydrogen' offtake deal signed in California by waste-to-H2 start-up, electronic resource,
https://www.rechargenews.com/energy-transition

New intermetallic magnesium compounds for hydrogen storage

Z. Matysina[1], N. Gavrylyuk [1,2], An. Zolotarenko[1,2], Al. Zolotarenko[1,2], M. Kartel[2], A. Veziroglu[3], T. Veziroglu[3], D. Schur[1,4], T. Ramazanov[4], M. Ualkhanova[4],N. Akhanova[4,5], M. Gabdullin[4,5], V. Mashira[1]

[1]*Frantsevich Institute for Problems of Materials Science, NASU, Kyiv, Ukraine*
[2] *Chuiko Institute of Surface Chemistry, NASU, Kyiv, Ukraine.*
[3]*University of Miami, International Association for Hydrogen Energy, Miami, USA*
[4]*National Nanotechnology Laboratory, Al-Farabi Kazakh National University, Almaty, Kazakhstan*
[5]*Kazakh-British Technical University, Almaty, Kazakhstan*

Currently, special attention is paid to the study of materials for hydrogen storage. Among the promising materials for hydrogen storage, magnesium and its alloys occupy a special place due to the high reversible sorption capacity (up to 7.6 wt%) [1–3].

Numerous studies of magnesium intermetallic compounds during last years [1-7] can be explained by their attractive physicochemical properties. These materials are already widely used in electronic technology, for example, for creation of electrodes in power batteries. Composite materials based on magnesium can effectively absorb and release hydrogen with a capacity up to 5.4-7.6 wt.%. Their large reversible hydrogen sorption capacity contributes to the creation of low-temperature (close to room temperature) hydrogen accumulators - environmentally friendly fuel [4-7]. Moreover, magnesium alloys are easily accessible, simple for production and treatment, non-toxic, resistant to an amorphous state transition, and quite low in price.

In this review, we develop the statistical theory of the $MgRT_4$-H_2 system (R = Ce, La, Nd, Pr, Y; T = Co, Ni) during the hydrogen pickup of the alloy and the phase transitions under pressure. All such alloys are isostructural; they have a crystal lattice of the type $MgSnCu_4$. In theory, simplifying approximations are used: the average-energy method is used, the interaction of the nearest atomic pairs is taken into account, the crystal

lattice is assumed to be geometrically ideal, and the correlation in the filling of their positions by atoms is not taken into account [8-17].

For the calculations, we used some results of experimental studies of $MgRT_4$ alloys in a hydrogen environment [4-7, 18-20]. Fig.1 shows the literature and experimental isotherms and isoplethes of magnesium intermetallic compounds hydrides, performed as a result of studying their P-T-c diagrams.

From Fig.1 (a, b, c) it can be seen that bends are appeared on the isotherms with a change of pressure, there are two plateaus where the hydrogen saturation pressure is reached for hydrogen concentrations $x \approx 4$ and $x \approx 6$. This indicates the presence of different phases α and β and occurring of the phase transition $\alpha \rightleftarrows \beta$. For an alloy with cerium and cobalt, the chemical reaction proceeds according to the scheme

$$MgCeCo_4 + 3H_2 \xrightarrow{0{,}5\ \text{MPa}} MgCeCo_4H_4 + H_4 \xrightarrow{5{,}0\ \text{MPa}} MgCeCo_4H_6 \quad (1)$$

where we denote the phases

$$\alpha=MgCeCo_4H_{\sim 4};\ \beta=MgCeCo_4H_{\sim 6} \quad (2)$$

As a result of absorption-desorption processes, a hysteresis effect takes place. Fig. 1 (d) indicates that the composition of the system changes the shape of the hysteresis loop: replacing nickel atoms by cobalt ones lengthens and narrows it, the concentration x increases (from $x \approx 4$ to $x \approx 5.5$) for the saturation pressures of the alloy with hydrogen, the equilibrium pressure of the system decreases (the hysteresis loop goes down the ordinate). From Fig.1 (e, f, g) it is also seen that the appearance of cobalt atoms in the alloy and an increase of its concentration lead to the hysteresis loop being realized at lower pressures, and it also narrows and lengthens. In this case, the saturation pressure for the alloy with nickel is reached at a hydrogen concentration of $x = 4$, and the addition of cobalt increases the concentration for the saturation pressure to $x \approx 5$, and in the presence of only cobalt without nickel in the alloy - to a concentration of $x = 6.6$.

Fig.1 (h) shows isoplethes for alloys with cobalt, nickel, and also with an equal content of cobalt and nickel. All isoplethes correspond to the Vant Hoff law - a linear dependence of lnP values on of inverse

temperature. The enthalpy of the sample can be estimated from the slope of the lines, and the entropy can be estimated from the point of the lines intersection (their extrapolation) with the ordinate axis. As can be seen from Fig.1 (h), the inclination angle ω decreases (tgω increases in absolute value) with the appearance of nickel in the alloy and an increasing of its concentration. The entropy also increases due to the presence of nickel in the system.

Table 1 shows the experimentally established physical quantities of eight alloys with a structure of the $MgSnCu_4$ type for illustration of manifesting regularities. There are the lattice parameters, their relative change during hydrogenation, the radii of Co and Ni atoms, the ratio of the equilibrium pressures for the processes of absorption and desorption isotherms, the tangents of the isopleths slopes, and also the numerical values of the enthalpy and entropy of the systems.

Table 1. Experimentally established some physical quantities of eight alloys with the structure of the $MgSnCu_4$ type. [5, 6, 19, 21, 22, 23,]

Alloy	*a*, Å	Δ*a*/*a*	r_M, Å	P_{abs}/P_{des}	tgω	H, kJ/mol	ΔS, J/K.mol
$MgYCo_4$	7.0596	0.55	r_{Co} = 1.252	1.5	–0.32	–27.9	–93.4
$MgYCo_2Ni_2$	7.0247			1.45	–0.48	–28.8	–101.5
$MgYNi_4$	7.0129 7.0147	0.20	r_{Ni} = 1.246	3.2	–0.74	–33.1	–117.6
$MgCeCo_4$	7.501	0.585					
$MgNdNi_4$	7.0947 7.1024	0.528					
$MgNdCo_2Ni_2$	7.1184	0.571					
$MgLaNi_4$	7.1681 7.1443 7.1794 7.1557						
$MgPrNi_4$	7.1265 7.1024 7.1074					–42.4 –19.6	–12.68 –98.2

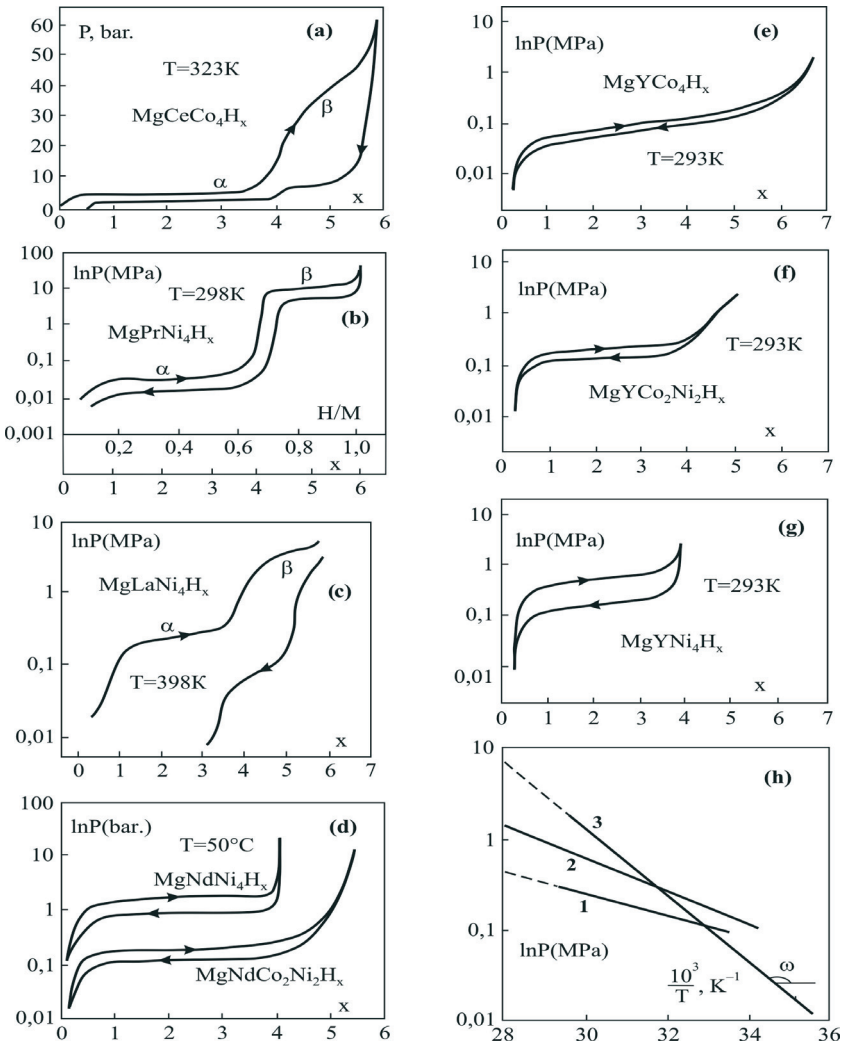

Fig. 1. Experimental isotherms (a, b, c, d, e, g, f), isoplethes (h) of magnesium intermetallic compounds hydrides: (a) $MgCeCo_4H_x$, $0 < x \leq 6$ [18, 19, 20]; (b) $MgPrNi_4H_x$, $0 < x \leq 6$ [4]; (c) $MgLaNi_4H_x$, $0 < x \leq 5.5$ [5]; (d) $MgNdNi_4H_x$, $0 < x < 4$; $MgNdCo_2Ni_2H_x$, $0 < x \leq 5.4$ [6]; (e) $MgYCo_4H_x$, $0 < x \lesssim 6.6$ [7]; (f) $MgYCo_2Ni_2H_x$, $0 < x \lesssim 5$ [7]; (g) $MgYNi_4H_x$, $0 < x \leq 4$ [7]; (h) $MgYCo_4H_x$, $MgYCo_2Ni_2H_x$, $MgYNi_4H_x$ (straight lines 1, 2, 3) [7].

It is interesting to develop a statistical theory of the abovementioned alloys to justify and explain experimentally observed regularities in P-T-c diagram of these systems.

Based on molecular kinetic concepts, the theory of magnesium crystals with a complex cubic structure C15b of the $MgSnCu_4$ type with composition $MgRT_4H_x$ (R = Ce, La, Nd, Pr, Y, T = Co, Ni, $0 \le x \le 6$) has been developed.

The hydrogen sorption properties of the $MgCeCo_4H_x$ hydrointermetalide have been studied. Under hydrogen pressure two α and β phases with $0 \le x \le 4$ and $4 \le x \le 6$ have been formed. The phases have been formed presumably due to the ordering of the distribution of hydrogen atoms by their position.

Free energy has been calculated, its dependence on temperature, pressure, hydrogen concentration, and order parameter and energy constants has been established. The equation of thermodynamic equilibrium, which determines the order parameter depending on the hydrogen concentration, temperature, pressure has been obtained; graphs of these dependencies have been constructed.

The dependence of the ordering temperature on the hydrogen concentration has been found. Isotherms and isopleths of hydrogen absorption-desorption in the α and β phases, which are consistent with the experimental Vant Hoff law, have been studied.

The dependence of the enthalpy and entropy of the crystal on the hydrogen concentration and the order parameter has been predicted. The possibility of a hysteresis effect has been established.

The hydrogen content of the alloy is calculated as a function of temperature. The graph of this dependence shows a sharp jump or kink at the phase transition temperature $\alpha \rightarrow \beta$.

The configuration heat capacity value has been estimated. The calculated isotherms and isopleths have been compared with the experimental ones.

We hope that the obtained calculation results can allow experimenters to select the temperature, pressure, alloy composition, atomic order (by the heat treatment mode) and work out the optimal solubility conditions and hydrogen extraction from the system.

The main publications in the frame of the project “Onboard hydrogen storage for a motorcycle”:

1. Z.A. Matysina, N.A. Gavrylyuk, A. Veziroglu, T.N. Veziroglu, A.P.Pomytkin, D.V. Schur, T.S. Ramazanov, M.T. Gabdullin, An.D. Zolonarenko, Al.D. Zolonarenko. Hydrogen sorption properties of new magnesium intermetallic compounds with $MgSnCu_4$ type structure», *Int. J. Hydrog. Energy*, 2021, vol. 46, pp. 25520-25532

2. An.D. Zolotarenko, Al.D. Zolotarenko, A. Veziroglu, T.N. Veziroglu , A.P.Pomytkin , N.A. Gavrylyuk , D.V. Schur , T.S. Ramazanov, M.T. Gabdullin. The use of ultrapure molecular hydrogen enriched with atomic hydrogen in apparatuses of artificial lung ventilation in the fight against virus COVID-19, *Int. J. Hydrog. Energy*, 2021, Mar 14. http://doi.org/10.1016/j.ijhydene.2021.03.025

3. Al.D. Zolotarenko, An.D. Zolotarenko, A. Veziroglu, T.N. Veziroglu, A.P.Pomytkin, N.A. Gavrylyuk , D.V. Schur, T.S. Ramazanov, M.T. Gabdullin. Methods of theoretical calculations and of experimental researches of the system atomic hydrogen – metal, *Int. J. Hydrog. Energy*, 2021, April 8,
https://doi.org/10.1016/j.ijhydene.2021.03.065

4. Z.A. Matysina, S. Yu. Zaginaichenko, DV Schur, Al.D Zolotarenko, An. D. Zolotarenko, M.T. Gabdulin, L..I Kopylova, T.I. Shaposhnikova. Phase transformations in the mixed lithium-magnesium imide $Li_2Mg(NH)_2$, *Rus. Phys.*, 2019, vol. 61, No.12, pp. 2244–2252. https://doi.org/10.1007/s11182-019-01662-7

References

[1] Matysina Z.A.,Gavrylyuk N.A., Veziroglu A., Veziroglu T.N., Pomytkin A.P., Schur D.V.,Ramazanov T.S., Gabdullin M.T., Zolotarenko An.D., Zolotarenko Al.D. Hydrogen sorption properties of new magnesium intermetallic compounds with $MgSnCu_4$ type structure», *Int. J. Hydrog. Energy*, 2021, vol. 46, pp. 25520-25532

[2] Zolotarenko An.D., Zolotarenko Al.D., Veziroglu A., Veziroglu T.N., Pomytkin A.P., Gavrylyuk N.A. , Schur D.V., Ramazanov T.S., Gabdullin M.T. The use of ultrapure molecular hydrogen enriched with atomic hydrogen in apparatuses of artificial lung ventilation in the fight against virus COVID-19, *Int. J. Hydrog. Energy*, 2021, Mar 14. http://doi.org/10.1016/j.ijhydene.2021.03.025

[3] Zolotarenko Al.D., Zolotarenko An.D., Veziroglu A., Veziroglu T.N., Pomytkin A.P., Gavrylyuk N.A. , Schur D.V., Ramazanov T.S.,

Gabdullin M.T. Methods of theoretical calculations and of experimental researches of the system atomic hydrogen – metal, *Int. J. Hydrog. Energy*, 2021, April 8,
https://doi.org/10.1016/j.ijhydene.2021.03.065
[4] Terastita N, Sakaki K, Nakamura Y, Akiba E. Hydrogenation properties of ternary intermetallics compounds $Mg_{2-x}Pr_xNi_4$, *Materials Transactions,* 2012, vol.53, pp. 513-517.
[5] Tan J, Zeng X, Zou J, Wu X, Ding W. Preparation of $LaMgNi_{4-x}Co_x$ alloys and hydrogen storage properties. *Trans. Nonferrous Met. Soc. China,* 2013, vol.23, pp.2307-2311.
[6] Shtender V.V, Denis R.V, Paul-Boncour V., Verbovytskyy Yu.V., Zavaliy I.Yu. Effect of Co substitution on hydrogenation and magnetic properties of $NbMgNi_4$ alloy. *J. Alloy Compd*., 2015, vol.639, pp. 526-532.
[7] Shtender V.V, Denis R.V, Paul-Boncour V, Riabov A.B, Zavaliy I.Yu. Hydrogenation properties and crystal structure of $YMgT_4$ (T = Co, Ni, Cu) compounds. *J. Alloys Comp.*, 2014, vol.603, pp.7-13.
[8] Smirnov A.A. Molecular kinetic theory of metals. – Moscow: Science. 1966, 488p.
[9] Smirnov A.A. Theory of implantation alloys. - Moscow: Science. 1979, 368 p.
[10] Matysina Z.A, Zaginaichenko S.Yu, Schur D.V. Solubility of impurities in metals alloys, intermetallic compounds, fullerites. - Dnipropetrovsk: Science and education. 2006, 514p.
[11] Lytvynenko Y.M, Schur D.V. Utilization the concentrated solar energy for process of deformation of sheet meta, *Renewable Energy*, 1999, vol. 16, pp. 753-756.
[12] Schur D.V, Dubovoy A.G, Zaginaichenko S.Yu. Method for synthesis of carbon nanotubes in the liquid phase. *Extended Abstracts, An International Conference on Carbon Providence. Rhode Island, USA: American Carbon Society*, 2004, pp. 196-198.
[13] Schur D.V, Lyashenko A.A, Adejev V.M, Voitovich V.B, Zaginaichenko S.Y. Niobium as a construction material for a hydrogen energy system. *Int. J. Hydrog. Energy*, 1995, vol. 20, pp. 405-407.
[14] Matysina Z.A, Zaginaichenko S.Y, Schur D.V. Hydrogen solubility in alloys under pressure. *Int. J. Hydrog. Energy*, 1996, vol. 21, pp.1085-1089.

[15] Anikina N.S, Zaginaichenko S.Y, Maistrenko M.I, Zolotarenko A.D, Sivak G.A, Schur D.V, Teslenko L.O. Spectrophotometric analysis of C60 and C70 fullerenes in toluene solutions. *Hydrogen Materials Science and Chemistry of Carbon Nanomaterials*. Proc. of NATO ARW on HMSCCN, Sudak. Series II. 2003; 172, pp. 207-216.

[16] Anikina N.S, Krivuschenko O.Ya, Schur D.V, Zaginaichenko S.Yu, Chuprov S.S, Mil’to K.A, Zolotarenko A.D. Identification of endohedral metallofullerenes by method of UV-VIS- spectroscopy. Proc. of 9th International Conference “*Hydrogen Materials Science and Chemistry of Carbon Nanomaterials”*, Sevastopol, Crimea, Ukraine, September 5-11, 2005, pp. 846-847.

[17] Matysina Z.A, Zaginaichenko S.Yu, Schur D.V, Viziroglu A, Viziroglu T.N, Zolotarenko Al.D, Zolotarenko An.D. Hydrogen in crystals. - Kiev: "KIM." 2017, 1060p.

[18] Denis R.V, Berezovets V.V, Kovalchuk I.V, Paul-Bonkur V., Cherni R, Zavaliy I.Yu. The structure and hydrogen sorption properties of new compounds and alloys based on magnesium. *Hydrogen materials science and chemistry of carbon nanomaterials*. – Kiev: AHEU, 2009, pp. 40-43.

[19] Matysina Z.A, Zaginaichenko S.Yu, Schur D.V. Sorption properties of hydrogen in magnesium intermetallic compounds. *Metallophysics and advanced technologies*, 2012, vol.34, No.7, pp. 883-893.

[20] Matysina Z.A, Botsva N.P, Elina E.V, Devyatkina M.E. Studies of hydrogen sorption isotherms in a system of magnesium intermetallic compounds. *Bulletin of the Dnipropetrovsk National University. Olesya Gonchar. Series “Physics. Radio Electronics”*, 2013, (34): 5.

[21] Kadir K, Noreus D, Yamashita I. Structural determination of $AMgNi_4$ (where A = Ca, La, Ce, Pr, Nd and Y) in the $AuBe_5$ type structure, *J. Alloys Compd.,* 2002, vol.345, pp. 140-143.

[22] Wang J-W, Yang F, Fan TW, Tang B-Yu, Peng Li-M, Ding W-J. Theoretical investigation of new type of ternary magnesium alloys $AMgNi_4$ (A = Y, La, Ce, Pr and Nd), *Physica B,* 2011, vol. 406, pp.1330-1335.

[23] Li R, Shen J, Tian F. A theoretical study of the thermodynamic properties of YM_gX_4 (X = Co, Ni, Cu) compounds, *AIP Advances*, 2014, vol. 4, 097123-3.

Technological complex for manufacturing of the cost-efficient and robust metal-plastic high-pressure tanks for hydrogen accumulation, storage and use

M. Savytsky, O. Savytsky, V. Vashenko, Yu. Shkrabalyuk

Paton Electric Welding Institute, NASU, Kyiv, Ukraine

The experience which has been saved up in the field of creation of easy combined high-pressure tanks testifies that working capacity and operational reliability of high-pressure tanks are strongly dependent on a material of which their tight cases are made. On the base of performed investigations of authors 08X18H10-, 12X18H9- type steels have been recommended for creation of welded cases of cylinders for hydrogen accumulation, storage and using. Such materials are characterized by the minimum factor of permeability of hydrogen and do not contain titanium in their structure. Titanium can create fragile compounds with hydrogen that negatively effects on the working capacity of cases. However according to HCS and HV_{max} characteristics for these steels they are prone to the formation of hot cracks and an overheat. The probability of formation of these defects decreases with reduction of heat supply to the welded connection. So, ATIG-welding process developed at Paton Electric Welding Institute has been applied to the welding of tight cases. It is provided the minimum heat supply and high resistance of metal welded connections against formation of abovementioned defects.

The following negative factor is non-uniform heating of a metal during the welding process. As a result, there are tensions and deformations within welded structures and also their destructions. The least resistant to destruction part of the case is its cylindrical part, ie the shell. Modern industrial technologies allow to create cylindrical parts of two types. In the first type of cases its cylindrical part has a direct longitudinal welded seam. In the second type of cases the cylindrical part has a spiral welded seam (Fig. 1). Studies of the character and conditions of their destruction have shown that despite the various peculiarities of destruction for two shell types both of them can be equally used for case production if their external strength cover is cocoon (Fig.1).

In this case the hermetic welded case is simply thin-walled capacity for hydrogen storage. And external strength cover ensures the total efficiency and working capacity under the conditions of high working pressures. Therefore, the durability and working capacity of the light combined high-pressure tanks for accumulation, storage and use of gases are determined by the type and quality of an external strength cover which is produced on the thin-walled tight case surface.

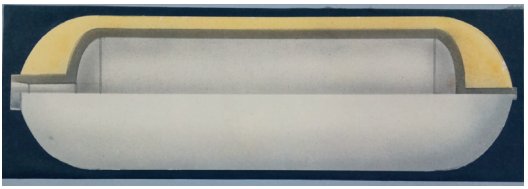

a

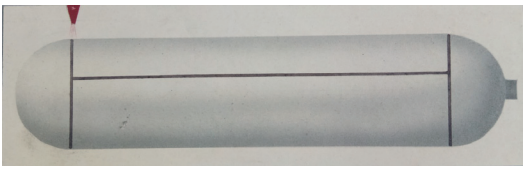

b

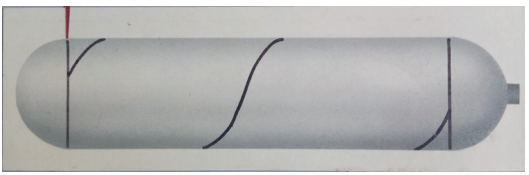

c

a – cylinder general view;
b – the case of a cylinder with a direct longitudinal welding seam;
c – the case of a cylinder with a spiral welding seam.

Fig. 1. The design of the combined high-pressure tank for hydrogen accumulation, storages and use:

As a result of preliminary studies, it was recommended to produce external strength covers from the composites reinforced by high strength fibers: glass fibers, basalt fibers, carbon fibers. All these types of fibers allow to produce qualitative external strength covers, which differ only in

their thickness, weight (Tab. 1) and cost. The maximum thickness and weight of a cover at its minimum cost are provided by glass fiber. Covers containing carbon fibers are characterized by minimum values of thickness and weight but at the same time they are the most expensive. The basalt fiber based covers had intermediate values of the abovementioned characteristics.

Table 1. Mass indicators of high-pressure tanks with volume of 30 L with strength covers from different fiber materials (a thickness of the case of 1 mm)

Case material	Material of a strength cover		Thickness of a power cover, mm		Weight of a power cover, kg		Weight of a cylinder, kg		M/V
	Fiber type	σ_T, MPa	$P_{w.}$= 35MPa	$P_{w.}$= 70MPa	$P_{w.}$= 35MPa	$P_{w.}$= 70MPa	$P_{w.}$= 35MPa	$P_{w.}$= 70MPa	
08X18H10 (12X18H9)	Glass fiber	1010	12.0	27.0	18.2	43.9	22.3	48.0	1.6
	Basalt fiber	1070	10.0	22.0	17.9	41.6	22.0	45.7	1.52
	Carbon fiber	4000	2.6	5.3	2.7	5.4	6.8	9.5	0.32
		6000	1.8	3.6	1.9	3.6	6.0	7.7	0.257

However, without the specialized equipment it is almost impossible to ensure the production of qualitative external strength covers. There is no serial production of such equipment in Ukraine and import installation is very expensive (about 500 000 USD). So the development of the automatic equipment for production of external strength covers was the main project task.

In the framework of this task three-dimensional computer modelling of the basic working units and mechanisms of the abovementioned equipment has been performed. Results of modelling have shown that for qualitative production of strength covers, the equipment should have the three-coordinate layout scheme. The first coordinate should provide a rotary motion of the case of a cylinder concerning its longitudinal axis with adjustable speed. The second

coordinate should provide longitudinal moving of the carriage with all necessary units and mechanisms along forming cases of a cylinder with adjustable speed and possibility of a short-term stop in points of fixation of a high-strength fiber material on a surface of the case of a cylinder. The third coordinate should provide moving of the mechanism of laying of a high-strength fiber material to a direction cross-section to the central axis of the case of a cylinder in extreme points of position of the carriage.

The special attention during the design of the equipment has been paid to configuration of unit for laying of a high-strength fiber material on the cylinder case. Without this unit it is possible to produce the strength cover, but in this case the requirements to the quality of welded case surface were significantly enhanced. In that case the surface should be equal without any differences at transition from a cylindrical part of the case to the bottoms and without strengthening of ring welded seams. It is in appropriate way enhances requirements to quality of manufacturing of a cylindrical part of the case and its bottoms. It is very difficult to ensure a necessary degree of quality at manufacturing of welded cases of cylinders from thin (to 3 mm) metal with relatively low strength values. In that case it is necessary to increase a thickness of the case up to 5-6 mm. As a result, metal consumption and weight of a cylinder, and also labour input during production process will be increased, and the cost will be increased too. Presence of the third co-ordinate in a design of the equipment for production of external strength covers reduces level of requirements to quality of a surface of the welded case of a cylinder and allows to solve the specified problems on thin-walled cases.

Prototyping and test of all units and mechanisms providing coordinated functioning of the specified layout scheme had shown that it is reasonable to use step-by-step or servomotors with programmed control for electric drives of this installation.

Also, the basic algorithms of formation of external strength covers have been developed. They provided formation of strength covers of "cocoon" type under *eigh*t and *spiral schemes.* The *eight* scheme provides a crossing of fibers in the centre cylindrical cases of a part of a cylinder. After the strength part of a cover reaches a necessary thickness, ring winding in some passes fixing basic layer of a fiber is carried out condensing the formed layer and pressing it to a surface of the case of a

cylinder. The *spiral* scheme provides spiral packing of a high-strength fiber material on the case of a cylinder with certain step. After formation of an intermediate layer of a certain thickness ring fixing winding of a fibre is carried out. The specified sequence of laying of a fibre is repeated till a necessary thickness of a strength cover will be achieved. At the next step ring winding of a fibre in some passes is performed similarly to the previous case.

It is also possible to carry out the preliminary winding for cylinder part of case to align it throughout the all case length.

To ensure the implementation of these algorithms for high-strength fiber laying on the body of the cylinder and the operation of the equipment without interruption for reconfiguration, program control of working in all three coordinates have been proposed.

Possible area of applications

Technological complexes can be used for production of high-pressure tanks for various applications: hydrogen energetics, aircraft industry, accumulation and transportation and use of natural gas, etc. Developed combined metal-plastic containers are intended for accumulation, storage and use of hydrogen.

Comparative estimation of the received results

Advantages, analogues

The cost of the foreign equipment for the production of high-pressure cylinders with power composite shells is about 500 thousand USD. According to preliminary estimates, the domestic complex will be 2-3 times cheaper and will provide a low mass/dimensional indicator (m/V) for combined cylinders.

Competitors

Production of equipment for the manufacturing of high-pressure combined cylinders: the company X-Winder (Europe), the company «Hurgo» (USA), the International Joint Stock Chinese Company «Honkong Tien» (China), the engineering center «Stankomposite» (Russia). Production of tanks for accumulation, storage and use of hydrogen: «ECD Ovonics» (USA), «HERA Hydrogen Storage Systems»

(Canada), «Dynetek» (Canada), «Millennium Cell» (USA), «Euro India Cylinders Ltd».

Level of technological readiness

The design of lightweight metal-plastic cylinders for hydrogen accumulation, storage, transportation and use with a welded metal body reinforced composite material had been developed. The design of the equipment for formation on a surface of the welded metal thin-walled case of a cylinder of external power covers has been developed. The equipment design provides programmed control by a work cycle.

The intellectual property

1. O.S. Pysmenny, M.M. Savytsky, O.O. Pysmenny, O.M. Savytsky, O.S. Prokofiev, R.C. Gubatuk, R.V. Yukhimets, V.O. Suprunenko. Design of a vessel which works under pressure in which tubular preparation of the case is made from a pipe the executed electric welding, UA patent No.80558, published June 10, 2013, bull. No.11.
2. M.M. Savytsky, O.M. Savytsky, V.M. Vashenko, Yu.M. Shkrabalyuk. Way of automatic arc welding of metals and alloys in the environment of protective gases. UA patent No.106118, published July 25, 2014, bull. No. 14.
3. M.M. Savytsky, O.M. Savytsky, V.M. Vashenko, M.M. Vashenko, I.A. Korovin. Yu.M. Shkrabalyuk. The automatic device for welding of not rotary joints of pipes, UA patent No. 106920, published Oct.10,2014, bull. No.20.
4. M.M. Savytsky, O.M. Savytsky, V.M. Vashenko, Metal-plastic high-pressure tank, UA patent No. 108948, published June 25, 2015, bull. No. 12.
5. O.S. Pysmenny, M.M. Savytsky, O.O. Pysmenny, O.M. Savytsky, O.S. Prokofiev, R.C. Gubatuk, R.V. Yukhimets, V.O. Suprunenko, O.Pf. Mujichenko, A.S. Shynkarenko, High-pressure tank in which the cylindrical case has covering a design, UA patent No. 107847, published Feb.25,2015, bull. No.14
6. M.M. Savytsky, O.M. Savytsky, V.M. Vashenko. Way of drawing of an activating gumboil, UA patent No. 1011243, published Apr.11,2016, bull. No.7.

7. M.M. Savytsky, O.M. Savytsky, V.M. Vashenko, I.A. Korovin. The combined pipe of a high pressure, UA patent No. 11292, published Jan.10, 2017, bull. No.1.

The main publications in the frame of the project “Development of the technological complex for the manufacture of combined metal-plastic tanks for hydrogen accumulation, storage and use”:

1. O. M. Savitskyi, M.M. Savitskyi, D. Bajic. Specifities of application of activating fluxes in electrical welding in protective atmosphere, *FME Transactions*, 2020, No.3, pp. 576-580.
2. O. M. Savitskyi, M.M. Savitskyi, D. Bajic.Influence of thermophysical properties of materials on formation conditions and quality of welded joints, *Proc.* of *ten-th international scientific-professional conference SBW 2019 «Engineering technologies in manufacturing of welded constructions and product, SBW 2019».* Slavonski Brod, Oct.16-18, 2019, pp. 27-36.

Development of physicochemical principles for the creation of high-capacity hydride-forming materials and their use in stationary hydrogen storage systems and as electrodes for electrochemical energy systems

O. Ershova, V. Dobrovolsky, Yu. Solonin

Frantsevich Institute for Problems of Materials Science, NASU, Kyiv,Ukraine

The project aimed to develop high-capacity hydride-forming nanocomposites for applications in stationary hydrogen storage systems. For this purpose, Mg with catalytic additives of transition metals Ni and Ti have been used, because it is characterized by high hydrogen capacity, improved hydrogenation-dehydrogenation kinetics, reduced thermal and increased cyclic stability.

To achieve project goals it was planned to study the influence of methods and conditions of synthesis for mechanical Mg-based alloys - nanocomposites with alloying additives of transition metals Ni, Ti on their hydrogen sorption properties, hydrogenation/dehydrogenation kinetics, and decomposition temperature of the $Mg(Me)H_2$ hydride phases. It was also planned to study the role of Ni and Ti alloying elements in lowering the temperatures and improving decomposition kinetics of the MgH_2 hydride phase in obtained mechanical alloys-nanocomposites, and also in stabilizing their nanostructure during subsequent cyclic heating/cooling.

Two mechanical magnesium-based alloys - nanocomposite with an additive of 10% wt. Ni (denoted MA1 and MA2) were synthesized using one method of reactive mechanochemical alloying (RMA) but in two different manners. Mechanical alloy MA1 was obtained by reactive grinding of Mg powder mixed with Ni for 20 hours, and mechanical alloy MA2 was produced by reactive grinding under the same conditions of MgH_2 powder (obtained by hydrogenation of Mg powder from the gas phase on a Sievers type facility) with Ni additives. Similarly, two mechanical magnesium-based alloys - nanocomposite with adding 10 % wt. Ti (denoted MA3 and MA4) were synthesized in the same two different manners. For comparison, the MgH_2 hydride phase was obtained without alloying elements of Ni and Ti (mechanical alloy MA5) under the

same reactive grinding of magnesium metal powder in a hydrogen atmosphere for 20 hours. Mechanical alloying by reactive grinding of all powder mixtures was performed in a Retch ball mill with 10 mm steel balls in hydrogen medium at a pressure of 1.2 MPa and a speed of 450 rpm. The ratio of the ball mass to the mass of the treated powder mixture was 20:1. Direct gas-phase hydrogenation (GPH) of MA1 - MA5 samples after synthesis completed was performed at hydrogen pressure of 5.0 MPa and reactor temperature 400 ^{0}C.

An automatic computerized DRON-3M diffractometer was used for the X-ray phase and structural analysis of all samples. The X-Ray patterns were obtained using CuKα -radiation with a graphite monochromator. The profiles of diffraction lines were plotted with scanning steps of $0{,}1^0$ and 15-20 sec exposure at each point of the spectrum. Crystal lattice parameters of the MgH_2 hydride phase in the obtained MA and the volume of its unit cell were analyzed using fullprof Powder Cell 2.4 software (https://powdercell-for-windows. software. informer. com /2.4/). The size of crystallites (grains) of the MgH_2 hydride phase in all MAs was determined by the approximation method according to Selyakov-Scherrer equation $D_{h,k,l} = 0{,}94\ \lambda / \beta \cos \Theta$.

The influence of Ni and Ti additives on hydrogen sorption properties, thermal stability, the kinetics of hydrogen desorption from the MgH_2 hydride phase was examined by thermodesorption spectroscopy (TDS) on a tailor-made automatic computerized facility [1]. It allows obtaining spectra and curves of hydrogen thermal desorption from hydride through an isobaric method, i.e., measuring the volume of desorbed hydrogen from a sample heated at a given rate in a hydrogen medium at the constant pressure in the reactor of 0.1 MPa**.**

Results and discussion

X-ray phase analysis showed that the mechanical alloys MA1, MA2, MA3, and MA4 synthesized by the RMA method are composites as a result of reactive mechanical doping of Ni and Ti. In addition to MgH_2 with a tetragonal structure, MA1 and MA2 contain the Mg_2NiH_4 hydride phase and the MgO phase, while MA3 and MA4 consist from the TiH_2 hydride phase and the MgO phase. After the first cycles of hydrogenation/dehydrogenation from the gas phase, all MAs showed no

changes in their phase composition. The average particle size of MA1, MA2, MA3, MA4, and MA5 powders was determined on the base of scanning electron microscopy data after their synthesis by RMA, obtained values were equal 0.27, 0.32, 0.40, 0.35, and 0.69 μm, respectively. These data and data on crystallites (grains) size of the MgH_2 hydride phase in all MAs determined by the approximation method using Selyakov – Scherrer equation $D_{h,k,l} = 0{,}94\ \lambda / \beta \cos \Theta$ are given in Table 1.

Table 1. Average particle size and crystallites (grains) size of the MgH_2 hydride phase in all MAs after 20 hours of RMA and the 5 cycles of the gas phase hydrogenation (GPH)

Mechanical alloy-composites	Crystallite size, nm		$D_{part.}$, μm
	After RMA	After GPH	RMA
MA1 (Mg+10wt.% Ni)	10.4	22.2	0.27
MA2 (MgH_2+10wt.% Ni)	12.6	29.2	0.32
MA3 (Mg+10wt.% Ti)	8.1	30.5	0.4
MA4 (MgH_2+10wt.% Ti)	11.4	31	0.35
MA5 (Mg without Ni i Ti)	12	142	0.69

The effect of Ni and Ti doping and the method of obtaining the hydride MgH_2 phase for synthesized MAs on its thermal stability and decomposition temperature was examined through hydrogen desorption from MA1-MA4 samples by the TDS method. Hydrogen desorption isobars from all MAs were obtained at a constant hydrogen pressure in the reactor of 0,1MPa and a heating rate of 3 deg./min. Fig.1 shows the isobars of hydrogen desorption from samples MA1 and MA2 obtained during their first heating after synthesis by the RMA method, and Fig.2 – after the first GPH. The obtained isobaric desorption allowed determining the hydrogen capacities and the beginning temperature of hydrogen desorption ($T_{beg.}$) from the MgH_2 hydride phase in MA1-MA5 during heating of samples both after RMA and direct GPH. Corresponding results are presented in Table 2.

Table 2. The beginning temperature ($T_{beg.}$) of hydrogen desorption from the MgH_2 hydride phase in MA1-MA5 and its hydrogen capacity

Mechanical alloys-composites	after RMA		after GPH 1-st cycle of hydrogenation	
	$T_{beg.}$, ^0C	C_{H2}, %wt.	$T_{beg.}$, ^0C	C_{H2}, %wt.
MA1 (Mg + 10wt.% Ni)	295	6.1	295	5.94
MA2 (MgH_2 +10wt.% Ni)	290	5.82	288	5.5
MA3 (Mg + 10wt.% Ti)	325	5.40	315	5.3
MA4 (MgH_2+ 10wt.% Ti)	295	5.47	307	4.8
MA5 (Mg without Ni and Ti)	288	7.40	290	6.3

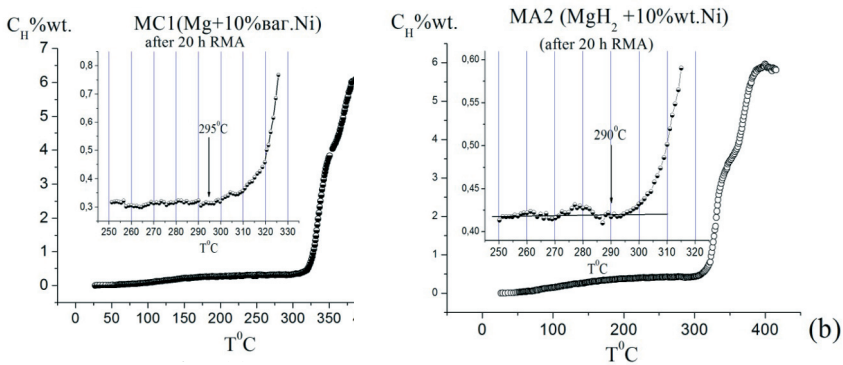

Fig.1. Isobar of hydrogen desorption obtained after synthesizing MAs by RMA method:(a)-MA1;(b)-MA2

As can be seen from Figs. 1 and 2, as well as from Table 2, the beginning temperature of hydrogen desorption ($T_{beg.}$) from mechanical alloys-composites MA1-MA 4 after their synthesis by the RMA method was 295, 290, 325, and 295 ^0C, respectively. After the first GPH of these MAs, the $T_{beg.}$ was 295, 288, 315, and 307 ^0C, respectively. It should be noted that above mentioned temperatures can be considered the beginning temperatures of hydrogen desorption from the main MgH_2 hydride phase,

taking into account the smaller number of other hydride phases (Mg_2NiH_4, TiH_2) in MC1-MC4 and the impossibility to record the beginning of the hydrogen release experimentally.

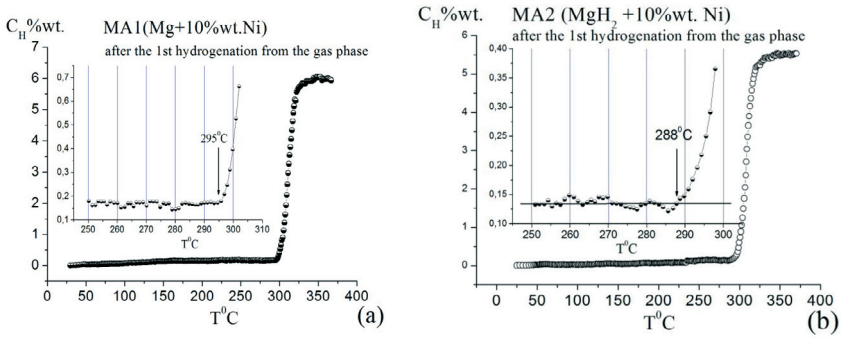

Fig.2. Isobars of hydrogen desorption after the first direct GPH of mechanical alloys: (a) - MA1; (b) - MA2

The comparison of the T_{beg} values in Table 2 for hydrogen desorption (release) from undoped Ni, Ti MgH_2 phase in MA5 (288 ^{0}C at a hydrogen pressure of 0,1 MPa) with corresponding values for MA1-MA4 alloys demonstrated that there are no effects of transition metal additives and method of obtaining MAs on the beginning temperature of hydrogen desorption and corresponding beginning temperature of their MgH_2 hydride phase decomposition for all MAs. It was not also observed the expected decrease in the equilibrium temperature of the MgH_2 hydride phase decomposition at a hydrogen pressure of 0.1MPa (288 °C according to [2]), which would indicate reduced of the MgH_2 phase due to its mechanical alloying with Ni or Ti. In our opinion, the thermodynamic stability of the MgH_2 phase was not decreased since within the chosen method of obtaining MAs (and, consequently, their main MgH_2 hydride phase), no solid solutions of Ti or Ni in magnesium were formed. According to [3], the resulting hydrides $Mg(Ti)H_2$ or $Mg(Ni)H_2$ should have a significantly lower formation enthalpy compared to that of the MgH_2 hydride phase, and, therefore, thermodynamic stability and decomposition temperature should reduced as well. As shown by X-ray phase analysis, the presence of the Mg_2NiH_4 phase

formed with a significant amount of the alloying Ni element may be the evidence of the absence or very insignificant amount of $Mg(Ni)H_2$ hydride formation after synthesizing MA1 and MA2 by the RMA method. The absence of the expected decrease of the unit cell volume in the MgH_2 hydride phase for MA1 and MA2 compared with that of the same hydride phase in composites without Ni can also indicate the absence of $Mg(Ni)H_2$ hydride formation in MA1 and MA2 under selected synthesis conditions.

Kinetics of the hydrogen desorption from mechanical alloys-composites MA1, MA2, MA3, MA4 obtained in different manner

The kinetics of hydrogen desorption from the MgH_2 hydride phase in all synthesized MAs after their GPH under the same conditions has been investigated at temperatures of 310 and 330 °C and a constant hydrogen pressure in the reactor of 0.1 MPa. Isobaric-isothermal kinetic curves of hydrogen desorption from MA1-MA5 at a temperature of 330 °C are presented in Fig. 3. Data on time for releasing half of the total hydrogen amount ($\tau 1/2$) and the total hydrogen amount (τf) for all MAs are summarized in Table 3. Analysis of the experimental data in Table 3 allows concluding that adding to magnesium as 10% wt. Ni to MA1, MA2 or 10% wt. Ti to MA3 and MA4 significantly improves the kinetics of hydrogen desorption from the MgH_2 hydride phase. The effect of improving the kinetics by adding Ni to magnesium is much more significant than in the case of Ti. It is confirmed by the experimentally recorded 16-fold and 11-fold reduction of the total desorbed hydrogen release time for MA1 and MA2, respectively, at a constant temperature of 330 ^{0}C and the constant pressure of 0.1 MPa. For MA3 and MA4, the release time decreased by 5,7 and 6,2 times, respectively, compared with the time of releasing of all hydrogen in the case of MA5 (Table 3, column "330 ^{0}C").

The analysis and comparison of the data in Table 3 for MA1 and MA2 samples allow stating that a method of reactive grinding of the Mg +10% wt. Ni powder mixture (rather than grinding a powder mixture of MgH_2 +10% wt. Ni) reveals the best kinetic characteristics of the mechanical alloys.

Table 3. Desorption time (min) of half ($\tau_{1/2}$) and total (τ_f) hydrogen amount from MgH_2 hydride phase in all MAs at 310 and 330^{0}C and the constant pressure of 0,1 MPa

Mechanical alloy - composites	310 ^{0}C		330 ^{0}C	
	$\tau_{1/2}$	τ_f	$\tau_{1/2}$	τ_f
MA1 (Mg+ 10 wt.%Ni)	2.2	7	1.6	5
MA2 (MgH_2 +10 wt.% Ni)	3.4	11	2.5	7
MA3 (Mg + 10 wt.%Ti)	8.5	25	4.7	14
MA4 (MgH_2 + 10 wt.%Ti)	5.2	14	3.1	13
MA5 (Mg without Ni,Ti)	55	160	30	80

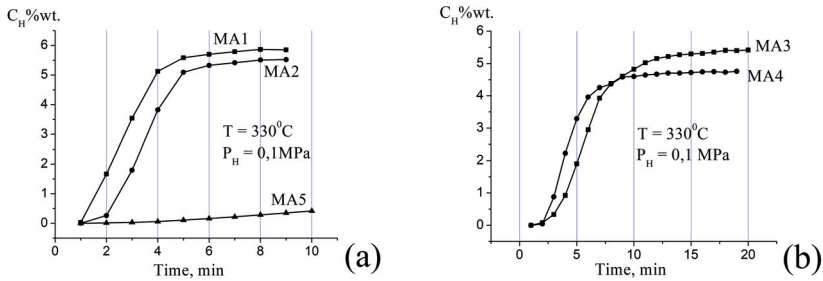

Fig. 3. Kinetic curves of hydrogen desorption from mechanical alloys MA1, MA2, MA5 - (a) and MA3, MA4 - (b), obtained at a hydrogen pressure in the reactor of 0.1 MPa and a temperature of 330 ^{0}C.

As shown in Table 3, the time needed to release half of total hydrogen $\tau_{1/2}$ from the sample MA1 (Mg + 10 wt.% Ni) and its total amount τ_f at a temperature of 330 ^{0}C is 1,6 and 5 minutes, respectively. For MA2 (MgH_2 + 10 wt.% Ni), it is 2.5 and 7 minutes, respectively. Such an outcome appeared rather unexpected for the authors since most researchers used reactive grinding of Ni powder with MgH_2 powder rather than with Mg powder to improve the kinetics of the hydrogen desorption from the MgH_2 hydride phase doped with transition metals (Ni, Ti) in synthesized MAs for its obtaining. To explain this outcome,

the crystallites (grains) size of the MgH_2 hydride phase was determined to be 29,2 and 22,2 nm for MA2 (MgH_2 + 10 wt.% Ni) and MA1 (Mg + 10 wt.% Ni), respectively, using the obtained X-ray diffraction spectra and the approximation method according to Selyakov-Scherrer equation $D_{h,k,l} = 0{,}94\ \lambda / \beta \cos \Theta$ after the first 5 cycles of their GPH (Table1). Based on these data, it is logical to assume that the faster kinetics of hydrogen desorption from the MgH_2 hydride phase in MA1 (Mg + 10 wt.% Ni) may be due to the smaller grain size (and correspondingly shorter diffusion paths for hydrogen atoms) compared to grain size of the MgH_2 hydride phase in MA2 (MgH_2 + 10 wt.% Ni). An interesting and important fact is noteworthy when analyzing the data in Table 1. After 5 cycles of heating/cooling the MA1 and MA 2 samples during their GPH, the grain size of the MgH_2 hydride phase increases by 2,13 and 2,32 times, respectively. However, under the same conditions of cyclic heating/cooling, the MA5 (without Ni), an increase in the grains of the MgH_2 hydride phase from 12 nm to 142 nm (almost 12 times) can be observed. This observation enables drawing a meaningful conclusion about the influence of nickel on the stability of the performance characteristics in studied Mg-based mechanical alloys with a Ni additive. By preventing the grain sizes of the MgH_2 hydride phase from growing, Ni ensures the stability of its nanostructure during cyclic operation and, thus, the stability of its operating kinetic and hydrogen sorption characteristics.

Hence, Ni as an additive to magnesium during MA1 and MA2 synthesis by the RMA method acts as a dispersant and nanostructure stabilizer during cyclic operation of these MAs, inhibiting the growth of crystallites (grains) in the MgH_2 hydride phase.

In the case of alloys with titanium (MA3, MA4), the effect of their production on the kinetics of hydrogen desorption is not so noticeable as for the alloys with nickel (MA1, MA2), which requires further study.

Conclusion

Four mechanical alloys-nanocomposites based on magnesium with the addition of 10 % wt.Ni (MA1, MA2) and 10% wt.Ti (MA3, MA4) were synthesized by one method of reactive mechanical alloying (RMA)

but in different manners. The hydrogen capacity, thermal stability, and kinetics of hydrogen desorption from the MgH_2 hydride phase of the obtained MAs were studied using thermodesorption spectroscopy at a constant hydrogen pressure of 0.1MPa.

It has been established that the time needed for the total hydrogen release from MA1, MA2, MA3, and MA4 was 5, 7, 14, and 13 minutes, respectively, at a constant hydrogen pressure of 0,1MPa and a temperature of 330 ^{0}C.

It was shown that method of obtaining a mechanical alloy-nanocomposite by reactive grinding of an Mg +10 % wt. Ni rather than MgH_2 +10 % wt. Ni powder mixture improves the kinetic characteristics. Faster kinetics of hydrogen desorption from the MgH_2 hydride phase of MA1 (Mg + 10 wt.% Ni) was due to the smaller grain size than the grain size of the MgH_2 hydride phase in MA2 (MgH_2 + 10 wt.% Ni). The effect of obtaining MA3, MA4 with Ti additives on the kinetics of hydrogen desorption from them is different and not noticeable compared to MA1, MA2 with Ni additive.

It was established the practical absence of the influence of Ni, Ti additives and the manner of MAs production on the temperature of the beginning of hydrogen desorption and the associated temperature of the beginning of decomposition of the hydride phase MgH_2 of MA1 - MA4.

The role of the alloying element Ni in improving the kinetics of the process of desorption of hydrogen from MAs obtained in different manners, as well as in stabilizing their nanostructure during cyclic operation by preventing (inhibiting) the growth of the crystallite (grain) of their hydride phase MgH_2, has been elucidated.

Possible area of applications

Hydrogen energetics is the main area where hydrogen-sorption materials developed during this project implementation can be applied. It is also expected to use the developed hydrogen-sorption materials based on magnesium and its alloys in high-power modules of energy converters, hydride heat pumps, and laboratory installations to research thermal hydrogen desorption features.

Comparative analysis of the study findings

As part of the project devoted to developing methods of deriving and improving the properties of hydrogen-sorption materials for hydrogen storage using Mg-based alloys, we planned to perform research aimed at achieving complex characteristics of these materials necessary for their practical application in hydrogen storage facilities. First and foremost, these characteristics include faster kinetics and lower temperature of full hydrogen release at a pressure of 0.1MPa. To achieve the specified improving performance of the obtained materials, new synthesis methods (mechanical and reactive mechanical alloying) were planned to be applied, also involving mechanical alloying and dispersion processes. That allowed modifying and generating the required hydrogen-sorption properties of alloys, chemical condition of their surfaces by affecting electronic and thermodynamic properties. Mechanical synthesis was carried out on magnesium-based alloys with the addition of Ni and Ti alloying elements, in particular, Mg+10%wt. Ni and Mg+10%wt.Ti. The role of the method and production conditions, size factor in lowering temperatures and improving the kinetics of the MgH_2 hydride phase decomposition in mechanical alloys-nanocomposites based on magnesium with Ni and Ti transition metals were examined. The optimal composition of alloys and their synthesis conditions providing an improved complex of performance characteristics were determined.

Advantages

It should be noted that most researchers determine the time of release of hydrogen from the MgH_2 hydride phase in obtained mechanical alloys from the kinetic curves of hydrogen desorption using a volumetric Sieverts-type apparatus rather than those obtained at a constant hydrogen pressure in the reactor 0.1MPa. This fact specified the relevance of this project. Therefore, this work is beneficial since the kinetics of the hydrogen desorption from the synthesized mechanical alloys-composites was studied at constant temperature and constant hydrogen pressure in the reactor 0.1MPa, as required by practice. We preferred the isobaric-isothermal method of obtaining kinetic curves over the isochoric-isothermal one used today by most researchers on MA (Mg + 10% wt. Ni) [4] and MA (MgH_2 + 10% wt. Ni) [5]. It allowed studying the role of

Ni and Ti alloying elements and the manners of obtaining MAs to improve kinetics and reduce the decomposition temperature of the MgH_2 hydride phase in synthesized MAs in more detail.

Competitors

Department for Mater.Sci.&Engineer., Zhejiang University, China
Department for Mater.Univer London, UK
Course in Materials Science &Chemistry, Tokai University, Numazu, Japan
Institute for Energy Technology, P.O. Box 40, N-2027 Kjeller, Norway.
Helmholtz-Zentrum Gentre for Materials and Coastal Research, Germany

Technology Readiness Level

Based on the authors' research in the last 10-15 years on the role of a small additives (10% wt.) separately for each of the alloying elements Ti, Ni in reducing thermal stability and improving the decomposition kinetics of stoichiometric MgH_2 hydride, the technology for obtaining high-capacity hydrogen-absorbing magnesium-based materials with complex characteristics was developed, ensuring the practical use of these materials in stationary hydrogen storage systems. At present, the synthesis modes and characteristics of the developed mechanical alloys-nanocomposites for hydrogen storage determined on laboratory equipment require further adjustment and verification on mechanical alloys obtained in industrial production conditions.

The main publications in the frame of the project “Development of physicochemical principles for the creation of high-capacity hydride-forming materials and their use in stationary hydrogen storage systems and as electrodes for electrochemical energy systems”:

1. O.G. Ershova, V.D. Dobrovolsky, Yu.M. Solonin, A.Yu.Koval. Hydrogen sorption properties, thermal stability, and kinetics of hydrogen desorption from the hydride phase of the MgH_2 of a mechanical alloy of magnesium with Ti and Y, *Met.Phys. and Adv.l Tech.* , 2019, vol.41, pp.981-1001.
2. O.G. Ershova, V.D. Dobrovolsky, Yu.M. Solonin. Hydrogen sorption properties, thermal stability and kinetics of hydrogen desorption from the hydride phase of the MgH_2 of a Mechanical Alloys of Magnesium with Ti, Ni and Y. *Physics and chemistry of solid state*; 2020, vol. 21,pp.167-175.

3. O.G. Ershova, V.D. Dobrovolsky, Yu.M. Solonin.The effect of transition metals and Y additives on decomposition kinetics and thermal stability of the MgH_2 hydride phase of mechanical alloy-composites. *International Independent Scientific Journal*, 2020, vol.1, No. 20,pp. 35-45.

References

[1] Ershova O. G., Dobrovolsky V.D., Solonin Yu.M., Khyzhun O.Y., Koval A.Yu. The effect of Al on thermal stability and kinetics of decomposition of MgH_2 prepared by mechanochemical reaction at different conditions, *Materials Chemistry and Physics,* 2015; vol.162, pp. 408-416.

[2] Stampfer J.F.,C.E. Holley, J.F. Suttle. The Magnesium-Hydrogen System. *J. Am. Chem. Soc*., 1960, vol.82, pp.3504 – 3508.

[3] Shang C.X., Bououdina M., Song Y., Guo Z.X. Mechanic alloying and electronic simulations of (MgH_2+M) systems (M = Al, Ti, Fe, Ni, Cu, Nb) for hydrogen storage. *Int J Hydrogen Energy*, 2004, vol. 29, pp. 73 - 80

[4] M.Y. Song. Effects of mechanical alloying of the hydrogen storage characteristics of Mg-xwt% Ni (x = 0,5,10,25,55) mixtures, *Int. J. Hydrogen Energy*,1995, vol.20, pp. 221-227.

[5] M.S. Yahya, M. Ismail, Synergistic catalytic effect of $SrTiO_3$ and Ni on the hydrogen storage properties of MgH_2, *Int. J. Hydrogen Energy*, 2018, vol. 43, pp.6244-6255 .
http://doi.org/10.1016/j.ijhydene2018.02.028

Hydrogen storage and generation properties of new MgH_2-based nanocomposites

I. Zavaliy[1], V. Berezovets[1], L. Vasylechko[2], P. Lyutyy[1], Yu. Kosarchyn[1]

[1]*Karpenko Physico-Mechanical Institute NASU, Lviv, Ukraine*
[2]*Lviv Polytechnic National University, Lviv, Ukraine*

MgH_2-based nanocomposites were synthesized by the reactive ball milling using 0.5-5 mol % of various catalytic additives (nano-Ti, nano-TiO_2, and $Nd_{0.5}Ho_{0.5}FeO_3$ powders). The composites were investigated by the TDS method to determine the activation energy of hydrogen desorption process. It was shown that additives facilitate the hydrogenation of magnesium during milling and significantly improve the kinetics of hydrogen absorption-desorption. The synthesized nanocomposites were tested as materials for hydrogen generation by hydrolysis in pure water and with the addition of magnesium chloride. It was shown that the synthesis of MgH_2-based materials by reactive ball milling can improve the rate and yield of hydrogen evolution in the hydrolysis reactions. The best parameters were observed for the MgH_2–$Nd_{0.5}Ho_{0.5}FeO_3$ composite. The degree of conversion was significantly improved by the addition of $MgCl_2$.

Keywords: *Magnesium hydride, Composite materials, Nanomaterials, Mechano-chemical synthesis, Hydrogen storage, Hydrogen generation*

Introduction

One of the problems that require an effective solution in the development of hydrogen energy as part of the alternative energy of the future is the problem of storage and transportation of hydrogen. From the point of view of practical application, researchers have recently paid very much attention to such a class of materials as hydrides of Mg-based composites [1,2] and the dependence of the properties of such materials on the dispersity and morphology of their particles. The addition of catalysts exhibited a significant positive effect on lowering temperatures and accelerating the kinetics of the reaction of sorption/desorption of hydrogen in Mg/MgH_2. It was shown [3,4] that the temperature of hydrogen release from MgH_2 depends on the size of nanoparticles of both magnesium

hydride and catalytic additive. Nanomaterials (when it comes to magnesium as the main component) are mainly characterized by better kinetics of hydrogen absorption and release due to the reduction of the required diffusion pathways. The main advantage of nanosized catalytic additives is the increase in their efficiency by improving the uniformity of distribution. Previously, the emphasis was on catalytic additives that form hydrides, in particular, TiFe, $LaNi_5$, etc. [5–7]. Various studies have shown that nanostructured materials that do not form hydrides also improve the hydrogen adsorption-desorption properties of magnesium hydride. Numerous catalysts have been studied for their catalytic action, including transition metals, rare earth metals, carbon materials, metal oxides, carbides and etc [8-11]. In particular, Ti and its compounds in the nanoscale state have shown very good catalytic properties in improving the characteristics of magnesium hydride composites as materials for hydrogen storage [12].

Experimental Details

Starting materials for the preparation of hydride nanocomposites were magnesium metal powder and $Nd_{1-x}Ho_xFeO_3$ powders. The low-temperature sol-gel method was used to prepare $Nd_{1-x}Ho_xFeO_3$ nanocrystalline powders [13]. Magnesium-based hydride composites were prepared by the reactive ball milling in the planetary mill Fritsch Pulverisette-6. Stainless steel balls (30 balls with a diameter of 10 mm) were used as grinding bodies. The ratio of the weight of grinding bodies (≈120 g) to the weight of the sample was 80:1. Milling was performed at the rotational speed of 400 rpm and a hydrogen pressure of 1 MPa.

Hydrogen sorption-desorption properties of the synthesized composites were investigated on a Sieverts-type unit. Thermodesorption spectroscopy (TDS) was performed by linear heating of the sample in a dynamic vacuum from room temperature to 350 °C (heating rate 0.5-4 °C/min.). X-ray phase analysis of the samples was performed using a powder X-ray diffractometer DRON-3.0 (Cu-Kα radiation). The lattice parameters and crystal structure were calculated by the Rietveld method.

For all investigated samples, hydrolysis was performed under pseudo-isothermal conditions in the temperature range of 20-25 °C using a specially designed unit. The hydrolysis unit consists of a glass flask with a flat flange lid and five necks placed on a magnetic stirrer, which allows it to be heated. The reaction powder and water were added under inert conditions (in a stream of Ar gas). The unit contains: a drop funnel with a pressure compensator; flow meter with Sierra 100 data logger. Temperature control of the source materials and reaction environment was carried out.

Results and Discussion

Synthesis of hydride composites Mg– nano-$Nd_{0.5}Ho_{0.5}FeO_3$.

Taking into account the known improvement in the kinetics of hydrogenation-dehydrogenation of magnesium by its reactive ball milling with nanosized transition metal oxides, a similar catalytic effect was expected when adding nanoparticles of complex oxides, such as perovskites. In this work, we studied the effect of nanosized $Nd_{0.5}Ho_{0.5}FeO_3$ on characteristics of the hydrogen sorption-desorption by mechanochemically synthesized MgH_2. Under experimental conditions (400 rpm and a hydrogen pressure of 2 MPa) full saturation (absorption ~5.5 wt.%) was achieved after 4 hours of milling. In the next hydrogenation cycle, the hydrogenation time to 20 minutes at 300 °C was reduced because of the added catalyst and the reduction of the milled powder particles to nanosize.

XRD analysis of the samples after ball milling showed the formation of a mixture of nanocrystalline magnesium hydrides, whereas the interaction of $Nd_{0.5}Ho_{0.5}FeO_3$ perovskite with hydrogen was not observed. In composite materials, agglomeration of magnesium hydride particles does not occur during high-energy grinding and a more uniform particle size distribution is achieved. The size of the magnesium hydride crystallites (obtained by the profile analysis of diffraction peaks for all composites) is in the range of 6…10 nm, and coincides with corresponding values obtained for pure magnesium hydride (7 nm). After

ten cycles of hydrogen sorption/desorption, an increase in magnesium crystallites size was observed when they were heated during desorption, and no interaction of magnesium with perovskite was detected.

Thermodesorption of hydrogen from hydride composites MgH_2–$Nd_{0.5}Ho_{0.5}FeO_3$.

The effect of the addition of $Nd_{0.5}Ho_{0.5}FeO_3$ nanoparticles on the hydrogen sorption properties of MgH_2 was investigated using Sieverts-type equipment. Desorption into vacuum occurred in one stage (Fig. 1). In Fig. 2, the dependences for the hydride nanocomposite Mg–2.5 mol % nano-$Nd_{0.5}Ho_{0.5}FeO_3$ obtained by the Kissinger method are shown. According to the slope of the averaged Kissinger line, the activation energy (E_A) for the composite Mg–2.5 mol % nano-$Nd_{0.5}Ho_{0.5}FeO_3$ was estimated as 136 kJ/mol. Desorption activation energy E_a= 136 kJ/mol^{-1} for this composite is close to the value of 147 kJ/mol for a similar composite Mg + 5 wt.% nano-$Nd_{0.5}Dy_{0.5}FeO_3$. Such values of activation energy are lower than for pure magnesium and significantly higher than that for Mg-nano Ti and Mg-nano TiO_2 composites [12,14].

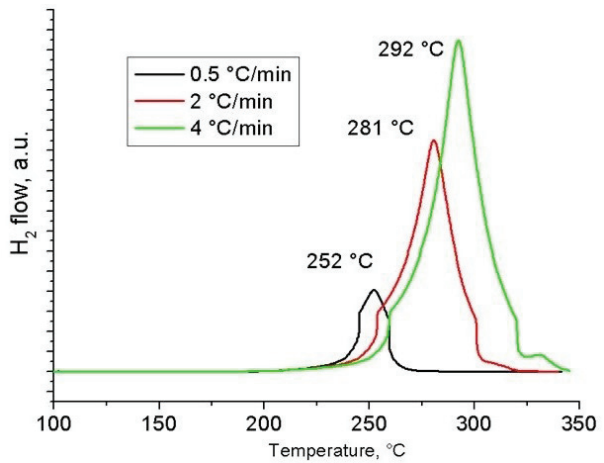

Fig. 1. TDS for Mg–2.5 mol % $Nd_{0.5}Ho_{0.5}FeO_3$ composite obtained at different heating temperatures.

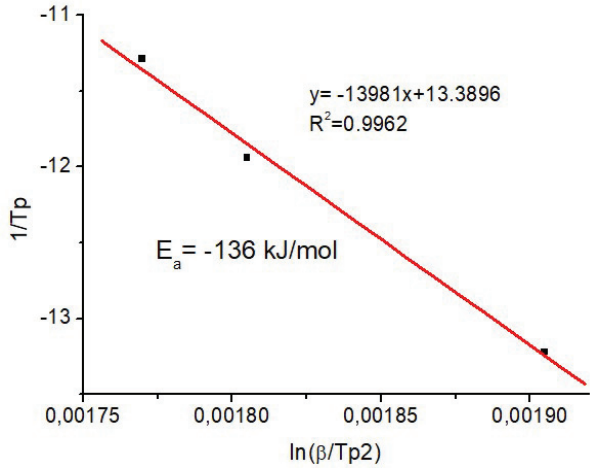

Fig. 2. Calculation of hydrogen desorption activation energy for Mg–2.5 mol % $Nd_{0.5}Ho_{0.5}FeO_3$ composite.

Hydrogen generation by hydrolysis.

All test samples were hydrolyzed under pseudo-isothermal conditions at room temperature using the unit described above. 50 ml of deionized water or magnesium chloride solution (0.04 mol/L) was introduced into the reaction flask containing 0.2 g of the composite. The reaction mixture was stirred well with a magnetic stirrer. After the hydrogen flow was stopped, a solution of citric acid was rapidly added to the reaction mixture to dissolve all the magnesium hydroxide in the reaction mixture and achieve complete interaction of the non-hydrolyzed magnesium hydride. Thus, the total yield of the hydrolysis reaction was established. The curves of hydrogen release from the composite material in the hydrolysis process are presented in Fig. 3.

In our previous works [12,14], a number of magnesium-based composite materials with catalytic additives were synthesized by the method of reactive grinding: Mg-10 wt.% nano-Ti; Mg-10 wt.% nano-TiO_2. Later the effect of nanoparticles of perovskites $Nd_{0.5}Ho_{0.5}FeO_3$ and $Nd_{0.5}Dy_{0.5}FeO_3$ and the effect of both the titanium and zirconium nitrides [15] on the hydrogen adsorption properties of magnesium were also

studied. The catalytic effect decreased in a row: nano-TiO_2 > nano-Ti > TiN > $Nd_{0.5}Ho(Dy)_{0.5}FeO_3$. Composites with nano-$TiO_2$ and nano-Ti slowly absorbed hydrogen even at room temperature. Conversely, $Nd_{0.5}Ho(Dy)_{0.5}FeO_3$ nanopowders demonstrated the effective sorption-desorption properties. However, the synthesized Mg–2.5 mol % nano-$Nd_{0.5}Ho_{0.5}FeO_3$ nanocomposites, tested as sources for hydrogen generation, showed promising results.

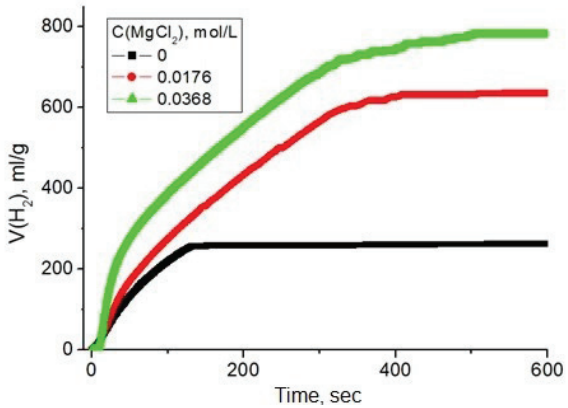

Fig. 3. Curves of hydrogen release from Mg–2.5 mol % nano-$Nd_{0.5}Ho_{0.5}FeO_3$ composite in the hydrolysis process.

The process of hydrolysis of magnesium hydride in pure water is not efficient due to the low overall yield of the hydrolysis reaction and blocking of the hydride surface. Currently, one of the best activators of the hydrolysis process is magnesium chloride. The aim of this work was also to confirm the positive effect of magnesium chloride on the reaction rate and hydrogen yield. Our studies of the effect of chloride ion on the hydrolysis reaction confirmed an increase in the reaction yield with increasing concentration of Cl^- (see Fig. 3). The depth of the reaction directly depends on the concentration of chlorine anions. This lowers the pH and leads to local destabilization of the hydroxide passivation layer on magnesium hydride. As a result, both the reaction kinetics and the hydrogen yield are improved.

Conclusions

In this work, nanopowders of $Nd_{0.5}Ho_{0.5}FeO_3$ perovskite was used as a catalyst for magnesium hydrogenation. The peculiarities of the microstructure of the obtained MgH_{2-x}–2.5 mol % nano-$Nd_{0.5}Ho_{0.5}FeO_3$ nanocomposite and the hydrogen sorption/desorption properties were studied in details. The nanocrystalline magnesium hydride synthesized by reactive ball milling is characterized by higher rates of hydrogen absorption/desorption compared to polycrystalline MgH_2. The activation energies from the hydrogen thermal desorption curves in vacuum with different heating rates for the composite with nano–$Nd_{0.5}Ho_{0.5}FeO_3$ additives were calculated. The difference between the desorption activation energies for pure magnesium hydride and composite with catalytic additives is about ~ 100 kJ/mol H_2. Synthesized composites with nano-$Nd_{0.5}Ho_{0.5}FeO_3$ additives were tested as materials for hydrogen generation by hydrolysis and demonstrated promising results. It was shown also that the degree of conversion increases with increasing concentration of $MgCl_2$.

The main publications in the frame of the project "Development of hydrogen storage and hydrogen generation materials based on magnesium hydride and optimization of hydrogen supply systems for fuel cells":

1. V.V. Berezovets, R.V. Denys, I.Yu. Zavaliy, Yu.V. Kosarchyn. Effect of Ti-based nanosized additives on the hydrogen storage properties of MgH_2. *Int J Hydrogen Ener*gy. *Accepted.* Available online 1 April 2021. https://doi.org/10.1016/j.ijhydene.2021.03.019

2. Y.V. Verbovytskyy, V.V. Berezovets, A.R. Kytsya, I.Yu. Zavaliy, V.A. Yartys. Hydrogen Generation by the Hydrolysis of MgH_2. *Materials Science.* 2020, 56, pp.1–14.
https://doi.org/10.1007/s11003-020-00390-5

3. I.Yu. Zavaliy, V.V. Berezovets, I.V. Oshchapovsky. Mg–TiN and Mg–ZrN nanocomposites as effective materials for hydrogen accumulation and generation. *Physicochemical Mechanics of Materials*. 2020, vol. 57, pp.52-59.

4. I.Yu. Zavalii, V.V. Berezovets’, R.V. Denys. Nanocomposites based on magnesium for hydrogen storage: achievements and prospects (a survey). *Materials Science*, 2019, vol.54, pp.611-626. https://doi.org/10.1007/s11003-019-00226-x

5. V. Berezovets, Y. Verbovytsky, D. Korablyov, Y. Solonin, I. Zavaliy, V. Yartys. Mg-based hydrides as a source of hydrogen for autonomous energy devices. *Proc. of the XX International Scientific and Practical Conference "Renewable Energy and Energy Efficiency in the XXI Century"*, May 15-16, 2019, Kyiv, Ukraine. pp.198-200

6. Zavaliy I.Yu., Berezovets V.V., Denys R.V., P. Zavalij, T. Zasadnyy. *H*ydrogen sorption/desorption properties of nanostructured Mg-based composites. *Abstr. Book of Ist Intern. research and practice conf. «Nanoobjects & Nanostructuring» (N&N–2020)*, Sept. 20–23, 2020, Lviv, Ukraine, p. 15.

References

[1] Sun Y., Shen C., Lai Q., Liu W., Wang D.W., Aguey-Zinsou K.F. Tailoring magnesium based materials for hydrogen storage through synthesis: Current state of the art. *Energy Storage Materials* 2018, 10, pp.168–198.
https://doi.org/10.1016/j.ensm.2017.01.010

[2] Lototskyy M., Denys R., Nyamsi S., Bessarabskaia I., Yartys V. Modelling of hydrogen thermal desorption spectra *Materials Today: Proceedings,* 2018, 5, pp.10440–10449.
http://doi.org/10.1016/j.matpr.2017.12.375

[3] Sadhasivam T., Kim H.T., Jung S., Roh S.H., Park J.H., Jung H.Y. Dimensional effects of nanostructured Mg/MgH_2 for hydrogen storage applications: A review. *Ren Sust Energy rev*. 2017, 72, pp.523–534. http://doi.org/10.1016/j.rser.2017.01.107

[4] Hanada N., Ichikawa T., Fujii H. Catalytic effect of nanoparticle 3*d*-transition metals on hydrogen storage properties in magnesium hydride MgH_2 prepared by mechanical milling. *J Phys Chem B.* 2005,109, pp.7188–7194.
http://doi.org/10.1021/jp044576c

[5] Halicioglu R., Bayrak M., Iscan B., Akbalik F. An Experimental Study on Hydrogen Storage Capabilities Improvement of the TiFe-H_2. *Energy Sources* 2012, 34, pp.1876–1882.

[6] Tibbetts G.G., Meisner G.P., Olk C.H. Hydrogen storage capacity of carbon nanotubes, filaments, and vapor-grown fibers. *Carbon* 2001, 39, pp.2291–2301.
http://doi/org/10.1016/S0008-6223(01)00051-3

[7] Züttel A. Materials for hydrogen storage. *Materials today.* 2003, 6(9), pp. 24–33. http://doi.org/10.1016/S1369-7021(03)00922-2

[8] Liang G., Huot J., Boily S., Van Neste A., Schulz R. Catalytic effect of transition metals on hydrogen sorption in nanocrystalline ball milled MgH_2-Tm (Tm= Ti, V, Mn, Fe and Ni) systems. *J Alloys Compd.* 1999, 292, pp.247–252.
http://doi.org/10.1016/S0925-8388(99)00442-9

[9] Oelerich W., Klassen T., Bormann R. Metal oxides as catalysts for improved hydrogen sorption in nanocrystalline Mg-based materials. *J Alloys Compd*. 2001, 315, pp.237–242.
http://doi.org/10.1016/S0925-8388(00)01284-6

[10] Barkhordarian G., Klassen T., Bormann R. Effect of Nb_2O_5 content on hydrogen reaction kinetics of Mg. *J Alloys Compd.* 2004, 364, pp.242–246.
http://doi.org/10.1016/S0925-8388(03)00530-9

[11] Kojima Y., Kawai Y., Haga T. Magnesium-based nanocomposite materials for hydrogen storage, *J. Alloys Compd.,* 2006, 424, pp.294–298.
http://doi.org/10.1016/j.jallcom.2005.11.088

[12] Berezovets V.V., Denys R.V., Zavaliy I.Yu., Kosarchyn Yu.V. Effect of Ti-based nanosized additives on the hydrogen storage properties of MgH_2. *Int J Hydrogen Energy*. Available online 1 April 2021.
http://doi.org/10.1016/j.ijhydene.2021.03.019

[13] Pavlovska O., Lutsyuk I., Kondyr A., Zhydachevskyy Ya., Vakhula Ya., Pieniazek A., Vasylechko L. Synthesis and structure characterisation of micro-and nanocrystalline powders of $Dy_{1-x}R_xFeO_3$ (R= La, Pr, Nd, Sm, Gd). *Acta Physica Polonica A.* 2018, 133, pp.802–805.

http://doi.org/10.12693/APhysPolA.133.802
[14] Zavaliy I.Yu., Berezovets V.V., Denys R.V., Shtender V.V. Research of new magnesium-based composites: synthesis and structure. Influence of phase and chemical composition on desorption properties and cyclic stability (pp.156-165). Section of the monograph "Fundamental aspects of renewable hydrogen energy and fuel cell technologies". K .: “KIM”, 2018. - 260 p.
[15] Zavaliy I.Yu., Berezovets V.V., Oshchapovsky I.V., Zasadnyy T.M. Mg – TiN and Mg – ZrN nanocomposites as effective hydrogen storage and generation material. *Physicochemical Mechanics of Materials.* 2021, vol.57, pp.52–59.

Metal-hydride stores as hydrogen supply systems for fuel cells

Y. Matsevity, A. Avramenko, N. Chorna

Pidhornyi Institute of Mechanical Engineering Problems, NASU, Kharkov, Ukraine

Introduction

The publications about using of hydrogen technologies together with renewable energy sources for energy technology complexes infrastructure, namely, for autonomous power supply of small consumers in remote areas are analyzed [1, 2]. The potential for the use of solar and wind energy in Ukraine is high enough for their including into energy systems. During the exploitation of autonomous power complexes based on renewable energy sources, in particular, solar and wind ones, emergency situations take place. Such emergency situations are caused by power outages due to inconsistency of power supply or emergency failures of individual elements of the power complex. Therefore, to ensure uninterrupted power supply of an autonomous private consumer, it is necessary to provide the additional energy supply equalization systems. For solving the problems of smoothing the uneven energy supply from renewable energy sources and conversion energy from primary sources using an electrolysis plant, a metal-hydride hydrogen storage system and a fuel cell have been proposed. It allows to solve technological problems and reduce environmental pollution in Ukraine.

Keywords: Power supply, Ecology, Power plant, Hydrogen, Fuel cells, Metal-hydride accumulator.

Scientific novelty

An alternative scheme of electric and heat supply for a stand-alone house without using additional imported fuel is proposed. The advantage of such a scheme is that it is closed and fully autonomous because hydrogen is produced on site to power the fuel cell, while the metal-hydride hydrogen storage system ensures hydrogen absorption and its release due to the hot and cold water resources available in the system.

Practical significance

The technology for energy conversion of primary sources by creating a wind-driven energy technological complex using an electrolysis plant and a metal-hydride hydrogen storage system will solve the problem of smoothing the irregular electric power supply from renewable sources.

Description

During wind-driven generator operation, the generated electric power is delivered to the high-pressure electrolyser via the control system [3]. The reaction of electrochemical dissociation of the liquid alkaline electrolyte yields oxygen and hydrogen that enter system of cylinders of gas storage system and used subsequently for fuel cell module operation. An invertor circuit is used to convert the DC voltage to alternating current. Then the converted electric power is delivered to the consumer. During hours when wind-driven generator power is excessive, hydrogen is stored in the metal hydride accumulator jointly with the gas cylinder storage system.

Hence, wind energy is accumulated to be used subsequently for stand-alone power supply to consumers. During peak load hours (morning and evening), as well as during an abrupt prolonged wind speed drop, hydrogen and oxygen in the storage system are used for generating additional electric power with the help of the fuel cell module (Fig. 1) [4–6].

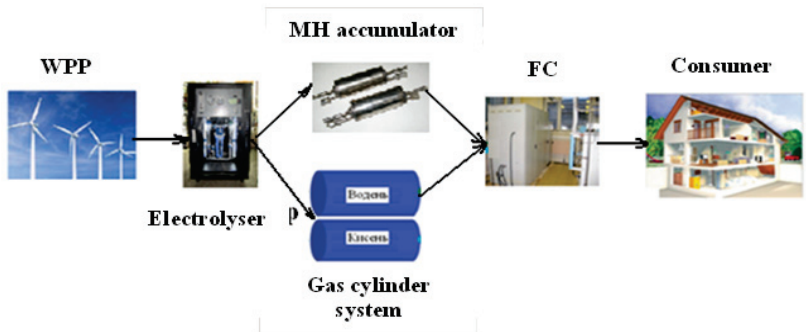

Fig.1. Schematic arrangement of a stand-alone wind-hydrogen energy technological complex

The use of hydrogen in fuel cells makes it possible to create efficient systems of autonomous power supply for private consumers. The most promising power plants for off-grid consumers are 1 kW to 20 kW power plants built around low-temperature alkaline fuel cells [7]. They are distinguished by high efficiency and are environmentally friendly and noiseless in operation. The analysis of publications showed that to provide power to fuel cells, the most compact, safe and environmentally friendly way is to use reusable metal-hydride batteries of high-purity hydrogen as part of an energy complex that meets the requirements for the placement of autonomous power supply systems [4, 6, 8, 9].

Possible applications

Research has shown that electrical energy supply systems built around fuel cells are interesting from different viewpoints: a high operating efficiency parameter [10], low environmental burden [11], flexible control of system parameters, and other parameters [12]. Systems for standby and stand-alone electrical energy supply built around fuel cells can also include renewable energy sources to create entirely closed systems. Furthermore, there is a big demand for automated systems of distributed and standby electrical supply for medical establishments, especially under conditions of the rapid spreading of the new COVID-19 coronavirus, and the need to support the serviceability of a huge number of artificial respiration units even under conditions of shutdown of centralised electric power supply. For today many small agricultural facilities are connected to centralised electric energy supply systems that causes a host of problems, namely, voltage drops, critical conditions of electric power grids, and frequent and prolonged power blackouts. The suggested solution based on fuel cells has an advantage over all other modern standby electric power supply systems.

Technique

The calculation method provides a set of optimal technical solutions for determining the effective operating modes of an autonomous power system for supplying hydrogen to a fuel cell based on the graphs of the electrical load of a particular consumer using a computational experiment.

Results

Based on the study, a technological scheme of an autonomous power supply system based on fuel cells has been developed, an approach to the creation of a metal-hydride system for accumulating hydrogen and its supply to fuel cells has been substantiated. A calculation algorithm has been developed that allows you to calculate the annual energy balance of a specific consumer and select the necessary equipment to implement the scheme based on the annual schedule of heat and electrical load (Fig. 2).

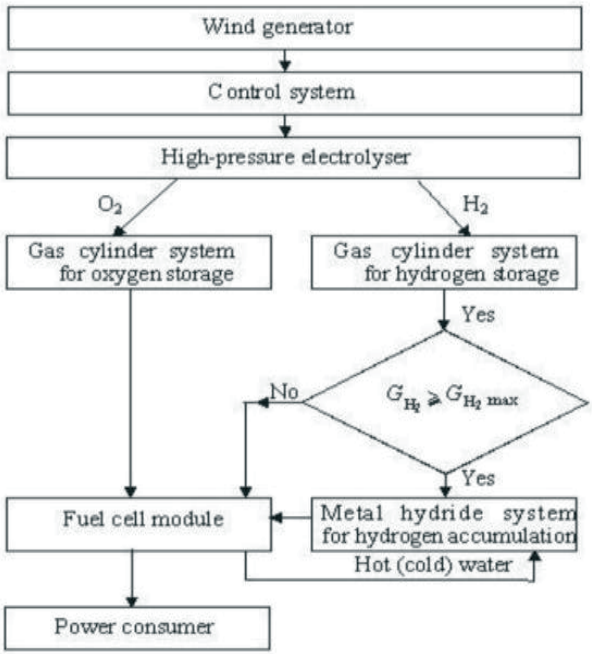

Fig. 2. Generalised algorithm for design of a stand-alone energy supply system

It is shown that, for stand-alone consumers, power supply systems built around low-temperature alkaline 20 kW fuel cell are exceptionally interesting. The use of a metal hydride hydrogen storage system in a wind energy technological complex meets the requirements to the installation of stand-alone power supply systems.

The operating modes of the selected fuel cell were studied and the parameters of influence on its output characteristics were investigated to determine the efficiency of the power plant for autonomous power supply systems for consumers in remote areas.

The operation of fuel cells with a metal hydride hydrogen accumulation system was analysed for hydrogen storage accumulators and the schemes of their joint operation for a stand-alone cottage. The design chosen was that of a metal hydride hydrogen accumulator with a length of L=0.15 m and an inner diameter of 0.04 m, and a productivity of up to 0.035 g/s (Fig. 3) [13].

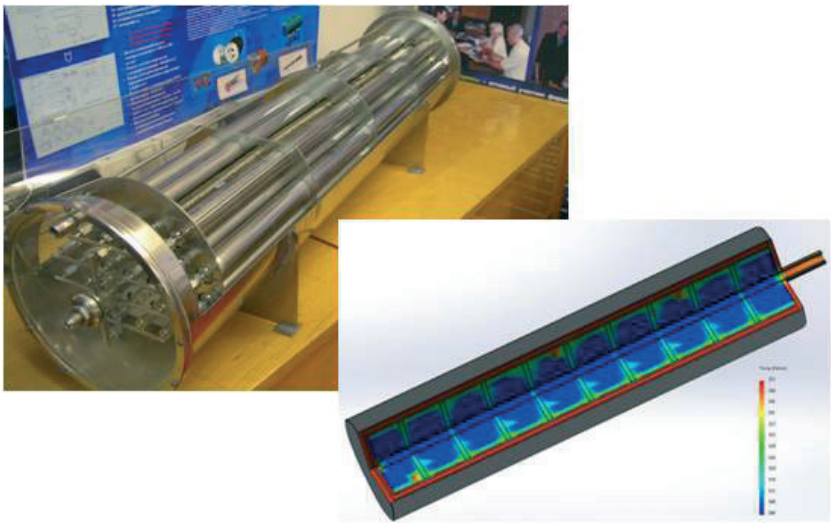

Fig. 3. Appearance and temperature field of a metal-hydride hydrogen storage system

Based on design, the electrolyser EBT 1.0 - 150 with the productivity of 1 nm^3 H_2 and 0.5 nm^3 O_2 was chosen. It produces high-pressure hydrogen and oxygen at 15.0 MPa without using a compressor and entirely meets the technical demands of a gas tank system for hydrogen and oxygen storage.

It was chosen fuel cell DBX5000 with a power of 5.0 kW that provides the maximum electric power load of a stand-alone house.

The modes of operation of the metal hydride system were optimized and the optimal operating conditions for the “metal hydride – fuel cell” were selected. Recommendations have been developed for the use of metal hydride hydrogen storage systems in autonomous power plants based on a fuel cell, considering the aspects of their fire and explosion hazardous operation.

Comparative assessment and level of technical training

Thus, as compared to present-day standby electric power supply systems based on storage batteries, fuel cells enable creating standby electric power supply systems with a 3 to 4 times longer time of operation in the stand-alone mode.

Hence, the combined application of advanced technologies for the production, storage and use of hydrogen increases energy conversion efficiency and significantly expands its application areas, especially for stand-alone power supply systems with a wind-driven power plant and a hydrogen energy accumulator.

List of the main publications in the frame of project “Application of high-efficient hydrogen generation and storage systems for autonomous energy support”:

1. N.A. Chorna. Prospects for application of hydrogen technologies for autonomous power complexes based on renewable energy sources. *Scientific and Applied Journal Vidnovluvana energetika,* 2021, No.3(66), pp. 18-32.
https://doi.org/10.36296/1819-8058.2021.3(66).18-32.

2. A.M. Avramenko, A.A. Shevchenko, N.A. Chorna, A.L. Koten ko. Application of highly efficient hydrogen generation and storage systems for autonomous energy supply, *Naukovyi Visnyk Natsionalnoho Hirnychoho Universytetu,* 2021, No.3, pp. 69–74.
https://doi.org/10.33271/nvngu/2021-3/069

3. Y. Matsevytyi, N. Chorna, A. Shevchenko. Development of a Perspective Metal Hydride Energy Accumulation System Based on Fuel Cells for Wind Energetics. *Journal of Mechanical Engineering,* 2019, vol. 22, No. 4, pp. 48–52.
https://doi.org/10.15407/pmach2019.04.048.

4. N.A. Chorna, V.V. Ganchin. Use of mathematical modeling to improve the mass and dimensions of metal hydride plants. *Mathematical methods and physical and mechanical fields,* 2019, Vol. 2, № 3, pp. 159–167.

References

[1] BP Statistical Review of World Energy, 68th edition, 2019. p. 62, electronic resource https://www.bp.com/content/dam/bp/business-sites/en/global/corporate/pdfs/energy-economics/statistical-review/bp-stats-review-2019-full-report.pdf.

[2] IEA report, «Renewables 2019: global status report», REN 21, 2020, p. 336. ISBN 978-3-9818911-7-1.

[3] Solovey V.V., Shevchenko A.A., Zipunnikov M.M., Kotenko A.L., Khiem N.T., Tri B.D., Hai T.T. Development of high pressure membraneless alkaline electrolyzer, *Int. J. of Hydrogen Energy,*2021*,* https://doi.org/10.1016/j.ijhydene.2021.01.209.

[4] Matsevytyi, Y.M., Chorna, N.A., Shevchenko, A.A. Development of a Perspective Metal Hydride Energy Accumulation System Based on Fuel Cells for Wind Energetics. *Journal of Mechanical Engineering*, 2019, vol.22, pp. 48–52. https://doi.org/10.15407/pmach2019.04.048.

[5] Chorna N.A., Hanchyn V.V. Modeling Heat and Mass Exchange Processes in Metal-hydride Installations, *Journal of Mechanical Engineering,* 2018, vol. 21, pp. 63–70. https://doi.org/10.15407/pmach2018.04.063.

[6] Avramenko A., Chorna N. Adaptation of metal-hydride hydrogen storage technologies for autonomous power supply systems based on fuel cells, XVI International Conference «Hydrogen materials science and chemistry of carbon nanomaterials» (ICHMS '2019), Kiev, September 23–30, 2019, pp. 88–89.

[7] Fuel Cell Technology Market: By Applications (Portable, Stationary, Transport), Types (PEMFC, DMFC, PAFC, SOFC, MCFC), Fuel (Hydrogen, Natural Gas, Methanol, Anaerobic Digester Gas) & Geography – Global Trends and Forecast to 2018, analytical report, M&M (MarketsandMarkets), (Dallas, TX Market Research Company and Consulting Firm): web-resource,

http://www.marketsandmarkets.com/Market-Reports/fuel-cell-market-348.html.

[8] Avramenko A.M. *et.al* Application of highly efficient hydrogen generation and storage systems for autonomous energy supply, *Naukovyi Visnyk Natsionalnoho Hirnychoho Universytetu*, 2021,No.3,pp. 69–74.

[9] Avramenko A.M. *et.al.* Using of hydrogen technologies for autonomous uninterrupted energy supply of customers in remote areas, *Information technologies: science, technique, technology, education, health*, XXIX international science and practice conference MicroCAD-2021, Kharkiv, NTU KhPI, *book of abstracts*, 2021, vol.1, p.180 (in Ukrainian).

[10] Fuel Cells Market by Type (Proton Exchange Membrane Fuel Cell, Phosphoric Acid Fuel Cell, Alkaline Fuel Cell, Microbial Fuel Cell), Application (Transport, Stationary, Portable), End-User, Region - Global Forecast to 2024,electronic resource,
http://www.marketsandmarkets.com/Market-Reports/fuel-cell-market-348.html.

[11] DOE Hydrogen and Fuel Cells Program.(2019). Annual Progress Report 2018:DOE/GO-102019-5156,April 2019, 1025p, electronic resource, https://www.nrel.gov/docs/fy19osti/73353.pdf.

[12] Zhang, X., Chan, S. H., Ho, H. K., Tan, S.-C., Li, M., Li, G., Feng, Z. Towards a smart energy network: The roles of fuel/electrolysis cells and technological perspectives. *Int. J. Hydrogen Energy*, 2015, vol. 40 (21). pp.6866-6919
https://doi.org/10.1016/j.ijhydene.2015.03.133. [in English].

[13] Chorna N.A., Ganchin V.V. Use of mathematical modeling to improve the mass and dimensions of metal hydride plants. *Mathematical methods and physical and mechanical fields,* 2019, vol. 2, No. 3, pp. 159–167. [published in Ukrainian].

Elaboration and study of materials for anodes and interconnects of lightweight solid oxide fuel cells

O. Ostash[1], B. Vasyliv[1], V. Podhurska[1], O. Vasyliev[2], Ye. Brodnikovskii[2], I. Polishko[2], I. Danilenko[3], A. Shylo[3], T.Prikhna[4], V. Sverdun[4] , O. Kuprin[5]

[1]*Karpenko Physico-Mechanical Institute, NASU, Lviv, Ukraine*
[2]*Frantsevich Institute for Problems of Materials Science, NASU, Kyiv, Ukraine*
[3]*Donetsk Institute for Physics and Engineering, NASU, Kyiv, Ukraine*
[4]*Bakul Institute for Superhard Materials, NASU, Kyiv, Ukraine*
[5]*National Science Center Kharkov Institute of Physics and Technology, Kharkov, Ukraine*

An important aspect of the development of modern industry is the need to move to environmentally friendly ways of electricity generation. Among them, one of the key places belongs to fuel cell technologies. From the point of view of efficiency, the most important place is occupied by Solid Oxide Fuel Cells (SOFCs). During long-term operation, materials of SOFC components degrade due to the influence of operating environments. SOFC anodes, which are traditionally made of 8YSZ–NiO ceramics, and interconnects made of the Crofer type ferritic steels are the most affected by the environments. It is known that a SOFC can consume all types of fuel. However, when hydrocarbons are used as fuel in a SOFC or there are impurities (CO_2, H_2S, H_2O, etc.) in the technological environment, a rapid degradation of the 8YSZ–NiO anode ceramics occurs. SOFC interconnect materials should possess a complex of high characteristics (strength, oxidation resistance, electrical conductivity, etc.). However, these characteristics are not reached in the Crofer type steel, and its high specific density results to a significant SOFC weight.

It was found [1] that 8YSZ–NiO ceramics obtained by the tape casting technology is more promising for the production of SOFC anode substrates than one obtained by sintering powders. It has finer grains and more homogeneous microstructure and as a result its strength increases by 63%. After its one-time reduction in the presence of carbon dioxide in a hydrogen-containing environment (N_2–10%H_2–5%CO_2), strength of 8YSZ–Ni cermet decreases by 15% compared to that reduced in Ar–5%H_2 mixture.

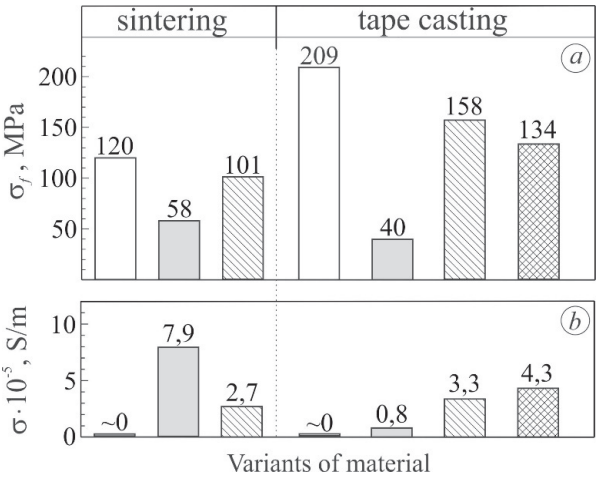

Fig. 1. Strength σ_f (*a*) and specific electrical conductivity σ (*b*) of the investigated ceramics in as-sintered state (white bars), and the cermets after reduction at 600 °C in 100%H_2 (gray bars), in Ar–5%H_2 mixture (hatched bars) and N_2–10%H_2–5%CO_2 mixture (cross-hatched bars) prepared by the sintering and tape casting technologies.

Electrical conductivity of the cermet increased by 30% (Fig. 1). This is due to the deposition of carbon at the ZrO_2–Ni interphases, which requires the improvement of such an anode material.

This problem can be solved by replacing nickel in the anode with copper. Copper, compared to nickel, has higher thermodynamic and kinetic barriers during the dissociation of hydrocarbons. It is also known that Al_2O_3 oxide has a positive effect on the mechanical properties of ceramics.

Technological modes for production of ceramics of 50% (ZrO_2 – 8 mol%Y_2O_3 – 2 wt% Al_2O_3) + 50% (NiO – 5 wt% CuO) composition were optimized in terms of the temperatures of calcination of powders (700 °C) and their sintering (1400 °C), which allowed to obtain a fine-grained microstructure and increased both strength and electrical conductivity of the corresponding cermet [2].

After reduction in N_2–10%H_2–5%CO_2 gas mixture, the cermet does not lose its physical and mechanical properties compared to the as-sintered ceramics (Fig. 2). However, to use it as anode material for a SOFC operating, for example, on syngas, it is necessary to increase its strength and electrical conductivity.

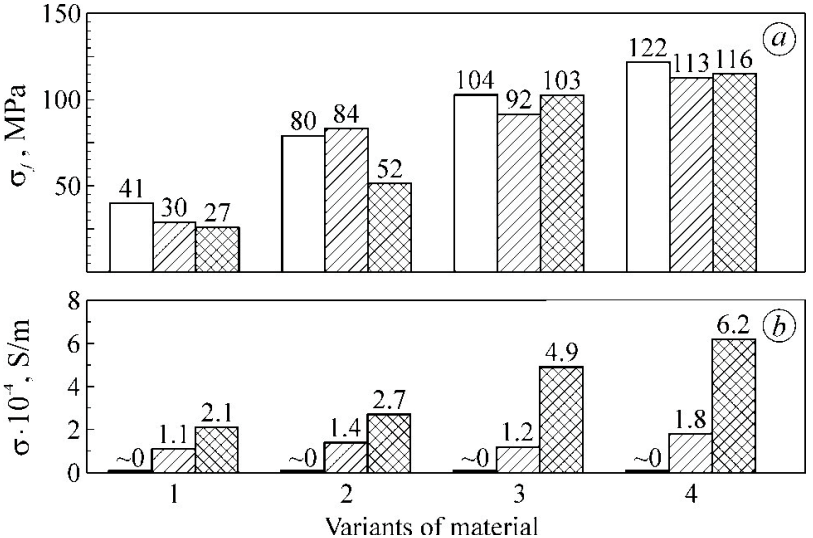

Fig. 2. Strength σ_f (*a*) and specific electrical conductivity σ (*b*) of the investigated ceramics in as-sintered state (white bars) and the cermets after reduction at 600 °C in Ar–5%H_2 mixture (hatched bars) and N_2–10%H_2–5%CO_2 mixture (cross-hatched bars): variant 1 – calcination temperature 900 °C/sintering temperature 1450 °C; variant 2 – 900°C/1400°C; variant 3 –700°C/1450°C; variant 4 –700 °C/1400 °C. The average values of the corresponding characteristics of at least 3 test specimens are given.

An alternative to the Crofer type steels (density of ~8 g/cm^3) are composites based on titanium MAX phase (density of 4.1…4.3 g/cm^3), especially for the intermediate temperature (550 °C…650 °C) SOFCs. Here, the Ti_2AlC phase is preferred over the Ti_3AlC_2 phase [3]. However, like Crofer steels, specimens of these MAX phases lose their electrical conductivity after long-term (1000 h) holding in air at 600 °C.

Interconnects made of thin (0.2 mm …0.5 mm) titanium sheets with a silver coating, as well as with a coating based on the MAX phases of the Ti–Al–C system, can be more efficient. It was shown [4] that silver-coated interconnects have high oxidation resistance under the above conditions but exhibit insufficiently high (~10^4 S/m) electrical conductivity. It was found [5-7] that high oxidation resistance and electrical conductivity under these conditions are demonstrated by the coating of the Ti–Al–C system, applied by vacuum-arc method on a thin (0.5 mm) plate made of a titanium of VT1-0 grade (Fig. 3 and Table 1).

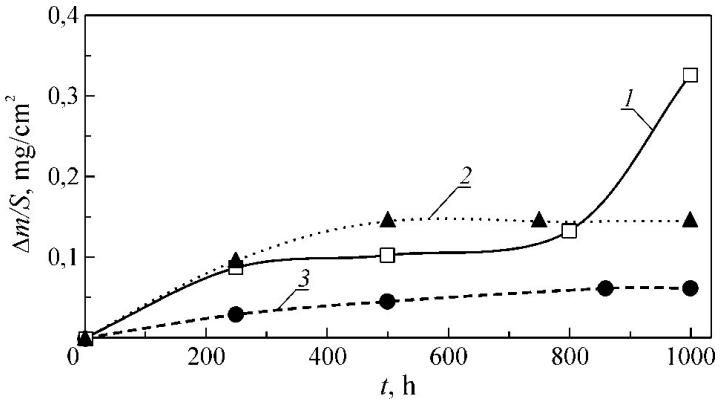

Fig. 3. Oxidation resistance of Crofer 22APU steel (curve 1), MAX phase Ti_2AlC based composite (curve 2), and Ti–Al–C coating on a Ti-plate (curve 3).

Table 1. Electrical conductivity, S/m, of investigated materials

Materials	Steel Crofer 22APU	MAX phase Ti_2AlC based composite	Ti–Al–C coating on a Ti-plate
As-received	$8.71 \cdot 10^5$	$1.63 \cdot 10^6$	$1.33 \cdot 10^6$
After holding in air at 600 °C for 1000 h	$2.05 \cdot 10^{-3}$	$1.73 \cdot 10^{-2}$	$1.30 \cdot 10^6$

This effect is explained by the formation of oxidation-resistant and electrically conductive Ti_3AlC (with antiperovskite crystal structure), TiAl, and Ti_3Al phases. On this basis, lightweight interconnects for SOFCs as an alternative to those made of the Crofer type steel can be created, which will significantly (by ~50%) reduce the weight of SOFC batteries.

The main publications in the frame of the project "Elaboration and study of materials for anodes and interconnects of lightweight solid oxide fuel cells" are presented in references.

References

[1] Vasyliv B.D., Podhurska V.Ya., Ostash O.P., Polishko I.O., Brodnikovs'kyi E.M., Ivanchenko S.E., Vasyl'ev O.D. Influence of the working media of fuel cells on the structure and physicomechanical characteristics of ceramics of the ZrO_2–Y_2O_3–NiO system, *Materials Science*, 2020,vol. 56, No. 1, pp. 15–21.
https://doi.org/10.1007/s11003-020-00391-4

[2] Podhurska V.Ya., Vasyliv B.D., Ostash O.P., Danilenko I.A., Shylo A.V., Burkhovetsky V.V. Influence of the reducing medium on the structure and physical and mechanical properties of ceramics of the ZrO2-Y2O3-Al2O3-NiO-CuO system, *Phys.-Chim. Mekhanika Materialiv*, 2020, vol.56, No.6, pp. 108–116. (in Ukrainian)

[3] Prikhna T.A., Ostash O.P., Serbenyuk T.B., Podhurska V.Ya., Sverdun V.B., Kozyrev A.V., Moshchil V.E., Karpets M.V., Javorska L., Podsiadło M., Cyboroń J., Figiel P., Starostina A.V., Zymych T.B. Lightweight Ti,Nb-Al-C MAX phases based materials: structure and heat-resistance in oxidizing and hydrogen atmosphere at 600 and 1200 °C, *Proceedings of the Euro PM2018 Congress & Exhibition*, 2020, Bilbao Exhibition Centre (BEC), Bilbao, Spain,code 156875, ISBN: 978-189907250-7.

[4] Ostash O.P., Prikhna T.O., Podhurska V.Ya., Sverdun V.B., Vasyliv B.D. Material for manufacturing of interconnect elements of solid oxide fuel cells. UA patent No. 137888, published Nov 11, 2019, bull. No.21.

[5] Ostash O.P., Prikhna T.O., Kuprin O.S., Podhurska V.Ya., Sverdun V.B., Vasyliv B.D. A production method of the thin interconnects

for solid oxide fuel cells, UA patent No.121831, published July 27, 2020, bul. No.14.

[6] Vasyliv B., Podhurska V. Development of the concept of a spheroidal shape anode for a solid oxide fuel cell // In: Ikhmayies S. (eds) Advances in Energy Materials. Advances in Material Research and Technology. Springer, Cham, 2020, pp. 77–103. https://doi.org/10.1007/978-3-030-50108-2_4

[7] Podhurska V., Brodnikovskyi D., Vasyliv B., Gadzyra M., Tkachenko S., Čelko L., Ostash O., Brodnikovska I. ,. Brodnikovskyi Ye, Vasylyev O. . Ti-Si-C in-situ composite as a potential material for lightweight SOFC interconnects, *Promising Materials and Processes in Applied Electrochemistry,* edited by V.Z. Barsukov, Yu.V. Borysenko, V.G. Khomenko, O.V. Linyucheva, Kyiv,KNUTD, 2020, pp. 54–68. https://er.knutd.edu.ua/handle/123456789/17000

Autonomous power supply based on fuel cells and Al-based hydrogen generator

Yu. Pirskyy, F. Manilevich, A. Kutsyi, T. Panchyshyn, B. Danil'tsev, A. Bogdanova, O. Krupennikova

Vernadsky Institute of General and Inorganic Chemistry, NASU, Kyiv, Ukraine

An autonomous power supply including a hydrogen generation unit and a portable battery of hydrogen-air fuel cells has been developed and investigated. Hydrogen was released from the water in the generation unit as a result of hydrolysis of activated aluminum. It was shown that introduction of zinc (3 wt.%) together with eutectic Ga-In-Sn alloy (5 wt.%) into the Al-based alloy leads to a significant increase in the rate of aluminum hydrolysis, particularly at low temperatures. Anodic and cathodic Pt (40 %)/XC72 electrocatalysts for hydrogen-air fuel cells have been synthesized and studied.

Keywords: *Autonomous power supply, Hydrogen generation, Activated aluminum, Aluminum alloys, Electrocatalysts for fuel cells*

Introduction

Over the past decades, hydrogen energetics has been actively developing, based on the use of hydrogen as an energy-intensive and environmentally friendly energy carrier and fuel [1]. In particular, the demand for fuel cells for various purposes has significantly increased, where an electric current is generated as a result of the anodic oxidation of hydrogen and the corresponding cathodic process [2]. The widespread use of fuel cells is constrained by the problems associated with the production, storage and transportation of hydrogen [3-4]. In nature, there are practically no reserves of free hydrogen, so it must be extracted from compounds, for example, from water, the reserves of which are colossal. The use of energy-storage substances (ESSs) for the extraction of hydrogen from water makes it possible to obtain hydrogen on demand directly at the place of its use. The development of a hydrogen generators of a hydrolysis type, in which ESSs are used to extract hydrogen from water, and their combination with improved fuel cells is an urgent task, since its solution will lead to the creation of autonomous current sources necessary in everyday life and in transport, in space research and in the defense sphere. The development of modern autonomous current sources

based on fuel cells and hydrogen generators solves the problem of power supply with electric current for a wide range of portable electrical and electronic devices. The generation of electricity in the developed current sources is an environmentally friendly process that does not degrade the environment.

Experimental procedures, results and discussion

To create an autonomous current source, within the framework of this work, studies were carried out to optimize the composition of aluminum-based ESSs, adapted to the release of hydrogen from water in an alumohydrogen generator at ambient temperature. Furthermore, cathode and anode electrocatalysts were improved for experimental samples of hydrogen-air fuel cells (FC) and efficient catalytic inks were developed for applying catalysts onto gas diffusion layers formed on a proton-exchange membrane.

New methods for the synthesis of highly efficient platinum electrocatalysts Pt(40 %)/XC-72 for the oxygen reduction and hydrogen oxidation have been developed, and the optimal conditions for their preparation have been determined. The starting materials for the preparation of such electrocatalysts were a solution of hexachloroplatinic acid H_2PtCl_6 and Vulcan XC-72 carbon black, which had been preliminarily subjected to oxidation in HNO_3. Ethylene glycol (EG) or formaldehyde was used as a reducing agent, and polyvinylpyrrolidone (PVP) was used as a stabilizer of platinum nanoparticles. Six methods for the preparation of Pt/C catalysts were proposed, and six corresponding groups of catalysts were obtained (for the designation and synthesis conditions, see Table) [5].

To assess the activity of the synthesized catalysts in the oxygen electroreduction reaction, potentiostatic cathodic polarization curves were recorded on a floating gas diffusion electrode (FGE) in a 0.5 M H_2SO_4 solution. In Fig. 1, the obtained polarization curves are presented in Tafel coordinates. It can be seen that a decrease in the synthesis temperature from 160 to 75 °C and the use of polyvinylpyrrolidone and formaldehyde improve the electrocatalytic properties of the materials obtained. An increase in the activity of electrocatalysts with an increase in the amount of PVP during their synthesis is associated with the stabilization of

platinum nanoparticles. Formaldehyde is a stronger reducing agent than ethylene glycol, therefore, it has a positive effect on the properties of the preparing catalysts.

Table. Designation of the obtained electrocatalysts Pt(40 %)/XC-72 and conditions of their synthesis.

Catalyst	EG additive, mL	Synthesis temperature, °C	Used alkali	Additives
A	100 EG	130	1 M NaOH	–
B	100 EG	160	1 M NaOH	–
C	100 EG + 30 H_2O	140	1 M NaOH	110 mg PVP
D	100 EG + 30 H_2O	140	1 M NaOH	330 mg PVP
E	100 EG	75	1 M KOH	330 mg PVP + 60 mL CH_2O
F	100 EG	75	1 M KOH	60 mL CH_2O

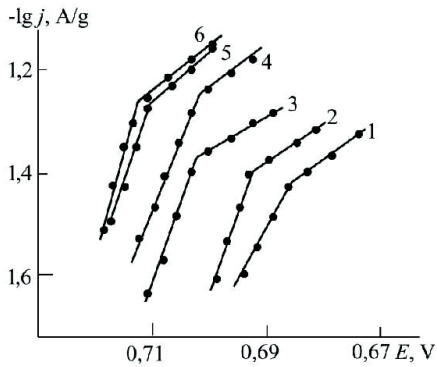

Fig. 1. Potentiostatic polarization curves of oxygen reduction in 0.5 M H_2SO_4 solution on FGE, superficially modified with Pt(40 %)/XC-72 catalysts: A (*5*); B (*3*); C (*4*); D (*2*); E (*6*); F (*1*).

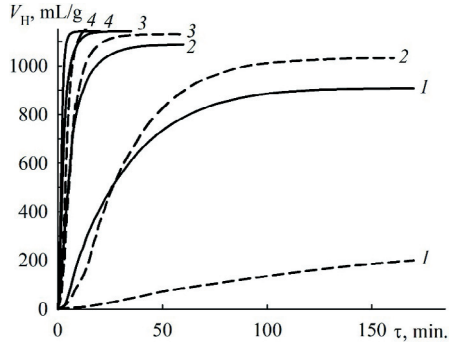

Fig. 2. Time dependencies of the volume of the evolved hydrogen during the hydrolysis of the aluminum alloys with 5 wt.% of eutectic Ga-In-Sn alloy (----) and 3 wt.% of Zn (—) at temperatures (°C): 25 (*1*); 40 (*2*); 55 (3); 70 (*4*).

On the basis of the obtained electrocatalysts Pt(40 %)/XC-72, a catalytic ink was prepared, which was tested in an operating laboratory model of a battery of hydrogen-air FCs with a Nafion® proton exchange membrane. The high efficiency of the obtained catalytic ink was shown. The power of the created FC battery was 8W, the operating voltage was 4.2V, the operating temperature was 5-30 °C, the maximum operating temperature was 55 °C, the hydrogen flow was 0.18 L/min, the time to reach the operating mode was 30 sec. at the temperature 20 °C, the efficiency of FC battery was 40 %.

To generate hydrogen, an aluminum-based ESSs were used, which was activated by alloying with low-melting and electropositive metals. In our previous studies, it was shown that aluminum alloys with 3 - 10 wt.% of the Ga-In-Sn eutectic enter into the hydrolysis reaction with the release of hydrogen from water at a temperature of 25 °C [6]. An increase in the content of the eutectic alloy in aluminum leads to an acceleration of its interaction with water. To increase the activity of aluminum alloys with the Ga-In-Sn eutectic (5 wt.%), zinc (3 wt.%) was used in this work as an additional alloying additive.

The dependences of the volume of evolved hydrogen on the duration of hydrolysis of the following alloys: 95 wt.% Al + 5 wt.% Ga-In-Sn eutectics and 92 wt.% Al + 5 wt.% Ga-In-Sn eutectic + 3 wt.% Zn

at four temperatures are compared in Fig. 2. It can be seen that the introduction of zinc into such ESSs led to an acceleration of the release of hydrogen from water during their hydrolysis, particularly at low temperatures (25 and 40 °C). The effective constants of the hydrolysis rate of optimized alloys, calculated using the modified Prout-Tompkins equation, were 1.33, 1.75, 2.19, and 2.58 min^{-1} at temperatures of 25, 40, 55, and 70 °C, respectively. The temperature dependence of the effective rate constant was used to calculate the effective activation energy of the process. It was 12.6 $kJ \cdot mol^{-1}$ and indicates a diffuse control of the rate of hydrolysis [7]. From Fig. 2, it also follows that an increase in temperature led to a sharp increase in the rate of hydrogen evolution during the hydrolysis of the studied alloys.

Activated aluminum powders PA-4 and ASD-1 were also used as ESSs in the hydrogen generator of the hydrolysis type. They were mechanochemically activated by the eutectic Ga-In-Sn alloy (5 wt.%) in a planetary ball mill with steel balls for 1 (PA- 4) or 4 (ASD-1) hours at a rotation speed of 400 rpm/min in a ceramic mortar manually. As a result of activation, the alloys of the aluminum with alloying elements were formed on the surface of the grains of aluminum powders, which made possible the interaction of aluminum with water. It was found that some part of the powders activated in the mill formed lumps, which, according to data obtained using an EVO 40XVP scanning electron microscope with an INCA Energy microanalysis system, was enriched by the Ga-In-Sn eutectic ($\gg$ 5 wt.%) localized on the surface of aluminum grains. Powder grains, which were not included in the composition of lumps, had an insignificant amount of eutectic alloy on their surface ($\ll$ 5 wt.%).

The regularities of hydrolysis of the obtained powders at 25 °C were investigated by periodically measuring the volume of hydrogen released during hydrolysis in a volumetric setup. It was found that the mechanochemical activation of aluminum powders with the Ga-In-Sn eutectic (5 wt.%) in a planetary ball mill and in a ceramic mortar makes it possible to obtain materials capable of releasing hydrogen from water with a high rate at a temperature of 25 °C, but the distribution of the eutectic alloy in materials obtained in mill is very non-uniform. The amount of generated hydrogen is sufficient to power the fuel cells or their

batteries and to ensure the operation of an autonomous power source. The design of the hydrogen generator is proposed.

Based on the results of the performed studies, samples of low-temperature hydrogen-air fuel cells and their batteries were developed, which included high-performance membrane-electrode blocks of a new generation. The necessary components (parts of the body of the combined fuel cell, hermetic gaskets, membrane-electrode blocks) of the autonomous power supply were manufactured. As a result of the combination of fuel cells and a hydrogen generator of a hydrolysis type, an autonomous power supply was created in which hydrogen, produced in the generator as a result of the interaction of Al-based ESSs with water, feeds the fuel cells. The scheme of the developed autonomous charger based on fuel cells and an alumohydrogen generator is shown in Fig. 3.

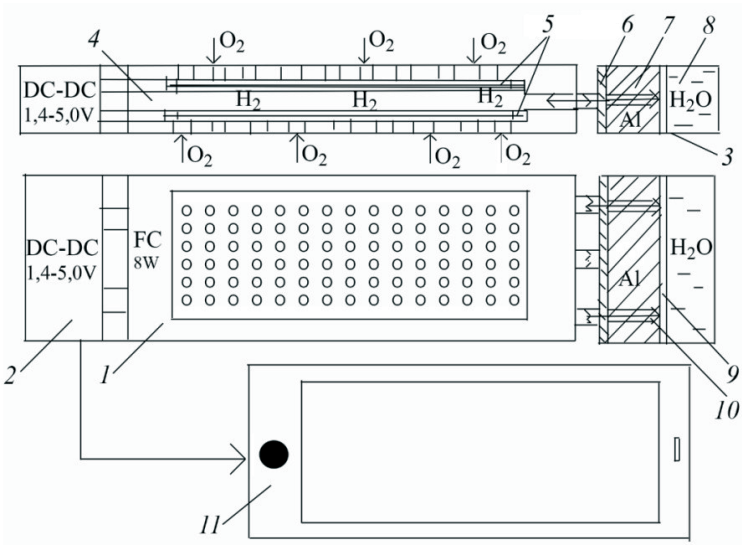

Fig. 3. Scheme of an autonomous charger based on fuel cells and an alumohydrogen generator: combined fuel cell (*1*); DC-DC voltage converter (*2*); hydrolysis-type hydrogen generator (*3*); hydrogen cell (*4*); membrane-electrode blocks (*5*); water-retaining separator (*6*); activated aluminum powder (*7*); container with water (*8*); porous membrane (*9*); activating needle (*10*); energy consumption device, e.g., smartphone (*11*)

The results of this work can find application in the creation of energy storage substances for use in highly efficient hydrolysis-type hydrogen generators for various purposes, including supplying hydrogen to fuel cells. The closest analogues of the developed autonomous charger based on an alumohydrogen generator and fuel cells with a power of 5-10 W are: MiniPAK/Horizon Fuel Cell (2.5 W, fuel – hydrogen, cartridge), Dynario™ Toshiba (5 W, fuel – methanol, cartridge), HandyPower (10 W, fuel – hydrogen obtained as a result of hydrolysis of activated aluminum, cartridge). The level of technological readiness of the development is IRL3, TRL4. The development is ready for the customer to issue a specific performance specification.

Intellectual property: Vernadsky Institute of General and Inorganic Chemistry, NAS of Ukraine, Palladina Prospekt, 32/34, Kyiv, Ukraine, 03142.

Conclusions

New methods for the synthesis of platinum-containing nanodispersed electrocatalysts immobilized on Vulcan XC-72 carbon black for hydrogen-ear fuel cells were developed, and anodic and cathodic Pt(40 %)/XC72 electrocatalysts were synthesized. The efficient catalytic inks were developed for applying catalysts onto gas diffusion layers formed on a proton-exchange membrane. The composition of aluminum based ESSs were optimized for the release of hydrogen from water in an alumohydrogen generator at ambient temperature and the design of such generator is proposed. The autonomous power supply has been developed based on the hydrogen generator of hydrolysis type and portable battery of hydrogen-air fuel cells.

The main publications in the frame of the project “Autonomous power supply based on fuel cells and alumohydrogen generator”:

1. F.D. Manilevich, Yu.K. Pirskyy, A.V. Kutsyi, B.I. Danil’tsev. Regularities of hydrolysis of aluminum activated by Ga-In-Sn eutectic alloy and zinc. *Ukr. Chem. Journal*, 2020, vol.86(2), pp. 63-77. (in Ukrainian)
https://doi.org/10.33609/0041-6045.86.2.2020.63-77

2. F.D. Manilevich, Yu.K. Pirskyy, B.I. Danil’tsev, A.V. Kutsyi, V.A. Yartys. Studies of the hydrolysis of aluminum activated by additions of Ga-In-Sn eutectic alloy, bismuth or antimony. *Materials Science*, 2020, vol.55, pp. 536-547.
https://doi.org/10.1007/s11003-020-00336-x
3. Yu.K. Pirskyy, F.D. Manilevich, T.M. Panchyshyn, Ya.V. Kolosovskiy, O.G. Alabut. Effect of polyvinylpyrrolidone on the synthesis and catalytic properties of platinum-containing oxygen electroreduction catalysts, *Ukr. Chem. Journal*, 2020, vol.86(7), pp. 53-64. (in Ukrainian).
https://doi.org/10.33609/2708-129X.86.7.2020.53-64
4. F.D. Manilevich, Yu.K. Pirskyy, A.V. Kutsyi. Promising hydrolytic methods of hydrogen generation for fuel cells // In: Electrochemistry of today: achievements, problems and prospects. - Kyiv: MPBP "Gordon", 2021, pp. 167-168. (in Ukrainian) https://doi.org/10.33609/978-966-8398-64-3.01.2021.1-191
5. Yu.K. Pirskyy, F.D. Manilevich, A.V. Kutsyi. Autonomous power supply based on fuel cell battery and hydrolysis type hydrogen generator // In: Electrochemistry of today: achievements, problems and prospects. - Kyiv: MPBP "Gordon", 2021, pp. 70-71. (in Ukrainian). https:// doi.org/10.33609/978-966-8398-64-3.01.2021.1-191

References

[1] Kozin L.H., Volkov S.V., Skryptun I.N. *Modern Hydrogen Energetics and Ecology*. K.: Akademperiodyka, 2019. 364 p.
[2] Debe M.K. Electrocatalyst approaches and challenges for automotive fuel cells. *Nature,* 2012, vol. 486, pp. 43–51.
[3] Pengtang Wang, Qi Shao, Xiaoqing Huang. Updating Pt-based electrocatalysts for practical fuel cells, *Journal Joule,* 2018, vol. 2, pp. 2511–2518.
[4] Chaojie Song, Jiujun Zhang. *Electrocatalytic Oxygen Reduction Reaction. PEM Fuel Cell Electrocatalysts and Catalyst Layers*, London: Springer, 2008, pp. 89-134.
[5] Pirskyy Yu.K., Manilevich F.D., Panchyshyn T.M., Kolosovskyi Ya.V., Alabut A.G. Effect of polyvinylpyrrolidone on the synthesis and

catalytic properties of platinum-containing oxygen electroreduction catalysts. *Ukr. Khim. Zh.,* 2020, vol. 86, No. 7, pp. 53-64.
[6] Manilevich F.D., Kozin L.H., Danil’tsev B.I., Kutsyi A.V., Pirskyy Yu.K. Regularities of hydrolysis of aluminum activated by eutectic alloy gallium,indium and tin. *Ukr. Khim. Zh.,* 2017, vol. 83, No. 7, pp. 51-59.
[7] Manilevich F.D., Pirskyy Yu.K., Kutsyi A.V., Danil’tsev B.I. Regularities of hydrolysis of aluminum activated by Ga-In-Sn eutectic alloy and zinc, *Ukr. Khim. Zh.* , 2020, vol. 86, No. 2, pp. 63-77.

Structural, impedance and electron-microscopic studies of multilayer systems for low-temperature (600° C) fuel cell

O. V'yunov[1], L. Kovalenko[1], O. Yanchevskii[1], I. Polishko [2], S. Ivanchenko [2], N.Lysunenko [2], D. Brodnikovskyi[2], V. Chedryk[3], I. Brodnikovska[2], O. Vasylyev[2]

[1]*Vernadsky Institute of General and Inorganic Chemistry, NASU, Kyiv, Ukraine*
[2]*Frantsevich Institute for Problems of Materials Science NASU, Kyiv, Ukraine*
[3]*Pisarzhevsky Institute of Physical Chemistry NASU, Kyiv, Ukraine*

Introduction

The creation of ceramic oxide fuel cells based on multilayer systems due to high efficiency, compactness and environmental friendliness is promising. The use of electrolyte, which has a high conductivity in oxygen, reduces ohmic losses, which can significantly increase the specific power of oxide fuel cells. Therefore, as a solid electrolyte, it is promising to use a zirconium matrix ZrO_2, stabilized by complex oxides of scandium (III) and cerium (IV), which are characterized by high oxygen conductivity. At the same time, the method of synthesis of powders of stabilized zirconium dioxide affects the electrophysical properties of the prepared electrolyte.

The main aim of the project is the development of preparation technology and structural, impedance and electron microscopic studies of multilayer systems based on thick films for low-temperature (600°C) fuel cell.

Thick films of electrolyte $ZrO_2 – Sc_2O_3 – CeO_2$ and ZrO_2-Y_2O_3 were prepared by tape casting of a suspension comprising organic (polyvinyl butyral, polyphthalate) and inorganic (weakly agglomerated nanopowders of appropriate compositions) components. The thick films were applied on a polymeric substrate with a hydrophobic layer, which allowed to cut loose the films after evaporation of solvents. The Film Applicator and Drying Time Recorder COATMASTER 510 equipped with a special knife was used for casting thick electrolyte films. Ultra-fast heating (thermal shock) from 20 to 500^{o}C with subsequent slow (1^{o}C / min) heating to the final synthesis temperature of 1200 - 1300^{o}C allowed significantly increasing the density of thick films.

Fig.1.Device for films deposition

Fig.2.Tapes of thick anode and electrolyte films

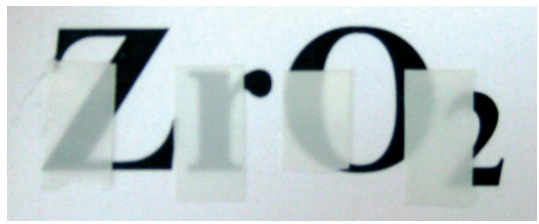

Fig.3.Films of different thickness: 80 μm, 160 μm and 320 μm (from left to right)

Nanopowders ZrO_2-Sc_2O_3-CeO_2 were synthesized by precipitation from aqueous solutions. $ZrCl_4$, $Sc(NO_3)_3$, $Ce(NO_3)_3$ and NH_4OH were used as starting reagents. It is established that when using sequential deposition at optimal pH values, weakly agglomerated nanopowders (Kfiltp = $(0.8 \div 1.5) \cdot 10^{-5}$ cm/s) are formed, which are easily washed, in contrast to sediments of the same composition, which are obtained by co-deposition (Kiltr = $(2 \div 5) \cdot (10^{-7}$ cm/s).

The synthesis of the ZrO_2-Sc_2O_3-CeO_2 system was also performed by the hydrothermal method. The autoclave was heated to 250°C for holding time 24 hours at pressure 20MPa. The starting reagents were the same as in the method of precipitation from solutions. Ceramic samples were obtained from hydrothermal powders. Sintering at the temperatures of 1390-1400°C / 10-12 h resulted in single-phase ceramics with a cubic structure of zirconium dioxide.

Brief description

The work was performed together with the staff of the laboratory of fuel cells of Frantsevich Institute for Problems of Materials Science of NAS of Ukraine.

The multilayered systems consisting from porous thick films of anode and cathode materials, which are connected through a dense electrolyte film, were developed by the method of tape casting. The chemical composition was optimized and the chemical stability of the multilayer systems was studied.

The multilayer system of dense thick films ZrO_2 - Sc_2O_3 - CeO_2 and ZrO_2-Y_2O_3 with different thicknesses (80-320 μm), prepared by the method of tape casting, were synthesised. Structural, impedance and electron-microscopic studies of multilayer, dense, thick films with different thicknesses (80-320 μm) were performed. It was established that the combination of two different methods (tape casting and lamination with subsequent heat treatment) allows the preparation of a multilayer system of dense thick films ZrO_2-Y_2O_3, which consists of mechanically inseparable thin films. It was found that at a temperature of 600 °C, the

increase in ZrO_2-Y_2O_3 film thickness results in an increase in conductivity, and a decrease in activation energy. Namely, the conductivity of film with a thickness of 80 μm is equal $8.5 \cdot 10^{-3}$ S/cm (1.04 eV), and for the film with a thickness of 320 μm corresponding value is equal $5.5 \cdot 10^{-3}$ S/cm (1.0 eV). The film with a thickness of 320 μm is not inferior in conductivity to the ceramic sample of the same composition (at 600 °C the conductivity of the ceramic sample is $5.2 \cdot 10^{-3}$ S/cm (0.98 eV), and the mechanical strength of the film is sufficient for subsequent deposition of layers of anode and cathode materials. It was established that multilayer, dense, thick films of ZrO_2 - Sc_2O_3 - CeO_2 composition are characterized by high oxygen conductivity, namely: $1.8 \cdot 10^{-2}$ S/cm at 600 °C and $9 \cdot 10^{-2}$ S/cm at 700 ºC, while the electron conductivity is 4 orders of magnitude lower compared to the oxygen conductivity.

A methodology for the preparation of ZrO_2-Y_2O_3-Ce_2O_3 powders by various methods (hydrothermal method and precipitation method) has been developed and electrophysical properties of ceramic samples based on them have been investigated. It was established that at a sequential deposition at optimal pH values, weakly agglomerated nanopowders are formed, which are easily filtered, in contrast to precipitates of the same composition, which are prepared by the method of co-deposition. Complex impedance investigations of ceramic samples in a wide frequency range (1 Hz – 32 MHz) and temperature interval (20-800 ºC) showed that the ceramics of the composition ZrO_2-Y_2O_3-Ce_2O_3 has high oxygen conductivity, namely, for deposition method is $1.1 \cdot 10^{-3}$ S/cm (at 600 °C), $4 \cdot 10^{-3}$ S/cm (at 700 ºC), $1.2 \cdot 10^{-2}$ S/cm (at 800 ºC), and activation energy is 1.015 eV; for the hydrothermal method is $9 \cdot 10^{-4}$ S/cm (at 600°C), $3.4 \cdot 10^{-3}$ S/cm (at 700 ºC), $1.2 \cdot 10^{-2}$ S/cm (at 800 ºC), and activation energy is 1.07eV. For both methods, the electron conductivity of ZrO_2-Y_2O_3-Ce_2O_3 ceramics obtained is 4 orders of magnitude lower compared to oxygen conductivity.

The low-temperature (600 °C) fuel cell based on the investigated multilayer systems was developed and its electrical and physical properties were studied.

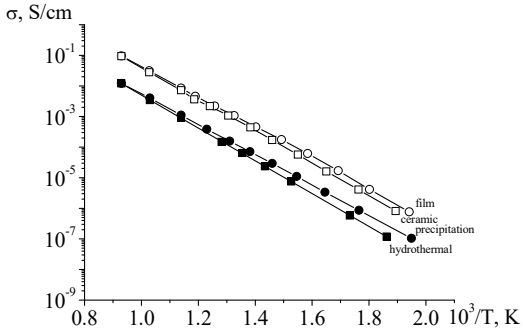

Fig.4. Temperature dependence of specific conductivity of ceramics ZrO_2-Y_2O_3 prepared by different methods.

Table 1. Characteristics of ZrO_2-Y_2O_3 samples produced by different methods

Method of preparation ZrO_2-Y_2O_3	Activation energy, eV	Conductivity at 600°C, S/cm	Conductivity at 700°C, S/cm	Conductivity at 800°C, S/cm
Hydrothermal	1.07	$9 \cdot 10^{-4}$	$3.4 \cdot 10^{-3}$	$1.2 \cdot 10^{-2}$
Precipitation	1.015	$1.1 \cdot 10^{-3}$	$4.0 \cdot 10^{-3}$	$1.2 \cdot 10^{-2}$
Film	1.03	$8.5 \cdot 10^{-3}$	$3.1 \cdot 10^{-2}$	$9.5 \cdot 10^{-2}$
Ceramic	0.98	$5.2 \cdot 10^{-3}$	$2.7 \cdot 10^{-2}$	$9.3 \cdot 10^{-2}$

Area of applications

Low-temperature (600 °C) fuel cells, oxygen sensors.

Comparative evaluation of the obtained results

Produced low-temperature (600 °C) fuel cell has higher characteristics compared to a commercial analogue. Thus, when the fuel cell uses a model fuel gas, the maximum specific power of the developed

one demonstrated 4.2 mW / cm^2, while of commercial one demonstrated only 2.8 mW/cm^2.

Level of technological readiness

The technology for preparation of vacuum-dense polycrystalline bulk materials, gas-tight thin and thick films with a high level of oxygen conductivity in the region of average temperatures (500-600 °C) based on zirconium oxide with a structure of cubic fluorite, stabilized with complex scandium-containing additives was developed. A low-temperature (600 °C) fuel cell has been manufactured, which has the highest characteristics compared with its commercial counterpart.

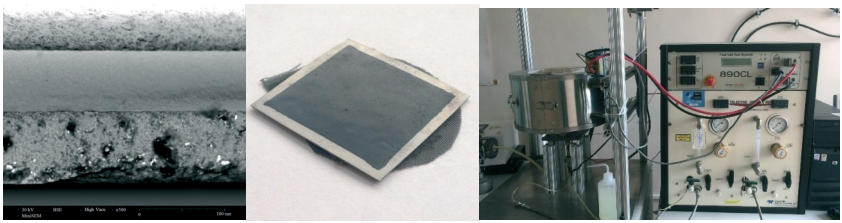

Fig.5. Photo and photomicrograph of a fuel cell made by tape casting; photo of the universal stand for testing fuel cells Scribner Teledyne Medusa RD 890CL

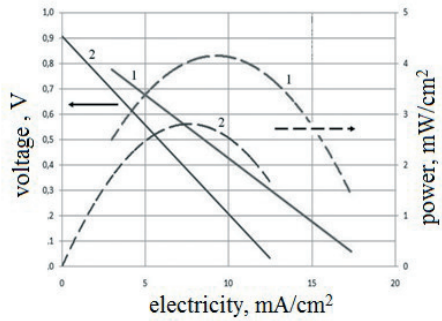

Fig.6. Comparison of the electrical properties of the prepared fuel cell (1) with a commercial analogue (2); devices were tested under the same conditions.

List of the main publications within the project “Elaboration of tape-casting technique for ceramic fuel cell production”:

1. Y.Brodnikovskyi, N. McDonald , D. Brodnikovskyi, I. Brodnikovska, M. Brychevskyi, L. Kovalenko, O. Vasylyev, A.Belous, R. Steinberger-Wilckens Properties of 10Sc1CeSZ-3.5YSZ (33-, 40-, 50-wt.%) Composite Ceramics for SOFC Application. *Materials Today*: *Proceedings,* 2019, vol.6, pp. 26-35.
https://doi.org/10.1016/j.matpr.2018.10.071

2. I. Polishko, S. Ivanchenko., R. Horda, Y. Brodnikovskyi, N. Lysunenko, L. Kovalenko Tape casted SOFC based on Ukrainian 8YSZ powder, *Materials Today*: *Proceedings*, 2019, vol.6, pp. 237–241.
https://doi.org/10.1016/j.matpr.2018.10.100

3. Y.M.Ostroverkh , I.Polishko , D.Brodnikovskiy , L.L.Kovalenko , A.Samelyuk , A.Vasilev , A.Ostroverh. Mechanical behavior and electrical conductivity of zinc-oxide ceramics, *Uspikhi materialoznavstva*, 2020, No,1, pp. 46-55.

4. I.A.Rusetskii, L. L. Kovalenko, I. A. Slobodyanyuk, M. O. Danilov, S. S. Fomanyuk, V. O. Smilyk, A. G. Belous, G.Ya. Kolbasov. Photoelectrochemical systems for hydrogen evolution using ion-conducting membranes. *ECS Trans*, 2020, vol. 99, pp. 221-230. http://doi.org/10.1149/09901.0221ecst

5. M.A. Gumenna, N.S. Klimenko, A.V. Stryutsky, L.L. Kovalenko, V.V. Kravchenko, A.V. Shevchuk, V.V. Shevchenko. Polymeric proton exchange media with ionic bonds in the main chain of the polymer. *Dopov. Nac. akad. nauk Ukr.* 2020, No.12, pp. 60-66.(in Ukrainian)
http://doi.org/10.15407/dopovidi2020.12.060

Development of tape casting technique regimes for manufacturing of solid oxide fuel cells

Y. Brodnikovskyi[1], O. Vasylyev[1], I. Polishko[1], N. Lysynenko[1], L. Kovalenko[2], S. Ivanchenko[1], D. Brodnikovskyi[1], V. Chedryk[3], I. Brodnikovska[1], R. Horda[4], M. Smyrnova-Zamkova[1], I. Marek[1], O. Myslyvchenko[1], A. Ragulya[1], S. Orlyk[3], A. Belous[2], V. Vereshchak[5], A. Nosyk[6].

[1] *Frantsevich Institute for Problems of Materials Science,NASU, Kyiv,Ukraine*

[2] *Vernadsky Institute of General and Inorganic Chemistry, NASU, Kyiv, Ukraine* [3] *Pisarzhevsky Institute of Physical Chemistry, NASU, Kyiv, Ukraine*

[4] *Ovcharenko Institute of Biocolloidal Chemistry, NASU, Kyiv,Ukraine*

[5] *Ukrainian State University of Chemical Technology, Kyiv, Ukraine*

[6] *Zirconia Ukraine Ltd., Ukraine*

Introduction

Fuel Cells (FC) are devices, which directly convert chemical energy of gaseous fuel and oxidant into electrical energy, heat and water. Solid oxide fuel cells are the most promising class of fuel cells due to their highest efficiency among other fuel cell types, feasibility of the fuel choice (C_mH_n, CO, H_2 etc.) and have no needs in noble materials for catalyst application. Solid Oxide Fuel Cells (SOFC) are power generators that can convert the chemical energy of a fuel gas into electricity and heat with the highest efficiency and low environmental pollution (Fig. 1).

Zirconia is one of the main SOFC component: it is part of the porous anode, dense electrolyte membrane, and sometimes – a part of porous cathode. Porosity of electrodes is required for pathways of gas supply, removing reaction byproducts, and also optimizing the catalytic sites providing the triple phase reactant boundary between electrolyte, electron conducting phase of the electrodes, and gas phase.

Zirconia, stabilized in the cubic phase and referred to as fully stabilized zirconia (FSZ), is the most developed, widely used electrolyte material for SOFC manufacturing due to its electrical properties, chemical and mechanical stability in both oxidizing and reducing

atmospheres at operating temperatures. Generally, for SOFC electrolytes, the zirconia is stabilized with trivalent dopants (Y^{3+}, Sc^{3+}, Gd^{3+}, Sm^{3+} etc.) in order to create oxygen vacancies in the zirconia crystal lattice. Zirconia stabilized with 8-mol. % Y_2O_3 (8YSZ) is the state-of-the-art electrolyte material for SOFC applications. Due to this 8YSZ was used for development of the laboratory type casting technique for SOFC

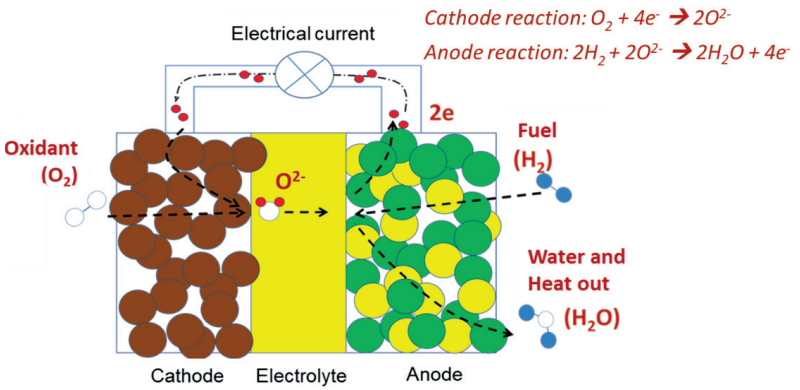

production.

Fig. 1. Principal scheme of SOFC operation.

The main aim of the project is the development of laboratory tape casting technique to produce solid oxide fuel cells based on zirconia powder (8YSZ) developed and produced in Ukraine. The main project motivations are the following:

- Ukraine has one of the largest zircon-sand deposits in the World – the basic raw material for production of stabilized zirconia powders.
- The tape casting technique is considered as the most promising for the SOFC production due to its relative simplicity and high productivity. This method ensures a relatively easy transition from laboratory technology to industrial production of SOFC.
- Elaborated tape casting techniques are the basement for the creation of industrial manufacturing of SOFC energy systems in Ukraine.

Development of stabilized zirconia powders

The laboratory method for production of zirconia powders with different stabilizers (8YSZ, 8Ce2YSZ, 1Ce10ScSZ and others) was developed. Typical morphology of the powders is shown in Fig. 2. The developed zirconia powders were produced in necessary quantities to elaborate the tape casting technique for production of the SOFC anode and electrolyte films. Also such powders used for preparation of the ceramic samples to study their electrical and mechanical properties.

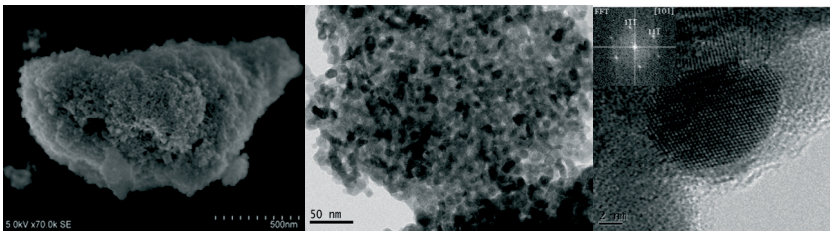

Fig. 2. TEM images of the synthesized zirconia powders.

The tape-casting regimes for SOFC component production

Tape casting is an important technology, which allows to manufacture thin elastic tapes of high density with predetermined thickness and uniform distribution of powder in a volume of the tape. It is possible to produce thin tapes of all materials from their powders using of comparatively simple equipment within such technology. (Fig. 3). The method is widely used as a basis for manufacturing of many modern electronic devices and permanently upgraded. For the last time, SOFC manufacturing by the tape casting technique became an important task due to its high performance, low cost and environmental friendliness.

To obtain high-quality films some technical and scientific problems must be solved. The tapes should be of different thickness and porosity with uniform powder distribution by volume. Furthermore such tapes must be defect-free with low surface roughness. The influence of casting conditions and rheological behavior of suspension on tapes properties must be studied deeply in order to predict these properties before casting. Traditional approaches to determining the influence of casting conditions on tape properties should be reviewed and supplemented by taking into account rheological parameters such as shear rate and shear stress. Particular attention should be paid to the mechanisms of defects

formation in tapes (Fig. 3b) and special methods to avoid defect appearance should be suggested. More attention must be paid to the analysis of the technology of multilayer ceramic packages assembling because the SOFC lifetime depends on the package's integrity.

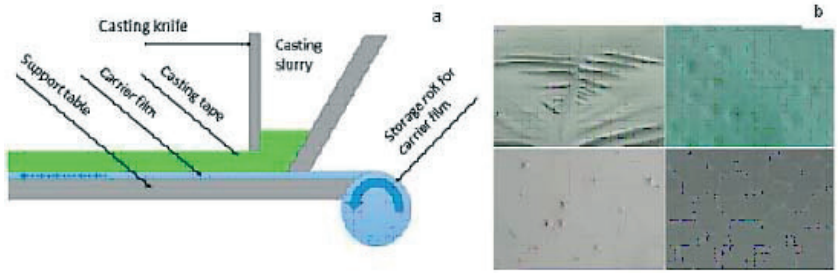

Fig. 3. Principal scheme of tape casting technique (a) and CEM images of examples of the casted tape defects (b).

As a result of the work, suspensions with an optimal component composition for manufacturing of non-defect types for SOFC anode and electrolyte were formulated. It was found that increasing the viscosity of the suspensions will result in thicker and stronger tapes, however, high viscosity creates difficulty in mixing and increases the suspension irretrievable losses. The control of anode and electrolyte film thickness could be achieved by step-by-step lamination of thin films. The obtained tapes were successfully laminated and sintered into an SOFC (Fig. 4).

Influence of the thickness of electrolyte samples on their electrical properties were studied

Electrolyte films with different thickness were manufactured. The thickness of the films was controlled by assembling of different amount of the tapes in one set for further lamination and sintering at 1400 °C. Also, bulk ceramic samples were produced. In that case powders were uniaxially pressed at 30 MPa into disc shaped samples with disc diameter of 20 mm and its thickness of 1.2 mm . The samples were sintered at temperature 1400 °C for 2 h in air environment. The electrical impedance of the manufactured zirconia samples was measured as a function of AC frequency. Measurements were performed using Solartron 1260 impedance/gain-phase analyzer within the frequency range 10^{-2}-10^{6} Hz at 600 ºC in air. The electrodes of the samples were prepared using

silver paste. In order to compare conductivities of ceramic samples with different porosity, measured total conductivity was normalized by porosity using V.I. Odelevsky’s formula for conductive properties of material with the porosity between 0 and 66.7%. Ceramic samples made from 8Ce2YSZ powder had porosity about 8 %, for all other samples corresponding values were less than 2 %.

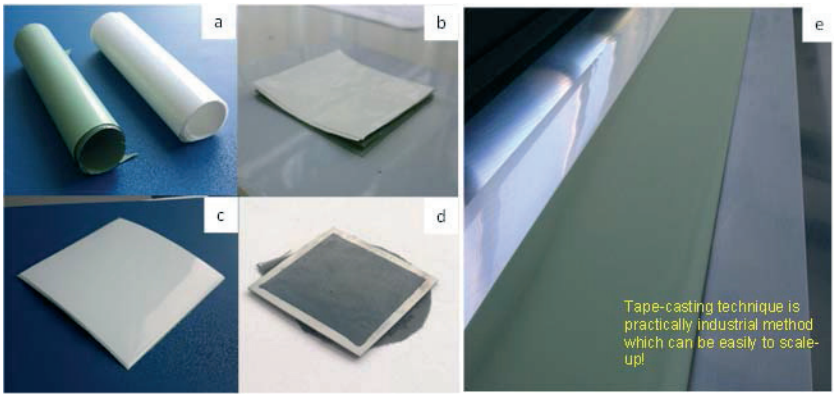

Fig. 4. Type casted films of anode (green) and electrolyte (white) (a); cut anode and electrolyte types into square-shaped samples for further half-cell preparation (b); laminated types in half-cell (c); sintered SOFC (d); drying of just casted anode type (e).

Obtained data on electrical conductivity of the stabilized zirconia samples are summarized in Table 1. It is clear that thickness of the zirconia electrolyte samples is one of the key factors, which influence on its electrical conductivity. The difference of electrical conductivity of the 8YSZ type casted films of 80 μm thickness is a little more than a half higher than bulk ceramic samples obtained by conventional powder metallurgy method. Moreover, the values of electrical conductivity are practically equal for both tape casted films of 320 μm thickness and bulk ceramic samples with a thickness about 1 mm. Probably, the dependence of electrolyte films electrical conductivity on the thickness can be explained by the special properties of their structure, as a result of combining process of several thin tape layers into one thick film.

Also, it was found that the developed 8Ce2YSZ material is promising for SOFC anode application; it can replace 3YSZ material that is widely used today. The manufactured 8Ce2YSZ ceramic samples demonstrate relatively high values of electrical conductivity at low temperatures (600° C) and similar level of strength in comparison with 3YSZ samples, 542 and 577 MPa, respectively. Moreover, the presence of cerium oxide under reduction media (SOFC anode operating conditions) can improve spreading the anode reaction zone due to the appearance of the electronic component of conductivity.

Table 1. Electrical conductivity of stabilized zirconia taped casted films and pressed ceramic samples

Sample/ thickness, μm	Electrical conductivity at 600°C, S/cm	Activation energy, eB
8YSZ Film / 80	8.5×10^{-3}	1.04
8YSZ Film / 167	7.1×10^{-3}	1.03
8YSZ Film / 252	6.5×10^{-3}	1.015
8YSZ Film / 320	5.8×10^{-3}	1.0
8YSZ Ceramic sample / 1 mm	5.2×10^{-3}	0.98
3YSZ Ceramic sample / 1 mm	1.0×10^{-3}	–
8Ce2YSZ Ceramic sample / 1 mm	1.3×10^{-3}	1.02

Comparison of the developed SOFC with commercial one

The tape-casted SOFC (electrolyte 8YSZ, anode NiO – 8YSZ, cathode LSM – 8YSZ) made using elaborated laboratory technology and commercially available anode-supported SOFC (electrolyte 8YSZ, anode NiO – 8YSZ, cathode LSM – 8YSZ) were tested with the stand for measuring of fuel cells electrical properties ("Scribner Teledyne Medusa RD 890CL" USA), at the same conditions. The tests of SOFC were performed at 800 °C, and fuel mixture 5 % H_2 – 95 % Ar and air were fed into the anode and the cathode, respectively.

The results of this study are shown in Fig. 5. The SOFC developed demonstrates much higher level of power density (4.2 mW/cm^2) in comparison with the commercial one (2.8 mW/cm^2) at the same testing conditions (800 °C, 5 % H_2+Ar, air).

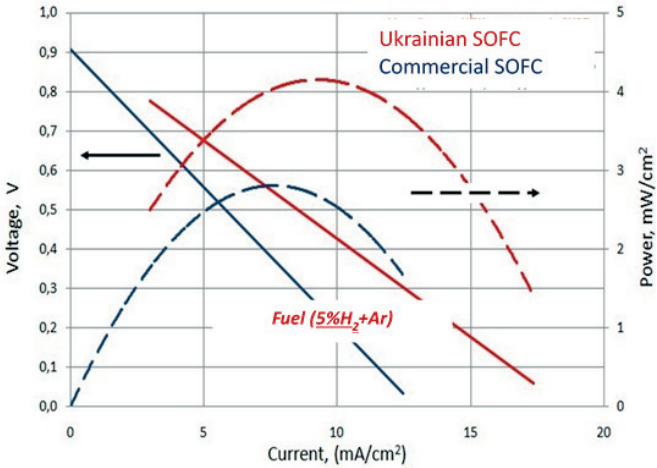

Fig. 5. Comparison of electrical properties of developed tape-casted SOFC and commercial one at the same testing conditions (800 °C, 5 % H_2+Ar, air).

Conclusions

A lot of different studies focused on the development of new promising materials for SOFC application have been already done. Despite that, zirconia-based materials remain the most common in use because they meet many requirements and have relatively low cost. Currently, progress in development of SOFC is primarily concentrated on the development and implementation of new methods of SOFCs production to improve their structure and optimize properties of its components, rather than through the introduction of new materials.

The next stage in the introduction of hydrogen energy and fuel cells in the economy of Ukraine should be the creation and testing of pilot technologies for production of SOFC combine heat and power (CHP) systems. Extensive demonstration activities should attract new investment in this field. The main attention should be focused primarily on the

creation of pilot productions of stabilized zirconia powders and fuel cells from them and creation of SOFC-CHP systems prototypes.

Today, there is an intellectual and raw material basis for the organization of high-tech production of power generation facilities based on SOFC in Ukraine. Production and implementation of fuel cell technology in Ukraine can make a precedent for the "economic miracle" that took place in Germany, Japan and Korea due to high-tech productions.

List of the main publications within the project “Elaboration of tape-casting technique for ceramic fuel cell production”:

1. I. Polishko, S. Ivanchenko., R. Horda, Y. Brodnikovskyi, N. Lysunenko, L. Kovalenko Tape casted SOFC based on Ukrainian 8YSZ powder, *Materials Today*: *Proceedings*, 2019, vol.6, pp. 237–241. https://doi.org/10.1016/j.matpr.2018.10.100

2. Y.Brodnikovskyi, N. McDonald , D. Brodnikovskyi, I. Brodnikovska, M. Brychevskyi, L. Kovalenko, O. Vasylyev, A.Belous, R. Steinberger-Wilckens Properties of 10Sc1CeSZ-3.5YSZ (33-, 40-, 50-wt.%) Composite Ceramics for SOFC Application. *Materials Today*: *Proceedings,* 2019, vol.6, pp. 26-35.
https://doi.org/10.1016/j.matpr.2018.10.071

3. I.V. Brodnikovska, Y.M. Brodnikovskyi, M.M. Brychevskyi, O.D. Vasylyev. Joint Impedance Spectroscopy analysis of 10Sc1CeSZ and 8YSZ Solid Electrolytes for SOFC, *Powder Metallurgy and Metal Ceramics,* 2019, vol.57, issue 11–12, pp. 723–730.
https://doi.org/10.1007/s11106-019-00037-4

4. Y.M.Ostroverkh , I.Polishko , D.Brodnikovskiy , L.L.Kovalenko , A.Samelyuk , A.Vasilev , A.Ostroverh. Mechanical behavior and electrical conductivity of zinc-oxide ceramics, *Uspikhi materialoznavstva*, 2020, No,1, pp. 46-55.
https://doi.org/10.15407/materials2020.01.046

5. N.O.Lysunenko, Y.M. Є.M. Brodnikovskyi , V.M.Mokiychyk, I.O.Polishko, D. M. Brodnikovskyi, V.I.Chedryk, O.D. Vasylyev. Influence of hydrogen concentrations in Ar–H2 mixture on electrical properties of SOFC, *Poroshkova metalurgia*, 2021, No.5-6, pp.118-127.

Conferences:

1. O. Vasylyev, Y Brodnikovskyi, I. Polishko et. al. From powder to Power. *International conference on the Cooperation and Integration of Industry, Education, Research and Application*. 11-14 July, Nanchang, Jiangxi, China, 2019

2. O.Vasylyev, Y Brodnikovskyi, I.Polishko et. al. *Advanced Technologies for Energy Application China (Ningbo) International Advanced Material, Technology and Industry Exposition* 28-30 August, Ningbo, China, 2019

3. I.Polishko, Y. Brodnikovskyi, N. McDonald , D. Brodnikovskyi, I. Brodnikovska, M. Brychevskyi, N. Lysunenko, L. Kovalenko, O. Vasylyev, A. Belous, R. Steinberger-Wilckens Properties of advanced yttria- and scandia-stabilized zirconia composite for solid oxide fuel cell application. *13th Conference for Young Scientists in Ceramics, CYSC-2019, Novi Sad, Serbia*, October 16-19, 2019, p. 112

4. O. Vasylyev, Y. Brodnikovskyi, I. Polishko, D. Brodnikovskyi, O. Ostash, V. Podhurska, B. Vasyliv. *Fuel Cell Energy Systems for Aviation International Symposium on Electric Aviation and Autonomous Systems; 2020 International Symposium on Aircraft Technology; MRO & Operations 2020 International Course on Unmanned Aerial Vehicle* 2020 22 - 24 September 2020 Kyiv, Ukraine / Online

5. Y .Brodnikovskyi, O. Vasylyev, I Polishko. et. al. Fuel Cell as a key technology for Hydrogen Energy. *International Conference on Industry-University-Research-Application Cooperation.* 28 July, Nanchang, Jiangxi, China, 2021 / On-line

Development of hybrid oxygen reduction electrocatalysts derived from nanostructured organic conjugated polymers or deep eutectic solvents for hydrogen-oxygen fuel cells

Ya. Kurys, O. Pariiska, D. Mazur, V. Koshechko, V. Pokhodenko

Pysarzhevsky Institute of Physical Chemistry, NASU, Kyiv, Ukraine

Oxygen reduction reaction (ORR) is an important electrochemical process usually realized for low-temperature fuel cells (FCs), but in that case in order to reduce ORR overpotential it is necessary to use electrocatalysts, usually based on platinum. The limited resources of Pt and its high cost make Pt catalysts one of the main barriers to the commercial mass market of such FCs. So, it is attractive to obtain highly active and stable ORR electrocatalysts, which do not contain precious metals. Metal-nitrogen-carbon composites (Fe-N-C, Co-N-C) obtained by pyrolysis of various nitrogen precursors, salts of the corresponding d-metal and nanosized carbon materials are considered as a possible alternative to platinum ORR electrocatalysts.[1-3]. Compared to iron-based analogs, Co-N-C catalysts are usually characterized by slightly less activity in ORR, but they are much more stable under the service conditions of real FCs [1]. At the same time, despite the progress made in the development of such catalysts, their functional characteristics (low stability or catalytic activity) need further improvement to meet the requirements of practical applications.

During the project implementation new effective precious metals free cobalt-nitrogen-carbon hybrid electrocatalysts for oxygen reduction, obtained by pyrolysis of cobalt-containing precursors based on nitrogen-containing conjugated polymers or deep eutectic solvents, have been developed. These catalysts are characterized by the potential where oxygen reduction starts (E_{onset}, vs. RHE) ~ 0.97-0.99 V in 1.0 M NaOH and 0.79- 0.81 V in 0.5 M H_2SO_4, by halfwave potential ($E_{1/2}$, vs. RHE) ~ 0.87-0.89 V (1.0 M NaOH) and 0.67-0.69 V (0.5 M H_2SO_4), as well as by high stability during long-term operation, and by resistance to carbon monoxide and methanol poisoning.

The main scientific results of the project are given below.

By pyrolysis of the system 2,6-diaminopyridine (monomer)/ammonium persulfate (oxidant) (instead of pre-synthesized poly-2,6-diaminopyridine) together with MultiLayer Graphene (MLG) and salt of Co (II), Co-N-C composite, containing the particles of cobalt sulfide (Co_9S_8/Co-N-C_{MLG}) was obtained. It was found that Co_9S_8/Co-N-C_{MLG} is characterized by higher ORR activity in comparison with analogue obtained on the basis of acetylene black – AB (Co_9S_8/Co-N-CAB) [4], which may be due to the dominance in the composition of such catalysts of different active sites (CoN_x, C/N_x, Co_9S_8), where adsorption, activation and catalytic transformations of O_2 take place. Based on the analysis of the calculated main parameters of ORR – E_{onset}, $E_{1/2}$, Tafel slope (b), number of electrons (n) and the percentage of electrons involved in the four-electron process (4e%), as well as the yield of hydrogen peroxide (H_2O_2%) (Table) – it was assumed that the reduction of oxygen on Co_9S_8/Co-N-C_{MLG} is mainly controlled by both charge transfer and migration of intermediates, while on Co_9S_8/Co-N-C_{AB} – by electrochemical stage of transfer of the first electron and adsorption of O_2 on active sites. Moreover, for both catalysts, the direct 4-electron reduction of oxygen to water is dominant, and a small contribution of the 2-electron process (~ 6%) decreases with increasing of overpotential. The obtained Co_9S_8/Co-N-C_{MLG} has a high tolerance to CO and methanol, which are able to poison ORR catalysts, in particular Pt-containing, in the service conditions of hydrogen and methanol FCs, which determines the prospects for its practical application.

Table. Electrochemical characteristics of Co_9S_8/Co-N-C_{MLG} and Co_9S_8/Co-N-C_{AB} catalysts in ORR, calculated based on RRDE data in different electrolytes [4].

Catalyst	E_{onset}, mV	$E_{1/2}$, mV	b, mV/decade	$\%H_2O_2$, %	n	4e %,
0.5 M H_2SO_4						
Co_9S_8/Co-N-C_{MLG}	775	680	71	6	3.9	94
Co_9S_8/Co-N-C_{AB}	720	500	158	16	3.7	84
0.1 M NaOH						
Co_9S_8/Co-N-C_{MLG}	900	830	71	6	3.9	94
Co_9S_8/Co-N-C_{AB}	900	840	64	4	3.9	95

In order to explain the contribution of Co_9S_8 to the electrocatalytic activity in the ORR of Co_9S_8/Co-N-C catalysts, the properties of Co_9S_8 (both in the individual state and deposited on Vulcan XC72 soot – Co_9S_8/C) in this process were investigated. It is shown that in contrast to Co_9S_8 itself, which is inactive in ORR in 0.5 M H_2SO_4 and 1.0 M NaOH, Co_9S_8/C has a sufficiently high ORR activity in the alkaline electrolyte, which does not exclude the contribution of cobalt sulfide as an active component of Co_9S_8/Co-N-C catalysts during their operation at high pH. It was found that the reduction of Co_9S_8 content in the Co_9S_8/Co-N-C catalysts obtained using poly-5-aminoindole, slightly affects the values of E_{onset} and $E_{1/2}$ in the alkaline electrolyte, but provides a higher limiting current density and lower H_2O_2 yield, which may be due to either a decrease in the degree of agglomeration of sulfide particles in the composite, or greater availability of CoN_x sites, which are likely to be more active in ORR compared to Co_9S_8. It is assumed that in the acid electrolyte Co_9S_8 particles in such hybrid materials only play the role of "spectator", without significantly affecting the performance of catalysts in ORR, which is provided by other active sites [5].

A convenient approach to the production of Co-N-C electrocatalysts based on PolyAniline (PAni) was suggested. The corresponding monomer, hydrogen peroxide, cobalt (II) salt and a catalytic amount of iron salt are using for the formation of a polymeric precursor composite which is subjected to the further carbonization. Such approach, on the one hand, excludes the stage of pre-obtaining of PAni, and on the other hand – avoids the formation of Co_9S8 nanoparticles in the composition of Co-N-C electrocatalysts during carbonization process, which may be promising for their use in acid electrolyte.

The possibility of effective replacement of traditional PAni by poly-o-aminobenzoic acid (PABA) in the creation of pyrolyzed Co-N-C electrocatalysts ORR is shown. Such possibility allows not to disturb the type of polymeric nitrogen source (because PABA undergoes decarboxylation with the formation of PAni already at ~ 200^o C), and also provides a more developed, porous catalyst structure due to CO_2 gassing in PABA decarboxylation process.

It is established that the use in the formation of Co-N-C catalyst of PAni, nanostructured using a "soft" template – β-cyclodextrin, allows to

increase the available for the electrolyte solution surface area of the catalyst, which determines its functional advantages over the composite, which is obtained on the basis of unstructured PAni.

It was shown, that carbonization of the phosphoric acid doped PAni together with the salt of Co (II) yielded carbon nanocomposites co-doped with cobalt, nitrogen and phosphorus with CoP (preferably) and Co_2P particles – CoP_x/Co-N,P-C, which are able to possess high ORR activity in acidic and alkaline electrolytes (Fig. 1). It was shown that H_3PO_4 in the structure of the polymer precursor can play the role not only of a source of phosphorus, but also of a pore-forming agent, which provides an increase in the electrochemically active surface area of the catalyst. A significant effect of the polymer doping method on the ORR activity of CoP_x/Co-N,P-C electrocatalysts formed with its participation was revealed. It is shown that the catalyst obtained using PAni doped with phosphoric acid during in situ polymerization provides higher values of E_{onset} and $E_{1/2}$ in the alkaline electrolyte, as well as lower yield of hydrogen peroxide compared to the analogue derived from emeraldine base doped with phosphoric acid.

By means of high-temperature treatment of Co (II) nitrate together with poly-3-aminophenylboronic acid (PAPBA) or boric acid doped PAni (PAni-B), as complex simultaneous sources of carbon, nitrogen and boron, new Co-N,B-C nanocomposites were obtained and their electrocatalytic properties in ORR were investigated. It was found that the catalyst obtained using PAni-B is characterized by a more positive value of E_{onset} compared to that formed on the basis of PAPBA (by 10 and 15 mV in 0.5 M H_2SO_4 and 1.0 M NaOH, respectively). It is shown that the reduction of oxygen on the Co-N,B-C catalyst obtained using PAni-B in both investigated electrolytes occurs mainly by a direct 4-electron mechanism (yield of hydrogen peroxide ~ 1%), and the value of b is ~ 150 and 60 mV/dec in acidic and alkaline environments, respectively.

For the first time, it was shown the possibility of using a Deep Eutectic Solvent (DES) based on 1-butyl-3-methylimidazolium chloride ([Bmim]Cl) and hydrated Co (II) nitrate as a source of nitrogen and cobalt to create highly efficient carbonized Co-N-C electrocatalysts toward ORR. Such catalysts are characterized in alkaline electrolyte by $E_{1/2}$ ~ 0.88-0.89 V (vs RHE), that is almost not inferior to that for Pt/C (Fig. 2) [6].

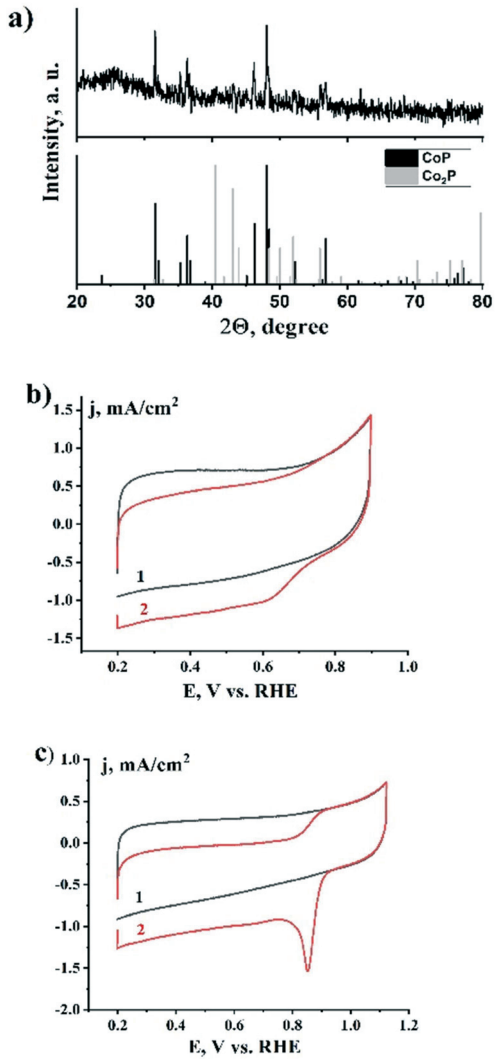

Fig. 1. XRD-patterns of CoP_x/Co-N,P-C, CoP (PDF № 29-0497) and Co_2P (PDF № 06-0595) (a); cyclic voltammograms CoP_x/Co-N,P-C in deaerated (1) and saturated with oxygen (2) 0.5 M H_2SO_4 (b) and 1.0 M NaOH (c).

It was found that ORR on obtained electrocatalysts passes mainly by a 4-electron mechanism, and the yield of H_2O_2, which is an undesirable intermediate in hydrogen FCs, does not exceed 15%. One of the reasons for the high performance of electrocatalysts may be the efficient formation of active CoN_x sites in them, which is facilitated by the fact that cobalt, forming a strong bond with the ligand, is uniformly distributed in DES.

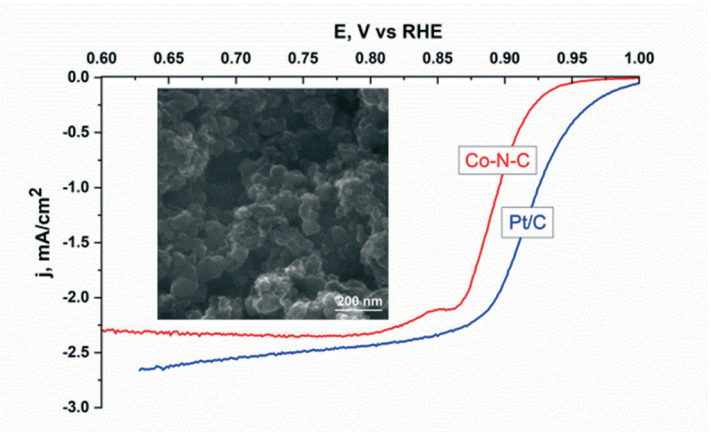

Fig. 2. Electrochemical oxygen reduction on commercial Pt/C catalyst and Co-N-C catalyst prepared using DES. Insert: SEM image of Co-N-C catalyst.

The possibility of using Co-containing DES based on choline chloride – $[(CH_3)_3N{+}CH_2CH_2OH]Cl^-$, which is much cheaper compared to [Bmim]Cl and other alkylimidazolium salts, in the production of Co-N-C catalysts has been shown. Although such catalysts are somewhat inferior in ORR activity (E_{onset} ~ 0.92-0.95 and ~ 0.75-0.81 V, vs RHE in 1.0 M NaOH and 0.5 M H_2SO_4, respectively) by analogues derived from [Bmim]Cl-DES, further optimization of their preparation can, in our opinion, improve their performance.

The ability of the best of the developed catalysts to stable operation as a part of the membrane-electrode block based on a commercial ion-conducting membrane Nafion in the model of the low-temperature FC is established.

Areas of application and advantages

The possibility of using the obtained hybrid materials as precious metals free ORR electrocatalysts for low-temperature FCs, including a solid polymer electrolyte FCs, are assumed. It is also possible to use them as ORR electrocatalysts in direct alcohol FCs and metal-air power sources, as electrocatalysts for overall water splitting, as heterogeneous catalyst for organic chemistry processes, etc. Developed cobalt-nitrogen-carbon ORR electrocatalysts can be produced by relatively simple manufacturing technology. They have low cost due to the absence of precious metals in the composition, high stability in the process of long-term operation, tolerance to methanol and CO. Compared with analogues, the obtained catalysts are characterized in the alkaline electrolyte by higher values of E_{onset} and $E_{1/2}$, and in the acid – comparable.

The level of technological readiness of development: experimental proof of commercial prospects (IRL3); experimental proof of technology concept (TRL3).

Intellectual Property

Technical solutions are know-how; an application for a Ukrainian patent was filled for the developed electrocatalysts and methods of their production.

The main publications in the frame of the project "Development of oxygen reduction hybrid electrocatalysts based on carbonized nanostructured organic conjugated polymers for hydrogen-oxygen fuel cells":

1. Y.I. Kurys, O.O. Pariiska, D.O. Mazur, V.G. Koshechko, V.D. Pokhodenko. Electrochemical synthesis of multilayered graphene and its use in Co–N–C electrocatalysts of oxygen reduction and hydrogen evolution, *Russian Journal of Electrochemistry*, 2020, vol.56, pp. 271-284.
https://doi.org/10.1134/S1023193520040072

2. O. Pariiska, D. Mazur, Y. Kurys, R. Socha, V. Koshechko, V. Pokhodenko. Poly-5-aminoindole and and graphene-like materials derived bifunctional Co-N-C electrocatalysts for oxygen reduction and

hydrogen evolution. *Journal of Solid State Electrochemistry*, 2021, vol.25, pp. 2309-2319.
https://doi.org/10.1007/s10008-021-05009-6
3. Ya. Kurys, O. Pariiska, K. Cherchenko, D. Mazur, V. Koshechko, V. Pokhodenko. Cobalt-nitrogen-carbon electrocatalyst for oxygen reduction, obtained using a deep eutectic solvent, *Ukrainian Patent Application* No a202008235, December 12, 2020.

References:

[1] He Y, Tan Q, Lu L, et al. Metal-Nitrogen-Carbon Catalysts for Oxygen Reduction in PEM Fuel Cells: Self-Template Synthesis Approach to Enhancing Catalytic Activity and Stability. *Electrochem. Energy Rev.,* 2019, vol.2, pp.231–251.
[2] Zhang J, Chen G, Müllen K, Feng X. Carbon-rich nanomaterials: fascinating hydrogen and oxygen electrocatalysts, *Adv. Mater.*, 2018, vol.30, article number 1800528.
[3] Gewirth A.A, Varnell J.A, DiAscro A.M. Nonprecious metal catalysts for oxygen reduction in heterogeneous aqueous systems, *Chem. Rev*., 2018, vol.118, pp. 2313-2339.
[4] Kurys Ya.I, Pariiska O.O, Mazur D.O, et al. Electrochemical synthesis of multilayered graphene and its use in Co–N–C electrocatalysts of oxygen reduction and hydrogen evolution, *Russ. J. Electrochem.,* 2020, vol.56, pp.271–284.
[5] Pariiska O., Mazur D., Kurys Y., et al. Poly-5-aminoindole and graphene-like materials derived bifunctional Co-N-C electrocatalysts for oxygen reduction and hydrogen evolution, *J. Solid State Electrochem.* 2021, vol.25, pp.2309–2319.
[6] Kurys Ya.I, Pariiska O.O, Cherchenko K.O, et al. Cobalt-nitrogen-carbon electrocatalyst for oxygen reduction, obtained using a deep eutectic solvent. *Ukrainian Patent Application* No a202008235, Dec. 12, 2020.

Development of proton-exchange systems for fuel cells based on polymeric membranes and oligomeric ionic liquids

V. Shevchenko, A. Stryutsky, M. Gumenna, N. Klimenko

Institute of Macromolecular Chemistry, NASU, Kyiv, Ukraine

Introduction

Polymer electrolyte Fuel Cells (FCs) are characterized by high efficiency of conversion of chemical energy of fuel into electrical one and environmental safety [1-3]. They are used as energy sources in both stationary and mobile devices for different purposes. The heart of such FCs is a membrane-electrode unit comprising a polymeric Proton-Exchange Membrane (PEM) as a key component [1, 2]. The most widespread polymer electrolyte FCs are based on aliphatic sulfoacidic perfluorinated polymers as PEMs known as Nafion. The performance of these membranes has significant limitations due to the need for high humidity to achieve the required level of proton conductivity, the high requirements for hydrogen fuel purity, use of expensive catalysts, fuel crossover, etc. These shortcomings combined with the high cost of perfluorinated PEMs are a limiting factor in improving FCs performance, competitiveness and large-scale implementation. The main way to eliminate these shortcomings is to provide polymer electrolyte FCs with the ability to operate in the temperature range of 100 ^{o}C -200 ^{o}C under dry conditions that puts forward new requirements for performance of PEMs [1-6].

Among the effective ways to solve this problem is the appropriate functionalization of commercially available thermally stable polymers including formation of non-aqueous proton-conducting medium in their composition [4, 5]. Protic Ionic Liquids (ILs) are widely used as dopants for this purpose [6, 7]. However, ILs are prone to diffuse from the composition of PEMs during performance that impairs their functional characteristics.

This work is devoted to the development of the direction of synthesis of oligomeric and polymeric ILs (OILs and PILs correspondingly) of different structure and molecular architecture and use

of such compounds as proton-conducting media for creating the thermostable PEMs capable of performance at temperatures above 100°C in the absence of moisture. In this case the used compounds form non-aqueous proton-conducting medium as a part of PEMs and their macromolecular nature counteracts diffusion of them from the membranes.

Developing OILs as anhydrous proton-exchange media

Methods for synthesis of protic cationic and anionic OILs of highly branched structure (silicone star-like and hyperbranched ester ionomers) as anhydrous proton-conducting media were proposed in this work. The developed compounds were used as dopants in obtaining the thermally stable PEMs on the basis of commercial thermally robust polymers both by impregnating them with solutions of the proposed compounds or combining the polymers with the compounds in solutions (casting method). The obtained membranes were characterized by high thermal stability and ability to ionic conductivity in the absence of moisture.

Star-shaped basic oligosilsesquioxanes with tertiary amine groups in combination with primary and secondary hydroxyl groups in an organic frame, as well as those containing secondary amine, secondary hydroxyl groups and imidazole rings in the organic shell of the silsesquioxane core were developed and used by us as highly branched initial oligomers for the synthesis of OILs. Also, the sulfonic acid derivative of the third generation hyperbranched oligoester polyol containing 32 terminal functional groups was developed and used by us as a highly branched initial acidic oligomer. OILs based on the star-shaped basic oligosilsesquioxanes and the hyperbranched sulfonic acid oligoester were obtained via the partial or complete neutralization of them by developed by us oligoethylene oxide derivatives with terminal sulfonic acid or ternary amine groups respectively. The developed OILs are shown in the Figure.

It should be noted that the highly branched structure and polyfunctionality of the synthesized compounds provide a high charge density which promotes realization of proton conductivity and the presence of a silsesquioxane core contributes to their high thermal stability. Moreover, the ethylene oxide component of the compounds is

capable of solvating small cations, in particular protons, with their

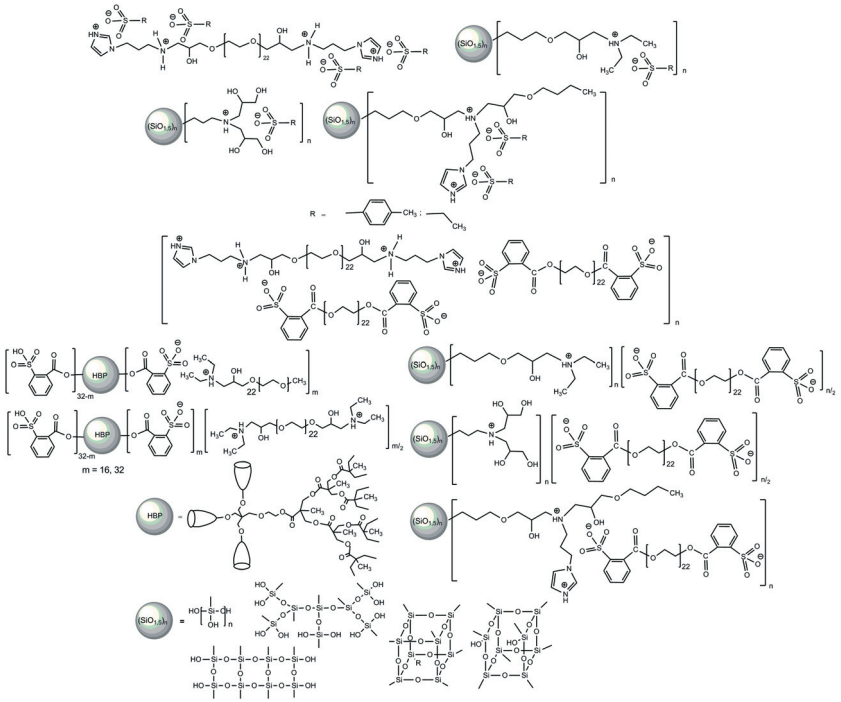

subsequent transport under anhydrous conditions.

Also, the low molecular weight sulfonic acids (ethane and p-toluenesulfonic acid) were used as neutralizing agents in the synthesis of OILs. The linear protic cationic OILs were obtained with use of the latter by neutralizing the basic centers of the oligoethylene oxide derivative developed by us with terminal imidazole fragments and secondary amine groups.

Developing PEMs based on the OILs

Polyethylene terephthalate in the form of track membranes (due to limited solubility it was used only for impregnating with the developed OILs) with different pore sizes (0.1 μm and 1.0 μm) as well as aromatic polysulfone in the form of porous membranes of a given porosity (up to 80%) were used as a starting commercially available thermostable

polymer. In this case, the latter was used both for impregnating with the synthesized OILs and for mixing with the OILs in a solution followed by film casting.

Structure and properties of the obtained OILs and PEMs

The structure of the synthesized compounds was proved by the methods of FTIR, ^{1}H and ^{13}C NMR spectroscopy, as well as by the method of functional analysis. Their structure and thermophysical properties were studied by the method of dynamic scanning calorimetry. It was shown that depending on the composition, the synthesized compounds can be characterized by both a completely amorphous structure (facilitating proton conductivity) and presence of a crystalline phase formed by oxyethylene component. According to the data of thermogravimetric analysis the obtained compounds are thermally stable up to 200 ^{o}C -280 ^{o}C and the dielectric relaxation spectroscopy data indicate a proton conductivity level of 10^{-3} S/cm at the temperatures 100 ^{o}C -120 ^{o}C in the absence of humidification that indicates their prospects as anhydrous proton-conducting media for PEMs.

The developed PEMs are characterized by thermal stability up to 250 ^{o}C -290 ^{o}C and ionic conductivity of (10^{-6}-10^{-4}) S/cm at 100 ^{o}C -120 ^{o}C under anhydrous conditions. The obtained membranes according to these characteristics are at the level of the best domestic and foreign analogues of this type.

Area of application

The obtained OILs and PEMs can be used not only in FCs but also in chemical separation processes, sensors, energy storage devices (supercapacitors), windows with controlled permeability of light ("smart windows"), electrochromic displays, process of electrolysis of water, etc.

Comparative evaluation of the results

The developed methods of PEMs obtaining are based on the use of commercially available thermally stable polymers that makes it possible to implement this approach on an industrial scale. The synthesized PEMs are characterized by small thickness (10 μm -80 μm), high mechanical strength and thermal stability, acceptable ionic conductivity in anhydrous

conditions, ease of synthesis and low cost of production compared to common perfluorinated sulfoacidic membranes (type Nafion) manufactured by DuPont Co., Asahi Glass Co. Ltd, Asahi Chemicals Co. Ltd , Dow Chemical Co.

The main publications in the frame of the project “Development of proton-exchange systems for fuel cells based on polymeric membranes and oligomeric ionic liquids”:

1. M.A. Gumenna, N.S. Klimenko, A.V. Stryutsky, L.L. Kovalenko, V.V. Kravchenko, A.V. Shevchuk, V.V. Shevchenko. Polymeric proton exchange media with ionic bonds in the main chain of the polymer, *Dopov. Nac. akad. nauk Ukr.,* 2020, No.12, pp. 60-66. https://doi.org/10.15407/dopovidi2020.12.060
2. A.V. Stryutsky, O.O. Sobko, M.A. Gumenna, N.S. Klimenko, A.V. Kravchenko, V.V. Kravchenko, A.V. Shevchyuk, V.V. Shevchenko. Polymeric organic-inorganic proton-exchange membranes based on anionic oligomeric ionic liquid of hyperbranched structure, *Polym. J.*, 2019, vol. 41, No. 2, pp. 123-129. https://doi.org/10.15407/polymerj.41.02.123

References

[1] Tellez-Cruz M.M, Escorihuela J, Solorza-Feria O, Compañ V. Proton exchange membrane fuel cells (PEMFCs): Advances and challenges. *Polymers* 2021; 13: article number 3064.

[2] Karimi M.B, Hooshyari K, Salarizadeh P, Beydaghi H, Ortiz-Martinez V.M, Ortiz A, Uribe I.O, Mohammadi F. A comprehensive review on the proton conductivity of proton exchange membranes (PEMs) under anhydrous conditions: Proton conductivity upper bound, *Int J Hydrogen Energy,* 2021, vol. 46, pp. 34413-34437.

[3] Elwan H.A, Thimmappa R, Mamlouk M, Scott K. Applications of poly ionic liquids in proton exchange membrane fuel cells: A review, *J. Power Sources,* 2021, vol. 510, article number 230371.

[4] Araya S.S, Zhou F, Liso V, Sahlin S.L, Vang J.R, Thomas S, Gao X, Jeppesen C, Kaer SK. A comprehensive review of PBI-based high temperature PEM fuel cells, *Int J Hydrogen Energy,* 2016, vol.41, pp. 21310-21344.

[5] Hooshyari K, Amini Horri B, Abdoli H, Fallah Vostakola M, Kakavand P, Salarizadeh P. A review of recent developments and advanced applications of high-temperature polymer electrolyte membranes for PEM fuel cells, *Energies*, 2021, vol.14, article number 5440.

[6] Ebrahimi M, Kujawski W, Fatyeyeva K, Kujawa J. A review on ionic liquids-based membranes for middle and high temperature polymer electrolyte membrane fuel cells (PEM FCs). *Int. J. Mol. Sci.*, 2021, vol. 22, article number 5430.

[7] Greaves T.L, Drummond C.J. Protic ionic liquids: Evolving structure–property relationships and expanding applications, *Chem. Rev.*, 2015, vol. 115, pp.11379-11448.

Development of nanostructured catalysts and new technological solutions for the processing of biogas with the production of hydrogen fuel for the methane conversion unit of high-temperature fuel cells

S. Soloviev, P. Kyriienko, D. Samoylenko, Ya. Kurylets, A. Kapran

Pysarzhevsky Institute of Physical Chemistry, NASU, Kyiv, Ukraine

1. Brief description of the development and main results

It is shown that Ni-Al_2O_3 composites deposited on ceramic block matrices of honeycomb structure are efficient catalysts for Carbon Dioxide Conversion of Methane (CDCM). Improving the stability of the catalysts is achieved by adjusting the acid-base properties of the surface by introduction the additives of alkali metal oxides, which contribute to a more complete decomposition of nickel-aluminium spinel and the formation of metallic nickel (Ni^0) particles at the stage of catalyst reduction.

Fig.1. Catalyst on ceramic monolith

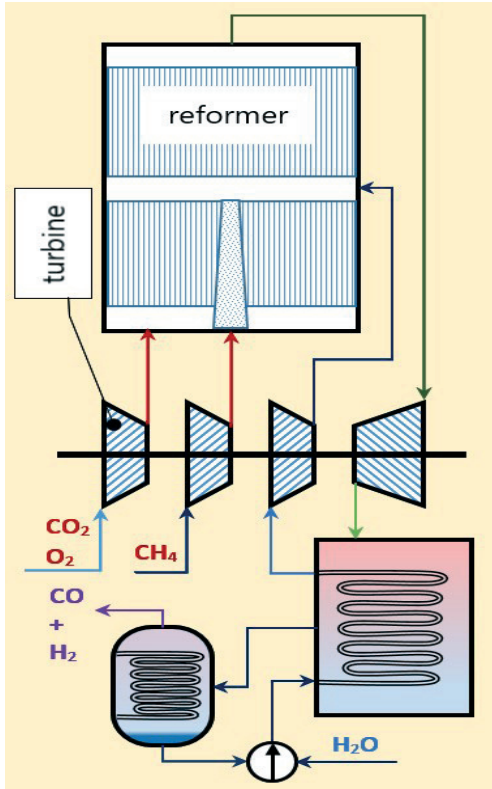

Fig. 2. Scheme of methane/biogas tri-reforming

High initial activity of Ni/Al_2O_3/cordierite catalyst decreases over the time due to surface carbonization, which is typical for compositions based on $Ni\text{-}Al_2O_3$. Alkaline additives (K_2O, Na_2O) slow down the process of carbon accumulation on the surface, increasing the stability of the catalyst, though catalytic activity is somewhat reduced. Increasing the oxidant (CO_2) content reduces the conversion of methane on nickel-aluminium catalysts modified with alkali metal oxides, which may be due to the formation of stable and low-reactive alkali metal carbonates.

The increase in the stability of operation of the catalysts modified by the addition of alkali metal oxides is due to the slowing down of the

carbonization processes of the surface. Moreover, additives with high basicity (K_2O, Na_2O) slightly reduce the catalytic activity by slowing down the dissociation of methane, by the formation of inactive alkali metal carbonates, as well as by some increase in the strength of the nickel-oxygen bond, which is revealed itself in decreased reduction of nickel-aluminium catalysts modified with alkali metals.

Modification of Ni-Al_2O_3/cordierite catalysts by Rare Earth Oxides (REO: La_2O_3, CeO_2) provides increase of their activity and stability in operation in the processes of deep and partial oxidation of methane and CDCM. In the partial oxidation of methane, the nickel-aluminium catalyst modified with lanthanum oxide provides high, close to 100%, selectivity with respect to hydrogen.

The use of structured catalysts with a small wall thickness will eliminate the diffusion limitations of the CDCM process and, due to this, reduce the coke formation process. It is shown that the productivity of the structured nickel-aluminium catalyst in the CDCM process significantly exceeds the productivity of the granular industrial catalyst.

It was shown for the first time that Ni-BEA zeolites with high Si/Al modulus, prepared by postsynthetic treatment, show high activity and operation stability in the process of low-temperature carbon dioxide conversion of methane – a mixture that simulates biogas (99% of methane conversion at $T \leq 700$ °C). It was shown that dealumination increased the activity of catalysts in the CDCM process, which may be associated with a decrease in the concentration of aluminium-containing acid sites (complete absence of Brønsted acid sites) on the catalyst surface.

It was found that dealuminated Ni-BEA catalysts can withstand several CDCM catalytic cycles without loss of activity. The results of the studying catalysts by the X-ray photoelectron spectroscopy after the course of this process showed the stabilization of nickel cations in the structure of the zeolite.

It was shown for the first time that the use of cold plasma in the presence of metal oxide and zeolite catalysts can significantly (by 300°C-400°C) reduce the temperatures of achieving high degrees of conversion of methane and carbon dioxide to CO and H_2.

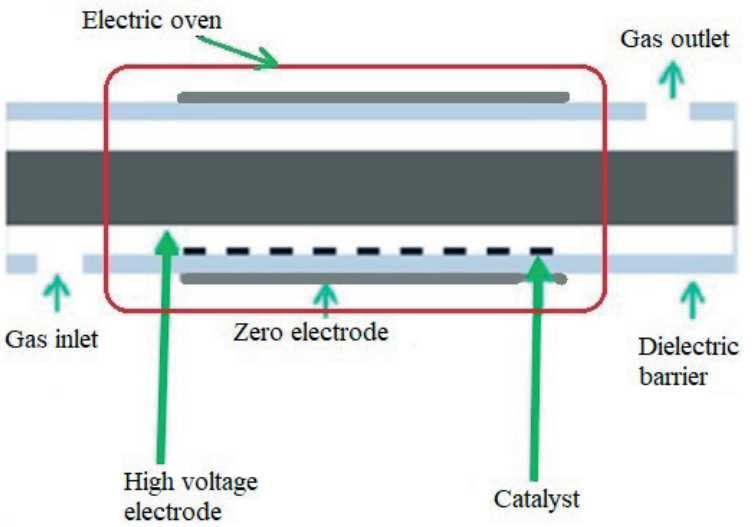

Fig. 3. Scheme of the plasma catalytic unit

The obtained results are important for the development of the industrial process of converting biogas into syngas with different H_2/CO ratios (1÷3).

The composition of nickel-aluminium catalysts on structured ceramic supports for the carbon dioxide conversion of methane is optimized. It is found that the introduction of rare earth oxides (CeO_2, La_2O_3) in the composition of Ni/Al_2O_3/cordierite catalysts prevents the formation of nickel-aluminium spinel ($NiAl_2O_4$), which decreases the reduction temperature of nickel oxide with the formation of Ni crystals and, as a result, increases the resistance to oxidation of the active phase of the catalysts.

It was found that La_2O_3 doesn't form a separate crystalline phase on the surface of the Ni-Al_2O_3 catalyst but may be a part of the secondary support (together with Al_2O_3) or be in a finely dispersed state, preventing sintering processes and phase transformations of alumina, which lead to thermal recrystallization of the catalytic coating.

It is shown that the role of REO modifying additives (La_2O_3, CeO_2) in the composition of Ni-Al_2O_3-catalysts is to ensure their stable operation

in the CDCM process also by creating additional oxygen vacancies and increasing the mobility of surface oxygen, which accelerates the oxidation of carbon-containing structures (Ni-C) and prevents carbonization of the catalyst.

It is shown that nickel-aluminium catalysts are prone to loss of activity in the carbon dioxide reforming of methane during prolonged exposure to SO_2. Catalysts, modified with La_2O_3 and CeO_2, are characterized by the highest resistance to the action of sulfur.

Restoration of catalytic activity is possible when treating catalysts with hydrogen at high temperatures, including under pre-oxidation with oxygen. Restoration of catalyst activity can occur due to complete oxidation of nickel, which removes the vast majority of sulfur-containing compounds. The ability of catalysts to be regenerated is decreased when repeating the cycles of poisoning-regeneration. Modification of catalysts with La_2O_3, CeO_2 allows to regenerate the catalyst without pre-oxidation.

It was found that increasing the degree of dealumination of Ni-BEA zeolites helps to increase their catalytic activity in the conversion of CH_4-CO_2 mixture and resistance to carbonization, while modification with ceria provides an additional increase in their activity. The Ni-Ce-BEA sample showed high stability in operation over several catalytic cycles. The presence of sulfur compounds in the reaction mixture leads to partial deactivation of the catalyst.

It was shown that in the process of plasma-catalytic conversion of methane with CO_2 the nature of the electrode affects the conversion of reagents and the selectivity with reference to products; the highest rates of reagent conversion were achieved on copper and steel (grade 9XC) electrodes. Varying the ratio of CH_4:CO_2 under conditions of plasma catalysis allows to change the ratio of H_2:CO in the produced syngas.

2. Possible areas of application

Chemical, bio-, petrochemical and processing industries, the agrarian sector for the processing of natural and biogas to the synthesis gas for the subsequent production of ammonia, methanol, diethyl ether, Fischer-Tropsch syntheses as well as for high-temperature solid oxide fuel cells.

3. Comparative evaluation of the obtained results (analogues, competitors)

Compared with analogues (Haldor Topsøe), the developed structured catalysts of high productivity have a significantly lower content of active components; they are resistant to carbonization and catalytic poisons (sulfur) and high temperatures (500–1000 °C); they do not contain noble metals; they have low gas-dynamic resistance, which reduces operating costs.

4. Level of technological readiness

Custom-made industrial designs are manufactured, licensing of production is carried out.

5. Intellectual property

Ie.V. Gubareni, S.O. Soloviev, S.M. Orlyk, Ya.P. Kurylets. Nickel based catalyst for methane tri-reforming, UA patent No. 108461, published July 25, 2016, bull. No.14.

The main publication in the framework of project “Development of nanostructured catalysts and novel technological solutions for processing of biogas with hydrogen fuel production for methane conversion module of high-temperature fuel cells”:

S.M. Orlyk, M.R. Kantserova, V.I. Chedryk, P.I. Kyriienko, Y.Millot, S. Dzwigaj, Influence of acid–base surface characteristics of GAxSIBEA Zeolites on their catalytic properties in the process of oxidative dehydrogenation of propane to propylene with participation of CO_2. *Theoretical and Experimental Chemistry*, 2021, vol. 56, pp.387–395. http://doi.org/10.1007/s11237-021-09667-5

Outlook

A comprehensive, large scale introduction of hydrogen as an energy carrier and its utilisation in hydrogen energy systems are on the global agenda. The priority for Europe and for the world is to achieve a climate neutrality by implementing zero pollution goals. Development of the hydrogen technologies and production facilities of renewable hydrogen, obtained mainly using wind and solar energy, is the main trajectory in moving towards these goals.

Winning the price competition is a key factor in reaching a success in a broad use of hydrogen. Today, fossil-based hydrogen is much cheaper (around 1.5 €/kg; the cost of CO_2 is disregarded) as compared to both renewable hydrogen (3-5 €/kg) and low-carbon hydrogen (2 €/kg). Every kg of a fossil-based hydrogen produced by steam reforming releases 8 kg of CO_2, which is an incredibly high number. Carbon dioxide removal process prices in the range of 55-90 €/ton of CO_2 are required to make the production of the fossil-based hydrogen with carbon capture competitive with fossil-based hydrogen today.

Reaching this latter, very challenging, target is one of the aimed developments. The other target is in markedly growing the industrial capacities for producing clean hydrogen. By 2030, hydrogen needs to become an intrinsic part of an integrated energy system with a strategic objective to install in the EU at least 40 GW of renewable hydrogen electrolysers and to produce of up to 10 million tonnes of renewable hydrogen. Between 2030 and 2050, renewable hydrogen technologies should reach maturity and be deployed at a large scale.

Use of hydrogen requires significant advances in not only hydrogen production technologies, but also in hydrogen storage and transportation efficiencies, together with a parallel progress in the performance and in lowering of the costs of the fuel cell stacks. For hydrogen storage systems, as ultimate goal is to reach the energy storage efficiency of 2.2 kWh/kg at a system level and, storage of 6.5 kg of hydrogen in 100 kg of the system in total (DoE, USA).

As reaching these goals is challenging in many aspects, an international joint effort, supported by the funding from the national and international sources, is in need. This book presents a contribution to the R&D efforts in this field, which were supported by the NATO Science for Peace and Security Programme (collaborative project G5233 “Portable Energy Supply” executed in collaboration between the Institute for Energy Technology in Norway (Coordinator) and three research institutes

of the National Academy of Sciences of Ukraine, Karpenko Physico-Mechanical Institute, Frantsevich Institute for Problems of Materials Science and Vernadsky Institute of General and Inorganic Chemistry). Furthermore, a 3-years Ukrainian Research Program "Development of scientific principles for hydrogen production, storage and use in autonomous energy supply systems" has been completed and enjoyed contributions from more than 20 projects, being focused on the efficient hydrogen production, hydrogen storage and its use in energy systems.

Ukraine recently became an associated country of the EU research programme HORIZON 2020 and contributes to the growing year-by-year joint with EU R&D activities as a partner. For Ukraine, depletion of fossil hydrocarbon fuels together with a presently rather limited use of alternative energy sources, put a demand for a sufficient energy supply into a strategic national priority interests. Total annual energy consumption in Ukraine is about 200 million tons in a fuel equivalent. In Ukraine a share of renewable energy, including solar, wind, geothermal energy, into the overall energy supply is only about 2 % (2020), with a total renewable energy systems (RES) capacity of about 650 MW. That's why hydrogen-based energy supply becomes prioritized in Ukraine, in a similar way as in the EU countries.

Thus, it is very important that Ukraine will utilize its unique opportunities to expand the use of renewable energy sources. The potential resources of wind energy and solar energy in Ukraine are estimated at a level of 20-30 and 400 mln tons in a fuel equivalent per year, respectively, with biomass energy resources of 22 mln tons in a fuel equivalent per year, and their efficient use is a national target.

Increased utilization of hydrogen, and the use of RES for its production are the key focus areas to achieve the future energy and environmental security in Ukraine. Progress in this field will contribute to the creation of a low-carbon national economy and for a diversification of energy supply by utilizing both central and also distributed energy generation systems.

As the use of hydrogen-powered fuel cells together with renewable energy sources allows a drastic reduction of carbon-containing emissions, thus hydrogen and fuel cells technologies require further fundamental and applied research efforts, focused on the creation of the new materials, development of advanced processes and technologies, and their practical implementation via the targeted demonstration projects.

Methods of hydrogen production with use of renewable energy sources, utilization of the various organic wastes, energy storage materials and processes, need further advances, efficient dissemination and implementation by joining the efforts of the research community, financial, governmental and industrial sectors.

Fundamentally new solutions are needed to achieve the required progress in the development of hydrogen storage materials and systems, with a focus on new H storage compounds, metal hydrides, complex hydrides and highly efficient hydrogen sorbents. Such materials will allow to improve the efficiency of use of hydrogen-based energy storage for the stationary, mobile and portable applications.

Furthermore, it is necessary to continue the research on the novel advanced materials for the fuel cells - polymer-based proton conductive membrane fuel cells and solid oxide fuel cells. Future studies should be performed to achieve a significant improvement in the ionic conductivity of the solid electrolytes, and to create new, inexpensive and platinum-free catalysts, increasing the fuel cell service life while aiming at a significant cost reduction.

Finally, it is also very important to implement various pilot demonstration projects, including development of autonomous energy supply systems based on the use of hydrogen and renewable energy sources to power farms, houses, portable and electronic devices.

Joint efforts of the research community are required to reach these goals and the participants of the NATO SPS programme and Ukrainian Research Program “Development of scientific principles for hydrogen production, storage and use in autonomous energy supply systems” will be happy to contribute to the success of such an effort.

The Editors

Prof.	Prof.	Prof.
Volodymyr Yartys	Yuriy Solonin	Ihor Zavaliy
IFE, Norway	IPMS, Ukraine	PhMI, Ukraine

8 November 2021

Content

Yartys Volodymyr A.

Professor of materials science and hydrogen technologies, Doctor of Chemical Sciences, Senior Scientist I. Institute for Energy and Technologies, Norway.
Prof. V.A.Yartys is an expert in hydrogen based energy storage working on: (a) Nanomaterials for energy storage; (b) Rechargeable Batteries; (c) H2 as an Energy Carrier; (d) Materials for Hydrogen Storage and Battery Applications; (e) H storage systems; (f) Use of metal hydrides in energy management.
He acted as a project leader in a number of research projects funded by EU, Norwegian Research Council, Nordic Energy Research, industry. Prof. Yartys is the Editor of Journal of Alloys and Compounds, Elsevier and is a representative of Norway in the International Society of Electrochemistry.
Author of more than 250 papers (H-index 49). https://www.researchgate.net/profile/Volodymyr-Yartys; Volodymyr Yartys-Google Scholar; orcid.org/0000-0003-4207-9127.

Solonin Yuriy M.

Academician of the NAS of Ukraine (Materials Science, Materials for Hydrogen Engineering),
Professor, Doctor of Physical and Mathematical Sciences, Institute for Problems of Materials Sciences of the NAS of Ukraine, Director
Prof. Yu.M. Solonin is an expert in hydrogen based energy storage working on: (a) Materials for Hydrogen Storage and Battery Applications; (c) H storage systems, (d) Chemistry of refractory compounds. He acted as a project leader in a number of domestic and international research projects.
Editor-in-Chief of the journal “Poroshkova Metallurgiya” (“Powder Metallurgy and Metal Ceramics”). Author of more than 200 papers (H-index 15). Scopus ID: 7003333526: https://orcid.org/0000-0002-8068-1023

Zavaliy Ihor Yu.

Corresponding Member of the NAS of Ukraine (Materials Science, Materials for Hydrogen Engineering),
Professor, Doctor of Chemical Sciences,
Karpenko Physico-Mechanical Institute of the NAS of Ukraine, Head of the Department of hydrogen technologies and materials of alternative energy. Prof. I.Yu. Zavaliy is an expert in hydrogen based energy storage working on: (a) Materials for Hydrogen Storage and Battery Applications; (b) Nanomaterials and their properties; (c) H storage systems.
He acted as a project leader in a number of domestic and international research projects.
Author of more than 150 papers (H-index 16).
https://www.researchgate.net/profile/Ihor-Zavaliy
https://orcid.org/0000-0002-9825-6922

Acknowledgements

We sincerely thank the institutions hosting the NATO SPS Programme Project G5233 “Portable Energy Supply” – Institute for Energy Technology, Norway, Karpenko Physico-Mechanical Institute of the National Academy of Sciences of Ukraine, Frantsevich Institute for Problems of Materials Science of the National Academy of Sciences of Ukraine, and Vernadsky Institute of General and Inorganic Chemistry of the National Academy of Sciences of Ukraine for their support in execution of the program of the work.

This work has received a continuous support from the staff of the NATO SPS Programme. The Editors / Project Directors of the Project G5233 Portable Energy Supply are very much grateful to Mr. Richard Brewin, the Programme Manager for Energy & Environmental Security and Science for Peace & Security at NATO, Dr. Deniz Beten, Senior Science for Peace, Security & Partnership Cooperation Advisor and Mrs. Klavdija Kaliope, SPS Projects Assistant, for their continuous guidance and help and for their article presenting the Science for Peace and Security Programme of NATO in this book.

Furthermore, we also thank the participants of the research Programme “Development of scientific principles for hydrogen production, storage and use in autonomous energy supply systems” (2019-2021) supported by the National Academy of Sciences of Ukraine, who presented their projects in this book and cooperated during the preparation of the book.

Volodymyr Yartys is grateful for the colleagues from the IEA Tasks 32 and 40 for the fruitful collaboration.

Our special thanks to Dr. Iryna BILAN and Dr. Igor Morozov from IPMS NASU, Mr. Roman KOKOT and Dr. Vasyl BEREZOVETS from the PhMI NASU for their dedicated and highly valuable contribution to the work on the Project G5233 and for their preparation of the book.

THE EDITORS

Volodymyr Yartys Yuriy Solonin Ihor Zavaliy

Водневі технології зберігання енергії: стан та перспективи розвитку. [Текст] колективна моногр. / За редакції В.А. Яртися, Ю.М. Солоніна, І.Ю. Завалія. – Львів : Простір-М, 2021 – 268 с.

ISBN 978-617-8055-08-0

Представлено останні досягнення в галузі використання енергії відновлювальних джерел (сонця і вітру), хімічних реакцій, біосировини для ефективного одержання водню, його акумулювання та використання для систем живлення на основі паливних комірок. Нові значні результати були одержані в рамках двох науково-дослідних програм, а саме, проекту G5233 "Portable Energy Supply" (2019-2021 рр.) програми НАТО Science for Peace and Security та цільової комплексної програми НАН України "Розвиток наукових засад отримання, зберігання та використання водню в системах автономного енергозабезпечення" (2019-2021 рр.).

Книга рекомендована для наукових працівників, викладачів та аспірантів, які спеціалізуються у галузі матеріалознавства, енергетики, зокрема, в дослідженнях та впровадженні матеріалів та технологій водневої енергетики.

УДК 620.9.546.11

Наукове видання

Інститут енергетичних технологій, Норвегія

Національна академія наук України

ВОДНЕВІ ТЕХНОЛОГІЇ ЗБЕРІГАННЯ ЕНЕРГІЇ: СТАН ТА ПЕРСПЕКТИВИ РОЗВИТКУ

За редакцією: В.А. Яртися, Ю.М. Солоніна, І.Ю. Завалія

Колективна монографія

(англійською мовою)

Технічний редактор І.І. Білан

Художнє оформлення обкладинки О. Зубар

Комп'ютерна верстка І.А. Морозов

ТзОВ "Простір-М"

Свідоцтво про внесення до Державного реєстру суб'єктів видавничої справи серії ДК № 5068 від 22.03.2016.

79000, Львів, вул. Чайковського, 8

Тел.: (032) 261-09-05, e-mail: prostir.druk@gmail.com

Підписано до друку 15.11.2021. Формат 60×90/16. Папір офсетний 80 г/м^2. Друк офсетний. Ум. друк. арк. 16,25. Обл.-вид. арк. 15,35. Наклад 120 прим. Зам. № 181121.

Друк ТзОВ "Простір-М". 79000, Львів, вул. Чайковського, 8